REMOVAL OF TOXIC METALS IN A MULTI METAL SYSTEM USING SORBENTS FOR POTENTIAL APPLICATION TO URBAN STORMWATER TREATMENT

Abdul Majeed Mohamed Ziyath
B.Sc. (Chemical and Process Engineering, Honours)

A thesis submitted in partial fulfilment of the requirements of the degree of

Doctor of Philosophy

Science and Engineering Faculty
Queensland University of Technology
February, 2012

Keywords

Freundlich isotherm, Kinetics modelling, Rate-limiting step, Seaweed, Sorbent mixtures, Sorption enthalpy, Stormwater treatment, Toxic metals, Zeolite

Abstract

In the context of increasing demand for potable water and the depletion of water resources, stormwater is a logical alternative. However, stormwater contains pollutants, among which metals are of particular interest due to their toxicity and persistence in the environment. Hence, it is imperative to remove toxic metals in stormwater to the levels prescribed by drinking water guidelines for potable use. Consequently, various techniques have been proposed, among which sorption using low cost sorbents is economically viable and environmentally benign in comparison to other techniques. However, sorbents show affinity towards certain toxic metals, which results in poor removal of other toxic metals. It was hypothesised in this study that a mixture of sorbents that have different metal affinity patterns can be used for the efficient removal of a range of toxic metals commonly found in stormwater.

The performance of six sorbents in the sorption of Al, Cr, Cu, Pb, Ni, Zn and Cd, which are the toxic metals commonly found in urban stormwater, was investigated to select suitable sorbents for creating the mixtures. For this purpose, a multi criteria analytical protocol was developed using the decision making methods: PROMETHEE (Preference Ranking Organisation METHod for Enrichment Evaluations) and GAIA (Graphical Analysis for Interactive Assistance). Zeolite and seaweed were selected for the creation of trial mixtures based on their metal affinity pattern and the performance on predetermined selection criteria. The metal sorption mechanisms employed by seaweed and zeolite were defined using kinetics, isotherm and thermodynamics parameters, which were determined using the batch sorption experiments. Additionally, the kinetics rate-limiting steps were identified using an innovative approach using GAIA and Spearman correlation techniques developed as part of the study, to overcome the limitation in conventional graphical methods in predicting the degree of contribution of each kinetics step in limiting the overall metal removal rate.

The sorption kinetics of zeolite was found to be primarily limited by intraparticle diffusion followed by the sorption reaction steps, which were governed mainly by the hydrated ionic diameter of metals. The isotherm study indicated that the metal

sorption mechanism of zeolite was primarily of a physical nature. The thermodynamics study confirmed that the energetically favourable nature of sorption increased in the order of Zn < Cu < Cd < Ni < Pb < Cr < Al, which is in agreement with metal sorption affinity of zeolite. Hence, sorption thermodynamics has an influence on the metal sorption affinity of zeolite. On the other hand, the primary kinetics rate-limiting step of seaweed was the sorption reaction process followed by intraparticle diffusion. The boundary layer diffusion was also found to limit the metal sorption kinetics at low concentration. According to the sorption isotherm study, Cd, Pb, Cr and Al were sorbed by seaweed via ion exchange, whilst sorption of Ni occurred via physisorption. Furthermore, ionic bonding is responsible for the sorption of Zn. The thermodynamics study confirmed that sorption by seaweed was energetically favourable in the order of Zn < Cu < Cd < Cr ≈ Al < Pb < Ni. However, this did not agree with the affinity series derived for seaweed suggesting a limited influence of sorption thermodynamics on metal affinity for seaweed.

The investigation of zeolite-seaweed mixtures indicated that mixing sorbents have an effect on the kinetics rates and the sorption affinity. Additionally, the theoretical relationships were derived to predict the boundary layer diffusion rate, intraparticle diffusion rate, the sorption reaction rate and the enthalpy of mixtures based on that of individual sorbents. In general, low coefficient of determination (R^2) for the relationships between theoretical and experimental data indicated that the relationships were not statistically significant. This was attributed to the heterogeneity of the properties of sorbents. Nevertheless, in relative terms, the intraparticle diffusion rate, sorption reaction rate and enthalpy of sorption had higher R^2 values than the boundary layer diffusion rate suggesting that there was some relationship between the former set of parameters of mixtures and that of sorbents. The mixture, which contained 80% of zeolite and 20% of seaweed, showed similar affinity for the sorption of Cu, Ni, Cd, Cr and Al, which was attributed to approximately similar sorption enthalpy of the metal ions. Therefore, it was concluded that the seaweed-zeolite mixture can be used to obtain the same affinity for various metals present in a multi metal system provided the metal ions have similar enthalpy during sorption by the mixture.

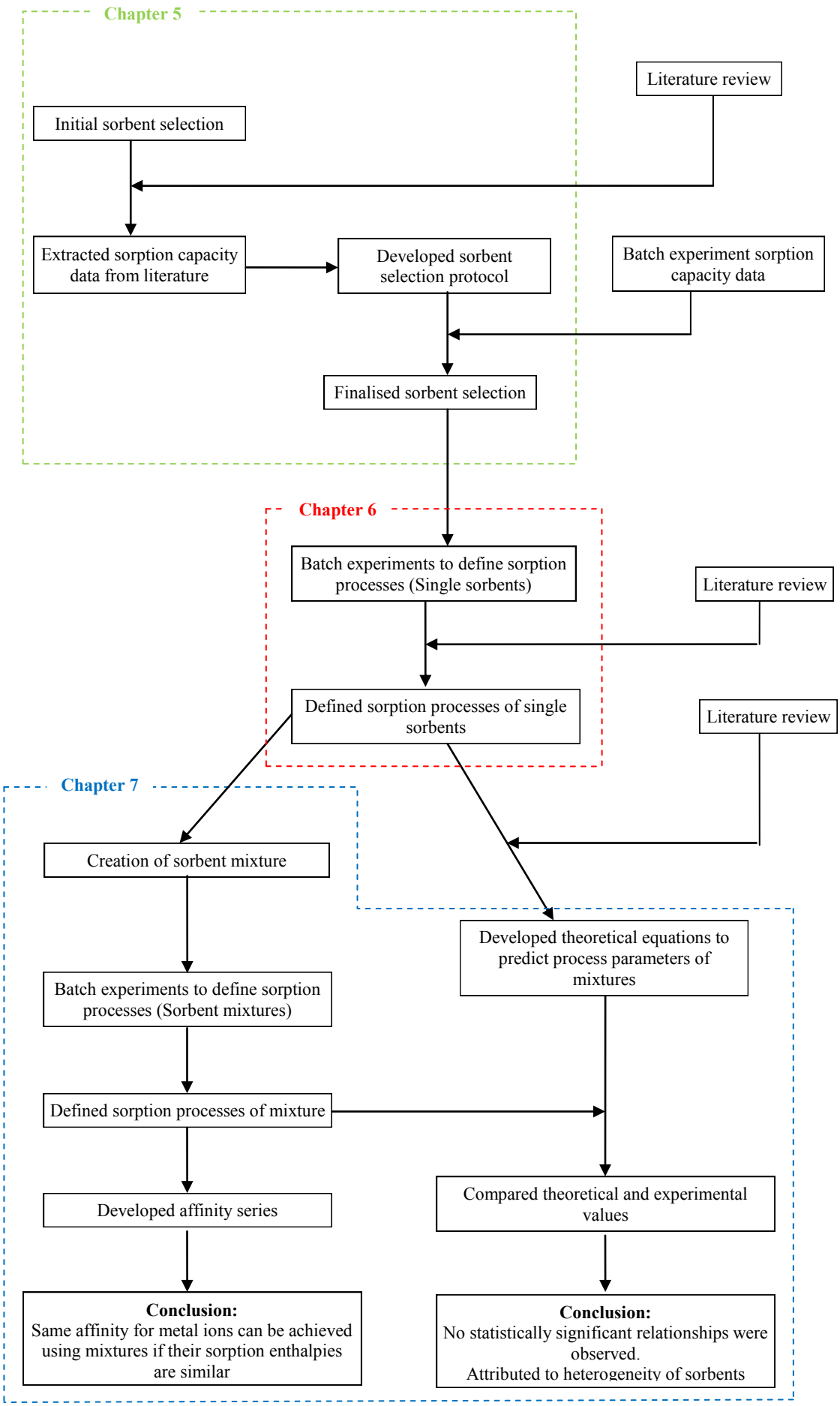

Schematic diagram showing the research methodology and the development of analytical chapters

Table of Contents

List of Figures

List of Tables

List of Appendices

List of Abbreviations

As	Arsenic
A_s	Electron affinity
AgCl	Silver chloride
$AgNO_3$	Silver nitrate
Al	Aluminium
BLDR	Boundary layer diffusion rate
C_0	Initial metal concentration
C_5	Concentration of metal ion after 5 minutes
C	Tendency to form covalent bond
Ca^{2+}	Calcium ion
Cd	Cadmium
C_e	Equilibrium metal concentration
CEC	Cation exchange capacity
Cl^-	Chloride
C_N	Concentration of ammonium ion
CO_2	Carbon dioxide
CO_3^{2-}	Carbonate
COO	Lactonic functional group
COOH	Carboxylic acid
Cr	Chromium
C_t	Metal concentration in solution at time 't'
Cu	Copper
d_p	Average particle size
D_v	Vermeulen intraparticle diffusion coefficient
D_{WM}	Weber-Morris intraparticle diffusion rate
E	Tendency to form ionic bond
ECEC	Effective cation exchange capacity
ELECTRE	ELimination and Choice Expressing REality
Fe	Iron
GAIA	Graphical Analysis for Interactive Assistance
H_2O	Water

H_2S	Hydrogen sulphide
H_3O^+	Hydronium ion
H	Chemical hardness
H^+	Hydrogen ion/proton
HCl	Hydrochloric acid
Hg	Mercury
HNO_3	Nitric acid
I	Boundary layer thickness
I^-	Iodide
ICP-MS	Inductively coupled plasma-mass spectrometry
ICP-OES	Inductively coupled plasma-optical emission spectrometry
I_s	Ionisation potential
ISRIC	International Soil Reference and Information Centre
K_1	Pseudo first order reaction rate
K_2	Pseudo second order reaction rate
K^+	Potassium ion
K_a	Langmuir constants related to energy of sorption
K_D	Distribution coefficient
K_F	Freundlich constant
K_{WM}	Weber-Morris constant
$M_2(CO_3)_n$	Metal carbonate
M_2S_n	Metal sulphide
M	Metal ion/ extra framework cation
Mg^{2+}	Magnesium
$M(OH)_n$	Metal hydroxide
m_m	Amount of metal ions sorbed
m_{mix}	Amount of metals in the mixture
m_s	Mass of the sorbent
m_{sw}	Amount of metals in a gram of seaweed
m_z	Amount of metals in a gram of zeolite
N	Number of samples
n	Freundlich exponent
Na_2CO_3	Sodium carbonate
Na^+	Sodium ion

NaCl	Sodium chloride
$NaHCO_3$	Sodium bicarbonate
NaOH	Sodium hydroxide
NH_3	Ammonia gas
NH_4^+	Ammonium ion
NH_4Ac	Ammonium acetate
NH_4Cl	Ammonium chloride
Ni	Nickel
OH^-	Hydroxide
P	Significance of Spearman correlation analysis
Pb	Lead
PC	Principal component
pKa	Acid dissociation content
PROMETHEE	Preference Ranking Organisation METHod for Enrichment Evaluations
Q	Electric charge
Q_e	Equilibrium sorption capacity
Q_t	Sorption capacity at time 't'
q_m	Maximum sorption capacity
R	Hydrocarbon chain/ Alkyl or aryl group/Universal gas constant
r	Ionic radius
R^2	Coefficient of determination
RC	Relative coefficient
r_s	Spearman ranking coefficient
S^{2-}	Sulphide
SD	Standard deviation
SMART	Simple Multi Attribute Ranking Technique
SSE	Normalised sum of squares error
T	Absolute temperature
t	Time
t_e	Equilibrium time
v	Volume
$\bar{y}$	Mean
y_i	i^{th} data point

Z	Average specific metal removal rate
Ze	Zeolite
Zn	Zinc

Abbreviations with Greek Symbols

ΔG^0	Gibbs free energy change
ΔH^0	Enthalpy change
ΔS^0	Entropy change
η_s	Absolute hardness
φ	PROMETHEE net ranking flow

Statement of Original Authorship

The work contained in this thesis has not been previously submitted for a degree or diploma from any other higher education institution to the best of my knowledge and belief. The thesis contains no material previously published or written by another person except where due reference is made.

Abdul Majeed Mohamed Ziyath Date

Acknowledgments

I wish to express my sincere gratitude to my principal supervisor Prof. Ashantha Goonetilleke for his invaluable guidance, support and constructive criticisms throughout this research. I also wish to extend my sincere thanks to Prof. Adekunle Oloyede for the advice and support at the crucial points of this research project. I am indebted to both of you for helping me understand the 'art of doing research', the concept of 'philosophy' and the importance of the word 'why'. My appreciation is further extended to Dr. Moses Adebajo for clarifying several questions regarding zeolite. Special thanks to Adjunct A/Prof. Serge Kokot for the lengthy discussions that helped me enormously to gain valuable insights into various data analysis techniques. Sincere thanks to Dr. Prasanna Egodawatta for the support and advice whenever I needed.

I am grateful to the Science and Engineering Faculty of Queensland University of Technology (QUT) for providing the financial aid to pursue this doctoral research. I would also like to thank QUT technical staff, especially Mr. Shane Russell, Mr. James Brady, Mr. Matthew Mackay, Mr. Bill Kwiecien and Ms. Leonora Newby, for their friendly and generous support during my laboratory experiments. I am also thankful to my fellow researchers; Dr. Nandika Miguntanna, Ms. Nadeeka Miguntanna, Dr. Chandima Gunawardana, Dr. An Liu, Ms. Noraliani Alias, Mr. Kehinde Yusuf and Ms. Melissa Chan for their valuable support and encouragement. I also wish to express my gratitude to the Azharis and the Noorus for their support throughout my study.

Dedication

I wish to dedicate this thesis to my dearest parents, Abdul Majeed and Ummu Salma, my lovely siblings, Zimar, Zano and Zeeras, and my wonderful wife, Zaynab Azhari, for their loving support, care, encouragement and the utmost patience, without which my childhood dream of obtaining a PhD would have remained as a dream forever!

Chapter 1: Introduction

1.1 BACKGROUND

Access to safe drinking water has been declared as a basic human right by the United Nations (WHO 2000). Some 884 million people do not have access to safe water due to the pollution of conventional water sources, such as groundwater and surface water (WHO 2008). In addition, water scarcity is one of the most critical resource issues for dry countries, such as Australia. A report by the Australian Bureau of Statistics (ABS 2005) notes that the gap between water supply and demand increases every year as water demand is growing despite highly constrained water supply sources. In this context, there has been an increased focus on utilising largely unused stormwater for potable purposes due to its availability in large volumes and accessibility in most parts of the world (Burns and Mitchell 2007; Hatt et al. 2007; Begum et al. 2008). Reusing stormwater has an additional advantage because it can reduce the hydrological impacts and water quality deterioration in receiving water bodies caused by stormwater runoff. However, the presence of toxic pollutants in stormwater restricts its direct use for potable applications, for which a high degree of treatment is required to avoid human health consequences (Tsihrintzis and Hamid 1997; Carpenter et al. 1998; NHMRC 2004).

Among the pollutants in stormwater, metal ions are some of the most toxic and persistent pollutants, which can cause significant health impacts on humans and animals (Dayan and Paine 2001; Terry and Stone 2002; Satarug and Michael 2004; Ziyath et al. 2011). Metals are found in both particulate (particle size > 0.45 μm) and dissolved (particle size < 0.45 μm) phases. Though particulate metals can be effectively removed using secondary treatment techniques such as filtration, removal of dissolved metals using these techniques is not efficient (Pontier et al. 1998). Unfortunately, dissolved metals are relatively more hazardous than the particulate form because the former is readily bioavailable to organisms (Dils and Heathwaite 1998). Therefore, removal of dissolved metals is one of the primary objectives of tertiary treatment and developing an efficient and inexpensive technology for this purpose is imperative for practical reuse of urban stormwater for potable purposes.

1.2 RESEARCH PROJECT

Several physico-chemical treatment techniques, such as coagulation-flocculation and chemical precipitation have been investigated for the treatment of dissolved metals in water (Eisenman et al. 1962; Patterson et al. 1977; Martin 1988; Bose et al. 2002; Inglezakis et al. 2006). However, these techniques have environmental and economic consequences resulting from the generation of contaminated sludge and high capital and operational costs (Ayoub et al. 2001; Kurniawan et al. 2006; Ziyath et al. 2011). Consequently, sorption technique is preferred for the removal of dissolved toxic metals from water due to economic and environmental benefits. This study investigated the use of sorption technique for the removal of dissolved metals from water for potential application in tertiary stormwater treatment.

The removal of metals by various sorbent materials have been investigated in past research studies (Genç-Fuhrman et al. 2007; Adebowale et al. 2008; Minceva et al. 2008). However, these studies have noted that sorbents selectively remove certain metal ions over the others leading to poor removal of the less preferred metal ions. This behaviour is influenced by factors such as kinetics and thermodynamics of the metal sorption mechanisms employed by the sorbent materials. Therefore, using a mixture of sorbents can be a logical approach to ensure similar affinity for the sorption of all metal ions since a range of kinetics and thermodynamics characteristics will simultaneously be in operation.

Investigating metal removal using typical urban stormwater is complex due to the presence of a range of other pollutants, which can mask and/or interfere with the metal removal processes. As such, it is difficult to characterise the specific metal removal processes, which come into play under a given set of circumstances. Therefore, the research study was undertaken using deionised water spiked with varying concentrations of dissolved metals typically found in urban stormwater as identified in research literature.

1.3 RESEARCH HYPOTHESES

- A mathematical relationship can be established between the metal sorption kinetics and thermodynamics of the sorbent mixture and those of the individual sorbents based on mass conservation principle.
- Mixtures of sorbents with different metal affinity patterns can be utilised to obtain similar affinity for the sorption of a range of dissolved metal ions in a multi metal system such as urban stormwater.

1.4 AIMS AND OBJECTIVE

Aims

The project aims were:

- To develop a multi-criteria protocol for the selection of sorbents to create sorbent mixtures for the removal of a range of metal ions in water;
- To define the kinetics and thermodynamics of the metal removal mechanisms of selected sorbents;
- To investigate the effect of sorbent mixtures on the kinetics and thermodynamics of metal sorption mechanisms and the affinity for the sorption of metal ions.

Objective

The primary objective of this research was to investigate whether the kinetics and thermodynamics of metal sorption mechanisms can be enhanced by mixing selected sorbents in order to improve the affinity for the sorption of dissolved metal ions from a multi metal solution such as urban stormwater.

1.5 INNOVATION AND CONTRIBUTION TO KNOWLEDGE

- This study created fundamental knowledge in relation to the kinetics and thermodynamics of the mechanisms employed by sorbent mixtures. This knowledge is important for the effective utilisation of sorbent mixtures for the removal of dissolved metal ions in tertiary stormwater treatment and

can be extended to investigate the sorption of other pollutants by different sorbent mixtures.

- Conventional techniques used for the identification of kinetics rate-limiting step cannot predict the influence of each kinetics step on limiting the overall metal removal rate. This study developed a novel approach to predict the influence of the kinetics steps on limiting the overall metal removal rate. This procedural innovation can contribute to the advancement of knowledge in the area of sorption kinetics investigations.
- The study identified the kinetics rate-limiting steps in the sorption of metal ions in a multi metal system by sorbents. This knowledge is crucial for increasing the overall metal removal rate and, consequently, reducing the treatment time.
- Mathematical relationships developed for predicting metal sorption kinetics and thermodynamics of mixtures based on those of individual sorbents provide essential knowledge relating to the use of mixtures for metal sorption. These equations can be extended to include a range of different sorbent mixtures.
- In this research study, a multi-criteria protocol was developed for the selection of sorbent materials to create sorbent mixtures based on a range of criteria in addition to their affinity for metal ions. This multi criteria approach can be extended to create mixtures for the simultaneous removal of various pollutants in a real-world water treatment application.

1.6 SCOPE

- This study focused on the removal of dissolved metals from road stormwater runoff at the tertiary treatment stage. Traffic activities are considered as one of the major contributors of metals to road runoff. Lead (Pb), zinc (Zn), cadmium (Cd), copper (Cu), nickel (Ni) and chromium (Cr) are toxic heavy metals commonly found in road runoff (Sansalone and Buchberger 1997; Drapper et al. 2000). Furthermore, Mangani et al. (2005) observed very high concentration of soluble aluminium (Al) in road

runoff, which is regarded as highly toxic to humans and plants. Therefore, this research study investigated the removal of dissolved Pb, Cr, Ni, Cu, Zn, Cd and Al from a multi metal system.

- In this study, the metal sorption mechanism employed by the sorbents and the mixtures was defined based on the isotherm, kinetics and thermodynamics characteristics.
- Only six sorbents, namely, seaweed, activated carbon, zeolite, clay, corncob and sugarcane bagasse were investigated.
- Only five criteria, namely sorption capacity, cost, environmental, biodegradability and operational factors, were considered in the evaluation of the performance of sorbent materials.
- The research was confined to laboratory studies using synthetic metal solutions prepared by dissolving the metal nitrates in deionised water. The study did not focus on metal removal from typical tertiary stormwater system. In addition, there were no field investigations carried out.
- The study focused on the characterisation of the sorption mechanisms employed by the selected sorbents and their mixtures. Optimisation, regeneration or life cycle analysis of the technology was not investigated.

1.7 OUTLINE OF THESIS

This thesis has nine chapters. Chapter 1 introduces the research study by providing a brief background to the research problem and by outlining the hypothesis, aims and objective of the study. Chapters 2 and 3 consist of critical review of research literature on stormwater pollution, the techniques available for the removal of metals in water, the influence of physico-chemical factors on the sorption process and the sorption modelling approaches. The design of the research study including the pertinent theory, experimental procedures and data analysis is discussed in Chapter 4.

The protocol developed for sorbent selection and the application of the protocol for the sorbents investigated in this study are presented in Chapter 5. Chapter 6 discusses the kinetics and thermodynamics of the metal sorption mechanism employed by

zeolite and seaweed, while Chapter 7 describes the metal sorption mechanism employed by their mixtures including the effect of mixing seaweed and zeolite on metal sorption affinity and the sorption kinetics and thermodynamics. Chapter 8 summarises the key findings, primary contributions to the knowledge and the recommendations for future research. The final chapter consists of the full list of the references used in this thesis.

Chapter 2: Stormwater pollutants and treatment methods

2.1 INTRODUCTION

Water is an essential resource for the existence of life and the delicate balance of its quantity on earth is maintained by the hydrologic cycle. Water evaporates from sources such as oceans and lakes to the atmosphere where it gets condensed and returns back to the surface of the earth in the form of precipitation, for example, rain, snow and hail. A portion of precipitated water is generally absorbed by the ground and is treated via a natural cleansing system consisting of soil, microorganisms and vegetation. The remainder flows as surface runoff and reaches receiving water sources such as seas, rivers and lakes.

In recent times, rapid urbanisation has significantly increased the amount of impervious surface coverage such as roofs and roads in catchment areas. Impervious surfaces have significantly reduced the infiltration of precipitated water into the ground. Consequently, there is an increase in stormwater runoff quantity, which causes erosion of stream banks and flooding (Tillinghast et al. 2011). Additionally, various pollutants such as suspended solids and toxic metals that are accumulated on impervious surfaces due to anthropogenic activities are incorporated into stormwater runoff resulting in the deterioration of the quality of receiving water bodies (Gnecco et al. 2005).

On the other hand, access to safe water is one of the most critical resource issues around the world (WHO 2008). On average 1700 m^3 per capita per annum fresh water is required to meet the needs of human population and the environment (Pigram 2006). However, 480 million people all over the world faced water shortage in 2000, which is expected to grow to almost 3 billion by 2025 (Gleick 2002). In addition, approximately 884 million people did not have access to safe drinking water in year 2006 according to the World Health Organization (WHO 2008).

Therefore, there has been an increased focus on utilising alternative water sources such as stormwater, wastewater, irrigation water and seawater in order to meet the increasing demand for clean water. Among them, stormwater is a logical alternative due to its availability in large volumes and accessibility in most parts of the world (Burns and Mitchell 2007; Hatt et al. 2007; Begum et al. 2008). Additionally, reuse of stormwater can minimise the hydraulic and water quality impacts due to increased stormwater runoff. However, the presence of toxic pollutants in stormwater restricts its direct use for potable applications, for which a high degree of treatment is required to avoid human health consequences (Tsihrintzis and Hamid 1997; Carpenter et al. 1998; NHMRC 2004). Consequently, it is necessary to develop an effective treatment system for stormwater pollutants, for which an in-depth knowledge on the physics and chemistry of stormwater pollutants is essential.

2.2 STORMWATER POLLUTANTS

The primary pollutants that are found in stormwater runoff are (Tsihrintzis and Hamid 1997):

- Suspended solids
- Organic carbon
- Nutrients
- Toxic metals
- Hydrocarbons.

Litter is also considered as a pollutant. However, its impacts on water resources are largely of aesthetic concern.

2.2.1 SUSPENDED SOLIDS

Suspended solids, which are particles typically larger than 0.45 μm in size, are contributed to stormwater runoff via various natural and anthropogenic sources such as soil erosion, vehicular emissions and industrial activities (Sansalone and Buchberger 1997). Clay, silt, abrasion products from vehicles and various types of organic matter are commonly found among suspended solids (Ellis 1976; Ogunlaja

and Aemere 2009). Concentration of suspended solids in stormwater runoff depends on various factors including rainfall intensity and duration (Egodawatta et al. 2006).

Suspended solids contribute to physical and chemical impacts on receiving water bodies. These impacts include the increase in turbidity of receiving water, which blocks light penetration. Consequently, photosynthesis and primary food production by aquatic plants are reduced (Henley et al. 2000). This can lead to the death of aquatic organisms and eventually to the collapse of the aquatic ecosystem.

The chemical impacts of suspended solids on receiving water bodies are more significant than their physical impacts. Suspended solids can adsorb toxic pollutants such as metals and hydrocarbons and transport them to receiving water bodies (Vaze and Chiew 2004; Lau et al. 2005). Particle size of suspended solids is one of the important factors that influence the adsorption and transportation of other pollutants by suspended solids. Based on size, particulates can be divided into coarse (>150 μm) and fine (<150 μm) fractions (Zafra et al. 2008). During a rainfall event, both coarse and fine suspended solids are washed from pervious and impervious surfaces. However, coarse particles generally tend to settle quickly due to gravity. In contrast, fine particles remain in suspension for a longer period due to their relatively larger surface area and surface electrostatic charge (Sansalone and Kim 2008). Furthermore, the relatively larger surface area of fine particles facilitates the adsorption of pollutants in higher concentrations compared to coarse particles.

Several studies have found that fine particles represent the majority of suspended solids in stormwater runoff and act as the most important pollutant carrier to receiving waters (Herngren et al. 2006; Miguntanna 2009). Herngren (2005) measured the concentration of total suspended solids for five particle size ranges from three different land uses. He observed higher fine particulate concentration compared to the coarse particles. For example, the mean concentration of fine suspended solids in build up samples was about 116 mg/kg for a residential site, while it was 5 mg/kg for coarse suspended solids. Therefore, it is essential to develop stormwater treatment technologies to facilitate the efficient removal of fine particles,

which, in turn, can reduce the toxic pollutant load transported to receiving water sources.

In stormwater runoff, solids are also present in the dissolved phase. Dissolved solids are defined as solids that are less than 0.45 μm in size (Herngren et al. 2010) and their mean concentration in urban Gold Coast region of Australia was found to be in the range of 27-175 mg/kg (Herngren 2005). Ions complexed with water molecules or colloidal particles are generally identified as dissolved solids. Dissolved form of hydrocarbons and toxic metals can be more hazardous than in their particulate form since the former is readily bioavailable to organisms (Dils and Heathwaite 1998). Additionally, the treatment of dissolved solids using conventional physical stormwater treatment processes such as filtration and settling is generally not efficient. Therefore, dissolved metals and hydrocarbons can easily reach receiving water bodies and can create significant human and ecosystem health impacts.

2.2.2 ORGANIC CARBON

Organic carbon is oxygen demanding material contributed to stormwater runoff from vegetation debris, animal wastes, vehicle exhaust and tyre wear (Rogge et al. 1993). Decomposition of organic carbon by microorganisms leads to the depletion of dissolved oxygen, which creates significant problems to aquatic life including failure or alteration of respiratory metabolism (Vijayavel and Balasubramanian 2006). Furthermore, ligands in organic compounds can bind metal ions via complexation. Consequently, organic carbon plays a crucial role in partitioning metal ions into particulate and dissolved forms depending on whether complexation has taken place with particulate or dissolved organic carbon (Hamilton et al. 1984; Beck et al. 2012). Similarly, organic carbon can also have an influence on the concentration and distribution of hydrocarbons. Several studies have reported positive correlation between polycyclic aromatic hydrocarbons (PAHs) and organic carbon in stormwater (Wang et al. 2001; Herngren et al. 2010). Adsorption of PAHs and toxic metals by dissolved organic carbon can make these substances readily bioavailable. Additionally, due to microbial decomposition, PAHs and toxic metals adsorbed to particulate organic carbon can be released back to water in dissolved form, which enhances their bioavailability.

Though high organic carbon concentration is associated to coarse particle size, weak structure of organic matter can eventually result in disintegration to fine particles (Sartor and Boyd 1974). Therefore, frequent street sweeping is necessary to reduce organic carbon load as it can prevent the process of coarse organic matter being grounded to fine particles. Similarly, a significant amount of dissolved organic carbon is also found in urban pollutant build–up. The dissolved organic carbon concentration was found to vary from 4 to 19 mg/kg depending on the land use compared to the coarse organic carbon concentration range of 4 – 24 mg/kg in Gold Coast, Australia (Herngren 2005). Physical treatment cannot be used for the removal dissolved organic carbon. Chemical or biological treatment is needed for the removal of dissolved organic carbon and associated toxic pollutants such as metals and hydrocarbons, which can be eventually released into the water environment due to subsequent decomposition.

2.2.3 NUTRIENTS

Nutrients encourage excessive growth of aquatic plants. The subsequent decomposition of these plants after the death will deplete the dissolved oxygen. (Carpenter et al. 1998). The resulting anaerobic conditions can result in acidic pH, dissolution of toxic substances and bad odour. Nitrogen and phosphorous are some of the most important nutrient pollutants responsible for the deterioration of water quality (Carpenter et al. 1998). The major source of nitrogen and phosphorous is the increased use of fertilisers (Schoonover and Lockaby 2006). Additionally, nutrients in stormwater runoff can originate from detergents and nitrous oxide that is produced by vehicular exhaust and lightening (Hogan and Walbridge 2007). Phosphorous is predominantly bound to particulates due to their reduced solubility, whereas nitrogen is primarily found in dissolved or colloidal forms due to its high solubility (Uusitalo et al. 2000; Vaze and Chiew 2004). Particulate nitrogen and phosphorous are mainly associated with the finer fraction of suspended solids regardless of land use type (Miguntanna et al. 2010). Therefore, the removal of fine particles can minimise the nutrient load transported to the receiving water sources. Miguntanna (2009) reported that the concentration of nitrogen in wash-off is high for low rainfall intensity, while phosphorous concentration is high for high intensity events. For example,

concentration of nitrogen in wash-off collected from Gold Coast, Australia after the first 5 minutes of a simulated rain event was about 16 mg/L for 20mm/hr intensity, while it was about 2 mg/L for 135 mm/hr intensity. In contrast, phosphorous concentration was 4 and 10 mg/L for 20 mm/hr and 135 mm/hr intensities, respectively. In addition, Miguntanna (2009) found that concentrations of nutrients in stormwater was high at the beginning of rainfall and then decrease with time. This suggests that the stormwater treatment aimed at removing nutrients have to target the first flush wash-off.

2.2.4 TOXIC METALS

Metal ions can be divided into heavy and light metals according to their specific weights. Heavy metals are elements that have specific weights higher than 5 g/cm^3, whilst metal ions with specific weights lower than 5 g/cm^3 are classified as light metals (Zenk 1996). Heavy metals can be toxic even at low concentrations and persistent in water (Davis et al. 2001). Additionally, certain light metals such as Al are toxic to plants and humans (White et al. 2012). Road runoff is a major source of these toxic metals in stormwater (Forman and Alexander 1998). The metals are primarily contributed to road runoff from traffic related sources including wear and tear of vehicle parts and additives in fuel and oil (Sansalone et al. 1996). Zn, Pb, Cu, Cd, Cr, Hg and Ni are the commonly found metals in road runoff. Additionally, roof runoff, corrosion of metal structures and some industrial activities can also contribute metals to stormwater runoff under specific circumstances (Davis et al. 2001).

Metals are found in both particulate and dissolved forms. Sartor and Boyd (1974) noted that high percentage of particulate bound metal ions are found attached to fine particulates. Contradictory observations have been reported in the literature regarding the distribution of toxic metals. For example, Bubb and Lester (1994) reported that Cu and Zn are primarily found to be particulate bound in stormwater, whilst Legret (1999) found that they are predominantly in dissolved form. Herngren (2005) reported a that high fraction of toxic metals are bound to fine particulates. These contrary findings can be attributed to the fact that the distribution of metals between dissolved and particulate phases is influenced by factors such as pH, concentration of colloidal particles and the type of ligands present in particles.

Distribution of organic carbon in stormwater can also be a reason for the above differences since Cu and Zn can form strong complexes with organic ligands (Qu and Kelderman 2001). As such, complexation of Cu and Zn with particulate and dissolved organic carbon could be the reason for the former and the latter observations, respectively. This complexity suggests that an in-depth investigation of the metal speciation under various physico-chemical conditions prevailing in the catchment is essential to develop effective stormwater pollution mitigation strategies targeting toxic metals.

Herngren (2005) reported variations in the metal concentrations in stormwater and these were generally below 1 mg/L, and in the order of µg/L (Concentration range for: Zn (3-3600 µg/L); Al (< 5-640 µg/L); Pb (< 1-25 µg/L); Cu (3-390 µg/L); Cd (< 1-288 µg/L); Cr (< 1-18 µg/L)). As toxic metal ions are present at a low concentration in stormwater, these do not degrade in the environment. However, they can bioaccumulate in the tissues of living organisms and create significant health problems in the long-term. The toxic nature of these metal ions inactivates the enzyme systems of aquatic plants, which finally die off due to disturbances to their biochemical processes such as photosynthesis and respiration (Maldonado-Magaña et al. 2011; Rai et al. 1981). Additionally, bioaccumulation of metals in humans and animals can cause health problems ranging from irritation to cancers (Jacobs et al. 1969; Dayan and Paine 2001).

2.2.5 HYDROCARBONS

Hydrocarbons, which are primarily made up of hydrogen and carbon, are contributed to stormwater by sources such as traffic, forest fires and industrial activities (Brown and Peake 2006). A range of hydrocarbon compounds is found in stormwater runoff, among which PAHs are of particular interest since they are mutagenic and carcinogenic even at low concentrations (Beasley and Kneale 2002). Additionally, PAHs with smaller molecular weights are vulnerable to bacterial decomposition. Decomposed PAHs can react with other chemical compounds in water and produce more toxic derivatives (Cerniglia 1992).

Herngren (2005) reported that naphthalene was the most common PAH in residential, industrial and commercial sites at Gold Coast, Australia with concentration varying from: residential (0.8 ± 0.43 mg/L), industrial (1.11 ± 0.81 mg/L) and commercial (2.01 ± 2.21 mg/L). Majority of PAHs are associated with particulates since they have low solubility in water. Therefore, only a small fraction of PAHs is readily bioavailable. However, Smith et al. (2000) noted that high concentrations of PAHs can be present in the dissolved phase because of adsorption by colloidal particles such as dissolved organic carbon. As the majority of PAHs are associated with suspended solids, physical treatment techniques such as settling basins can reduce their concentrations particularly if adsorbed to coarse particles. However, atmospheric fallout contributes a significant amount of PAHs associated with fine particles, which may not settle easily in settling basins (Takada et al. 1991). Herngren (2005) also confirmed that most PAHs were associated with fine particulate size range. This emphasizes the importance of fine particulate removal from urban stormwater.

2.3 TREATMENT OF STORMWATER POLLUTANTS

Currently, in Australia reuse of stormwater harvested from roofs and other urban catchment surfaces is primarily for non-potable applications such as toilet flushing and outdoor use. The Australian government has developed guidelines for this purpose (NWQMS 2009). Since the guidelines are intended for non-potable use, the primary concern is the associated health risks when humans are exposed to pollution when the water is discharged to the environment. Consequently, the guidelines provide a preliminary screening tool to assess whether these risks can be adequately reduced during a specific application of stormwater. Furthermore, in primary treatment, focus is limited to pollutants such as suspended solids, iron, phosphorous, pathogens and carbonates. However, removal of other pollutants such as metals and hydrocarbons is also necessary for potable reuse. Additionally, the maximum threshold values prescribed by these guidelines are higher than those prescribed by the Australian drinking water quality guidelines (NHMRC 2004). For example, the threshold value for iron in the guidelines for the non-potable reuse is 10 mg/L, while it is 0.3 mg/L in the drinking water quality guidelines.

Though the annual volume of stormwater runoff from Australian capital cities is comparable to the annual consumption of potable water in these cities, the utilisation of stormwater for potable purpose has not yet been realised in Australia (Dowsett et al. 1995). The primary reason is the stringent water quality standards compounded by the presence of a range of pollutants in stormwater (Section 2.2). As such, the development of an efficient, economically viable and environmentally benign technology is imperative for potable reuse of urban stormwater. This requires a combination of primary, secondary and tertiary treatment strategies.

The objective of the primary treatment stage is to remove gross pollutants from stormwater runoff in order to avoid blockages in the drainage system. Since targeted pollutants are large in size, physical treatment techniques such as screens, mesh and traps are adequate (Allison 1998). These techniques operate based on the size or weight of the targeted pollutants. For example, certain low-density gross pollutants such as plastics can be removed via a floating trap, whilst a mesh can be used to trap pollutants that are larger than the corresponding mesh size.

Secondary treatment targets mainly the removal of suspended solids using techniques such as wetlands, filters and detention/retention basins. Carleton et al. (2001) analysed the performance of 39 wetlands that were used to treat stormwater runoff. They found that there was significant removal of suspended solids by wetlands compared to other pollutants after a period of detention. However, high stormwater flow through a wetland during an intense storm event can resuspend settled particles, especially fine solids (Birch et al. 2004). Detention basins reduce the stormwater flow velocity and provide time for coarse particulates to settle (Guo 1997). Eventually, the settled pollutants are removed from the basin after water is drained out. On the other hand, during filtration, stormwater flows through the media such as sand, which filter out water, whilst retaining solids. These techniques are sometimes implemented in series to increase the treatment efficiency. Even though a secondary stormwater treatment system may effectively remove coarse particulates, they are not very efficient in removing fine particulates or dissolved solids, especially metals and hydrocarbons (Pontier et al. 2001; Yousef et al. 1990).

Removal of dissolved metals is important in order to use stormwater for potable purposes since they are relatively more hazardous than in particulate form due to their ready bioavailability. Consequently, the treatment of dissolved metals is one of the primary targets in tertiary treatment. As physical techniques are not suitable for this purpose, chemical or a combination of physical and chemical methods such as sorption, precipitation or flocculation are required (Babel and Kurniawan 2003).

2.4 TREATMENT OF DISSOLVED METALS IN STORMWATER

Several techniques such as membrane filtration, chemical precipitation, coagulation-flocculation and sorption have been investigated for the removal of dissolved metal ions in typical industrial wastewater (Kurniawan et al. 2006). However, stormwater differs from industrial wastewater in many ways. Firstly, concentrations of metals in stormwater are commonly several times lower than those of industrial wastewater (Herngren et al. 2005; Reddy and Parupudi 1997). Secondly, the types and concentrations of metals in stormwater even from the same catchment area can vary depending on factors such as rainfall intensity, duration and antecedent dry period (Herngren 2005), whilst, generally, there is no drastic variation in quantity and characteristics in wastewater from a specific industrial process (Kumar et al. 2008). The following discussion critically reviews the applicability of various treatment techniques, which have been investigated for the removal of dissolved metals primarily from industrial wastewater, for application in the removal of toxic metals from stormwater runoff.

2.4.1 METAL IONS IN WATER

A fundamental knowledge of the chemistry of metals in aqueous solution is necessary to better understand the scientific principles involved in toxic metal removal techniques. Water molecules are negatively polarised due to the difference in electronegativity between hydrogen and oxygen atoms as shown in Figure 2.1. Due to the polarity of water molecules, metal cations are attracted to water molecules once dissolved in water. Furthermore, water, especially urban stormwater, consists of

other ions and molecules, which can participate in various competitive interactions between themselves or with water molecules.

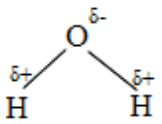

Figure 2.1 Polarised water molecule

The interaction of water molecules with metal cations leads to the formation of inner and outer sphere complexes. Negatively polarised oxygen atoms in water molecules can attract metal cations and form an inner sphere aqua complex as illustrated in Figure 2.2. Six water molecules are often found bound to metals ($[M(H_2O)_6]^{2+}$, where M is a metal cation) (Marcus 1988). The number of water molecules found in the metal complex is determined by various factors including the solution concentration and ionic size (Tunell and Lim 2006).

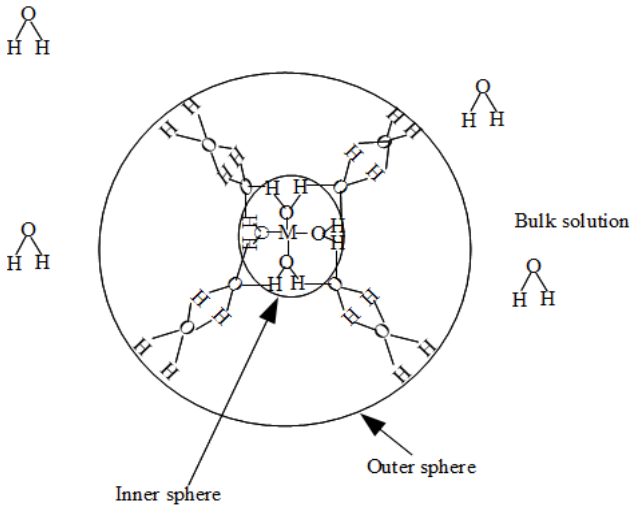

Figure 2.2 Inner sphere and outer sphere aqua metal complex; M is a metal ion

However, depending on the chemical composition of the solution, one or more of these water molecules may be replaced by thermodynamically preferred alternative anions such as chloride (Cl^-) and iodide (I^-) or more complex ligands such as dicarboxylic acids. This can change the chemical structure of the complex, for example to $[M\ (H_2O)_5Cl]^{1+}$from $[M(H_2O)_6]^{2+}$. Whilst anions such as Cl^- and I^- can bind directly to the metal in proportion to their respective charges, more complex

molecules such as dicarboxylic acids have several potential binding sites in one molecule and form rings around the metal ion as illustrated in Figure 2.3. This process is called 'chelation' (Norkus et al. 2003). The capacity for such interaction with metal ions is influenced by factors such as the properties of metal ions, pH and the chemical composition of solution (Ahmadi et al. 2009).

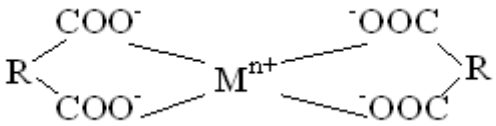

Figure 2.3 Dicarboxylic-metal ion chelate; R can be a hydrocarbon chain

A metal cation can be present in different ionic forms depending on solution pH (Bradl 2004). For example, chromium cation (Cr^{3+}) changes from predominantly free Cr^{3+} ion at pH 1 to $[CrOH]^{2+}$, $[Cr(OH)_2]^{+}$ and $[Cr(OH)3]^{0}$ as pH increases and reaches anionic $[Cr(OH)]^{4-}$ at pH 11. Similarly, lead cation (Pb^{2+}) changes to anionic $[Pb(OH)_3]^{-}$ at pH 11. Change in the chemical form of metal cations will have a significant influence on their interaction with other molecules and binding sites. Consequently, the speciation of metals will exert considerable influence on the treatment techniques, especially in chemical treatment techniques. Therefore, metal speciation in typical stormwater conditions must be investigated for the development of an effective chemical treatment technique. Additionally, the water molecules in the inner sphere complex develop hydrogen bonds with water molecules in bulk solution. This leads to the formation of the outer sphere complex as illustrated in Figure 2.2 (Martell and Hancock 1996).

2.4.2 MEMBRANE FILTRATION

Membrane filtration is a molecular sieving technique, in which particles that are smaller than the membrane pore size pass through, whilst larger particles are retained. Pressure is applied across the membrane to enhance the diffusion of water. Ultrafiltration (UF), nanofiltration (NF) and reverse osmosis (RO) are some of the membrane filtration techniques that have been investigated for the removal of dissolved metals (Chaabane et al. 2006; Ferella et al. 2007; Mohsen-Nia et al. 2007).

The pore size of the membranes used in UF is typically in the range of 50 - 200 A^0, which is larger than the hydrated ionic size of common metals (Table 2.1) (Vigneswaran et al. 2005). Thus, it is highly possible for dissolved metal ions to escape through the membrane without being trapped. Hence, UF membranes are generally modified in order to increase their removal efficiencies, for example, chitosan enhanced UF membrane (Juang and Shiau 2000). Chitosan is a linear polysaccharide that contains amino acid functional groups, which can form strong chelation with metal ions. Hence, the presence of chitosan enhances the metal removal efficiency of a UF membrane. Another example of modified UF technique is the addition of anionic surfactants to water. Anionic surfactants attract metal cations and assemble them into thermodynamically stable aggregates called micelles (Yurlova et al. 2002). A UF membrane can trap the micelles and the metal ions attached to them, as micelles are generally larger than the membrane pore size.

Table 2.1 Hydrated ionic diameter of common metal ions (Nightingale 1959)

Metal	Hydrated ionic diameter / A^0
Pb^{2+}	8.02
Cd^{2+}	8.52
Cu^{2+}	8.38
Cr^{3+}	9.22
Ni^{2+}	8.08
Zn^{2+}	8.60

NF membranes have pore sizes smaller than UF membranes. The smallest membrane pore size used in NF is approximately 10 A^0 (Yang et al. 2001). Additionally, NF membranes have an anionic surface charge in their structure, which can also attract metal cations to their surface. Hence, NF is more efficient in removing dissolved solids than UF. However, NF membrane pore size is still larger than hydrated ionic diameters of metal cations (Table 2.1). Hence, the membranes can still allow metal ions to pass through. Therefore, similar to UF, various surface modifications have been proposed to NF. Bougen et al. (2001) investigated the removal of Cu, Zn and Cd using NF modified with ethylenediamine (EDA) or pyrophosphate (PP) groups.

EDA is known to have strong affinity to form chelation with Cu, while PP can form weak complexation with Cu and Zn. Interestingly, the removal of Cu and Zn was about 50% regardless of the modification, while Cu removal increased to 80% from 50% for EDA modified NF. This indicates that specific modifications to a NF membrane are necessary for the removal of each metal ion, which will incur additional cost. Similar to UF modification, Muthukrishnan and Guha (2006) achieved 97 to 99.5% removal of Cr by adding a surfactant to the solution. However, the introduction of new chemical agents such as surfactants may result in human health impacts.

The maximum pore size of RO membranes is typically 1 A^0 (Bohdziewicz et al. 1999). Since the pore size is smaller than hydrated metal ionic size (Table 2.1), RO is the most efficient membrane filtration technique for the removal of dissolved metal ions. Additionally, it does not require any membrane modification. Liu et al. (2008) compared the efficiency of both NF and RO for the removal of metals in water. Greater than 95% removal was achieved using RO compared to 79% by NF. However, RO requires high pressure to facilitate the diffusion of water due to their very small pore size. Therefore, it may not be always economically feasible for the removal of metals due to the high energy needed to provide the necessary pressure for the diffusion of water across the RO membrane.

In summary, the efficiency of membrane filtration technique primarily depends on the pore size of the membrane. A higher efficiency can be achieved with smaller membrane pore size. However, small pore size will result in restricted diffusion of feed. Hence, high pressure is required to improve diffusion through the membrane. This will increase the operational cost due to the consumption of energy. Furthermore, a relatively clean feed that is free from any suspended particles is required to avoid membrane blockage. Even small oxidised compounds such as chloride oxides can block the small pores of RO membranes and cause membrane fouling (Matin et al. 2011; Potts et al. 1981). Hence, membranes have to be replaced frequently to achieve good performance, which will incur additional cost.

The application of membrane filtration for the treatment of dissolved metal ions in stormwater is not feasible due to a number of reasons. Firstly, stormwater consists of fine suspended solids and various organic and inorganic compounds, where complete removal using conventional secondary treatment techniques is generally difficult. Therefore, the membrane pores can be easily blocked. Secondly, treatment of relatively large volumes of stormwater within a short time span may be required to meet the high demand for potable water. Hence, stormwater may have to be pumped at high pressure to speed up the diffusion through membranes. This may require structurally strong membranes and high pressure, which will increase the capital and operational costs, respectively. Therefore, the use of membrane filtration for the removal of dissolved metal ions in urban stormwater may not be economically feasible even though good removal performance can be expected.

2.4.3 CHEMICAL PRECIPITATION

Chemical precipitation is a common technique used for the removal of dissolved metal ions from polluted water. Dissolved metal ions are precipitated as shown below, as their hydroxides, carbonates or sulphides with the adjustment of pH above the threshold value of precipitation and the addition of chemical reagents such as lime and iron sulphides (Fu and Wang 2011; Dean 1972):

$$M^{n+}_{(aq)} + n\ OH^{-}_{(aq)} \longleftrightarrow M(OH)_{n(s)}$$

$$2\ M^{n+}_{(aq)} + n\ S^{2-}_{(aq)} \longleftrightarrow M_2S_{n(s)}$$

$$2\ M^{n+}_{(aq)} + n\ CO_3^{2-}{}_{(aq)} \longleftrightarrow M_2(CO_3)_{n(s)}$$

The threshold pH of a certain ion can be theoretically calculated using the following equation:

$$\text{Threshold pH} = \frac{(\log_{10} K_{sp} - \log_{10}[M^{n+}] + 14n)}{n} \qquad (2.1)$$

where K_{sp} is the solubility constant and $[M^{n+}]$ is the concentration of metal ion 'M^{n+}'. Each metal ion has different threshold pH values depending on its solubility constant and concentration. According to equation (2.1), metal ions that have high solubility constants precipitate at relatively high pH.

Hydroxide precipitation using inexpensive lime is widely used compared to carbonate and sulphide precipitation (Lewis 2010). Heavy metal hydroxides generally have high K_{sp} values. Hence, pH of the solution has to be adjusted to the extreme basic region to ensure the precipitation of all heavy metals (Fu and Wang 2011). Though high pH does not cause any health risks, it can alter the taste of water (NHMRC 2004). Hence, further treatment is required to reduce the alkalinity of the treated water to the level prescribed by water quality guidelines (NHMRC 2004). However, sulphide and carbonate precipitation techniques can avoid this additional treatment step since K_{sp} values for heavy metal sulphides and carbonates are lower than that of heavy metal hydroxides (Fu and Wang 2011). Thus, the threshold pH for heavy metals is generally low, which ensures the precipitation of heavy metals even at neutral pH conditions. Charerntanyarak et al. (1999) found that utilising both hydroxide and sulphide precipitation in combination enhances the removal of heavy metals. Similarly, Feng et al. (2000) found that complete removal of heavy metals could be achieved using combined sulphide and hydroxide precipitation.

Patterson et al. (1977) investigated carbonate precipitation of Zn, Ni, Cd and Pb in detail and compared its efficiency with hydroxide precipitation. According to the results of their study, for Ni and Zn, carbonate precipitation technique did not have any additional advantages in terms of removal efficiency or sludge settling. However, Pb and Cd carbonate precipitates were found to have better sludge settleability than their hydroxide. However, there are significant disadvantages in using sulphide and carbonate precipitation techniques. Sulphide precipitation can produce toxic hydrogen sulphide gas (H_2S). On the other hand, carbonate precipitation process can produce carbon dioxide (CO_2), which is a greenhouse gas contributing to global warming (Crear 2001). Additionally, metal carbonates and sulphides tend to be colloidal precipitates, which can have settling problems (Sukola

et al. 2005). Therefore, sulphide and carbonate precipitation techniques have limitations in the application to stormwater treatment.

The main drawback of precipitation is the production of chemical sludge, which requires additional treatment and specialised handling. Furthermore, precipitation is generally a relatively slow process and not efficient in the low concentration range (Bose et al. 2002). In stormwater, toxic metals are found in low concentrations. Additionally, large amounts of chemicals are generally required to achieve complete removal of toxic metals (Jüttner et al. 2000). In the context of treating large volumes of stormwater for potable purposes, chemical precipitation is not economically feasible. Additionally, further treatment of any remaining chemical reagents in treated stormwater may be required.

Electrochemical precipitation is a modification of conventional chemical precipitation. Instead of chemical reagents, a voltage is applied across the metal solution, whilst pH is adjusted above the threshold pH (Kongsricharoern and Polprasert 1995). Though precipitation of metals is enhanced and accelerated by electrochemical precipitation, this technique is expensive and not economically viable to treat large volumes of water (Kurniawan et al. 2006).

2.4.4 COAGULATION-FLOCCULATION

Coagulation and flocculation occur in successive steps. During the coagulation step, a coagulant such as aluminium sulphate, ferrous sulphate or ferric chloride is added in order to form microflocs of colloids by neutralising the charges that keep the particulates apart. Following the coagulation step, flocculation occurs, in which the particle size of microflocs is increased using flocculants such as polyferric sulphate and polyacrylamide and removed via filtration or gravity settling (Semerjian and Ayoub 2003).

In general, coagulation-flocculation technique is used for the treatment of metals that are bound to particulates and is considered inefficient in the removal of metals

complexed with water or other small ligands such as Cl^- (Chang and Wang 2007). Hence, additional treatment steps are required for the complete removal of dissolved metal ions. In contrast, the potential of coagulation-flocculation technique for almost complete removal of dissolved Cu was reported by Li et al. (2003). They used sodium diethyldithiocarbamate as the coagulant agent and maintained a sodium diethyldithiocarbamate to Cu molar ratio of 0.8 to 1.2 to achieve complete removal.

Several novel coagulants have been developed for the removal of metals by grafting various ligands to existing coagulants. For example, Chaudhari and Tare (1999) investigated water-soluble starch xanthate for the removal of mercury (Hg), Cu, Cd and Ni. Starch xanthate was produced by incorporating a ligand called xanthate, which has a strong affinity for heavy metals, into starch. Notably, the removal of Cd and Ni was relatively ineffective compared to Hg and Cu. The ineffectiveness was attributed to the formation of colloidal cadmium-xanthate and nickel-xanthate complexes, which are difficult to remove from water. Formation of such colloids can be a potential problem in using the coagulation-flocculation technique in the removal of metal ions since it will result in relatively longer settling time. In such cases, the addition of further nucleating sites is required to increase the settling rate. It is worthy of note that the coagulation process is more efficient if the water is turbid, since the turbidity can provide more nucleating sites to form larger flocs (Gregor et al. 1997). Hence, the turbidity of stormwater can be used positively for this process.

Aluminium based coagulants are the most common coagulants used in water treatment. However, aluminium is considered toxic (White et al. 2012). Hence, the use of aluminium salts is not desired in the treatment of stormwater, especially for potable use. Another option is ferric-based coagulants, which are relatively safer than aluminium salts. However, it should be noted that high concentration of iron in water results in colour and taste issues, which could make the water unpalatable (NHMRC 2004). Hence, a clear understanding of the optimum dose of ferric salts required is essential to achieve an adequate level of metal removal without increasing the concentration of iron in water beyond the prescribed level for drinking water.

Large amounts of chemical coagulants may be required for the treatment of large volumes of stormwater. These chemical agents are often expensive and could increase the cost of treatment (Ayoub et al. 2001). As such, the use of stormwater for potable purposes can become economically unfeasible. Consequently, research studies have focused on the use of low cost and non-toxic natural coagulants based on vegetable and mineral products (Ndabigengesere et al. 1985). However, the coagulation-flocculation technique produces chemical sludge, for which additional treatment is required prior to disposal (Selcuk 2005). This will incur additional operational costs and has environmental consequences, which can make the technique unviable.

In recent years, electrocoagulation has gained considerable attention due to its efficiency (Biswas and Lazarescu 1991). In electrocoagulation, coagulants are produced by dissolving metal anodes instead of adding chemical coagulants. For example, an aluminium anode is used to produce aluminium coagulant. Thus, secondary pollution caused by the addition of chemical coagulants can be avoided in electrocoagulation. The cathode will release hydrogen gas, which carries the coagulated particles to the water surface and keeps them afloat (Chen 2004). Adhoum et al. (2004) investigated the removal of Cu, Zn and Cr from electroplating wastewater and reported that the removal of metals occurred at a rapid rate. The concentrations of investigated metals were reduced below the legal limits within 20 minutes. Furthermore, electrocoagulation can minimise the amount of chemical sludge, thereby reducing the additional treatment cost (Cenkin and Belevtsev 1985). However, the drinking water quality level for toxic metals is more stringent than for industrial wastewater quality limits. Hence, the mere reduction below the legal limits prescribed for industrial wastewater is not satisfactory. In the context of stormwater, electrochemical techniques may not be economically feasible since these are generally energy intensive.

2.4.5 SORPTION

Sorption is a general term used to encompass any physical or chemical process that retains the ‘sorbates’ on the surface of a ‘sorbent’ (Del Campillo et al. 1999). A sorbent is a material that has the required properties for retaining compounds or ions

or substances, which are collectively called sorbates. Various materials ranging from agricultural wastes (Ajmal et al. 1998; Garg et al. 2008) to commercial sorbents (Genç-Fuhrman et al. 2007; Minceva et al. 2008) have been investigated for the removal of metals from water.

The main advantages of the sorption technique include its effectiveness over a wide range of metal concentrations and simplicity of application (Minceva et al. 2008). For example, Conrad and Bruun Hansen (2007) investigated the sorption of Zn and Pb in low concentration solution (in the order of μg/L) and reported more than 90% removal for both metals. Similarly, peat exhibited more than 90% efficiency in removing Ni, Cu, Cd and Zn that were present at high concentrations (in the order of mg/L) (Gosset et al. 1986). However, capital and regeneration cost can limit the use of some sorbents for stormwater treatment, where large quantities of sorbent are required to treat large volumes of stormwater (Kesraoui-Ouki et al. 1994). For example, use of activated carbon is not economically viable for the treatment of metals in stormwater due to its high capital and regeneration cost (Minceva et al. 2008). However, many low cost natural sorbents such as zeolite, clay and biomass can be used for the sorption of metals (Bailey et al. 1999; Kurniawan et al. 2006). Hence, cost is an important criterion in selecting sorbents for the removal of metal ions from water.

Several reviews published on the use of low cost sorbents for the removal of metal ions in water highlight the significant potential that low cost sorbent materials have in water treatment (Bailey et al. 1999; Babel and Kurniawan 2003; Dabrowski et al. 2004; Kurniawan et al. 2006; Demirbas 2008; Wan Ngah and Hanafiah 2008; Gupta et al. 2009; Wang and Chen 2009). The disposal of sorbents after treatment is of concern as the sorbents will contain metal ions in high concentration. Some studies have noted that successful regeneration is possible, during which the sorbed metal ions are released back to a chemical reagent such as ammonium acetate (Baran et al. 2007; Yu et al. 2001). The quantity of chemical reagent required for this process is significantly low. Consequently, the metal ions can be recovered from the chemical reagent that contains the concentrated metals using chemical precipitation, if the

metal ions are economically valuable or otherwise the solution can be safely disposed.

However, the major drawback in the sorption technique is the preferential removal of certain metal ions over the others, which results in poor removal of less preferred metal ions. For example, Holan and Volesky (1995) reported that fungal biomass showed high affinity to sorb Pb over Cd and Ni. This resulted in moderate sorption of Cd and poor sorption of Ni since most active sites were occupied by Pb. Wang and Chen (2009) produced the following affinity series for metal sorption by biosorbents based on a number of research studies: Cd > Co > Cr > Fe (Iron) > Ni > Pb > Hg > Zn. This highlights that sorption of Cd is most preferred by biosorbents, whilst poor removal of Hg and Zn can be expected. Stormwater is a multi component system consisting of various pollutants including diverse species of metal ions. As such, the preferential sorption of sorbents can result in inadequate removal of certain metal ions. Consequently, the treated water will require additional treatment for the removal of these metal ions, which will incur additional cost.

Though sorption is an economically viable and environmentally benign technique compared to other techniques, preferential sorption needs to be rectified in order for use in the removal of metal ions in stormwater. Hence, fundamental knowledge of sorption science is essential for enhancing the affinity for the sorption of dissolved metal ions in a multi metal system such as stormwater.

2.5 CONCLUSIONS

The pollutants generated by anthropogenic activities in urban areas are transported by the stormwater runoff to receiving water bodies, consequently deteriorating the quality and degrading the ecosystem health. The primary stormwater pollutants are suspended solids, organic carbon, hydrocarbons, toxic metals and nutrients, among which metals and some hydrocarbons can result in adverse impacts even at low concentrations. Dissolved forms of metals and hydrocarbons are more hazardous than their particulate form due to their ready bioavailability to organisms.

On the other hand, water scarcity is a major problem facing many urban areas. Using stormwater as an alternative potable water source is a logical solution as it is available in large volumes, accessible in most parts of the world and can reduce the deterioration of the quality of natural water sources. However, treatment of stormwater to the level prescribed by drinking water guidelines is necessary for potable reuse and there are primary, secondary and tertiary strategies available for this purpose. Large particles and coarse solids in stormwater can be effectively treated by primary and secondary techniques, respectively.

However, these techniques are not efficient for the removal of dissolved pollutants such as dissolved metals, for which chemical techniques or physico-chemical techniques are necessary. Various removal techniques such as membrane filtration, precipitation and coagulation and flocculation have been investigated for the treatment of dissolved toxic metals. The use of membrane filtration technique is not economically viable and operationally complex for efficient treatment of metal ions in stormwater due to the need for high pressure and clean feed, respectively. On the other hand, the need for further treatment and specialised handling for the disposal of large quantities of chemical sludge are the primary drawbacks in using chemical precipitation or coagulation-flocculation techniques for the removal of dissolved metals in stormwater.

In contrast, use of low cost sorbents is an economically viable and environmentally benign technique in comparison to membrane filtration, chemical precipitation and coagulation-flocculation techniques. However, the preferential sorption of certain metal ions over the others by the sorbents is the main disadvantage of the sorption technique since it can result in inadequate removal of certain metals. Therefore, it is necessary to have an in-depth understanding of the sorption processes to modify the affinity of the sorbent materials to achieve the desired removal of metal ions.

Chapter 3: Review of sorption science and modelling

3.1 BACKGROUND

In Chapter 2, it was concluded that sorption is a preferred technique for the removal of dissolved metal ions from stormwater compared to other commonly available techniques such as chemical precipitation and membrane filtration due to better economic and environmental benefits. However, the preference of sorbent materials for the sorption of selected metal ions was identified as the key issue to be addressed to utilise the sorption technique for the treatment of metals in stormwater since preferential sorption could result in inadequate removal of other metal ions. Therefore, fundamental knowledge regarding the different sorption processes is essential to develop approaches to enhance the affinity of sorbents for the sorption of dissolved metal ions. As defined in Section 2.4.5, sorption is a common term to denote various mechanisms. The mechanisms employed by sorbent materials are complex and are often found operating in combination in the removal of metals in water (Panayotova 2001; Erdem et al. 2004). There are different types of surface retention mechanisms reported in the literature and the most common processes are ion exchange and adsorption.

3.2 ION EXCHANGE

Ion exchange is not a strict chemical reaction, but rather it is a redistribution of ions between solid and liquid phases (Inglezakis and Poulopoulos 2006). Several synthetic commercial cation exchange resins such as amberlite, dewex, ambersep and amberjet have been investigated for their efficiencies in removing dissolved metal cations (Sapari et al. 1996; Rengaraj et al. 2003). The resins contain H^+ ions that can be exchanged for metal cations in the solution as follows:

$$R^-H^+ + M^+ \longleftrightarrow R^-M^+ + H^+$$

where R^--H^+ is an ion exchange resin and M^+ is a metal ion.

The main advantages of these resins are high removal efficiencies and rapid removal rates (Kang et al. 2004). Therefore, they are ideal for the treatment of relatively large volumes of stormwater for potable use in shortest possible time. Amberlite, amberjet, dewex and ambersep have exhibited complete removal of Zn, Cr and Ni from initial metal concentrations ranging from 2-750 mg/L (Rengaraj et al. 2003; Sapari et al. 1996). However, commercial products are generally expensive, especially for use in the treatment of large volumes of stormwater.

Consequently, attention has been focused on the use of relatively inexpensive natural sorbent materials such as clay, zeolite and peat moss that have shown ion exchange properties due to the presence of exchangeable cations in their structure. For example, zeolite and clay have negative charges in their framework, which are generally balanced by exchangeable extra framework cations such as hydronium (H_3O^+), sodium (Na^+), calcium (Ca^{2+}) and potassium (K^+) (Bailey et al. 1999). Various research studies have noted a decrease in pH of solution due to the release of H_3O^+ during ion exchange. Bunzl et al. (1976) noted that two H^+ ions are released during the uptake of divalent metal cations by peat suggesting the existence of ion exchange process during sorption. Similarly, Pitcher et al. (2004) reported that Na^+ ions are released during the sorption of Pb, Cu, Zn and Cd by zeolite indicating the occurrence of the ion exchange process. However, most commonly, the amount of exchangeable cations released to the solution does not reflect the stoichiometric relationship of the ion exchange process between metal cations in solution and the exchangeable cations in sorbents (Angove et al. 1997). This suggests that other mechanisms such as adsorption often operate in combination with ion exchange during sorption.

The ion exchange process is driven by the Le Chatelier's principle and depends on the physical and chemical conditions prevailing in the system. Le Chatelier's principle states that if an equilibrium system is disturbed by a change in conditions such as concentration, the equilibrium will shift to counteract the effect of such

disturbance (Le Chatelier 1884). Introduction of a sorbent in metal solution divides the system into solids and liquid phases. Solid phase contains exchangeable cations such as H_3O^+, Na^+, Ca^{2+} and K^+ at higher concentration, whilst metal ions are found in higher concentration in the liquid phase. This uneven distribution of ions between solid and liquid phases disturbs the equilibrium of the system (De Villiers et al. 1997). Therefore, according to Le Chatelier's principle, some exchangeable cations will move into solution, whilst some metal ions will be transferred to the sorbent to restore the system back to equilibrium. The amount of exchangeable cations and metal ions, which engage in the exchange process, is influenced by a temperature dependent equilibrium constant. Furthermore, metals subject to ion exchange can be desorbed back to the bulk solution depending on the physical and chemical conditions of the system such as pH and temperature (Murzin and Salmi 2005). Consequently, sorbents can be regenerated in a controlled environment by providing favourable physico-chemical conditions for the desorption of metals, which can be eventually safely disposed.

A multi element system such as stormwater consists of various metal ions. The tendency of a metal ion for participating in the exchange depends on the strength of interaction between the specific metal ion and water molecules (Colella 1996). The strength of interaction is dependent on the hydration energy, which is defined as the energy released when one mole of a substance is dissolved into solution (Dimitriu et al. 2007). In other words, it is the energy released due to the formation of aqua metal complexes during the dissolution of a metal ion in water. Some metals release more energy during the formation of aqua complex. Hence, they have high hydration energy. As a result, more energy is required to detach water molecules from the metal cations in order to facilitate bonding with the active sites in the sorbents. As such, metals with high hydration energy will stay in solution instead of detaching the water molecules and being exchanged for cations in the sorbents (Eisenman 1962). Consequently, metals with low hydration energy are preferred for participation in the ion exchange process. Hydration energy of selected metal ions is given in Table 3.1.

Table 3.1 Hydration energies of common metal ions (Marcus 1991)

Metal ion	Hydration energy/ (kJ/mol)
Pb	-1425
Cd	-1755
Zn	-1955
Ni	-1980
Cu	-2010
Cr	-4010

Based on the hydration energy, it can be concluded that the affinity of metals for ion exchange must ideally follow Pb > Cd > Zn > Ni > Cu > Cr. Hence, poor preference of sorbents in relation to some metals such as Cu and Cr is a major drawback in using the ion exchange mechanism for the removal of metals from a multi metal system such as stormwater.

3.3 ADSORPTION

Adsorption or surface adsorption is a result of the attraction between negative and positive charges in the sorbent system. For example, metal cations in solution are attracted by a sorbent because of the negative charges present in its framework structure. The primary difference between ion exchange and adsorption mechanisms is that there is no exchange of ions involved in the adsorption mechanism. Adsorption can be broadly classified into physisorption and chemisorption depending on the characteristics of the bonding between metal cations and the sorbent active sites. During physisorption, dipole interaction is developed when metal cations approach the negative sites of sorbents. Due to this, a relatively weak van der Waals attractive force is developed between outer sphere of metal cations and sorbent framework (Inglezakis and Poulopoulos 2006). Therefore, physisorption is an outer sphere complexation process and strong chemical bonds are not formed since electron transfer does not occur between molecules. As such, physisorption causes only a very small change in enthalpy during the sorption of metals (Inglezakis and Poulopoulos 2006). Hence, heat of sorption for the physisorption mechanism is typically 20 - 40 kJ/mol (Inglezakis and Poulopoulos 2006). The sorption activation

energy (E) for the physisorption mechanism is typically less than 8 kJ/mol (Uluozlu et al. 2008).

The strength of physisorption largely depends on the strength of dipole interaction. Though dipole interaction is stable at low temperatures, increase in the temperature weakens the interaction, which causes desorption of metal ions (Murzin and Salmi 2005). The interaction is stronger when the molecules are closer to each other. Physisorption of metal ions by sorbent materials depends on the charge densities of the metal ions (Erdem et al. 2004). Charge density of an ion is given by the following equation:

$$\text{Charge density} = \frac{Q}{r^3} \tag{3.1}$$

where Q is the amount of electric charge of the cation and r is the ionic radius (Bosso and Enzweiler 2002). Charge densities of selected metal ions are given in Table 3.2 (determined based on the ionic radius extracted from Pfleger and wolf 1975).

Table 3.2 Charge densities of common metal ions

Metal ion	Charge density / (10^{-19}C/m)
Pb	8.6
Cd	9.8
Zn	3.4
Ni	2.2
Cu	10.1
Cr	14.8

Cations with high charge densities have a strong cationic field. Therefore, their interaction with an anionic field of sorbents is stronger than with the cations with low charge densities (Eisenman 1962). Consequently, the physisorption force is stronger for cations with high charge densities. Multilayer formation (Figure 3.1) is possible

during physisorption since physisorbed cations can form hydrogen bonding with water molecules in bulk solution (Nagao 1971).

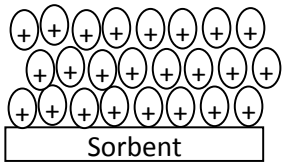

Figure 3.1 Schematic diagram of a multilayer formation in the external surface of a sorbent (+ denotes metal cation)

Many studies have reported the existence of the physisorption mechanism in the sorption of metals by various sorbents. Apiratikul and Pavasant (2008) found that the mean sorption activation energies for the sorption of Pb, Cu and Cd by coal fly ash were 2.55, 1.57 and 2.05 kJ/mol, respectively. This is within the range for physisorption mechanism. Horsfall Jnr and Spiff (2005) found that the sorption activation energies for Pb and Cd by wild cocoyam were negative indicating the sorption process is of a physical nature. Furthermore, based on the heat of sorption, Dorota (2011) concluded that the primary mechanism employed by the investigated commercial sorbents for the sorption of Cu was physisorption.

On the other hand, several studies have noted that the chemisorption mechanism plays a role during the sorption of metal ions. For example, Arámbula-Villazana et al. (2006) found that the activation energy for the sorption of Cd by Mexican zeolite was in the range for chemisorption. Ho et al. (2001) concluded that sorption of Pb on peat followed the chemisorption mechanism. The chemisorption mechanism was responsible in the sorption of Cd by akaganéite type crystals (Deliyanni and Matis 2005) and in the sorption of Pb, Cr, Cd and Ni by clinoptilolite (Mozgawa and Bajda 2005).

Chemisorption is an inner sphere complexation phenomenon, in which metal ions participate in the exchange of electrons with the active sites that are present on the external surface or inside the pores of the sorbent. This results in the formation of a

strong metal-ligand complex. For example, the metal-hydroxide complexation is illustrated in Figure 3.2.

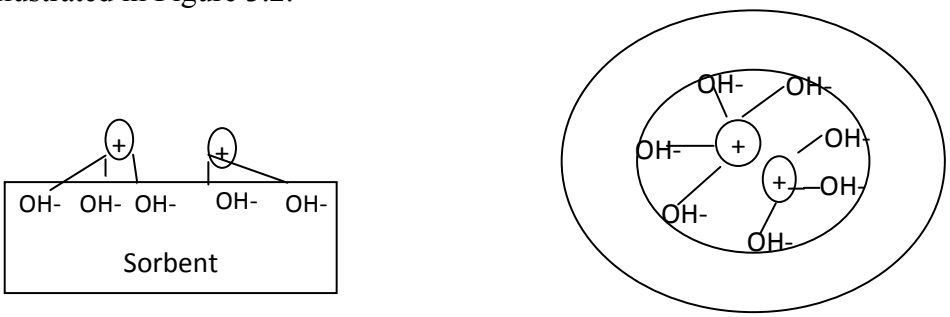

(a) (b)

Figure 3.2 Chemisorption of metal ions with hydroxyl functional groups: (a) on the external surface; (b) inside a pore explained using two dimensional schematic diagram (+ denotes metal cation)

Unlike physisorption, the chemisorption mechanism has to overcome an activation energy barrier. Therefore, significant enthalpy change is observed during the chemisorption process. Heat of sorption in the case of chemisorption is high, typically in the range of 40-800 kJ/mol (Haque et al. 1968; Inglezakis and Poulopoulos 2006).

In the case of physisorption, the distance between metal cations and the surface of sorbents is longer. In contrast, chemisorption bonds are formed close to the surface of the sorbents (Murzin and Salmi 2005). Metal ions strongly interact with the surface of sorbent, which prevents hydrogen bond formation with other molecules in the bulk solution. Therefore, a monolayer can be formed during chemisorption as illustrated in Figure 3.3.

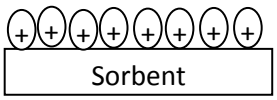

Figure 3.3 Schematic diagram of a monolayer formation on the external surface of sorbent (+ denotes metal cation)

Desorption of chemisorbed metal ions from the sorbent framework is difficult due to the strong bond that is formed. In contrast, metal cations sorbed via physisorption can be easily desorbed by means of chemical agents such as ammonium acetate.

Therefore, desorption studies with ammonium acetate have been used effectively to distinguish the contribution of chemisorption to the overall removal of metals (Mozgawa and Bajda 2005).

The chemisorption process can be explained by Lewis Hard Soft Acid Base (HSAB) theory, which is widely used to understand the chemical reaction between cations and anions in a qualitative context (Pearson 1963). Lewis acid is defined as any molecule that has the ability to accept electrons, while the molecule that donates the electrons is called Lewis base. Accordingly, metal cations act as Lewis acids, whereas ligands are Lewis bases. HSAB theory classifies metal ions and ligands into hard, intermediate and soft categories as listed in Table 3.3. 'Hard' and 'soft' are relative terms and the corresponding acids or bases are distinguished based on their properties including electronegativity, polarizability and ionic size (Pearson 1963). For example, a base with low electronegativity is regarded as a 'soft' species, which prefers to bond with a soft cation. Thus, according to HSAB theory, hard acids generally prefer to bind to hard bases, and soft acids prefer to bind to soft bases.

Table 3.3 Classification of acids and bases into hard, intermediate and soft categories (Pearson 1968)

	Hard	Intermediate	Soft
Acid	Na^+, K^+, Ca^{2+}, Mg^{2+}, Al^{3+}, Cr^{3+}	Ni^{2+}, Cu^{2+}, Zn^{2+}, Pb^{2+}, Fe^{2+}	Cd^{2+}, Ag^+, Hg^{2+}
Base	H_2O, NO_3^-, OH^-, CH^3COO^-, CO_3^{2-}, [1]RO^-, ROH	Br-, SO_3^{2-}, N_2, N_3^-	H^-, I^-, $S_2O_3^{2-}$, R_2S, RS^-

Note:

[1]R stands for an alkyl or aryl group

However, the main limitation of HSAB theory is that it is qualitative and the comparison of the 'hardness' or 'softness' of two acids or bases is not possible. For example, though Na^+ and K^+ are hard acids, the relative hardness of one over the other is not readily known. For this purpose, Parr and Pearson (1983) proposed a

property called 'absolute hardness (η)' based on the ionisation potential (I) and electron affinity (A) of a species 's' as shown in equation (3.2).

$$\eta_s = \frac{1}{2}(I_s - A_s) \tag{3.2}$$

The absolute hardness can be used to compare the hardness of two metals such that the metal ion with a high value is relatively harder. Klopman (1968) observed that 'softness' is correlated to the tendency of an acid or base to form covalent bonding, while 'hardness' is associated with the tendency of an acid or base to participate in ionic bonding. Based on this concept, Hancock and Marsicano (1978) proposed equation (3.3) for predicting the chemical hardness of acids and bases (H) based on the tendency of a metal ion or ligand to form ionic (E) or covalent bonds (C).

$$H = \frac{E}{C} \tag{3.3}$$

The above parameter (H) provides a reasonable estimation of hardness of metal acids (Hancock and Marsicano 1978). Thus, the parameter 'H' can be used for comparing the relative hardness or softness of different metal ions. The H values for some common metal ions found in stormwater are tabulated in Table 3.4.

Table 3.4 H values of metal ions (Hancock and Martell 1989)

Metal ion	H
Cu^{2+}	2.68
Cd^{2+}	3.31
Ni^{2+}	3.37
Zn^{2+}	4.26
Pb^{2+}	6.69
Cr^{3+}	7.14
Al^{3+}	10.50

Similar to ion exchange, the adsorption mechanism is also selective in the sorption of metals in water. The affinity for metal ions when the physisorption mechanism is in operation is primarily influenced by the charge densities, whilst chemical hardness of metals governs the affinity for the chemisorption mechanism. Therefore, it is essential to investigate potential methods for modifying the affinity of the adsorption mechanism.

The removal of metals using sorbents is a complex chemical process involving several sorption mechanisms such as physisorption, chemisorption and ion exchange operating simultaneously. The knowledge in relation to the isotherm, kinetics and thermodynamics of the mechanisms employed by sorbents for the removal of metal ions is useful in understanding the sorption system and in controlling the sorption process. Consequently, it is essential to model the isotherm, kinetics and thermodynamics of the sorption processes and, for this purpose, fundamental knowledge on various modelling approaches available is imperative.

3.4 SORPTION MODELLING

Two approaches are generally used for modelling a sorption system (Pagnanelli et al. 2002):

1. Mechanistic approach;
2. Empirical approach.

In the mechanistic approach, models are derived to represent the behaviour of a system based purely on fundamental scientific theories. In contrast, in the empirical approach, models are derived for a system based on experimental data (Volesky 2003). However, real world systems are generally too complex to be represented by theoretical models alone. On the other hand, though empirical models can provide real time information about a system, these details hardly have any physical meaning unless interpreted using established theories (Wang and Chen 2009). Therefore, modelling a system requires a combination of both approaches, where they can complement each other (Nestorov et al. 1999).

In modelling the behaviour of an unknown sorption system, experimental studies are conducted under well-defined conditions. The data obtained from the experiments are compared against the standard theoretical models that are developed by assuming well-defined sorption scenarios. Then, the sorption system under investigation is described based on how well the experimental data fit the standard models (Altin et al. 1998; Allen et al. 2004; Foo and Hameed 2010). For example, if a system fits a standard model, then it is concluded that the system closely resembles the sorption scenario, for which the model was developed.

3.4.1 ISOTHERM MODELLING

Isotherm models are used to describe the equilibrium of ions between solid and solution phases. Sorption isotherm models can also be used to calculate the maximum sorption capacity of a sorbent and to establish the affinity series.

Isotherm models are widely used in sorption studies and are derived by assuming that the equilibrium sorption behaviour only depends on the temperature of the system. Consequently, the temperature of the system is maintained constant. In contrast, in most experimental studies, pH of the system is not controlled (Ho et al. 2002; Erdem et al. 2004), even though, the equilibrium behaviour depends on the pH of the system (Bosma and Wesselingh 1998). Thus, it is recommended that the metal solution should be prepared using pH buffer solution instead of deionised water. This will ensure minimal change in the pH of solution during the sorption experiment.

Various isotherm models have been developed for different sorption scenarios. Among them, Langmuir and Freundlich models are widely used to determine whether the sorption is of monolayer or multilayer nature, which can be specifically useful to predict the type of adsorption mechanisms involved (Section 3.3).

(A) LANGMUIR ISOTHERM MODEL

Langmuir isotherm model is developed for an ideal homogeneous sorption scenario. Homogeneous sorption occurs if sorption sites of a sorbent are identical and equivalent. Thus, every sorption site in the sorbent has equal affinity to sorb metal ions (Kundu and Gupta 2006). Langmuir isotherm model also assumes that there is no further interaction or migration between sorbed metal ions (Vijayaraghavan et al. 2006). Therefore, a rigid layer of only one molecule in thickness (a monolayer) is formed during ideal Langmuir sorption. Additionally, no further sorption or desorption occurs once all sorption sites are occupied by metal ions. Langmuir isotherm equation is given as (Langmuir 1916):

$$Q_e = \frac{q_m K_a C_e}{1 + K_a C_e} \tag{3.4}$$

where C_e and Q_e are equilibrium metal concentration in the solution (mg/L) and equilibrium sorption capacity (mg/g), respectively. q_m (mg/g) and K_a (L/mg) are Langmuir constants related to maximum sorption capacity and energy of sorption (or affinity term) respectively.

The following linearised form of Langmuir isotherm is often used in sorption studies:

$$\frac{C_e}{Q_e} = \frac{1}{q_m K_a} + \frac{C_e}{q_m} \tag{3.5}$$

(B) FREUNDLICH ISOTHERM MODEL

Freundlich isotherm characterises a more complex scenario than the Langmuir isotherm. The scenario is that the sorption sites are heterogeneous, which means they are not identical and equivalent. Thus, the sorption sites have different degree of affinity for the sorption of metal ions in such a way that stronger sorption sites are occupied first by metal ions and sorption continues until the weakest site is occupied. In Freundlich sorption scenario, formation of multilayer sorption is possible since sorbed metal ions can attract other molecules from the bulk solution.

Freundlich isotherm model is governed by following equation (Freundlich 1906):

$$Q_e = K_F C_e^{(\frac{1}{n})} \quad (3.6)$$

where K_F is Freundlich constant (mg/g) and n is Freundlich exponent.

The K_F constant is an indicator of adsorption capacity, while n is the indicator of intensity of the reaction (Rengaraj et al. 2001). The n values can be used to predict the nature of the interaction between the metal ion and the sorbent (Foo and Hamid 2010). A 'n' value greater than 1 implies that the sorption of metal ions is modified in a way that the metal sorption capacity of sorbents is increased such as revealing previously inaccessible active sites (Jiang et al. 2002). In contrast, n value less than 1 indicates that the bond between active sites and metal ions are weaker. Consequently, metal ions are preferred to form a hydrogen bond with already sorbed metals instead of bonding with the active sites of sorbents. Therefore, n value less than 1 corresponds to physisorption or ion exchange.

Linear form of Freundlich isotherm is given by:

$$\log Q_e = \log K_F + \frac{1}{n} \log C_e \quad (3.7)$$

3.4.2 KINETICS MODELLING

Sorption kinetics describes the mobility of a metal ion in the bulk solution until it is immobilised by the active sites of the sorbent material. Typically, the metal sorption kinetics consists of four steps (Argun et al. 2007; McKay and Poots 1980):

1. Diffusion through the bulk solution;
2. Boundary layer diffusion;

3. Intraparticle diffusion;
4. Sorption to active sites (metal binding process).

The first three steps mentioned above are illustrated in Figure 3.4. The existence of intraparticle diffusion (step 3) has been noted for non-porous materials (Sağ and Aktay 2000). Hence, the term is not restricted to pore diffusion and can be extended to diffusion into cracks on the external surface of the sorbent.

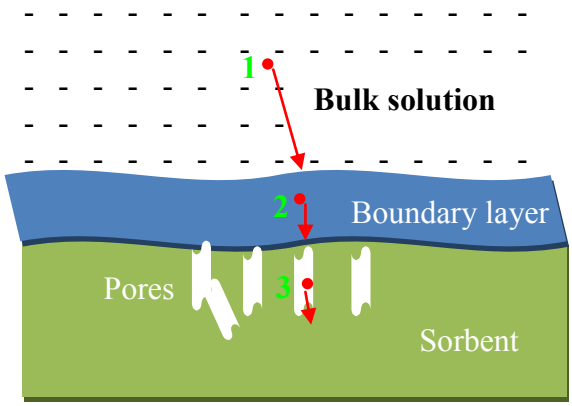

Figure 3.4 Schematic diagram illustrating the diffusion of an ion through the bulk solution, boundary layer and intraparticle site (Red circles denote the metal ion and the arrows indicate the diffusion directions)

The overall metal removal rate depends on the rates of each of these steps. The metal removal rate is of particular interest in the design of the treatment system since crucial design parameters such as residence time and reactor dimensions are determined based on the metal removal rate. Additionally, the diffusion rates can determine the affinity of a sorbent for a specific metal such that the metal with a rapid diffusion rate has a high probability to bond with the active sites of the sorbent provided such interaction is favourable in terms of energy. The rates are generally determined using kinetics models discussed below.

(A) DIFFUSION MODELLING

Weber and Morris (1965) noted the mathematical dependence of the diffusion processes on the square root of time. Consequently, sorption capacity (Q_t) vs. square

root of time (√t) plots are used to understand the diffusion processes and to determine the diffusion rates. As observed in a number of studies (Ho et al. 1996; Basha and Murthy 2007), a typical Q_t vs. √t graph generally consists of three regions (Figure 3.5):

1. Initial linear portion due to the boundary layer restriction;
2. Second linear portion corresponding to intraparticle restriction;
3. Plateau attributed to the equilibrium or near equilibrium.

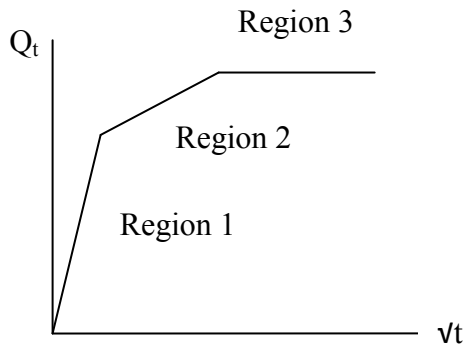

Figure 3.5 Q_t vs. √t graph showing the three linear regions

The boundary layer diffusion is significant at the early stage of diffusion (Ho et al. 1996; McKay et al. 1987). Hence, the boundary layer diffusion rate is generally determined from the slope of the initial linear portion of C_t/C_0 vs. t plot (C_0 is the initial metal concentration and C_t is the concentration of the remaining metal ions in the solution at time t) (McKay and Poots 1984; Forster et al. 1985) or simply using the following equation (Ho et al. 1996):

$$\text{Boundary layer diffusion rate} = \frac{(C_0 - C_5)}{5C_0} \qquad (3.8)$$

where C_5 is the concentration of metal ion in solution after 5 minutes.

The second linear region of Q_t vs. √t graph is attributed to the intraparticle diffusion phenomenon. Two models, Vermeulen (Vermeulen 1953) and Weber-Morris (Weber

and Morris 1962), are generally used to describe the intraparticle diffusion. The Vermeulen model is represented by the following equation:

$$Q_t = Q_e\sqrt{(1 - e^{\left(-\frac{4\pi^2 D_v t}{d_p^2}\right)})} \quad (3.9)$$

Where D_v is the Vermeulen intraparticle diffusion coefficient and d_p is the average particle size of sorbents.

The following equation describes the Weber-Morris model:

$$Q_t = K_{WM}\sqrt{t} + I \quad (3.10)$$

Where K_{WM} is the Weber-Morris constant related to intraparticle diffusion rate and I is the y-intercept related to the boundary layer thickness.

The parameter, K_{WM}, is generally determined by linear regression of sorption capacity data between t = 0 and t_{lim}, where t_{lim} is the first break point, i.e. the first point when the system achieves its equilibrium status. It should be noted that K_{WM} does not represent the intraparticle diffusion rate, rather it is a measure of intraparticle diffusion rate. Hence, Crank (1975) proposed the following equation to calculate the intraparticle diffusion rate (D_{WM}) from K_{WM}:

$$D_{WM} = \pi(\frac{d_p K_{WM}}{12 Q_e})^2 \quad (3.11)$$

(B) MODELLING METAL BINDING PROCESS

The metal binding rates can be calculated using the pseudo first order model proposed by Lagergren (1898) or pseudo second order model proposed by Ho and McKay (1998). Pseudo first order model is described by the following equation:

$$\frac{dQ_t}{dt} = K_1(Q_e - Q_t) \tag{3.12}$$

where K_1 is the pseudo first order reaction rate.

Integrating equation (3.12) with the boundary layer conditions (t = 0, Q_t = 0) and (t = t, Q_t = Q_t) gives:

$$\ln(Q_e - Q_t) = \ln Q_e - K_1 t \tag{3.13}$$

The metal binding rate can be found from the slope of the plot of ln(Q_e - Q_t) vs. t. As Ho et al. (1998) have pointed out, the equilibrium sorption capacity must be known to fit the pseudo first order model to the experimental data. Thus, Ho et al. (1998) argue that the model is complex since it is difficult to find the accurate equilibrium sorption capacity, if chemisorption, which is generally slow, is involved in the metal sorption. In such cases, complex trial and error analysis is required. Hence, Ho et al. (1998) proposed pseudo second order model given by the following equation:

$$\frac{dQ_t}{dt} = K_2(Q_e - Q_t)^2 \tag{3.14}$$

where K_2 is the pseudo second order reaction rate.

Integrating equation (3.14) with the boundary conditions (t = 0, Q_t = 0) and (t = t, Q_t = Q_t) gives:

$$\frac{1}{(Q_e - Q_t)} = \frac{1}{Q_e} + K_2 t \tag{3.15}$$

The linearised form of the equation is:

$$\frac{t}{Q_t} = \frac{1}{K_2 Q_e^2} + \frac{1}{Q_e} t \tag{3.16}$$

From the slope and intercept of t/Q_t vs. t plot, the pseudo second order metal binding rate can be found and the equilibrium sorption capacity is not required to fit the experiment data. In addition, Ho et al. (1998) concluded that pseudo second order model best describes the metal binding process than the pseudo first order model after testing both models using data available in research literature.

However, the necessity for equilibrium sorption capacity to fit the experimental data with the pseudo first order model can be avoided by rearranging equation (3.13) as shown in equation (3.17) and undertake non-linear regression using Solver function in Microsoft Excel®.

$$Q_t = Q_e(1 - e^{-K_1 t}) \tag{3.17}$$

Hence, it is necessary to fit both models with the experimental data and the model that best fits the experimental data can be used to determine the metal binding rate.

(C) IDENTIFICATION OF RATE-LIMITING STEP

Each sorption kinetics step occurs at a certain rate depending on the properties of the sorbent, the metal ion and solution. The step that controls the overall metal removal rate is defined as the rate-limiting step (Ray 1983). Identification of the rate-limiting step is necessary for process modification. For example, if the boundary layer is limiting the overall removal rate, high agitation can be used to increase the rate by reducing the boundary layer thickness.

Four steps are generally considered in the study of sorption kinetics as listed in Section 3.4.2. In general, step 1 is considered relatively rapid in an agitated system as the ions can move freely in the bulk solution, especially in water, the viscosity of which is relatively low. Similarly, in general, sorption of ions to active sites (step 4) is a spontaneous process (El-Bishtawi and Ali 2001; Horsfall Jnr and Spiff 2005). Hence, this step is also regarded as relatively fast (Vadivelan and Kumar 2005). Thus, only the diffusion restriction (steps 2 and 3) is assumed to control the metal removal rate in most research studies (Guibal et al. 1998; Keskinkan et al. 2004; Hui

et al. 2005; Herrero et al. 2011). However, sorption of metals to active sites (step 4) can also be rate limiting, especially in the case of chemisorption (Ho and McKay 1998). Hence, considering step 4 of sorption kinetics as rapid may not be suitable in all cases.

The diffusion rate in step 2 depends on the properties of the boundary layer formed at the surface of the sorbent, while the porosity of the material primarily determines the rate of intraparticle diffusion (step 3). In case the material has very large pores, but a thick boundary layer, then, in relative terms, the diffusion through the boundary layer (i.e. the boundary layer diffusion) is the rate-limiting step. In contrast, intraparticle diffusion is the rate-determining step if the sorbent has small pore sizes and a thin boundary layer.

Primarily graphical methods are used for the identification of the rate-limiting step. One of the methods is based on the Weber-Morris model (equation 3.10). In Weber-Morris model, the parameter 'I' corresponds to the thickness of the boundary layer. Consequently, intraparticle diffusion is considered as the sole rate-limiting step if I = 0, which implies that no boundary layer exists to resist the diffusion. In contrast, both intraparticle and the boundary diffusion are the rate-limiting stages if $I > 0$ (Kalavathy et al. 2005; Shen and Duvnjak 2005).

The other commonly used graphical method is based on the relationship between K_{WM} and the initial metal concentration (C_0):

$$K_{WM} = A\,(C_0)^x \tag{3.18}$$

where A is a constant and x is 0.5 if the intraparticle diffusion is the only rate-limiting step (Keskinkan et al. 2004). That is, a plot of K_{WM} vs. $\sqrt{C_0}$ should be a straight line passing through the origin if intraparticle diffusion is the sole rate-limiting step.

However, there is a fundamental issue in the use of these methods to determine the rate-limiting step. In the equations (3.10) and (3.18), it is assumed that only intraparticle and boundary layer diffusion contribute to the metal removal rate. However, sorption to active sites can also contribute to the overall metal removal rate. Hence, it is necessary to account for the metal binding rate when determining the rate-limiting step. Another problem is that these methods do not provide any information as to what extent these steps limit the overall removal rate. Such knowledge is necessary for deciding whether any process modification is required. For example, if the contribution of the boundary layer diffusion in controlling the overall metal removal rate is minimal, it may not be economically viable to provide energy intensive agitation to reduce the boundary layer thickness.

Apiratikul et al. (2008) suggested a relative coefficient (RC) to evaluate the degree of each rate-limiting step in controlling the overall metal removal rate as given in equation 3.19:

$$RC = \frac{I}{Q_e} \tag{3.19}$$

Low RC indicates that sorption is controlled predominantly by intraparticle diffusion. Thus, the lower the RC, the higher the degree of influence of intraparticle diffusion in limiting the overall metal removal rate. However, the main drawback of this approach is that it does not have any mathematical basis. Therefore, it is necessary to develop a mathematically rigorous methodology for the analysis of the rate-limiting step that would provide more insight in relation to the degree of contribution by each kinetics step in limiting the overall metal removal rate.

3.4.3 THERMODYNAMICS MODELLING

The primary thermodynamics parameters are enthalpy change (ΔH^0), entropy change (ΔS^0) and free energy change (ΔG^0), which can be used to predict the feasibility and the spontaneity of the sorption process. The following equations are used to calculate these parameters (Adebowale et al. 2008):

$$\Delta G^0 = -RT \ln K_D \tag{3.20}$$

where R is the universal gas constant, T is the absolute temperature and K_D is the distribution coefficient given as:

$$K_D = \frac{(C_0 - C_e)}{(\frac{m_s}{v})C_e} \tag{3.21}$$

where m_s and v are the mass of the sorbent and volume of solution, respectively.

In addition, ΔG^0 can be defined in terms of ΔH^0 and ΔS^0, which is:

$$\Delta G^0 = \Delta H^0 - T\Delta S^0 \tag{3.22}$$

Thus, combining equations 3.20 and 3.22 gives:

$$\log K_D = \frac{\Delta S^0}{2.303R} - \frac{\Delta H^0}{2.303RT} \tag{3.23}$$

ΔH^0 and ΔS^0 can be calculated from the slope and intercept of log K_D vs. (1/T) plot, respectively.

It is worthy of noting that the sorption process depends on the physico-chemical conditions of the system such as pH. Hence, the experimental conditions in the sorption system have to be properly controlled to study the isotherm, kinetics and thermodynamics of the metal sorption mechanisms employed by the sorbent materials. Hence, it is important to understand the impacts of the experimental conditions such as temperature, initial metal concentration, sorbent dose and pH on the removal of metals.

3.5 INFLUENCE OF EXPERIMENTAL CONDITIONS ON SORPTION

Ziyath et al. (2011) published a review on the influence of physical and chemical parameters on the treatment of metals in polluted stormwater by zeolite, which is a low cost sorbent. The sections related to the effect of experimental conditions of solution on metal sorption by zeolite are reproduced from the paper in the following subsections with minor changes. Though the discussion is based on zeolite, it should be noted that the fundamental science in relation to the influence of these parameters is generally similar for any sorbent.

3.5.1 pH

pH values are used as an indirect measurement of the concentration of H_3O^+ ions in solution and it is one of the crucial parameters in the sorption of metals by zeolites. pH of stormwater is typically in the range of 6.5-7.7 (Herngren et al. 2005). However, it is possible to have stormwater with lower pH, especially if it flows over acidic soils or due to acid rain. At low pH, H_3O^+ can effectively compete with metal cations for sorption sites of zeolites. As a result, the sorption of metals can be reduced (Inglezakis et al. 2003; Motsi et al. 2009). Furthermore, the competition by H_3O^+ can slow down the rate of metal uptake. For example, Hui et al. (2005) noted that complete removal of metal ions occurred within 60 minutes at pH 4, whereas it took 120 minutes at pH 3. This emphasizes that the development of sorption technique for stormwater treatment needs to select a suitable retention time at optimum pH for the effective removal of metals. The competition of H_3O^+ with metal ions for sorption sites depends on several factors such as the concentration and type of metal ions. For instance, metals that are selective to zeolite and present in high concentration can out-compete H_3O^+ ions for the sorption sites of zeolite.

In such cases, the metal solution becomes basic after the introduction of zeolites due to the uptake of H_3O^+ ions from solution by zeolites. This occurs mainly via the exchange of extra framework cations for H_3O^+ ions as shown below:

$$Ze\text{-}M^+ + 2H_2O \longleftrightarrow Ze\text{-}H_3O^+ + M^+ + OH^-$$

where Ze and M^+ denote zeolite and extra framework cation respectively.

Metal hydroxide precipitation can occur if pH of solution increases above the threshold pH level of precipitation of a particular metal ion. Ok et al. (2007) reported substantial increase in the sorption of metals at pH higher than 6 due to the possible precipitation of the metal ions. The hydroxide precipitation of metal ions in the basic region has been reported in several studies including Oren and Kaya (2006), Wark et al. (1993), Pitcher et al. (2004) and Hui et al. (2005). However, hydroxide precipitation can re-dissolve when pH of the solution is changed to the acidic region and the metal ion can be released back to solution (Pitcher et al. 2004).

Furthermore, pH has a profound effect on the formation of metal complexes. Metals can form various metal complexes depending on the pH of the solution. For example, Cr ion is predominantly present as $[Cr(OH)_2]^+$ at pH 7 and as $[Cr(OH)_4]^-$ at pH 10 (Vaca Mier et al. 2001). In general, zeolites have very little affinity to anionic complexes due to their negative framework structure (Haggerty and Bowman 1994). Therefore, sorption of a particular metal can be reduced if pH of the solution is favourable to form anionic metal complexes.

Apart from affecting the characteristics of metal ions and their sorption, pH can also affect the structure of zeolites. The aluminosilicate structure is vulnerable to strong basic and acidic environments. Strong bases can lead to desilication, whereas strong acids can dissolve Al atoms. Consequently, the zeolite structure can be destroyed at extreme pH values, which in turn can reduce sorption (Mishra and Tiwari 2006; Rao et al. 2006). Since zeolite is capable of changing pH of the solution as discussed above, there is a possibility for these processes to occur during the treatment of polluted water. Dealumination is of particular concern due to potential health impacts on humans. Australian drinking guidelines has set 0.1 mg/L as the maximum allowable limit of Al (NHMRC 2004). However, this limit is not based on health considerations due to the lack of data to set a health-based guideline. Hence, it has been highly recommended to keep the Al concentration as low as possible if the treated stormwater is intended to be used for potable purposes. This emphasises the

importance of detailed investigation of the dealumination processes of zeolite when introduced to polluted stormwater.

3.5.2 TEMPERATURE

Temperature of solution influences metal sorption mainly by enhancing the diffusion of hydrated metal ions (Inglezakis et al. 2004). Energy of metal ionic complex in solution increases with increasing temperature. As a result, hydrated metal ions strip off some of the water molecules from their hydrated complexes leading to the reduction of their ionic size (Barros et al. 2004). This facilitates the diffusion of metal cations into the pores and consequently increases sorption as the metal ions can access the extra sorption sites available. Seward et al. (1999) reported that the increase in temperature from 25 ^{0}C to 300 ^{0}C only reduced the distance between metal ion and water by approximately 0.005 nm resulting in only a slight reduction in the size of metal aqua complex. However, the size reduction can have an impact on some metal ion complexes that only have a few water molecules. In addition, studies have reported that increasing the temperature to 60 ^{0}C results in only a slight increase in sorption by zeolites possibly due to the insignificant impact on the size reduction of the metal aqua complex (Wang et al. 2006; Stylianou et al. 2007; Ismail et al. 2010). Hence, enhancing sorption by increasing the temperature is not economically attractive as it involves the consumption of energy (Ismail et al. 2010).

In contrast, some studies have observed a significant increase in the sorption of metals with the increase in temperature. For example, Curkovic et al. (1997) reported that the Pb sorption capacity of zeolite increased from approximately 0.30 mmol/g at 4 ^{0}C to 0.55 mmol/g at 70 ^{0}C. Similarly, sorption capacity for Cd increased from 0.13 to 0.28 mmol/g. Malliou et al. (1994) also reported that sorption of Pb and Cd increased with temperature. Therefore, the effect of temperature appears to be dependent on other physical and chemical factors such as the strength of metal-water complexes and the characteristics of the sorbent pores. Thus, knowledge on the contribution of these factors can provide a basis for the selection of an optimum treatment temperature.

3.5.3 SORBENT DOSE

Increasing zeolite dose increases the amount of available sorption sites. Therefore, in theory, metal sorption must increase with increasing zeolite dose. In addition, metal sorption rate increases at high zeolite dose since it reduces the competition between metal ions due to the availability of more sorption sites (Oren and Kaya 2006; Apiratikul and Pavasant 2008; Ismail et al. 2010; Jamil et al. 2010). However, high zeolite dose increases pH of the system, which successively affects the removal of metals.

In addition, sodium pretreated zeolites contain extra framework cations, mainly Na ions in the structure. Consequently, a high amount of Na ions can be released into solution due to the exchange with metals and/or H_3O^+ ions when a high zeolite dose is used. Na ions cannot be easily removed from water and can alter the taste if the concentration exceeds 180 mg/L (NHMRC 2004). Furthermore, there can be health impacts (NHMRC 2004). On the other hand, an adequate amount of zeolite must be available to ensure the removal of metals below the safe level. Zeolite dose, therefore, needs to be optimised considering the factors discussed above. For this optimisation, the impact of increasing zeolite dose on sodium concentration in solution needs to be systematically studied. Alvarez-Ayuso et al. (2003) used 10 g/L as the optimum zeolite dose to obtain the maximum possible removal of metals. 10g/L of zeolite has been used by other researchers such as Kocaoba et al. (2007) and Garcia-Sanchez et al. (1999) as a standard dose. However, this concentration cannot be taken as a datum value since it is also dependent on the initial metal concentration.

Large volumes of stormwater need to be treated to meet the demand for the potable water. Hence, a large quantity of zeolite is required for the treatment. Disposal of a large quantity of used zeolite can be another operational issue that needs to be addressed. The prospect of regenerating zeolite after use has been discussed in research literature (Blanchard et al. 1984; Katsou et al. 2011).

3.5.4 INITIAL METAL CONCENTRATION

Research studies report contradictory observations regarding the effect of initial metal concentration on the removal of metals. The following three different sorption behaviours have been reported in the literature when the initial metal concentration is increased:

1. Decrease in percentage uptake of metal ions (Erdem et al. 2004; Hui et al. 2005; Wang et al. 2006; Ibrahim et al. 2010);
2. No effect on metal sorption (Ouki and Kavannagh 1997);
3. Increase in sorption capacity of zeolite for up to a certain initial metal concentration, above which there is only a slight increase in sorption (Oren and Kaya 2006; Kocaoba et al. 2007).

In a typical experimental study to evaluate the influence of initial metal concentration, zeolite dose is usually kept constant, meaning the number of available sorption sites is fixed. When the initial metal concentration is increased, the sorption sites available for the uptake of metal ions can become inadequate. This may be the possible reason for the first type of observation mentioned above. As for the observation by Ouki and Kavannagh (1997), the availability of an abundance of sorption sites in zeolite could have been the reason for the complete removal of metal ions in the concentration range studied. In the case of the third observation given above, zeolite could have been exhausted since the active sites were occupied by the ions. Thus, a significant increase in metal uptake was not observed beyond a certain initial metal concentration. These observations demonstrate that there is a close relationship between the metal concentration and zeolite dose. Thus, some research studies use metal concentration to zeolite dose ratio to discuss the effect of these inter-dependent parameters (Ahmed et al. 1998; Alvarez-Ayuso et al. 2003).

Depending on the catchment characteristics, stormwater can contain a range of metal ions such as Na^{+} and magnesium (Mg^{2+}), which can compete for the sorption sites of zeolite along with the common toxic metals. However, the effect of the presence of other metal ions on the sorption of the toxic metals has been investigated in relatively few studies (Ouki et al. 1997; Baker et al. 2009). Therefore, knowledge of the

chemical composition of stormwater can be the starting point in the development of sorption technology.

3.6 CONCLUSIONS

Ion exchange and adsorption are the two common sorption mechanisms involved in the removal of metals by sorbents. Ion exchange is primarily influenced by hydration energy and the adsorption mechanism can be divided into physisorption and chemisorption. Physisorption is a weak interaction between active sites and metal ions and is influenced by charge densities of metal ions. In contrast, electron transfer occurs between metal ions and active sites during chemisorption. Hence, the bond is relatively stronger than in the case of physisorption. Chemisorption is generally governed by HSAB theory. The major drawback in the sorption technique is that depending on the hydration energies, charge densities and chemical hardness of metal ions, sorbents have a preference for the removal of certain metal ions leading to the poor removal of less preferred metal ions.

Sorption of metal ions is a complex process involving various mechanisms operating in parallel. Consequently, both mechanistic and empirical approaches are necessary in modelling a sorbent system. In general, a sorbent system is modelled based on isotherm, kinetics and thermodynamics characteristics. Freundlich and Langmuir isotherm models are generally used to investigate the sorption mechanisms, while the thermodynamics parameters such as enthalpy change and free energy change are useful in predicting the feasibility and spontaneity of the sorption process. The knowledge of the metal sorption kinetics is useful to enhance the overall metal removal rate. Though there are methods to identify the step that limits the overall metal removal rate, they are primarily based on the assumption that only diffusion processes restrict the overall metal removal rate. However, metal binding process can also be rate limiting when the chemisorption mechanism is influencing the sorption of metal ions. Furthermore, there is no mathematically established approach to determine the degree of contribution of each kinetics step in limiting the overall metal removal rate. Additionally, the sorption technique is sensitive to physical and chemical conditions of the system such as pH, temperature, initial metal

concentration and sorbent dose. Hence, these parameters must be appropriately managed in sorption experiments.

Chapter 4: Research methods and design

4.1 BACKGROUND

Sorption is an economically viable and environmentally benign technique for the removal of dissolved metals in water. However, fundamental knowledge regarding the mechanisms employed by sorbents is essential for the design of an effective water treatment system. Defining the metal sorption mechanisms is complex, especially when the sorbent is introduced into a multi metal system such as stormwater, due to competition between metal ions for binding sites of the sorbent. Additionally, as discussed in Section 3.5, physico-chemical conditions of the solution such as pH and temperature can have an influence on the sorption mechanism. Therefore, these factors need to be taken into consideration in the research design.

This chapter describes the research design adopted to achieve the aims and objective of the research study. The discussion includes an outline of the research methodology, the experimental procedures, the test methods and the data analysis techniques. The experimental procedures describe the isotherm, kinetics and thermodynamics studies undertaken, whilst the test methods explain the equipment and procedures used to measure various physical and chemical parameters needed for the envisaged analysis to be undertaken.

4.2 RESEARCH METHODOLOGY

The research methodology comprised of the following phases:

- Critical review of literature;
- Sorbent selection;
- Experimental procedures;
- Test methods;
- Data analysis.

4.2.1 CRITICAL REVIEW OF LITERATURE

A comprehensive state-of-the-art review of research literature was carried out to gain an in-depth understanding of current state of knowledge in the following areas:

- Stormwater pollutants and their adverse impacts;
- Treatment of stormwater pollutants, specifically dissolved metals;
- Mechanisms associated with sorption process;
- Influence of physical and chemical parameters on sorption;
- Approaches in modelling a sorption system and identification of input parameters for modelling.

Based on the critical review, the knowledge gaps with research significance were identified and research problem and hypotheses were formulated. Furthermore, the knowledge acquired from the literature review formed the basis for the formulation of research methods and the identification of data required to test the research hypotheses.

4.2.2 SORBENT SELECTION

The literature review highlighted that the metal removal performance of sorbents is dependent on the experimental conditions (Section 3.5). Hence, the comparison of sorbent materials must be undertaken based on the metal removal performance determined under similar experimental conditions. However, there are large number of sorbents available. Hence, it is difficult to evaluate the performance of each of them for comparison. Therefore, based on the review of the literature, six sorbents, namely, zeolite, clay, activated carbon, seaweed, corncob and sugarcane bagasse were selected as they encapsulate a diversity of the following selection criteria:

- Sorption affinity for metals;
- Cost;
- Environmental impacts in relation to sourcing of sorbents;
- Biodegradability;

- Degree of leaching of toxic compounds.

Selected sorbents were then evaluated using a multi criteria analytical protocol for their performance in relation to the above criteria and the best performing sorbents were selected for further investigation in the research project (Chapter 5).

4.2.3 EXPERIMENTAL PROCEDURES

The common approach adopted to define any metal sorption process is the investigation of different aspects of the mechanisms, such as isotherm, kinetics and thermodynamics behaviour individually, and then, the knowledge created from these individual studies being extended to define the overall sorption mechanism. This approach has been successfully used in past studies. For example, Argun et al. (2007) used this approach to characterise the mechanism employed by oak sawdust for the sorption of Cu, Ni and Cr. Similarly, Panayotova (2001) defined the mechanism employed by zeolite for the sorption of Cu, based on kinetics and thermodynamics.

Accordingly, batch sorption experiments were conducted to characterise the isotherm, kinetics and thermodynamics characteristics of the mechanisms (Section 3.4) employed by the individual sorbents in removing a particular metal. One of the aims of this research project was to define the mechanism employed by mixtures of sorbents, which in theory, should help to overcome the constraints associated with the affinity of sorbents for the sorption of specific metal species. Accordingly, mixtures of sorbent materials were prepared and their metal removal mechanisms were investigated.

4.2.4 TEST METHODS

The mechanisms employed by the sorbent materials can be classified as ion exchange and adsorption (Sections 3.2 and 3.3). Ion exchange is related to the cation exchange capacity of sorbents (CEC), whilst adsorption is associated with the type and amount of negative sites in sorbents. These two properties of sorbents were characterised using ammonium acetate method (Section 4.4.2) and the titration

method (Section 4.4.3), respectively. The concentration of metals is the main input parameter needed by the theoretical models (Section 3.4) for defining the relevant mechanisms. The metal concentration was measured using Inductively Coupled Plasma Optical Emission Spectrometry (ICP-OES) and Inductively Coupled Plasma Mass Spectrometry (ICP-MS) (Section 4.4.4). Relevant quality control procedures (Section 4.5) were adopted to maintain the validity of the test data.

4.2.5 DATA ANALYSIS

Univariate and multivariate techniques were used to analyse the data generated from the laboratory experiments. Univariate analysis included linear regression analysis and basic statistical operations such as mean and standard deviation, whilst PROMETHEE (Preference Ranking Organisation METHod for Enrichment Evaluations) and GAIA (Graphical Analysis for Interactive Assistance) were the key multivariate techniques used (Section 4.6). The data analysis primarily focused on defining the sorption mechanism based on the data acquired from the kinetics and thermodynamics experiments. Finally, metal removal performance and mechanisms of the mixtures were compared with that of the individual sorbents in order to identify the influential parameters responsible for the effective removal of metal ions from water.

4.3 EXPERIMENTAL PROCEDURES

4.3.1 SORBENTS

The sorbent materials investigated in this study are listed in Table 4.1. Photographs of the materials are shown in Figure 4.1.

Table 4.1 Sorbent materials

Sorbents	Species	Source
Zeolite	Clinoptilolite	Zeolite Australia Pty Ltd
Granular activated carbon	Untreated charcoal	Sigma Aldrich Pty Ltd
Clay	Montmorillonite	Sigma Aldrich Pty Ltd
Sugarcane bagasse	-	Centre for Sugar Research and Innovation, Queensland University of Technology
Corncob	-	Local market
Seaweed	Ecklonia radiata	Murdoch, Western Australia

(a) (b) (c) (d) (e) (f)

Figure 4.1 Sorbent materials: (a) Zeolite; (b) Granular activated carbon; (c) Clay; (d) Sugarcane bagasse; (e) Seaweed; (f) Corncob

Physical and/or chemical pretreatment of a sorbent enhances its metal removal capacity and various techniques have been proposed for this purpose (Inglezakis et al. 2001; Wan Ngah and Hanafiah 2008). However, in this study, extensive chemical pretreatment was avoided to prevent secondary pollution resulting from potential leaching of these chemicals from sorbents. Additionally, if large volumes of stormwater need to be treated, it will require large quantities of sorbents. Thus, using expensive chemicals to pretreat large amounts of sorbents will increase the capital cost. Therefore, the following relatively inexpensive pretreatment techniques were adopted in this research study.

Zeolite was pretreated by equilibrating with 1 M sodium chloride (NaCl) for 24 hours. This has been proven to enhance the sorption capacity since the extra framework cations, such as Ca^{2+} and K^{+} are replaced with easily exchangeable Na^{+} ions (Zamzow et al. 1990; Wingenfelder et al. 2005). Activated carbon and sugarcane bagasse were thoroughly washed with deionised water and oven dried overnight. Corncob and seaweed were coarsely crushed using mortar and pestle before washing with deionised water and drying overnight. The sorbents were washed with deionised water in order to reduce the discoloration of water during treatment. Clay was used as received.

4.3.2 METAL SOLUTION

As identified from the review of research literature, Zn, Cu, Cd, Pb, Ni, Cr and Al are the common toxic metals present in stormwater (Herngren 2005) and their removal using sorbents were investigated in this study. Synthetic metal solutions containing these metals ions were prepared by dissolving the corresponding metal nitrates sourced from Sigma Aldrich Pty Ltd (Table 4.2) in deionised water or pH buffer. The metal nitrates were used since nitrate anions neither form any metal-anion complexes nor hydrolyse (Peric et al. 2004). Hence, the nitrate anions do not interfere with the metal sorption process of the sorbent materials.

Table 4.2 Metal nitrates used in this study

Name	Formula	Grade
Zinc nitrate	$Zn(NO_3)_2.6H_2O$	Reagent, 98%
Copper nitrate	$Cu(NO_3)_2.3H_2O$	Reagent, 98%
Cadmium nitrate	$Cd(NO_3)_2.4H_2O$	Reagent, 98%
Lead nitrate	$Pb(NO_3)_2$	Reagent, 99%
Nickel nitrate	$Ni(NO_3)_2.3H_2O$	Reagent, 99%
Chromium nitrate	$Cr(NO_3)_3.9H_2O$	Reagent, 99%
Aluminium nitrate	$Al(NO_3)_3 \cdot 9H_2O$	Reagent, 98%

Multi metal stock solutions (concentration: 1 g/L) were prepared and serially diluted to the required metal concentration. Two types of metal solutions were prepared. The first type was high concentration solutions (20, 50, 100 and 200 mg/L), which was used to define the metal sorption mechanisms. The high metal concentration values were selected to investigate the mechanism in order to ensure that the system was not exhausted, i.e. complete removal of metals from solution, which will not provide adequate information regarding the equilibrium characteristics of the sorbent materials. Additionally, pH buffer was used for the preparation of stock solution and its dilution in order to avoid any changes during the experiment since pH has an influence on the sorption mechanism (Section 3.5).

As discussed in Section 2.2.4, the typical concentrations of metals in stormwater are in the order of µg/L (concentration range for: Zn (3-3600 µg/L); Al (< 5-640 µg/L); Pb (< 1-25 µg/L); Cu (3-390 µg/L); Cd (< 1-288 µg/L); Cr (< 1-18 µg/L)) (Herngren 2005). Hence, low concentration solutions (200 µg/L) were prepared to investigate the metal removal performance of sorbents in a tertiary stormwater treatment scenario, i.e. stormwater with the presence of dissolved metals. Consequently, the stock solution for low concentration solution was prepared using deionised water and serially diluted to 200 µg/L concentration using deionised water. The pH was adjusted to replicate typical stormwater pH of approximately 6.5, using sodium hydroxide (NaOH) and nitric acid (HNO_3) as appropriate.

4.3.3 PERFORMANCE OF SORBENT MATERIALS

Performance of sorbent materials in removing metals from stormwater was investigated by introducing the sorbents to the low concentration solution, which replicated a tertiary stormwater treatment system (concentration: 200 μg/L; pH 6.5) (Figure 4.2).

Figure 4.2 Batch experimental set up

As identified in the literature review, a sorbent dose of 10 g/L is suggested for optimal metal removal performance for an initial metal concentration in the order of mg/L (Alvarez-Ayuso et al. 2003). However, in this study, the metal removal performance of the sorbents was evaluated for a lower concentration range. Consequently, the use of high sorbent dose can result in the complete removal of metals from the solution, which will make it difficult to compare the metal removal performance of different sorbents. Consequently, a low sorbent dose of 1 g/L, which can sufficiently accommodate measurement error, was selected.

The system was agitated at 200 rpm using a magnetic stirrer in a constant room temperature (22±1 ^{0}C). pH of the solution was not modified in order to reflect a practical treatment scenario, where controlling the pH of a large volume of water can be difficult. 20 mL sample was withdrawn after 24 hours, which was generally sufficient to reach equilibrium for the investigated sorbents (Kadirvelu and

Namasivayam 2003; Bektas et al. 2004; Gupta et al. 2005; Karnitz et al. 2007; Murphy et al. 2008; Tan et al. 2010). The withdrawn samples were filtered through 0.45 µm glass fibre membrane filters, acidified with HNO_3 and stored in plastic vials until analysis. The metal concentrations in the samples were measured in triplicate using Inductively Coupled Plasma-Mass Spectrometry (ICP-MS) and the sorption capacity (Q_t) was calculated using the following equation (Hui et al. 2005):

$$Q_t = \frac{(C_0 - C_t)}{m_s/_V} \quad (4.1)$$

where C_t is the metal concentration in solution at time 't'. In this case, C_t and Q_t were equal to equilibrium metal concentration (C_e) and equilibrium metal sorption capacity (Q_e), respectively. The metal sorption capacities were used in the evaluation of the performance of sorbent materials (Chapter 5).

4.3.4 DEFINING THE METAL SORPTION MECHANISM

As identified in the review of research literature, the mechanisms employed by the sorbents for the removal of metals are defined based on the kinetics, thermodynamics and isotherm behaviour (Argun et al. 2007). The data required for the kinetics, isotherm and thermodynamics investigation of sorption mechanisms were generated using batch experiments described below. Furthermore, it was identified from the review of research literature that pH, temperature, sorbent dose and initial metal concentration are the primary experimental parameters that influence the metal sorption mechanisms (Section 3.5). Therefore, these parameters were controlled throughout the batch experiments.

(A) KINETICS AND ISOTHERM STUDIES

Volumetric flasks containing 500 mL of metal buffer solution (200 mg/L) and the sorbent (dose: 10 g/L) were agitated using a magnetic stirrer at 200 rpm in a constant room temperature (22±1 ^{0}C). The experiment was conducted for 25 hours. 5 mL of sample was withdrawn after 5, 10, 20, 40, 60, 120, 180, 270, 360 and 1500 minutes

and diluted to 25 mL. The samples were filtered through 0.45 μm glass fibre membrane filters, acidified with HNO_3 and stored in plastic vials until Inductively Coupled Plasma-Optical Emission Spectrometry (ICP-OES) analysis. Additionally, pH of the solution was measured at the end of the experiment. The metal concentration in the samples were measured in triplicate using ICP-OES and the amount of metal removed at each time interval by a gram of sorbent was determined using equation (4.1). The experimental data was fitted to the theoretical kinetics models (Section 3.4.2) to analyse their diffusion characteristics and to identify the steps that limit the metal removal rate of sorbents. Additionally, the equilibrium sorption capacity for isotherm modelling was determined using the kinetics experimental data.

(B) THERMODYNAMICS STUDIES

The thermodynamics experiments were conducted by placing the volumetric flasks containing the sorbent (dose: 10 g/L) and metal buffer solution (200 mg/L) in a constant temperature water bath at temperatures of 20 ^{0}C, 30 ^{0}C, 40 ^{0}C and 50 ^{0}C (Figure 4.3). The system was manually agitated at 15 minute intervals. After the equilibrium time, which was determined based on the kinetics studies discussed in Section 4.3.4 (A), 20 mL of samples were withdrawn and filtered through 0.45 μm glass fibre membrane filters. The equilibrium metal concentration in solution was measured using ICP-OES. The thermodynamics parameters were determined using the models discussed in Section 3.4.3.

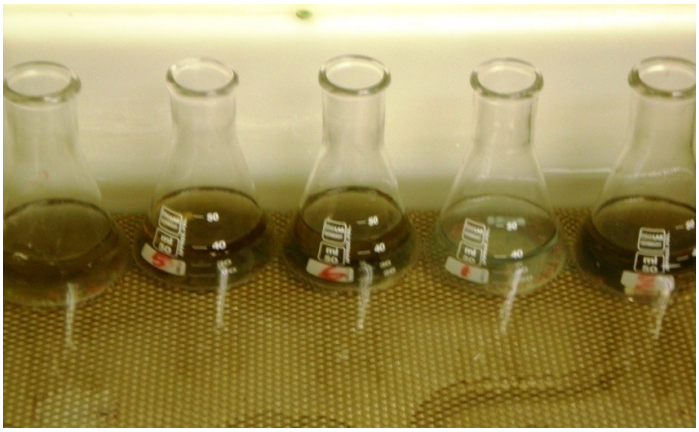

Figure 4.3 Experimental setup for thermodynamics studies

4.4 TEST METHODS

4.4.1 pH

pH is a measure of acidic or alkaline nature of a solution and it is calculated based on the concentration of H^+ ions according to the following equation:

$$pH = -\log_{10}[H^+] \quad (4.2)$$

where $[H^+]$ denotes the concentration of H^+ ions.

Metal removal mechanism is dependent on the pH of the solution (Section 3.5.1). Additionally, pH controls metal speciation, which has an influence on the interaction of metal ions with the active sites of a sorbent as discussed in Section 3.5.1. Therefore, controlling the pH of the solution is crucial in sorption studies. A pH probe (Model: TPS IJ44) attached to a combined pH/EC meter (Model: TPS AQUA-pH-mV-Temperature meter) was used for pH measurement (Figure 4.4). Calibration of pH/EC meter and verification of the method are discussed in Section 4.5.2. Calibrated pH/EC meter was immersed into solution to record its pH.

Figure 4.4 pH probe and pH/EC meter

4.4.2 CATION EXCHANGE CAPACITY

Cation exchange capacity (CEC) is a measure of the ability of a sorbent to exchange the cations present in the structure for the cations in the solution. Accordingly, CEC was determined in order to understand the ion exchange characteristics of a sorbent. Theoretically, CEC is measured based on the elemental composition of the sorbent (Kesraoui-Ouki et al. 1993). The amount of cations, which are generally considered involved in the cation exchange process in 1 g of sorbent, is used as the theoretical CEC. However, not all of these cations are available for exchange. For example, the cations present in inaccessible sites do not necessarily participate in the cation exchange process (Inglezakis 2005). Therefore, the parameter, 'effective cation exchange capacity (ECEC)'determined using experimental techniques is generally used for practical application (Robertson et al. 1999) since ECEC provides a practical estimation of the cation exchange property. In this study, the ammonium acetate method recommended by the International Soil Reference and Information Centre (ISRIC) (1992) was used to determine ECEC of the sorbents. Though this method was developed for soil analysis, it has been used as a standard technique to determine ECEC of various sorbent materials (Vazquez et al. 2008; Wu et al. 2008). ECEC determined using this technique is based on the amount of ammonium uptake from the solution by the sorbent.

2 g of sorbent was stirred with 1 M ammonium acetate (NH_4Ac) at pH 7 in a magnetic stirrer for three days. Then, the solution was decanted and a fresh batch of 1 M NH_4Ac was added to the system. After another three days, the sorbent was filtered and washed with 20 mL of 1 M NH_4Ac five times, 20 mL of 1 M ammonium chloride (NH_4Cl; pH 7) four times and with 0.25 M NH_4Cl (pH 7) once. Thereafter, the sorbent was washed with methanol to remove excess ammonium (NH_4^+) ions that were not held by the sorbent. Methanol washing was stopped if no silver chloride (AgCl) precipitation was observed when silver nitrate ($AgNO_3$) was added to effluent methanol. Finally, the beaker containing the sorbent was covered with a clean tissue and allowed to air dry for two days. Afterwards, 50 mL of deionised water was added to the beaker containing dry sorbent and the beaker was covered with a clean polythene wrap to minimise the escape of NH_4^+ ions as ammonia gas (NH_3) during the analysis. An opening was made on the wrap and an ammonia selective electrode

(Model: TPS ISE) connected to the combined pH/EC meter was immersed into solution through the opening. The electrode was firmly tapped to dislodge any air bubbles trapped in its membrane. 0.5 mL of 10 M NaOH was added to the solution, which moves the reaction given below to the left hand side to balance the increase in OH^- concentration in solution due to the addition of NaOH:

$$NH_{3(g)} + H_2O_{(l)} \longleftrightarrow NH_4^+{}_{(aq)} + OH^-_{(aq)}$$

This produces NH_3 gas, which diffuses through the membrane and creates a voltage difference inside the electrode proportional to the ammonium concentration in solution. The voltage difference was measured using the combined pH/EC meter and displayed in millivolts (mV).

The concentration of NH_4^+ in solution was determined from the calibration curve (Section 4.5.4) and ECEC of the sorbent was calculated using the following equation:

$$\text{ECEC} = \frac{50 \times C_N}{m_s \times 10^{-5}} \tag{4.3}$$

where ECEC is in meq/100g, 50 is the volume of water added to the dry sorbent in mL, C_N is the concentration of ammonium ion in solution (mol/L) and m_s is the weight of dry sorbent (g).

4.4.3 QUANTIFICATION OF NEGATIVE SITES

Several types of functional groups are available in a sorbent material and they are commonly found in acidic form due to the complexation with H^+ ion. For example, carboxylic functional group is found as carboxylic acid. The negativity of the functional groups present in sorbents can attract the metal cations and sorb them via either physisorption or chemisorption mechanisms. For example, carboxylic

functional group (COO^-H^+) can attract a metal ion (M^{n+}) via physisorption (COO^-H^+-M^{n+}) or chemisorption (COO^-M^{n+}) depending on the characteristics of the bonding. Spectroscopic techniques can be used to identify the available functional groups. However, these techniques quantify all the functional groups available in the sorbents instead of considering the ones that can participate in the sorption process. Hence, in this study, acid-base titration method was used to determine the types and to quantify the amount of negative sites in the structure of the sorbents.

The functional groups present in biosorbents can be broadly divided into carboxylic (-COOH), hydroxyl (-OH) and lactonic (-COO) groups (Basso et al. 2002), which can be quantified using Boehm titration technique (Boehm 1994). The technique uses three bases, namely, sodium hydroxide (NaOH), sodium carbonate (Na_2CO_3) and sodium bicarbonate ($NaHCO_3$) to quantify these acidic groups by means of back-titration. $NaHCO_3$ can neutralise the acids, which have acid dissociation constant (pKa) less than 6.37. Hence, it can only neutralise the carboxylic acidic group. In contrast, both carboxylic and lactonic groups can be neutralised by Na_2CO_3 due to its ability to neutralise acids with pKa less than 10.25. NaOH can neutralise acids with pKa less than 15.74. Thus, it can neutralise the carboxylic, hydroxyl and lactonic groups (Laszlo et al. 2001). Accordingly, 0.5 g of seaweed was equilibrated with 50 mL of 0.1 M NaOH, 0.2 M Na_2CO_3 and 0.1 M $NaHCO_3$ separately at a constant temperature water bath for five days (Figure 4.5a). Thereafter, 10 mL from the final solution was withdrawn and titrated with 0.1 M of hydrochloric acid (HCl) pHmetrically to quantify the excess basic compounds in solution (Figure 4.5b). The quantities of carboxylic, hydroxyl and lactonic sites were estimated based on the titration data.

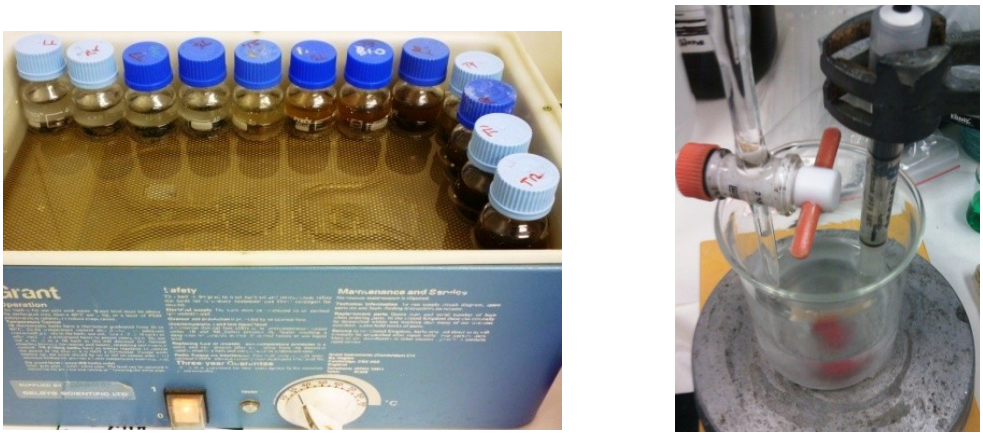

(a) (b)

Figure 4.5 Quantification of active sites: (a) Experimental arrangement; (b) pHmetric titration

On the other hand, zeolite is an aluminosilicate material with a tetrahedral framework structure, in which the presence of Al^{3+} results in a net negative charge as shown in Figure 4.6 (Ghobarkar et al. 1999). Consequently, zeolite requires a positive charge to maintain the neutrality, which can be provided by a proton (H^+) resulting in the formation of a hydroxyl functional group ($-OH^-$) in the zeolite framework (Hill et al. 1999; Rivera et al. 2000).

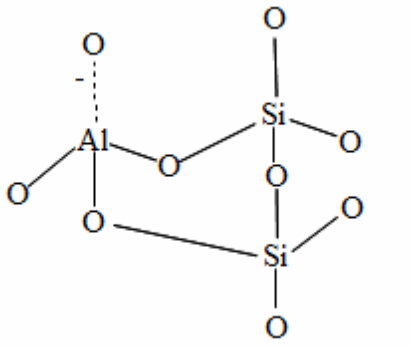

Figure 4.6 Tetrahedral framework of zeolite

Hence, based on Boehm titration philosophy, the amount of total hydroxyl sites present in zeolite was determined by firstly equilibrating 0.5 g zeolite samples with 0.1 M NaOH in excess at a constant temperature water bath for five days (Figure 4.5a; equation 4.4). Then, the amount of NaOH used for neutralising hydroxyl functional group was determined by pHmetrically back titrating the equilibrated solution with 0.1 M HCl (Figure 4.5b; equation 4.5).

$$\text{Ze-OH} + \text{NaOH} \longrightarrow \text{Ze-Na}^{+} + \text{H}_2\text{O} \qquad (4.4)$$

$$\text{NaOH} + \text{HCl} \longrightarrow \text{NaCl} + \text{H}_2\text{O} \qquad (4.5)$$

4.4.4 CONCENTRATIONS OF METAL IONS

Concentrations of metal ions in solution were measured using the ICP-MS (Model: Agilent 7500-cx; Figure 4.7a) and the ICP-OES (Model: Varian Vista-MPX; Figure 4.7b). ICP-MS was used to measure the concentrations of metal ions in very low concentration range (µg/L order), whereas ICP-OES was used for high metal concentration (mg/L). Both ICP-MS and ICP-OES were calibrated as described in Sections 4.5.1 and 4.5.2, respectively.

ICP-MS and ICP-OES require a method to be set up for data acquisition and analysis. A full quantitative analysis with five repetitive measurements was selected in order to increase the precision. Before the analysis, the ICP-MS was tuned in auto-tune mode, whilst the ICP-OES was manually tuned. In ICP-MS, the sample was introduced via a peristaltic pump and mixed with helium or argon gas to produce aerosols. On the other hand, in ICP-OES, the sample was introduced manually and argon gas was used to produce the aerosols. The droplet was sprayed through a chamber to the ICP torch, which strips the electrons of the metal element and ionises it. The ionised metal hits the detector producing a spectrum of electric signals. Concentration of metal ions was calculated using the calibration curve based on the intensity of the electric signal produced.

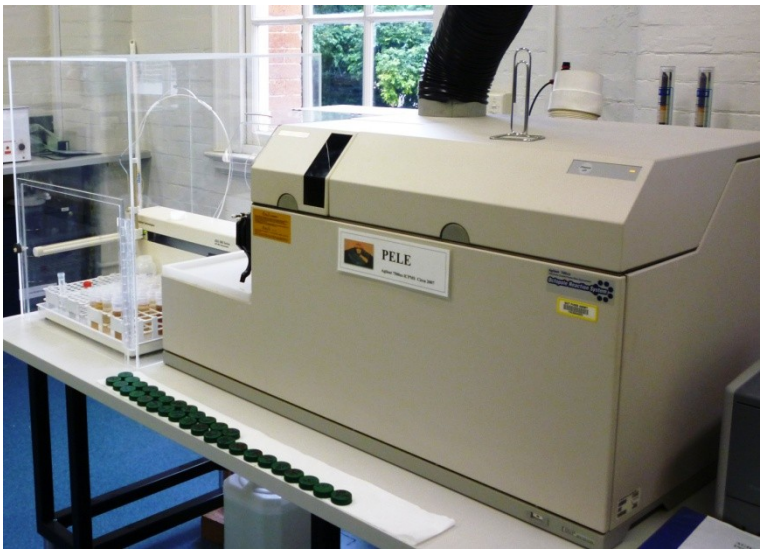

(a)

(b)

Figure 4.7 Inductively Coupled Plasma: (a) Mass Spectrometry; (b) Optical Emission Spectrometry

4.5 CALIBRATION AND VERIFICATION

The equipment used in this study was calibrated using standard calibration methods. The measured data was verified according to the standard verification techniques as discussed below.

4.5.1 INDUCTIVELY COUPLED PLASMA MASS SPECTROMETRY

Calibration

Calibration standards were prepared by diluting the stock multi metal standards sourced from AccuStandard (5% nitric acid matrix) using 5% nitric acid solution to preserve the matrix. Concentrations of calibration standards were 200, 100, 50, 25, 5, 1, 0.1 and 0.01 μg/L. Additionally, blank nitric acid was tested along with calibration standards. The calibration standards were run in ICP-MS and were accepted if coefficient of determination (R^2) was close to 1.

Verification

During the batch experiments, a blank sample containing 5% nitric acid was stirred under similar conditions to the samples to account for any leaching or sorption of metal ions by the consumables. Additionally, internal standards of known concentration was added to each sample, blank and calibration standards and the measured metal concentration was accepted if the response of internal standards was within 60-125% of the calibration blank.

4.5.2 INDUCTIVELY COUPLED PLASMA OPTICAL EMISSION SPECTROMETRY

Calibration

Calibration standards were prepared by diluting the stock multi metal standards of 1000 mg/L concentration prepared using the corresponding metal chlorides. Concentrations of calibration standards were 200, 100, 50, 25, 5, 1 mg/L and the blank. The calibration standards were run in ICP-OES and were accepted if R^2 value was close to 1.

Verification

During the batch experiments, a blank sample containing the buffer solution used for the preparation of metal solution was also stirred under similar conditions to the samples to account for any leaching or sorption of metal ions by the consumables. In order to increase the accuracy of the ICP-OES analysis, calibration reslope was performed after every 20 samples by checking the calibration curve using two standards for the deviation in the slope. The instrument was re-calibrated if the deviation varied by ±5% of the initial slope. In addition, a check standard of 10 mg/L

was tested after every 10 samples and the instrument was re-calibrated if the values varied by ±10%.

4.5.3 pH METER

Calibration

Two-point calibration technique was followed for the pH meter. Standard pH 6.8 and pH 4 solutions were used for this purpose. pH probe was thoroughly rinsed with deionised water and blot dried before first immersing it in pH 6.8 solution for calibration. Then, the probe was calibrated with pH 4 solution.

Verification

The pH meter was checked with pH 6.8 standard after every ten measurements to ensure its performance. The probe was re-calibrated if there was a significant variation (±10%) in pH.

4.5.4 AMMONIA SELECTIVE ION ELECTRODE

Calibration

Ammonia selective electrode was calibrated using freshly prepared NH_4Cl solution of 10^{-1}, 10^{-2}, 10^{-3}, 10^{-4} and 10^{-5} M concentrations. Stock solution of 1 M NH_4Cl was prepared and serial diluted to the required concentration. First, the electrode was kept in diluted NH_4Cl solution for 15 minutes to stabilise it. Then, it was immersed into each standard solution (adjusted to pH 7). The reading was recorded in millivolts when the change in reading was less than 0.2 mV/minute. The electrode was washed using deionised water and blot dried in between measuring each standard.

Verification

Each measurement was taken in triplicate and the mean value was accepted if the error was within ±10%.

4.6 DATA ANALYSIS TECHNIQUES

4.6.1 BASIC STATISTICAL OPERATIONS

Basic statistical operations, such as mean (equation 4.6) and standard deviation (equation 4.7) were used in this study. Standard deviation provides an indication of the error margin in the measurement.

$$\bar{y} = \frac{\sum y_i}{N} \tag{4.6}$$

$$SD = \sqrt{\frac{(y_i - \bar{y})^2}{N - 1}} \tag{4.7}$$

where $\bar{y}$ is the mean of the data, y_i is the i^{th} data point, N is the number of samples and SD is the standard deviation.

4.6.2 LINEAR AND NON-LINEAR REGRESSION

Linear and non-linear regression analyses have been used extensively in practical applications to fit experimental data to theoretical models (Bates and Watts 2008; Foo and Hameed 2010). Theoretical isotherm and thermodynamics models used in this study were in their linearised form. Hence, the corresponding experimental data were fitted using linear regression technique built in Microsoft Excel® software. On the other hand, the Solver add-in in Microsoft Excel® was used for non-linear regression analysis. The model parameters such as kinetics rates were determined when the normalised sum of squares error (SSE) given by the following equation was minimum (Sheppard et al. 2011):

$$SSE = \sum \frac{(\text{Predicted } Q_t - \text{Experimental } Q_t)^2}{(\text{Experimental } Q_t)^2} \tag{4.8}$$

4.6.3 SPEARMAN CORRELATION ANALYSIS

Spearman correlation analysis, a non-parametric method, was used to investigate the kinetics rate-limiting step. The analysis produces a ranking coefficient (r_s) that can be used to test the null hypothesis of no relationship between the variables. Accordingly, there is no correlation if $r_s = 0$. However, r_s values cannot be used to interpret the strength of the relationship between the variables (Bolboaca and Jantschi 2006).

4.6.4 MULTI CRITERIA DECISION MAKING (MCDM) TECHNIQUES

MCDM methods are used to aid the decision making process when multi variable problems are involved. There are various MCDM methods, such as ELECTRE (ELimination and Choice Expressing REality), PROMETHEE and Simple Multi Attribute Ranking Technique (SMART) available for comparing different alternatives based on their performance against a set of evaluation criteria (Keller et al. 1991). In this study, PROMETHEE and GAIA were used since they are generally regarded as more sophisticated techniques compared to the others (Brans et al. 1986; Keller et al. 1991). These methods have been increasingly used in various environmental research studies to evaluate different alternatives against a set of criteria (Carmody et al. 2007; Khalil et al. 2010; Miguntanna et al. 2010).

PROMETHEE algorithm

It is important to note that PROMETHEE does not provide a direct solution to a MCDM problem; rather it only aids to make a decision. Thus, it is the scientist who ultimately makes the decision based on MCDM modelling and the nature of the problem. The PROMETHEE analysis was performed in this study with the help of Decision Lab software (Visual Decision Inc. 2000). The PROMETHEE algorithm used in this software has been explained in detail in several research papers (Keller et al. 1991; Kokot and Phuong 1999) and only a brief description is presented here.

In PROMETHEE, a ranking order is developed according to the net ranking flow, the φ values, for a number of available objects or actions on the basis of a range of

criteria (variables). To calculate the φ values, each criterion must be provided with three conditions: a preference function, a preference order (maximise/minimise) and a weighting. The following steps are performed to calculate the φ values between objects 'a' and 'b':

Step 1: Creation of a difference matrix (d_j) between 'a' and 'b' from raw data matrix:

$$d_j = y_j(a) - y_j(b) \tag{4.9}$$

where y_j (a) and y_j (b) are the data points of objects 'a' and 'b' for criteria y_j.

Step 2: Definition of the preference for 'a' over 'b':

A preference function P (a,b) is used to define the preference for 'a' over 'b' for each criterion. The following preference functions (Table 4.3) are available for the user to choose depending on the characteristics of the criterion:

Table 4.3 Preference functions

Preference function	Shape of the graph[1]	Mathematical expression
Linear	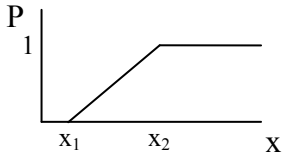	$y(x) = \begin{cases} 0 & x<x_1 \\ mx + c & x_1<x<x_2 \\ 1 & x>x_2 \end{cases}$
V-shape	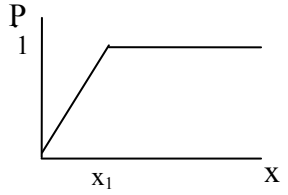	$y(x) = \begin{cases} mx & x<x_1 \\ 1 & x>x_1 \end{cases}$
Level	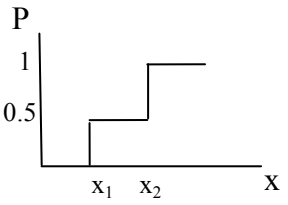	$y(x) = \begin{cases} 0 & x<x_1 \\ 0.5 & x_1\leq x<x_2 \\ 1 & x\geq x_2 \end{cases}$
U-shape	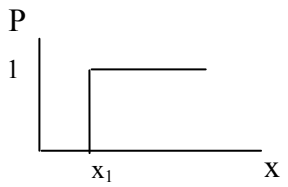	$y(x) = \begin{cases} 0 & x<x_1 \\ 1 & x\geq x_1 \end{cases}$
Usual	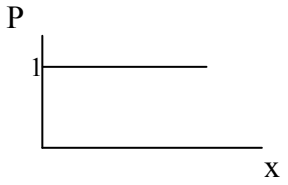	$y(x) = \begin{cases} 0 & x<0 \\ 1 & x\geq 0 \end{cases}$
Gaussian	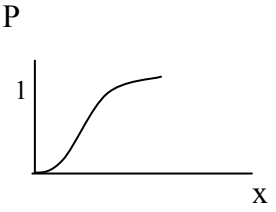	$y(x) = \frac{e^x}{1+e^x}$

Notes:

[1]Legends used in the preference graph: P (preference); X (difference); x_1 (indifference threshold); x_2 (preference threshold)

Step 3: Calculation of global preference index, π:

$$\pi(a,b) = \sum_{j=1}^{k} W_j \times P_j(a,b) \tag{4.10}$$

where W_j is the weight, which is set to 1 by default. However, it can be changed subjectively in case one criterion needs to be emphasized in the selection of objects.

Step 4: Calculation of outranking flows:

$$\text{Positive outranking flow } \varphi^{+}(a) = \frac{1}{(n-1)} \sum_{x \epsilon A} \pi(a,x) \tag{4.11}$$

$$\text{Negative outranking flow } \varphi^{-}(a) = \frac{1}{(n-1)} \sum_{x \epsilon A} \pi(x,a) \tag{4.12}$$

Positive outranking flow corresponds to how much object 'a' is preferred over other objects, while negative outranking flow shows how much other objects are preferred relative to 'a'.

Step 5: Production of partial ranking

Partial ranking of the objects is produced according to the following rules:

Case 1

If $\varphi^{+}(a) > \varphi^{+}(b)$ and $\varphi^{-}(a) < \varphi^{-}(b)$

Or

$\varphi^{+}(a) > \varphi^{+}(b)$ and $\varphi^{-}(a) = \varphi^{-}(b)$

Or

$\varphi^{+}(a) = \varphi^{+}(b)$ and $\varphi^{-}(a) < \varphi^{-}(b)$

Then 'a' is preferred over 'b'.

Case 2

If $\varphi^+(a) = \varphi^+(b)$ and $\varphi^-(a) = \varphi^-(b)$

Then 'a' and 'b' are equally preferred.

Case 3

In all other cases, 'a' and 'b' are incomparable.

Step 6: Production of complete ranking:

Complete ranking is produced based on the net outranking flow, φ (a), calculated from the following equation:

$$\varphi(a) = \varphi^+(a) - \varphi^-(a) \tag{4.13}$$

Complete ranking eliminates the obstacle in comparing 'a' and 'b', even if they are directly incomparable (Case 3 in Step 5). However, the compromise may also reduce the reliability of the outcome. In addition, the φ values can be used to understand how far two objects are discriminated in PROMETHEE ranking. In the case where the difference between the φ values of two objects is over 10% of the whole range, which is the difference between the maximum and the minimum values in the data matrix for that particular criterion, they may be considered well-discriminated (Ni et al. 2009). This is because an error over 10% in the measurement is generally not acceptable in analytical chemistry.

GAIA

GAIA is a PC1 vs. PC2 biplot that provides visual complement to the PROMETHEE ranking. Additionally, it is useful in understanding the correlation between the objects and the variables. The GAIA biplot is the result of principal component analysis of the data matrix constructed from the decomposition of the PROMETHEE

net outranking flows (φ values) (Keller et al. 1991). Espinasse et al. (1997) listed a set of rules to interpret the GAIA biplot. In this study, the following rules were found to be useful for the data interpretation:

1. An acute angle between two vectors indicates positive correlation and they represent similar information. In contrast, two vectors represent conflicting information if the angle between the vectors is obtuse. The information explained by two vectors is considered independent if they are orthogonal. For example, in Figure 4.8, criteria 'a' and 'b' represent similar information, while 'a' and 'c' explain conflicting information. The information represented by vectors 'a' and 'd' is independent.
2. An object that is best performing in a criterion is generally located in the direction of the corresponding criterion vector, e.g. 'A' is the best performing object in criteria 'a' and 'b' (Figure 4.8).
3. Longer criterion vector in the PC1 vs. PC2 space has more influence in ranking the objects, e.g. Criterion 'a' has more influence in ranking the objects compared to the rest (Figure 4.8).
4. The decision axis, also known as the pi-axis, points towards the approximate position of the object that is preferred on the basis of all criteria.
5. Long pi-vector indicates a good decision.

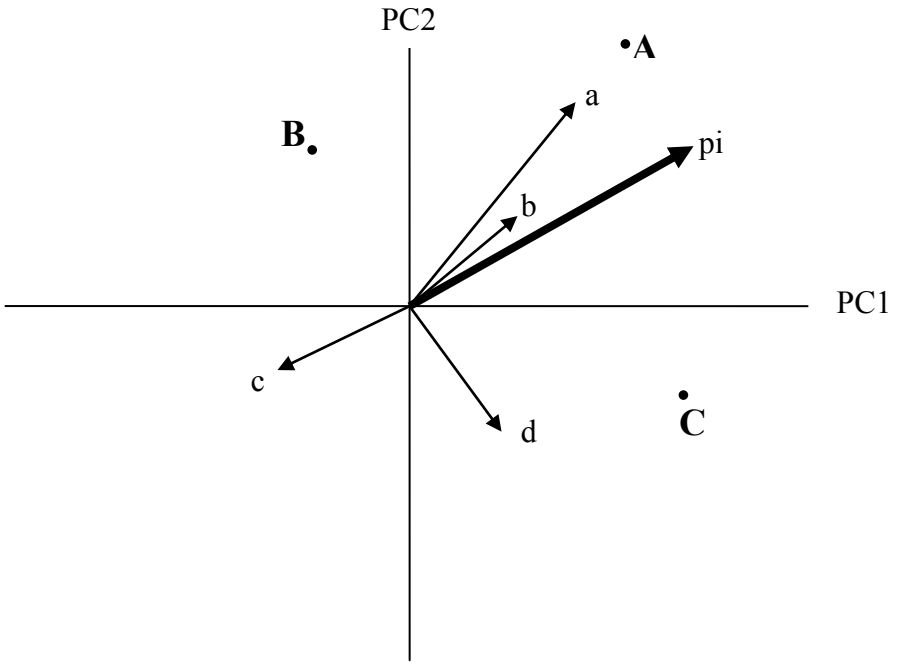

Figure 4.8 GAIA biplot

4.7 SUMMARY

This chapter has discussed the research methods and design adopted to achieve the objectives and aims of the research study. The research methods consisted of critical review of the literature, selection of sorbents for the research project, development of experimental procedures and test methods to generate data to test the research hypotheses and the techniques employed to analyse the data. The experimental procedures primarily described the batch sorption experiments in relation to the evaluation of the metal removal performance of sorbent materials and the definition of sorption mechanisms. Furthermore, the equipment used to measure the relevant parameters such as pH, metal concentration and cation exchange capacity was discussed along with the calibration of the equipment and verification of the measured data to ensure the data quality. Finally, a detailed discussion of the univariate and multivariate analytical techniques employed for the data analysis was provided.

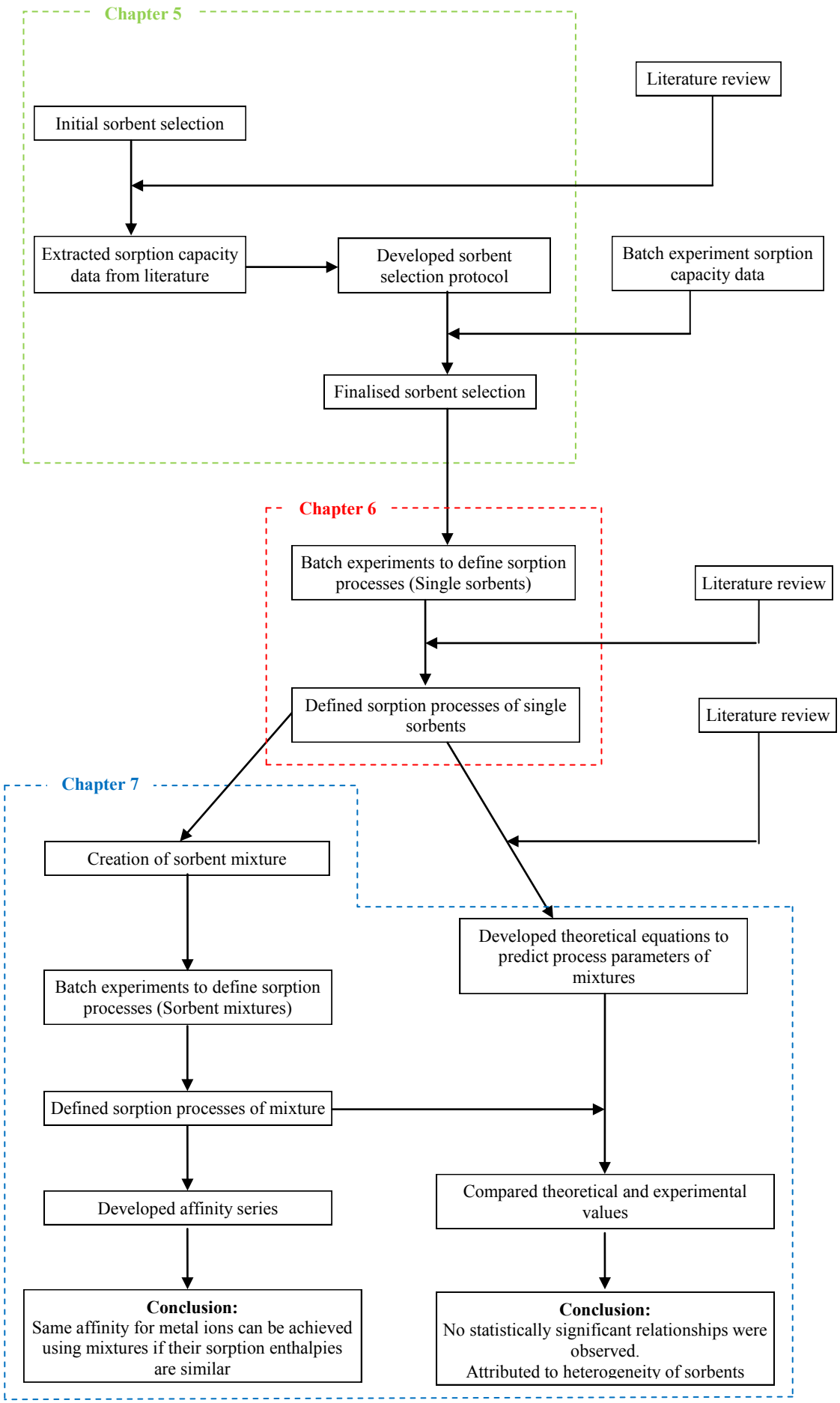

Schematic diagram showing the research methodology and the development of analytical chapters

Chapter 5: Selection of sorbents

5.1 INTRODUCTION

Various materials ranging from low cost agricultural wastes (Ajmal et al. 1998; Garg et al. 2008) to commercial sorbents (Genç-Fuhrman et al. 2007; Minceva et al. 2008) have been investigated for the removal of metals from water. Most of these sorbent materials generally exhibit high metal sorption capacities indicating that they can be used for removing metal ions from polluted waters, such as industrial wastewater and stormwater runoff. However, the effectiveness of a sorbent in removing metals is dependent on the physical and chemical properties of the solution (Section 3.5). For example, a material that is efficient in high pH solution may not be equally effective in removing metals from a low pH system. Therefore, it is important to identify the materials that are efficient for a particular system. This is generally achieved using batch sorption experiments, in which the sorbent is introduced to solution that has similar properties as the particular polluted water.

Several past studies have compared the performance of various sorbent materials in removing metal ions from water with varying degrees of success. This chapter first provides a critical overview of these studies and evaluation methods adopted. Then, a protocol based on Multi Criteria Decision Making (MCDM) technique for sorbent selection was developed using data extracted from published literature. The developed method was applied to the experimental data in order to select the sorbent materials for creating mixtures that can enhance the affinity for the sorption of metal ions commonly found in stormwater. Finally, the results and discussion of this analysis are presented.

5.2 CRITICAL OVERVIEW OF PAST RESEARCH STUDIES ON SORBENT SELECTION

The metal removal performance of sorbent materials is generally evaluated in a single sorbent-single metal solution system (Genc-Fuhrman et al. 2007). However,

comparative studies with the aim of evaluating the performance of various sorbents in removing metals from a multi metal solution are limited. One such study was undertaken by Genc-Fuhrman et al. (2007), in which the performance of eleven different sorbents were assessed for the simultaneous removal of arsenic (As), Cd, Cr, Cu, Ni and Zn from stormwater. The sorbents were ranked based on the distribution coefficient (K_d) as given in equation 5.1:

$$K_d = \frac{Q_e}{C_e} \tag{5.1}$$

Both Q_e and C_e were determined from sorption experiments conducted under similar experimental conditions. Sorbents that had high average K_d values were considered as efficient for the removal of metals. Overall, alumina was the best performing sorbent followed by bauxsol-coated sand and granulated ferric hydroxide, while natural materials, such as zeolite, bark and sand were the least efficient.

A similar study was conducted by Wu and Zhou (2009) to rank various sorbents by adopting a similar approach to that described by Genc-Fuhrman et al. (2007). They found that a mixture of zeolite and a commercial sorbent called ferrosorp Plus was most effective. However, these studies did not consider the economic viability and environmental sustainability, which are critical factors in the real-world decision making process. For example, according to Genc-Fuhrman et al. (2007), alumina emerged as the best performing material because of its high average K_d value. However, it is generally more expensive compared to natural materials such as zeolite and bark. Furthermore, treatment of stormwater may require large amounts of material depending on the amount to be treated. Hence, the use of expensive materials may not be economically feasible.

Based on the data extracted from research literature, Kurniwan et al. (2006) and Babel and Kurniwan (2003) compared the use of selected low cost sorbents with relatively expensive activated carbon for removing metals from wastewater. Their approach was more detailed in comparing the sorbents due to the inclusion of cost analysis, even though sorption capacities remained as the main performance criteria

for evaluation. They concluded that low cost chitosan, zeolite, waste slurry and lignin were the best performing sorbents in terms of both cost and removal performance when compared to activated carbon. Furthermore, zeolite was found to be the best option because it was the least expensive among the best performing low cost sorbents.

In addition to the cost and sorption capacities, factors such as environmental impacts and operational restrictions of using a sorbent often play a vital role in the real-world decision making. This clearly introduces additional criteria, which can transform the analysis to a complex MCDM problem. Though such an elaborate analytical approach has been used in other research areas (Brucker et al. 2004; Mostert et al. 2010), it is not generally undertaken when comparing sorbent materials for the removal of metals. Among various MCDM analytical techniques, PROMETHEE aided by GAIA has been commonly used in selecting the best option/s among several potential alternatives (Keller et al. 1991).

Kokot et al. (1992) used PROMETHEE for selecting suitable microwave digestion methods for solids, whilst Khalil et al. (2004) applied the technique for selecting appropriate sites for sewage effluent renovation. The latter is one of the earliest use of PROMETHEE and GAIA in the field of environmental engineering (Behzadian et al. 2010). Furthermore, Carmody et al. (2007) used PROMETHEE to compare various potential sorbent materials for cleaning oil spills. It is interesting to note that in the study by Carmody et al. (2007), non-technical qualitative criteria, such as ease of use and biodegradability were introduced into the analysis along with the conventional technical criteria, such as sorption and retention capacities. Importantly in the approach by Carmody et al. (2007), the data matrix was expanded stepwise, i.e. by adding one criterion at a time, which was helpful in extracting information on the influence of each criterion in ranking the sorbents. Such an approach could be particularly useful in multi disciplinary forums, where an immediate response regarding the influence of a particular criterion in decision making is of interest.

5.3 EVALUATION OF SORBENT PERFORMANCE USING MCDM METHODS

Firstly, a comprehensive protocol for the evaluation of sorbent materials on their performance in removing metals in water was developed based on PROMETHEE and GAIA techniques. For this purpose, the metal sorption capacities extracted from the data provided in past research publications were used being cognisant of the fact that these sorption capacities were determined under different experimental conditions. As such, it was evident that these values could not be used directly to compare the performance of sorbents in the removal of metals. The sorption capacity data obtained from literature were used only to develop the protocol for sorbent selection. The sorption capacities were determined from the batch sorption experiments that were conducted using water spiked to replicate dissolved metal concentrations in stormwater such as in the case of a tertiary treatment scenario. These sorption capacities were used for identifying the sorbents for further investigation by applying the protocol developed.

5.3.1 PROMETHEE ANALYSIS – CRITERIA

Six sorbents namely seaweed, corncob, sugarcane bagasse, activated carbon, zeolite and clay were evaluated for their performance in the metal removal on the basis of the following criteria:

- Sorption capacity (SC);
- Cost factor (Co.);
- Biodegradability factor (Bio.).
- Environmental factor (En.);
- Operational factor (Op.).

PROMETHEE analysis requires the assignment of three modelling parameters for each criterion: a ranking sense, a preference function and a weighting. A weight of 1 was selected for all criteria in order to ensure all variables were given the same importance in the analysis. The ranking sense and preference function assigned for each criterion are discussed below.

(A) SORPTION CAPACITIES

Two types of metal sorption capacities were used. First was the data extracted from past literature, which were used in developing the protocol for sorbent selection. Second was the sorption capacities determined from the batch experiments conducted using water spiked to replicate stormwater in a tertiary treatment system, which were used for the selection of sorbent materials for further investigation.

PROMETHEE modelling parameters

(a) Ranking sense:

A sorbent with high sorption capacity is preferred for metal removal application. Hence, sorption capacity criterion was maximised.

(b) Preference function:

The sorption capacity data matrix contained values that are very close to each other, e.g. 0.40 and 0.49 mmol/g. Hence, providing indifference threshold values can enhance the discrimination between objects rather than considering the objects with very close values in the low sorption capacity range as dissimilar. Consequently, the linear preference function (Table 4.3) was selected for sorption capacity criterion.

(B) COST FACTOR

Cost of a sorbent generally varies from one geographic location to the other depending on various factors, such as local availability and extraction cost. Sorbents used in this study were specifically purchased for the research study. Therefore, the price may not reflect the actual cost when using them in a practical application. As such, a qualitative criterion, cost factor, was developed by assuming sorbents with no other significant uses are likely to be inexpensive. A value from a scale of 1 to 3 (high cost - 3; moderate cost - 2; low cost - 1) was assigned to each sorbent (Table 5.2) based on whether it has other significant uses (Table 5.1).

Table 5.1 Uses of sorbents

Sorbents	Uses	References
Seaweed (SW)	• Mainly used for human consumption • Important ingredient in certain cosmetic and pharmaceutical products	Mabeau and Fleurence 1993; Bansemir et al. 2006
Corncob (CC)	• Fibre source in animal food • Charcoal production • However, not widely used	Sultana et al. 2007
Sugarcane bagasse (SB)	• Primary source of fuel in sugar mills • Main ingredient in paper and disposable container production	Broek et al. 2000; Horvath et al. 2009
Activated carbon (AC)	• Various environmental applications including water treatment • Medical applications, e.g. in poison and overdose treatment • Gas purification in nuclear reactors	Suzuki 1994; Barnes et al. 2009; Smolka and Schmidt 1997
Zeolite (Z)	• Soil treatment • Odour control	Terzano et al. 2005; Luo and Lindsey 2006
Clay (C)	• Building industry • Agricultural uses	Murray 1991

PROMETHEE modelling parameters

(a) Ranking sense:

This criterion was minimised since low cost sorbents are usually preferred in real-world applications.

(b) Preference function:

Since a value from the 3-point scale was assigned for cost factor, the difference matrix had discrete data, which were best suited in LEVEL preference function. Accordingly, the LEVEL preference function (Table 4.3) was selected.

(C) BIODEGRADABILITY FACTOR

In general, seaweed, corncob and sugarcane bagasse are easily biodegradable, while activated carbon, zeolite and clay do not easily biodegrade.

PROMETHEE modelling parameters

(a) Ranking sense:

Biodegradability is a concern when using a sorbent for the treatment of stormwater for potable application since biodegradation can lead to the growth of harmful microorganisms in water. This can result in significant human health impacts (Pitter and Chudoba 1990). Therefore, the biodegradability criterion was minimised.

(b) Preference function:

The selected preference function was USUAL for this criterion (Table 4.3), which reflects a scale of 1 or 0 (non-biodegradable - 0; biodegradable - 1).

(D) ENVIRONMENTAL FACTOR

Environmental factor corresponds to the direct negative impacts of using a sorbent on the environment, especially on fauna and flora. For example, seaweed harvesting can disturb the delicate balance in the marine environment. Though seaweed farming can help in overcoming this problem, it needs to be monitored to avoid any adverse impacts on the environment. Depending on the raw material source and activation process, production of activated carbon on an industrial scale can have negative impacts on the environment. For example, the use of wood as a raw material can have greater adverse impacts on the environment in comparison to the use of agricultural waste products. Additionally, zeolite and clay are extracted from the earth's surface, which can also lead to adverse impacts on the environment. Corncob and sugarcane bagasse are agricultural products, use of which as sorbents generally do not have any adverse impacts on the environment. Similar to the cost factor, a

value was allocated to each sorbent investigated (Table 5.2) based on a 3-point scale (high impact – 3; moderate impact – 2; low impact – 1).

PROMETHEE modelling parameters

(a) Ranking sense:

The criterion was minimised since it is preferred to keep the adverse impacts on the environment to a low level.

(b) Preference function:

The LEVEL preference function (Table 4.3) was selected for the same reason as applicable to cost factor.

(E) OPERATIONAL FACTOR

Some sorbents release toxic substances or cause discoloration on their introduction to water. It has been reported that zeolite and clay release toxic aluminium to water at low pH (Wang and Peng 2010). Hence, pH of the system must be continuously monitored and controlled to avoid aluminium leaching (Oumi et al. 2001). Similarly, activated carbon can cause discoloration, which can be minimised by washing it thoroughly with water before use. Similarly, corncob, sugarcane bagasse and seaweed can cause discoloration due to leaching of certain organic compounds and extensive chemical pretreatment is required to minimise its occurrence. The 3-point scale system was also used for this criterion and points were allocated as follows:

- 3 - if leachate is toxic and chemical pretreatment is required to avoid leaching;
- 2 - if leachate is not toxic and chemical pretreatment is required to avoid leaching;
- 1 - if leaching can be controlled without any chemical pretreatment.

The points allocated for each sorbent is presented in Table 5.2.

PROMETHEE modelling parameters

(a) Ranking sense:

Leaching of toxic compounds is a serious concern if treated water is intended to be used for potable applications. Similarly, discoloration can create aesthetic concerns. Therefore, this criterion was minimised.

(b) Preference function:

For this criterion, the sorbents were under, either the moderate (2) or low (1) category. Hence, the difference matrix contained either 1 or 0, which is best described by the USUAL preference function (Table 4.3).

5.3.2 DEVELOPMENT OF SELECTION PROTOCOL

The data matrix (Table 5.2) consisted of the sorption capacities extracted from past literature (Table A.1 of Appendix A) and the non-technical criteria discussed in Section 5.3.1.

Table 5.2 Data matrix for PROMETHEE analysis – Published data

	Ni[2]	**Cu[2]**	**Zn[2]**	**Cd[2]**	**Pb[2]**	**Co.[3]**	**Bio.[3]**	**En.[3]**	**Op.[3]**
Function	Linear	Linear	Linear	Linear	Linear	Level	Usual	Level	Usual
Min/Max	Max	Max	Max	Max	Max	Min	Min	Min	Min
Weight	1	1	1	1	1	1	1	1	1
Unit	mmol/g	mmol/g	mmol/g	mmol/g	mmol/g	-	-	-	-
SW[1]	0.61	0.99	0.50	0.76	1.16	3	1	3	2
CC[1]	0.37	0.49	0.40	0.49	0.40	1	1	1	2
SB[1]	2.80	2.09	2.54	2.78	1.51	3	1	1	2
AC[1]	1.72	1.16	0.18	0.17	0.72	3	0	2	1
Z[1]	0.03	0.09	0.05	0.04	0.07	1	0	2	1
C[1]	0.48	0.40	0.23	0.29	0.16	2	0	2	1

Notes:

[1]Seaweed (SW); Corncob (CC); Sugarcane bagasse (SB); Activated carbon (AC); Zeolite (Z); Clay (C)

[2]Sorption capacity of the corresponding metal ion

[3]Cost factor (Co.); Biodegradability factor (Bio.); Environmental factor (En.); Operational factor (Op.)

The matrix consisting of sorption capacities was first analysed using PROMETHEE and GAIA techniques. Then, the data matrix was further expanded by adding cost, environmental, operational and biodegradability factors stepwise and re-analysed using PROMETHEE and GAIA techniques. Table 5.3 summarises each analytical scenario and the corresponding variables used in this study:

Table 5.3 Analytical scenarios and corresponding variables

Scenario	Variables
1	Metal sorption capacity
2	Metal sorption capacity and cost factor
3	Metal sorption capacity, cost and environmental factors
4	Metal sorption capacity, cost, environmental and biodegradability factors
5	Metal sorption capacity, cost, environmental and biodegradability operational factors

(A) SCENARIO 1: METAL SORPTION CAPACITIES

The data matrix for Scenario 1 consisted of sorption capacities of six sorbents for five metals (Table 5.2). The net outranking flow (φ) for Scenario 1 is presented in Table 5.4. According to the φ values, sugarcane bagasse is the most preferred sorbent for the removal of toxic metals as it clearly outranks the rest by a large margin. The difference between the φ values of the second ranked sorbent (seaweed) and sugarcane bagasse is 0.82 scale units, which was over 66% of the whole net outranking flow range (φ = 0.85 to φ = -0.39). On the other hand, the gap between activated carbon and seaweed is not substantial, i.e. less than 1% of the whole range, though seaweed has slightly higher φ value than activated carbon. Hence, seaweed is ranked second, while activated carbon occupies the third rank. Corncob, clay and zeolite have high negative φ values. Thus, they are less preferred for metal removal applications. However, the φ value gap between the less preferred sorbents is less than 10% of the whole range, i.e. they are, arguably, not well separated. As per the above discussion, the sorbents can be divided into three groups:

1. The most preferred sorbent: Sugarcane bagasse
2. The moderately preferred sorbents: Activated carbon and seaweed

3. The less preferred sorbents: Corncob, clay and zeolite

Table 5.4 Net outranking flow values – Published data

Rank	Scenario 1 [2]*SC*		Scenario 2 [2]*SC+Co.*		Scenario 3 [2]*SC+Co.+ En.*		Scenario 4 [2]*SC+Co.+ En.+ Bio.*		Scenario 5 [2]*SC+Co +En. +Op.+Bio.*	
		φ		φ		φ		φ		φ
1	**SB**[1]	0.85	**SB**	0.63	**SB**	0.61	**SB**	0.46	**SB**	0.34
2	**SW**[1]	0.03	**SW**	-0.05	**CC**	-0.02	**AC**	0.01	**AC**	0.07
3	**AC**[1]	-0.01	**CC**	-0.07	**AC**	-0.08	**CC**	-0.06	**Z**	-0.02
4	**CC**[1]	-0.22	**AC**	-0.08	**SW**	-0.15	**Z**	-0.09	**C**	-0.03
5	**C**[1]	-0.29	**Z**	-0.21	**Z**	-0.19	**C**	-0.10	**CC**	-0.12
6	**Z**[1]	-0.39	**C**	-0.22	**C**	-0.21	**SW**	-0.20	**SW**	-0.25

Notes:

[1]Seaweed (SW); Corncob (CC); Sugarcane bagasse (SB); Activated carbon (AC); Zeolite (Z); Clay (C)

[2]Sorption capacity (SC); Cost factor (Co.); Biodegradability factor (Bio.); Environmental factor (En.); Operational factor (Op.)

The grouping of sorbent materials can also be observed in the GAIA biplot (Figure 5.1; 96% variance accounted). On PC1, the most preferred sorbent, sugarcane bagasse, is separated from the rest with high positive scores and the scores of activated carbon and seaweed are close to zero. The less preferred sorbents have negative scores on this axis. Hence, this axis reflects the PROMETHEE ranking order such that the sorbent's score on PC1 reduces when its preference, the φ value, is reduced. When projected on PC1, the vectors related to sorption capacities of metals are closely associated with sugarcane bagasse indicating that it has affinity for the sorption of all metals investigated.

In PC2, the moderately preferred sorbents, i.e. activated carbon and seaweed, have negative scores, whereas the rest have positive scores. Hence, PC2 discriminates the moderately preferred sorbents from the most preferred and the less preferred ones. The projection of the sorption capacity vectors on PC2 shows that activated carbon and seaweed have more affinity to Pb, Cu and Ni than Zn and Cd. In contrast, Zn and Cd are preferred by corncob, clay and zeolite.

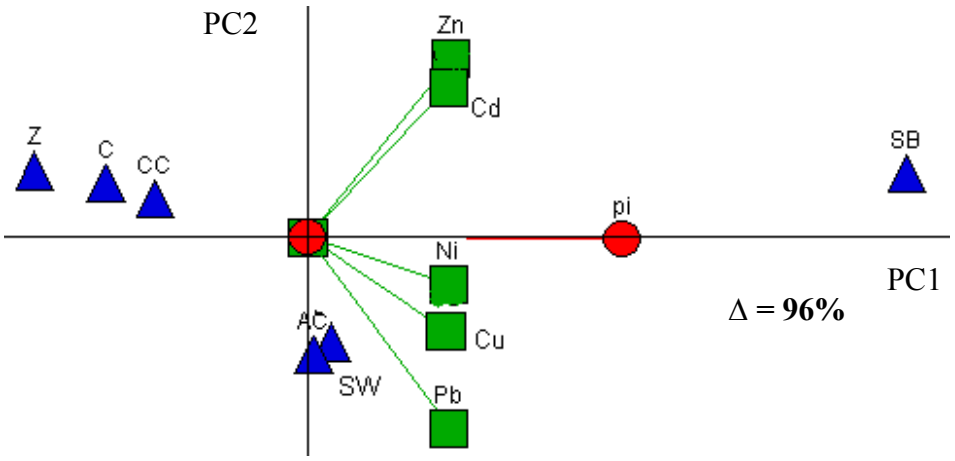

Figure 5.1 GAIA biplot for Scenario 1 – Published data
Legends: Seaweed (SW); Corncob (CC); Sugarcane bagasse (SB); Activated carbon (AC); Zeolite (Z); Clay (C)

The following information can be obtained from PC1 vs. PC2 biplot by applying the rules outlined by Espinasse et al. (1997) (Section 4.6.4). The pi-axis is longer and points towards sugarcane bagasse indicting that it is the preferred sorbent, which is in agreement with the PROMETHEE results. According to the biplot, sorption of Ni, Pb and Cu is strongly associated with sugarcane bagasse, seaweed and activated carbon. Hence, these sorbents are preferred for the sorption of these specific metals. On the other hand, zeolite, corncob and clay are least preferred as they are negatively correlated. Additionally, sugarcane bagasse also performs well in the sorption of Zn and Cd, whereas seaweed and activated carbon are negatively correlated with the sorption of Zn and Cd vectors. Therefore, sugarcane bagasse emerges as the best option for the sorption of Ni, Pb, Cd, Zn and Cu compared to the other sorbents.

(B) OTHER SCENARIOS: EFFECT OF COST, ENVIRONMENTAL, BIODEGRADABILITY AND OPERATIONAL FACTORS

Qualitative criteria such as cost, environmental, biodegradability and operational factors were added to the data matrix stepwise and new PROMETHEE and GAIA analyses were conducted. The φ value for each analytical scenario is presented in Table 5.4. The φ values and the GAIA biplots can be interpreted in detail as explained in Section 5.3.2 (A). However, only important changes in the ranking and the patterns in the GAIA biplots are discussed here.

In Scenario 2, the criterion representing the cost factor was added to the data matrix. The φ value of sugarcane bagasse significantly reduced compared to Scenario 1, though the reduction was not adequate to change its rank due to the very low φ value of the rest of the sorbents. This indicates that the sorption capacity criteria are still influential in ranking sorbent materials. However, the changes in the φ values of other sorbents resulted in modification to the PROMETHEE ranking such that corncob advanced as a moderately preferred sorbent. In the GAIA biplot for Scenario 2 (Figure 5.2; 95% variance accounted), activated carbon and seaweed are negatively correlated to the cost factor, as they are considered relatively expensive, whilst materials that are not used in other economically significant applications such as clay, zeolite and corncob are strongly correlated to the cost vector. According to Table 5.4, the φ value gap between seaweed, corncob and activated carbon was less than 10% of the whole range. Hence, seaweed, corncob and activated carbon should be close to each other in the GAIA biplot. However, corncob is located away from seaweed and activated carbon in the GAIA biplot given in Figure 5.2. This is because of the low cost factor of corncob compared to seaweed and activated carbon, which moved corncob close to the cost vector. Furthermore, the longer pi-axis indicates a good decision and it points in the direction of sugarcane bagasse showing that it is the most preferred sorbent for this scenario.

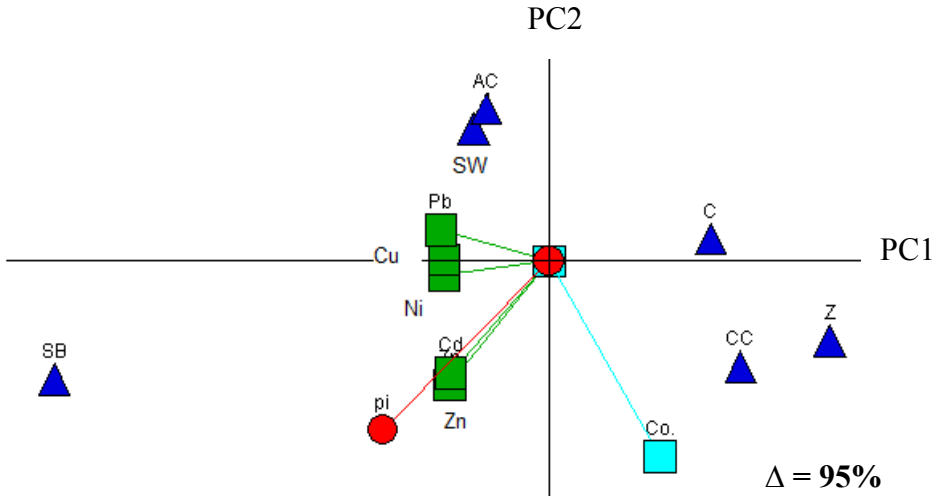

Figure 5.2 GAIA biplot for Scenario 2 – Published data
Legends: Seaweed (SW); Corncob (CC); Sugarcane bagasse (SB); Activated carbon (AC); Zeolite (Z); Clay (C)

When the environmental factor criterion was added to the matrix (Scenario 3), corncob and activated carbon moved to the second and third rank, respectively, while seaweed dropped to the fourth rank. According to the GAIA biplot for Scenario 3 (Figure 5.3; 94% variance accounted), seaweed and activated carbon are negatively correlated with cost and environmental factors, which is consistent with the data matrix in Table 5.2. According to the φ values presented in Table 5.4, seaweed is expected to be located near to zeolite and clay in the GAIA biplot (Figure 5.3). This is because cost and environmental factors were minimised in PROMETHEE analysis and therefore, the sorbent that has low values for these factors stays closer to the vectors corresponding to cost and environmental factors. Seaweed has high values for cost and environmental factors (Table 5.2), which moved seaweed away from the cost and environmental vectors. Thus, it is not positioned near zeolite and clay. The length of environmental and cost vectors is approximately the same. Thus, the influence of both factors in discriminating the objects is similar.

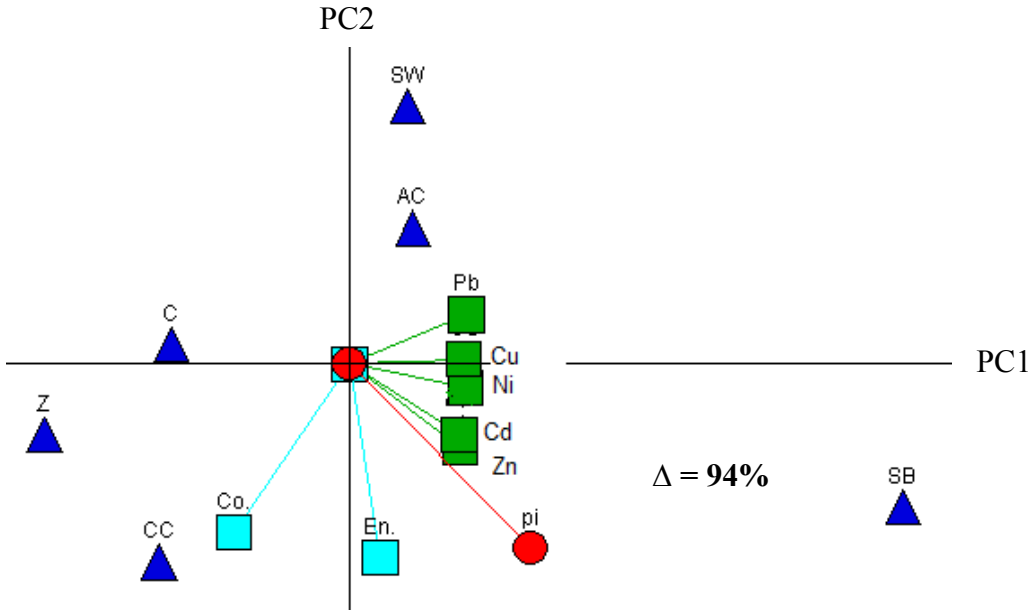

Figure 5.3 GAIA biplot for Scenario 3 – Published data
Legends: Seaweed (SW); Corncob (CC); Sugarcane bagasse (SB); Activated carbon (AC); Zeolite (Z); Clay (C)

Addition of the biodegradability factor to the data matrix (Scenario 4) resulted in changes in PROMETHEE ranking and the φ values. Especially, zeolite and clay moved to the fourth and fifth ranks, respectively. Furthermore, the φ value of seaweed was further reduced. Hence, it eventually became the least preferred sorbent, while sugarcane bagasse remained the most preferred. However, the

introduction of the biodegradability factor reduced the length of the vector representing the environmental factor in Scenario 4 (Figure 5.4; 84% variance accounted). Hence, the discriminating power of the environmental factor weakened in the presence of the biodegradability factor.

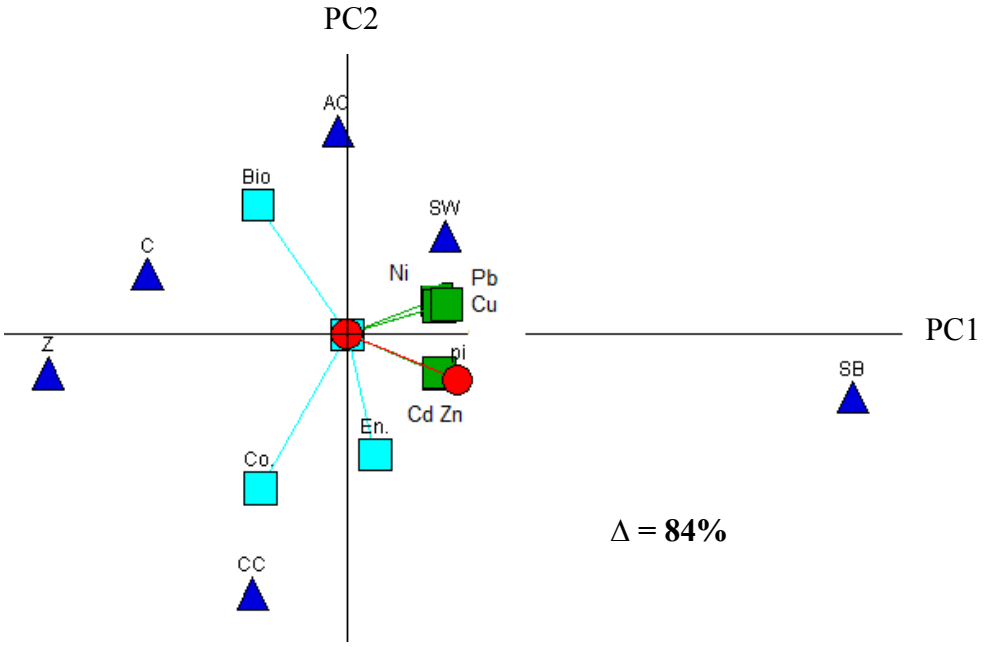

Figure 5.4 GAIA biplot for Scenario 4 – Published data
Legends: Seaweed (SW); Corncob (CC); Sugarcane bagasse (SB); Activated carbon (AC); Zeolite (Z); Clay (C)

Finally, the operational factor criterion (Scenario 5) was added to the data matrix. Zeolite and clay advanced further to the third and fourth ranks, respectively, while corncob dropped to the fifth rank (Table 5.4). The influence of the environmental factor was further reduced when the operational factor was introduced to the data matrix in Scenario 5 (Figure 5.5; 84% variance accounted). In such cases, sorption capacities, cost, biodegradability and operational factors were primarily responsible for the PROMETHEE ranking.

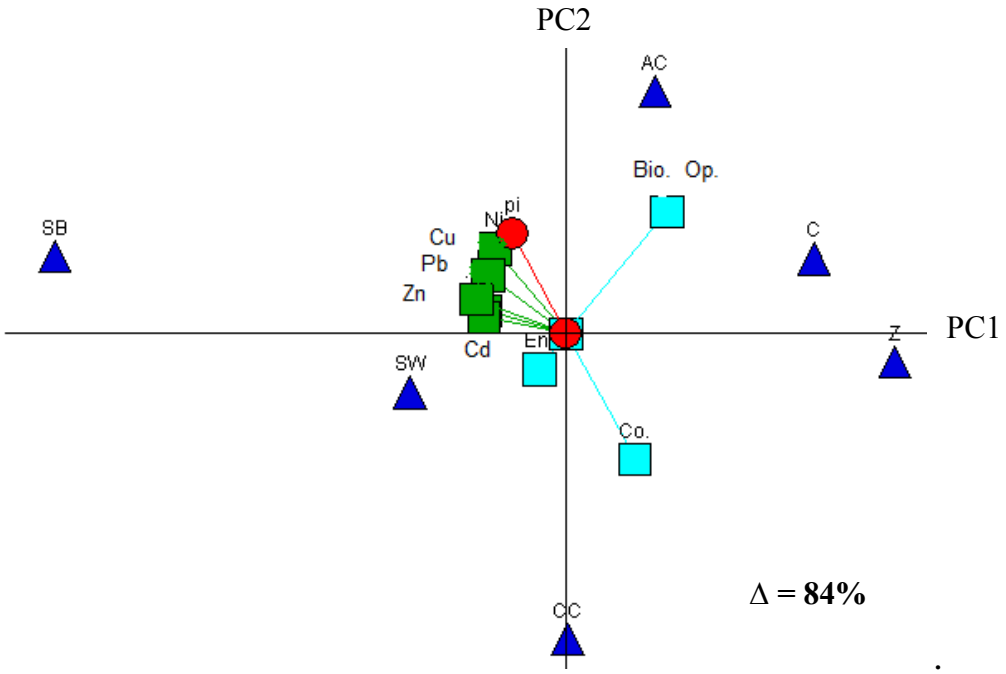

Figure 5.5 GAIA biplot for Scenario 5 – Published data
Legends: Seaweed (SW); Corncob (CC); Sugarcane bagasse (SB); Activated carbon (AC); Zeolite (Z); Clay (C)

Overall, sugarcane bagasse remained as the best sorbent for all scenarios, that is, the φ value gap between sugarcane bagasse and second ranked sorbent was always over 10% of the whole range, even though its φ values reduced significantly from Scenario 1 (φ = 0.85) to Scenario 5 (φ = 0.34). Activated carbon was considered as the next best performing sorbent since it occupied the second and third ranks in almost all scenarios. Though seaweed performed well in the first two scenarios, it was the least preferred sorbent when all the criteria were considered. Corncob performed well in Scenarios 2 and 3. However, on the basis of all criteria, it was ranked in the fifth place. Hence, corncob could be considered as one of the best options when cost and environmental factors are important in decision making. Zeolite and clay exhibited similar behaviour throughout the analysis. On the basis of all the criteria, zeolite and clay could be considered as good options, though not the best.

The discrimination of sorbents in the GAIA biplots from Scenario 2 to Scenario 5 did not clearly explain the PROMETHEE ranking as it did in Scenario 1. This is because the location of the sorbent materials was rearranged when a new criterion was introduced. For example in PC1, sugarcane bagasse had positive scores in Scenarios 3 and 4 and negative scores in Scenarios 1 and 2. This was due to the rearrangement

of the sorption capacity vectors due to the introduction of other factors to the data matrix. This confirmed that the discrimination of sugarcane bagasse was primarily influenced by the sorption capacity rather than the other factors. Activated carbon was negatively correlated to the cost vector in all scenarios investigated. Hence, the position of activated carbon in GAIA biplots was primarily determined by the cost vector. Similarly, seaweed appeared to be influenced by all qualitative criteria since it generally had negative correlation with these vectors. On the other hand, biodegradability and cost factors had a significant influence in discriminating clay and zeolite. Clay and zeolite were generally close to each other in all scenarios as in the case with their φ values, which were almost the same for the entire analysis.

It is important to note that PROMETHEE and GAIA techniques describe a compromise scenario. Hence, it is the individual user's discretion to decide which compromise best suits requisite objective/s. For example, in terms of metal removal (Scenario 1), seaweed performed better than zeolite. However, when all the criteria were considered (Scenario 5), seaweed was less preferred in comparison to zeolite. Hence, if the removal performance is the prime concern at the expense of the rest of the criteria, seaweed is a better option than zeolite. In addition, the GAIA biplots demonstrated how each criterion is correlated to the others and the effect of the compromise of one criterion on the others. An interesting example is the correlation between the cost factor and the sorption capacity in Scenario 5 (Figure 5.5), which showed that they both were negatively correlated. In other words, the cost will increase if a high performing sorbent is to be used.

The univariate analysis based solely on K_d values employed in studies such as by Genc-Fuhrman et al. (2007) and Wu and Zhou (2009) is limited to ranking the materials based only on their metal sorption ability. In contrast, the protocol developed in this chapter based on a multi criteria decision making method, PROMETHEE and GAIA, is comprehensive as the sorbent materials can be ranked on the basis of a set of criteria and the underlying correlations between criteria and objects can be investigated. The GAIA analysis was particularly useful in predicting the metal affinities of sorbents. Furthermore, non-technical criteria that are important in real-world decision making such as cost and environmental impacts were also incorporated into this approach.

5.3.3 SELECTION OF SORBENTS

The protocol developed in Section 5.3.2 was applied on the basis discussed above, to the data matrix consisting of the sorption capacities determined from the batch experiments, with the aim of selecting suitable sorbents for creating mixtures to enhance the affinity for the sorption of metal ions in water (Table A.2 in Appendix A). The data matrix for the analysis is presented in Table 5.5. Two factors were primarily considered in the selection of sorbents:

- Affinity of the sorbents for specific metals (Based on Scenario 1);
- Overall performance on the basis of metal sorption capacity, biodegradability, cost, environmental and operational factors (Based on Scenarios 1-5).

Table 5.5 Data matrix for PROMETHEE analysis – Experimental data

	[2]Al	[2]Cr	[2]Ni	[2]Cu	[2]Zn	[2]Cd	[2]Pb	[3]Co.	[3]Bio.	[3]En.	[3]Op.
Function	Linear	Linear	Linear	Linear	Linear	Linear	Linear	Level	Usual	Level	Usual
Min/Max	Max	Max	Max	Max	Max	Max	Max	Min	Min	Min	Min
Weight	1	1	1	1	1	1	1	1	1	1	1
Unit	µmol/g	µmol/g	µmol/g	µmol/g	µmol/g	µmol/g	µmol/g	-	-	-	-
[1]SW	0.08	0.40	0.75	0.47	0.34	0.08	0.13	3	1	3	2
[1]CC	0.07	0.06	0.09	0.06	0.03	0.04	0.03	1	1	1	2
[1]SB	0.00	0.50	0.27	0.25	0.08	0.16	0.05	3	1	1	2
[1]AC	0.00	0.10	0.25	0.01	0.04	0.10	0.02	3	0	2	1
[1]Z	0.00	0.31	0.28	0.39	0.08	0.20	0.50	1	0	2	1
[1]C	0.00	0.42	0.42	0.53	0.00	0.31	0.27	2	0	2	1

Notes:

[1]Seaweed (SW); Corncob (CC); Sugarcane bagasse (SB); Activated carbon (AC); Zeolite (Z); Clay (C)

[2]Sorption capacity of the corresponding metal ion

[3]Cost factor (Co.); Biodegradability factor (Bio.); Environmental factor (En.); Operational factor (Op.)

(A) SCENARIO 1 – METAL SORPTION CAPACITIES

The data matrix for Scenario 1 consisted of sorption capacities of the six sorbent materials for seven metals and the rank order obtained from PROMETHEE analysis is presented in Table 5.6. According to the φ values, seaweed is the most preferred sorbent followed by clay, zeolite, sugarcane bagasse, corncob and activated carbon. The gaps in φ value between adjacent sorbents in PROMETHEE ranking are generally over 10% of the whole range. Thus, the sorbents are generally well separated. However, the gap between zeolite and clay is about 10% indicating that these sorbents can almost be grouped together.

Table 5.6 Net outranking flow values – experimental data

Rank	Scenario 1 [2]*SC*		Scenario 2 [2]*SC+Co.*		Scenario 3 [2]*SC+Co.+En.*		Scenario 4 [2]*SC+Co.+En.+Bio.*		Scenario 5 [2]*SC+Co.+En.+Op.+Bio.*	
		φ		φ		φ		φ		φ
1	[1]**SW**	0.41	**SW**	0.29	**SW**	0.18	**Z**	0.20	**Z**	0.23
2	[1]**C**	0.19	**Z**	0.18	**Z**	0.15	**C**	0.19	**C**	0.23
3	[1]**Z**	0.11	**C**	0.17	**C**	0.14	**SW**	0.10	**SW**	0.04
4	[1]**SB**	-0.07	**SB**	-0.12	**SB**	-0.05	**SB**	-0.11	**SB**	-0.15
5	[1]**CC**	-0.26	**CC**	-0.14	**CC**	-0.07	**CC**	-0.12	**CC**	-0.17
6	[1]**AC**	-0.37	**AC**	-0.38	**AC**	-0.35	**AC**	-0.26	**AC**	-0.18

Notes:

[1]Seaweed (SW); Corncob (CC); Sugarcane bagasse (SB); Activated carbon (AC); Zeolite (Z); Clay (C)

[2]Sorption capacity (SC); Cost factor (Co.); Biodegradability factor (Bio.); Environmental factor (En.); Operational factor (Op.)

Further information regarding the PROMETHEE ranking can be obtained from the GAIA biplot (Figure 5.6; 83% variance accounted). The sorbents that occupy the first four ranks have positive scores on PC1 and their location reflects the PROMETHEE order except for seaweed, which has low scores, even though it is ranked first. The reason for this exception is that seaweed, which has a high sorption capacity for Ni and Zn, has relatively weaker discrimination power on PC1 as a result of the low loading of Ni and Zn vectors when projected on PC1. Furthermore,

the poor performers, i.e. activated carbon and corncob, have negative scores on PC1. All metal sorption capacities have an influence in the distribution of sorbents on PC1 except for Zn.

Activated carbon, zeolite, clay and sugarcane bagasse have positive scores on PC2, while seaweed has a negative score. Corncob is close to 0 on the PC2 axis. This discrimination is influenced mainly by Al, Ni and Zn and to a relatively lesser extent by Cu, Cr, Cd and Pb. High negative score for seaweed is attributed to the influence of Ni, Zn and Al, for which seaweed has a high sorption capacity. Similarly, zeolite and clay have positive scores due to the influence of the high sorption capacities for Cd and Pb.

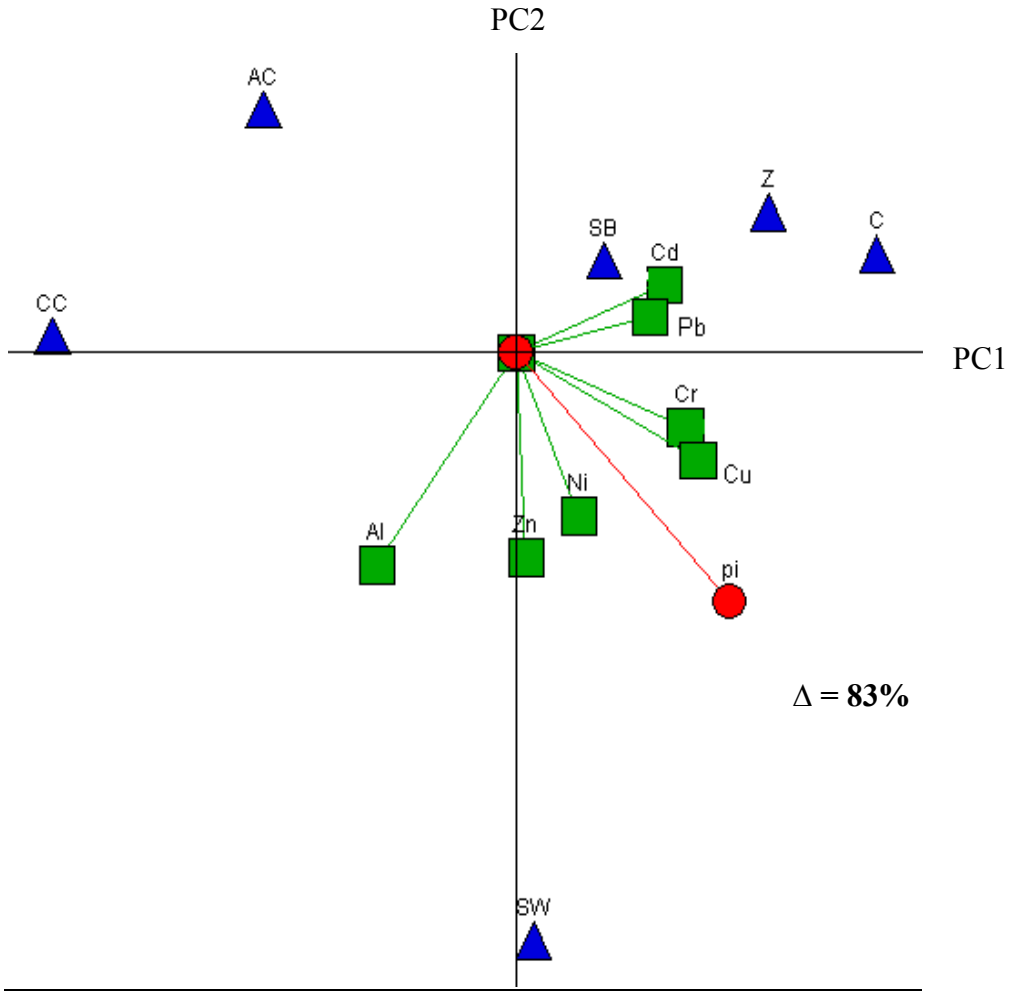

Figure 5.6 GAIA biplot for Scenario 1 – Experimental data
Legend: Seaweed (SW); Corncob (CC); Sugarcane bagasse (SB); Activated carbon (AC); Zeolite (Z); Clay (C)

The most important information that can be extracted from the GAIA biplot is the correlation between variables and objects using the rules described in Section 4.6.4. In Figure 5.6, it can be observed that the vectors are approximately the same size indicating that the sorption capacity for every metal ion has about equal weight in PROMETHEE ranking of sorbent materials. Furthermore, Pb and Cd vectors point towards zeolite and clay indicating that these sorbent materials have a relatively high affinity for Pb and Cd sorption. This was in agreement with the affinity series reported for zeolite and clay in past studies (Zamzow et al. 1990; Malliou et al. 1992; Kwon et al. 2010).

Similarly, according to Figure 5.6, seaweed exhibits high affinity for the sorption of Al, Zn, Ni and Cr in comparison to the rest of the sorbent materials. In the case of sugarcane bagasse, it is close to Pb and Cd vectors indicating that it has some affinity for these metal ions. Corncob did not perform well in the sorption of metals except for Al, for which it had weaker affinity relative to seaweed. Activated carbon was the least preferred sorbent since it performed poorly in the sorption of all of the investigated metals relative to other sorbents. It could possibly be due to the characteristics of activated carbon used in the study, i.e. untreated activated charcoal, which is known to have reduced affinity for cations (Boehm 2002). In the case of Cu, seaweed, zeolite and clay approximately have equal affinity. The decision vector in the GAIA biplot is long indicating a good decision. In addition, the decision vector roughly bisects the acute angle formed by zeolite and clay with seaweed, though the axis leans towards seaweed. This reflects the outcome of PROMETHEE analysis, in which the ranking was in the order of seaweed > clay ≈ zeolite.

It is hypothesised that various factors such as physico-chemical properties of metals, sorbents and solution, sorption kinetics, and sorption thermodynamics are responsible for the above-observed differences in the affinity of sorbents for metals. A detailed discussion of the factors influencing the affinity of selected sorbents for the sorption of metals can be found in Chapters 6 and 7.

(B) OTHER SCENARIOS: EFFECT OF COST, ENVIRONMENTAL, BIODEGRADABILITY AND OPERATIONAL FACTORS

The data matrix was expanded by adding the qualitative criteria, such as cost, environmental, biodegradability and operational factors progressively in order to rank the sorbent materials under different analytical scenarios. The φ value for each analytical scenario is presented in Table 5.6. The φ values and the GAIA biplots can be interpreted in detail similar to the discussion in Section 5.3.3 (A). However, only the changes in PROMETHEE ranking and the GAIA biplots are discussed here.

The data matrix was expanded in Scenario 2 by adding the cost factor. In the GAIA biplot for Scenario 2 (Figure 5.7; 72% variance accounted), the cost vector was approximately equal to the sorption capacity vectors showing that sorption capacities and cost factor have equal importance in the ranking of sorbent materials. The low cost factor of zeolite and corncob contributed significantly to the increase in their φ values, whereas the relatively high cost factor of sugarcane bagasse and seaweed reduced their φ values. Compared to Scenario 1, there was a change in the second and third ranks due to the increase in the φ value of zeolite, which advanced to the second rank. However, the φ values of zeolite and clay were the same. Seaweed was still the most preferred sorbent, though its φ value reduced significantly. There was no significant difference in the φ value of activated carbon. Activated carbon was already low performing in terms of metal sorption capacity. Hence, cost factor has a relatively minor effect in the discrimination of activated carbon though the GAIA biplot showed a correlation between activated carbon and cost vector. Similarly, the influence of the cost factor on the ranking of clay was not significant since the object, clay, is approximately perpendicular to the cost vector despite the fact that clay is only moderately expensive. This is the reason why the φ value of clay in Scenario 2 (Table 5.6) is not significantly different from that in Scenario 1.

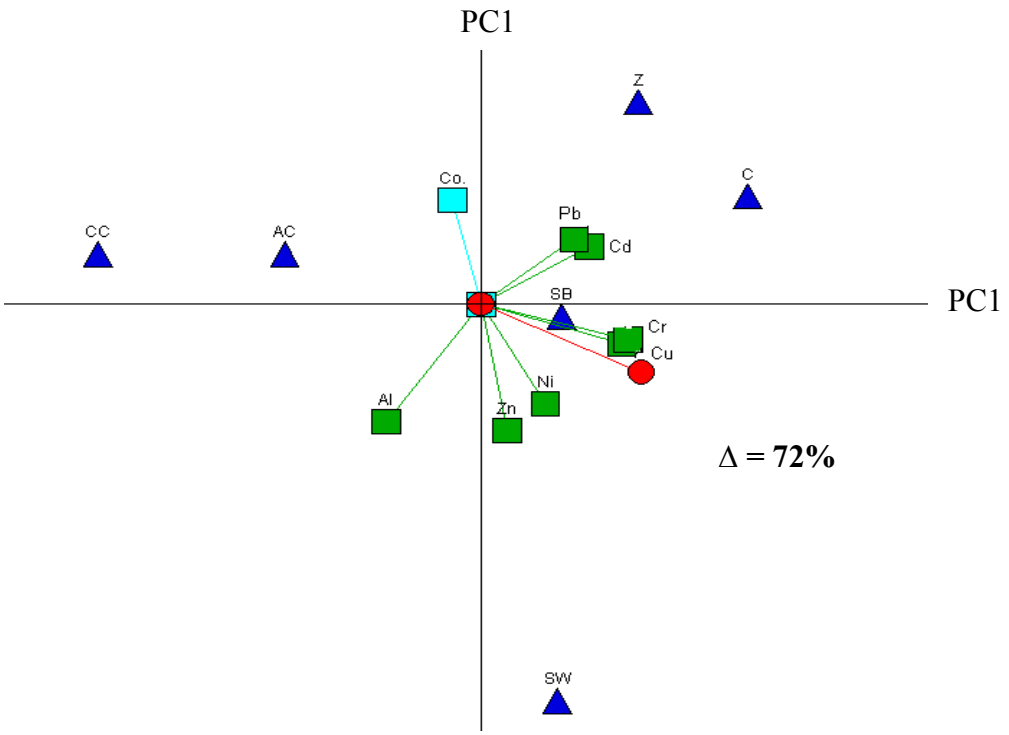

Figure 5.7 GAIA biplot for Scenario 2 – Experimental data
Legend: Seaweed (SW); Corncob (CC); Sugarcane bagasse (SB); Activated carbon (AC); Zeolite (Z); Clay (C)

The data matrix was further expanded in Scenario 3 by including the environmental factor. The ranking order remained the same, though the φ value for seaweed reduced significantly due to the potential negative environmental impact of using it as a sorbent material. The introduction of the environmental factor in Scenario 3 slightly reduced the influence of the cost factor in the discrimination of sorbents as evident in the corresponding GAIA biplot (Figure 5.8; 71% variance described), in which the length of the cost vector is smaller than in Scenario 1. Additionally, the pi-axis has further moved away from the direction of seaweed towards the direction of clay and zeolite. This indicates that the preference for the former has reduced in favour of the latter. This is primarily due to the fact that cost and environmental vectors are negatively correlated to seaweed, while positively correlated to clay and zeolite. However, according to the PROMETHEE ranking, seaweed still occupied the first rank, though the φ value gap between seaweed, zeolite and clay was small, i.e. less than 8%. This confirmed that the sorption capacity vectors still dominated the ranking compared to the cost and environmental factors as clearly evident in the GAIA biplot (Figure 5.8), in which the length of the environmental and cost vectors are relatively smaller than the sorption capacity vector.

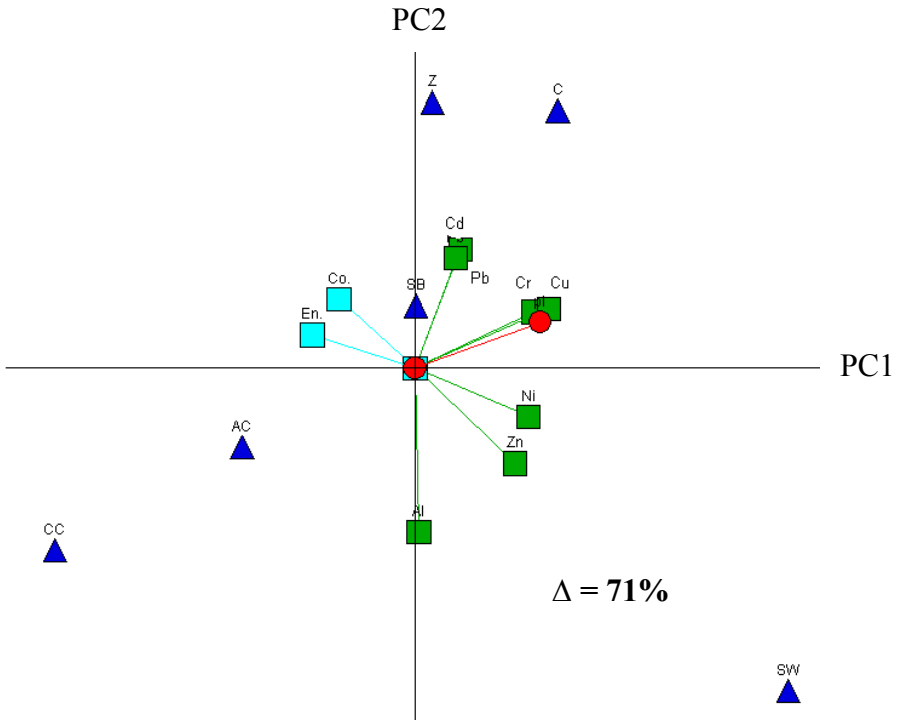

Figure 5.8 GAIA biplot for Scenario 3 – Experimental data
Legend: Seaweed (SW); Corncob (CC); Sugarcane bagasse (SB); Activated carbon (AC); Zeolite (Z); Clay (C)

However, a decisive reduction in the φ value for seaweed occurred when the biodegradability criterion was introduced to the data matrix (Scenario 4). The φ value of seaweed was substantially reduced to the extent that seaweed dropped to the third rank, while zeolite and clay moved to the first and second ranks, respectively. The φ value gap between clay and zeolite was negligible. However, the gap was over 20% of the whole range between seaweed and clay or zeolite. This showed that the ranking of clay and zeolite is arguably the same, while seaweed was well separated in the third rank from zeolite and clay. The corresponding GAIA biplot is presented in Figure 5.9 (70% variance accounted). The decision axis moved further away from seaweed reflecting the PROMETHEE ranking and the φ values tabulated in Table 5.6 for Scenario 4. Furthermore, the introduction of the biodegradability vector slightly reduced the size of sorption capacity vectors indicating that the influence of sorption capacities in ranking sorbents has reduced. This is in agreement with the PROMETHEE ranking, in which zeolite and clay were ranked in the first two places, even though their correlation with sorption capacity vectors was weaker than with

seaweed. In contrast, they are strongly correlated to the cost, environmental and biodegradability vectors.

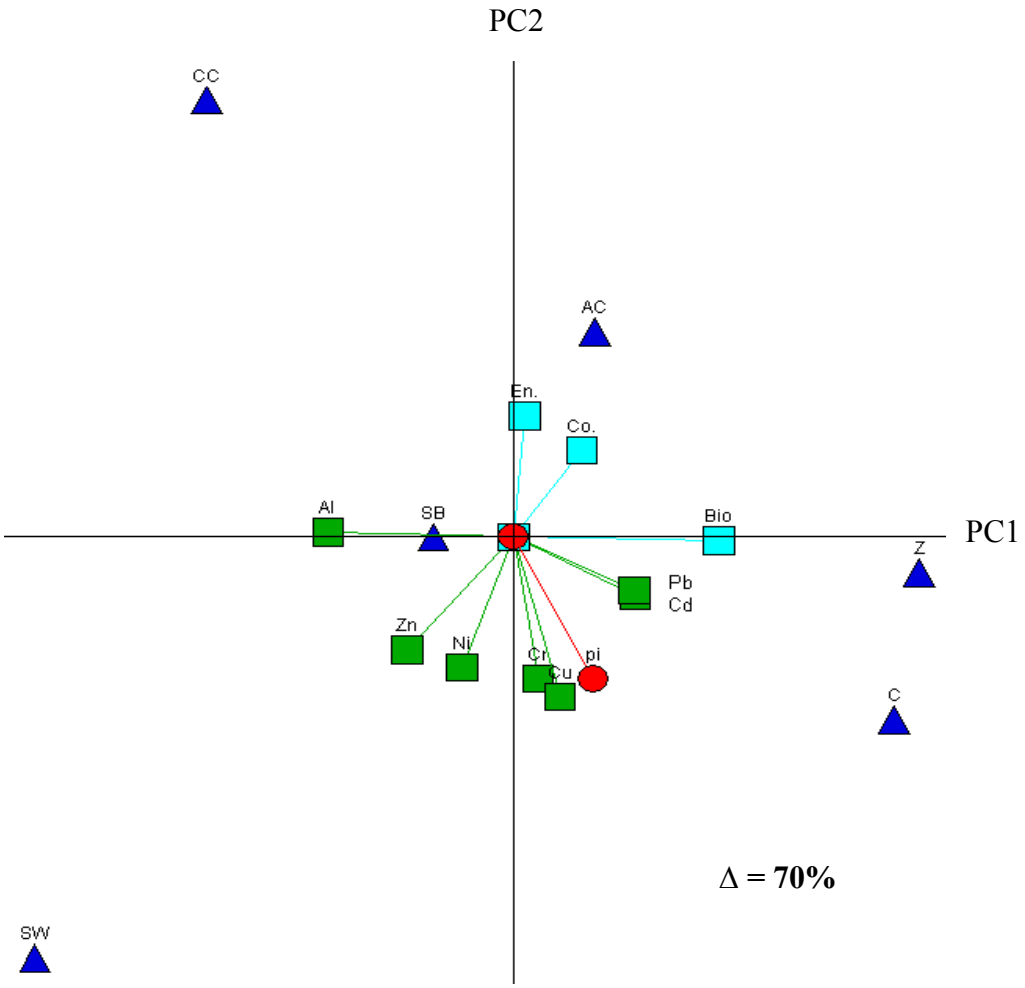

Figure 5.9 GAIA biplot for Scenario 4 – Experimental data
Legend: Seaweed (SW); Corncob (CC); Sugarcane bagasse (SB); Activated carbon (AC); Zeolite (Z); Clay (C)

The criterion related to the operational factor was added to the data matrix (Scenario 5). The PROMETHEE ranking was similar to that of Scenario 4. However, the φ values of zeolite and clay increased, whilst that of seaweed decreased. As a result, zeolite and clay outranked seaweed by a large margin, i.e. the φ value gap was about 40% of the whole range. Hence, it can be concluded that considering the overall performance of the sorbent materials on the basis of all criteria, zeolite and clay were the best performing sorbents followed by seaweed, while sugarcane bagasse, corncob and activated carbon were the least preferred. From the GAIA biplot for Scenario 5 (Figure 5.10; 70% variance accounted), it can be observed that length of the vectors

related to the sorption capacities, cost, environmental, biodegradability and operational factors are approximately equal. Hence, they have approximately equal influence in ranking sorbent materials. Therefore, when analysing the complete data matrix, zeolite and clay become highly preferred due to their low cost, relatively low negative environmental impacts, non-biodegradability and reasonably good metal sorption capacity. On the other hand, despite its superior removal capacity, seaweed was ranked third due to its relatively high cost, high negative environmental impacts and biodegradable nature.

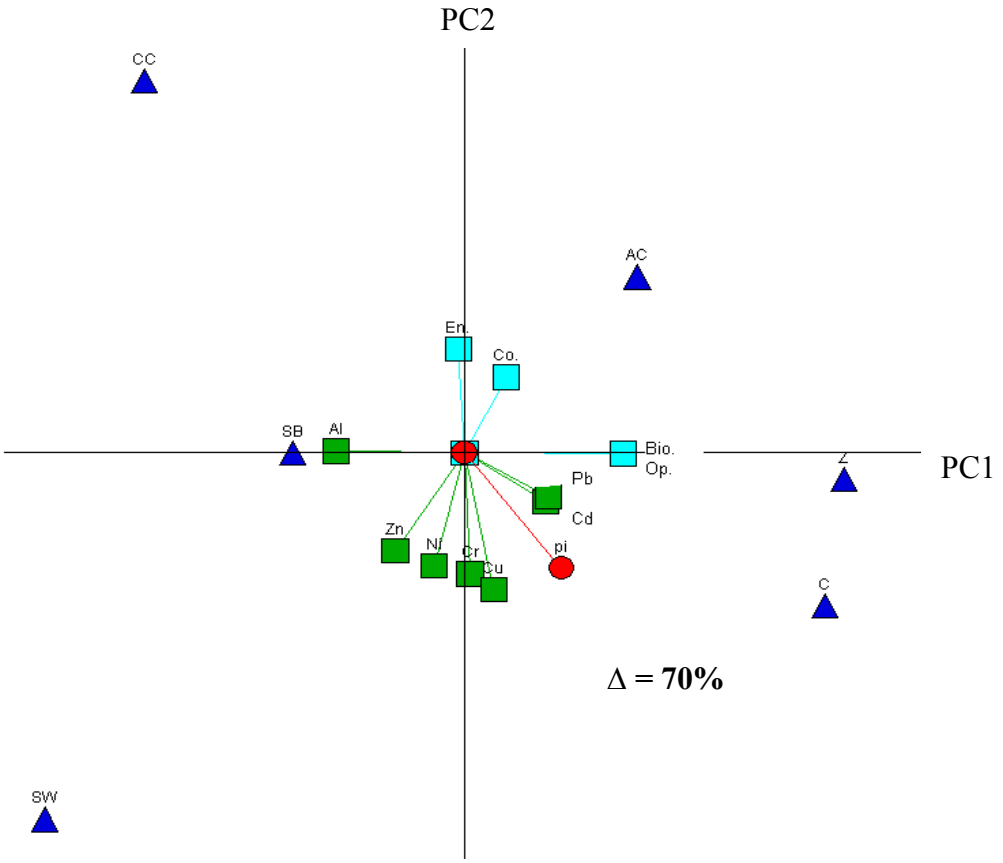

Figure 5.10 GAIA biplot for Scenario 4 – Experimental data
Legend: Seaweed (SW); Corncob (CC); Sugarcane bagasse (SB); Activated carbon (AC); Zeolite (Z); Clay (C)

In general, for all Scenarios, the gaps in φ values between sorbents are over 10% of the whole range, except between clay and zeolite. This indicates that the sorbents were generally well separated. The PROMETHEE ranking order reflected the raw data matrix, in which seaweed, clay and zeolite had high sorption capacity for

metals, whilst sugarcane bagasse, corncob and activated carbon generally exhibited low sorption capacity. It is interesting to note that the affinity pattern generally remained the same for all analytical scenarios. This indicated that affinity illustrated in the GAIA biplots can be used as a reliable guide. Based on the affinity pattern and the overall performance on all the criteria, zeolite, seaweed and clay were selected for further investigation.

5.4 CONCLUSIONS

Commonly, univariate techniques are used to compare the performance of sorbent materials in removing metals in water. However, economic, environmental and operational factors inherent in using sorbents are important in real-world decision making. Therefore, the application of MCDM techniques such as PROMETHEE and GAIA are appropriate for the selection of sorbents for metal removal due to the influence of a range of factors. Consequently, a multi criteria analytical protocol for sorbent selection was developed based on PROMETHEE and GAIA using the sorption capacity data extracted from past literature. The advantages of using the developed protocol over univariate analysis for sorbent evaluation include the understanding of the underlying correlation between criteria and objects, which can be used as an important guide for predicting metal affinities of sorbents.

Batch sorption experiments were conducted using water spiked to replicate typical stormwater quality in order to determine the metal sorption capacities for sorbent evaluation. The analytical protocol was applied to the data matrix, which consisted of experimental sorption capacities, in order to select suitable sorbents for creating sorbent mixtures to enhance the affinity for the sorption of metal ions in urban stormwater. Two analytical scenarios, which were primarily considered with regards to the selection of sorbent materials were their affinity series and overall performance on the basis of all selection criteria, i.e. metal sorption capacity, cost, environmental, operational and biodegradability factors. According to the PROMETHEE ranking, overall, zeolite, clay and seaweed ranked best, whilst sugarcane bagasse, corncob and activated carbon performed poorly. Based on the GAIA biplot, it was noted that seaweed had strong affinity for the sorption of Al, Ni,

Cr and Zn, whereas Pb and Cd were preferred by zeolite or clay. Seaweed, zeolite and clay have approximately similar affinity for Cu. This conclusion is generally in agreement with the findings reported in research literature thereby confirming that the findings from this study can be used as a reliable guide to predicting the sorption affinities of sorbent materials. Hence, zeolite, seaweed and clay were selected for further investigation due to their affinity characteristics and overall performance on all of the criteria considered.

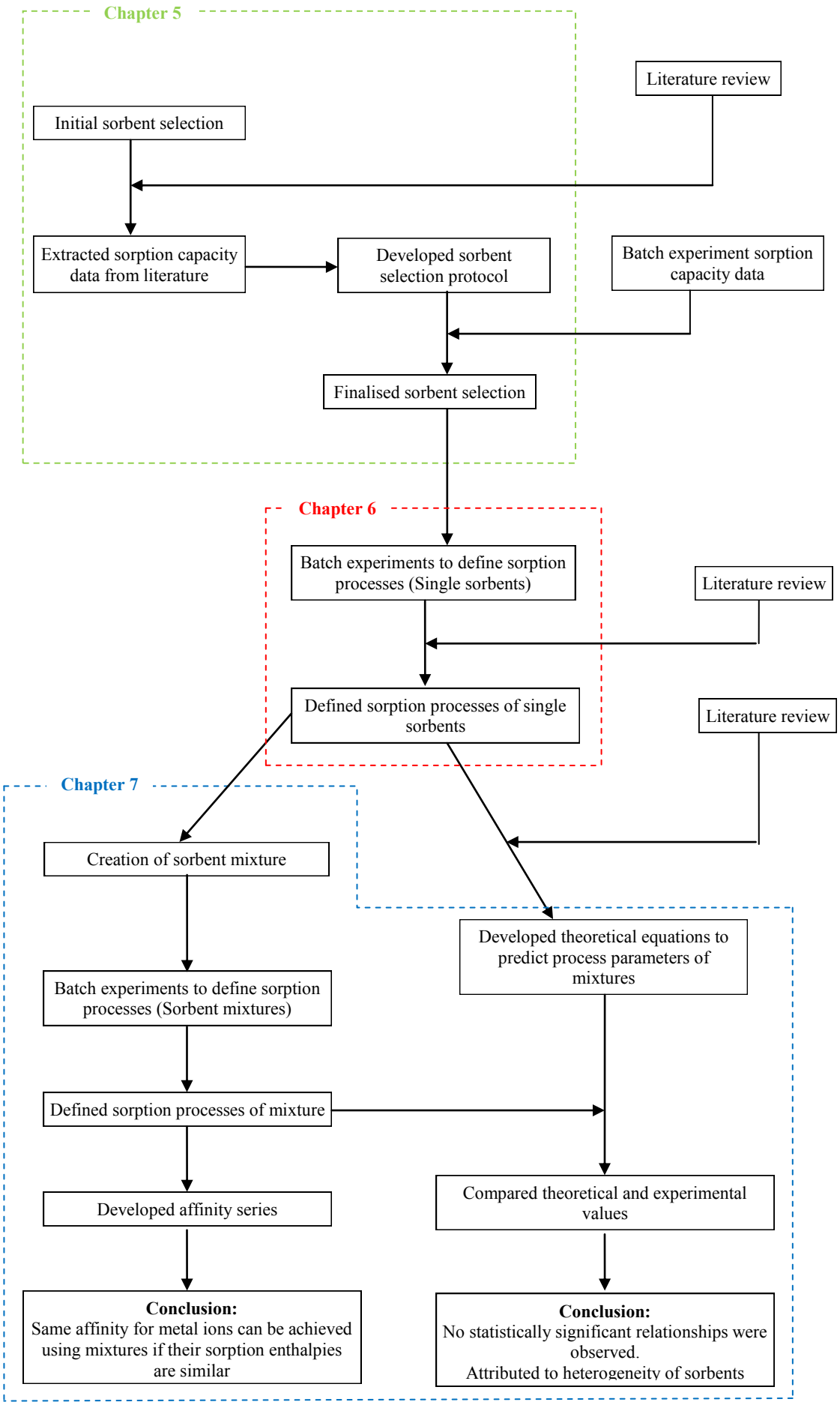

Schematic diagram showing the research methodology and the development of analytical chapters

Chapter 6: Isotherm, kinetics and thermodynamics of metal sorption by zeolite and seaweed

6.1 INTRODUCTION

In Chapter 5, six sorbent materials were investigated in order to select appropriate sorbents for creating mixtures that can remove a range of metals commonly present in stormwater. The metal affinity and the overall performance in relation to predetermined criteria were the two primary factors considered in the selection of sorbents. Based on the analysis of the experimental data, zeolite, seaweed and clay were selected, among which zeolite and clay had similar metal affinity characteristics and overall performance in relation to the selection criteria. Hence, it was considered adequate to consider either zeolite or clay for further analysis. Accordingly, seaweed and zeolite were chosen for creating the mixture as the metal affinity range of the two sorbents encompasses the metal ions investigated in the research study.

An in-depth knowledge on kinetics pathways, thermodynamics and chemical processes inherent in the metal sorption mechanisms employed by the individual sorbent materials is imperative for process modification and treatment system design. Additionally, this knowledge is essential to assess the mechanisms of the mixture/s in relation to individual sorbents in order to identify key factors, which can contribute to the enhancement of affinity for metal cations. Consequently, the kinetics, isotherm and thermodynamics characteristics of the mechanisms employed by zeolite, seaweed and their mixtures in the sorption of metal ions in a multi metal solution were investigated using the mathematical models discussed in Section 3.4. The input data for the models were obtained from a series of laboratory experiments described in Section 4.3.4. In this Chapter, the metal sorption mechanisms employed by zeolite and seaweed are discussed.

6.2 CHARACTERIZATION OF SORBENTS

Sorption process can be divided into ion exchange and adsorption mechanisms (Chapter 3). The ion exchange mechanism is associated with ECEC, while the negative functional groups present in sorbent materials are responsible for the adsorption mechanism. The ECEC was determined using the ammonium acetate method described in Section 4.4.2 and the functional groups were characterised using the titration methods as described in Section 4.4.3.

6.2.1 EFFECTIVE CATION EXCHANGE CAPACITY

The calibration curve for the ammonia selective electrode was developed as described in Section 4.5.4 and is presented in Figure 6.1.

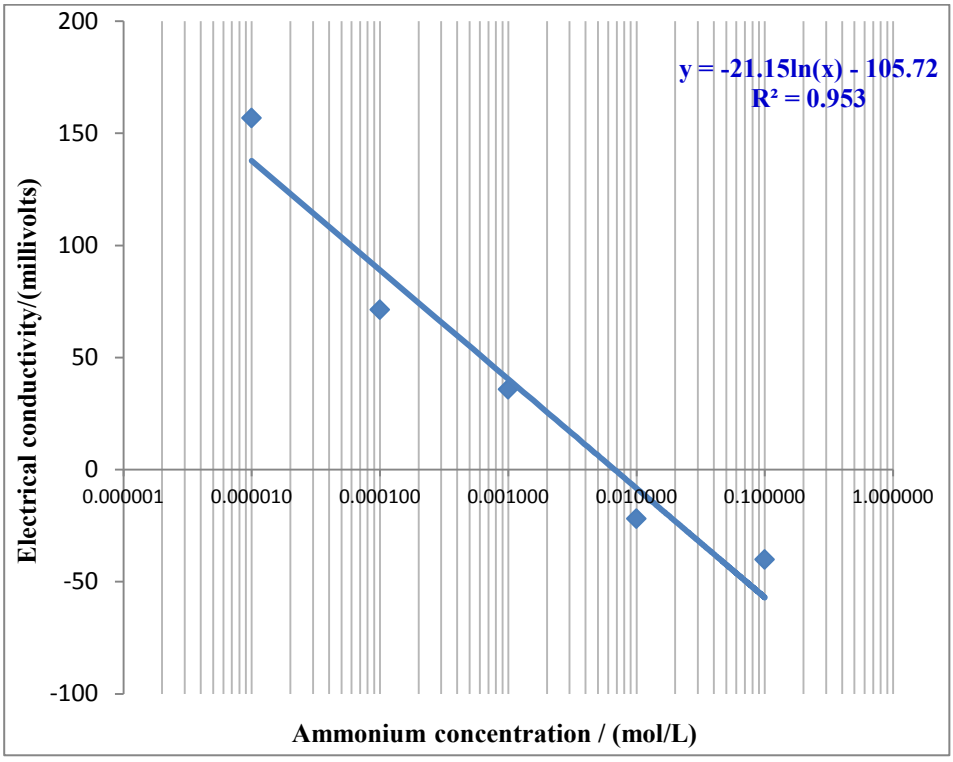

Figure 6.1 Calibration curve for ammonia selective electrode

The R^2 value for the calibration curve is 0.953 indicating a good fit. Hence, the ECEC calculated from the curve was considered reliable. The ECEC for zeolite and seaweed were 122 ± 23 and 1960 ± 369 meq/100g of sorbent, respectively. The standard deviation is relatively large indicating that the cation exchange property of zeolite and seaweed can vary from one batch of samples to the other. This is to be

expected as these are naturally occurring products and this needs to be taken into consideration in practical applications. Consequently, their metal sorption characteristics may vary for each batch. Additionally, ECEC of seaweed was about sixteen times higher than that of zeolite. Hence, seaweed can be expected to exhibit high ion exchange activity than zeolite. Seaweed used in this study was Ecklonia radiata, which is a brown seaweed species that has high cation exchange capacity, typically in the range of 1700-3100 meq/100g (Rupérez et al. 2001). The ECEC of sodium treated zeolite sourced from Zeolite Australia Pty Ltd. was previously determined by Aharon (2001), as approximately 112 meq/100g. This value is within the range found for ECEC in this study.

6.2.2 NEGATIVE SITES

The amount hydroxyl sites present in zeolite was determined based on stoichiometric relationship of the equations (4.4) and (4.5) and was found to be 4.90 ± 0.78 mmol/g. Boehm method was used to quantify the carboxylic, lactonic and hydroxyl groups in seaweed and the values were 2.90 ± 0.41, 0.05 ± 0.01 and 0.60 ± 0.09 mmol/g, respectively. The total amount of negative sites in seaweed was 3.55 ± 0.46 mmol/g. Accordingly, the carboxylic group is the primary binding site in seaweed. Several studies have also confirmed that the carboxylic functional groups are the main binding sites present in seaweed (Yun 2004; Davis et al. 2000; Romero-González et al. 2001).

6.3 METAL SORPTION MECHANISM – ZEOLITE

In this section, the kinetics, isotherm and thermodynamics characteristics of the mechanisms employed by zeolite for the sorption of metals are discussed.

6.3.1 DETERMINATION OF EQUILIBRIUM TIME

The equilibrium time is defined as the time, after which there is no increase in the removal of metals, subject to experimental error (Vuckovic et al. 2010). Batch kinetics experiments were conducted as described in Section 4.3.4 (A) and the plots of the kinetics experimental data (Tables B.1-B.7 in Appendix B) are given in Figure 6.2.

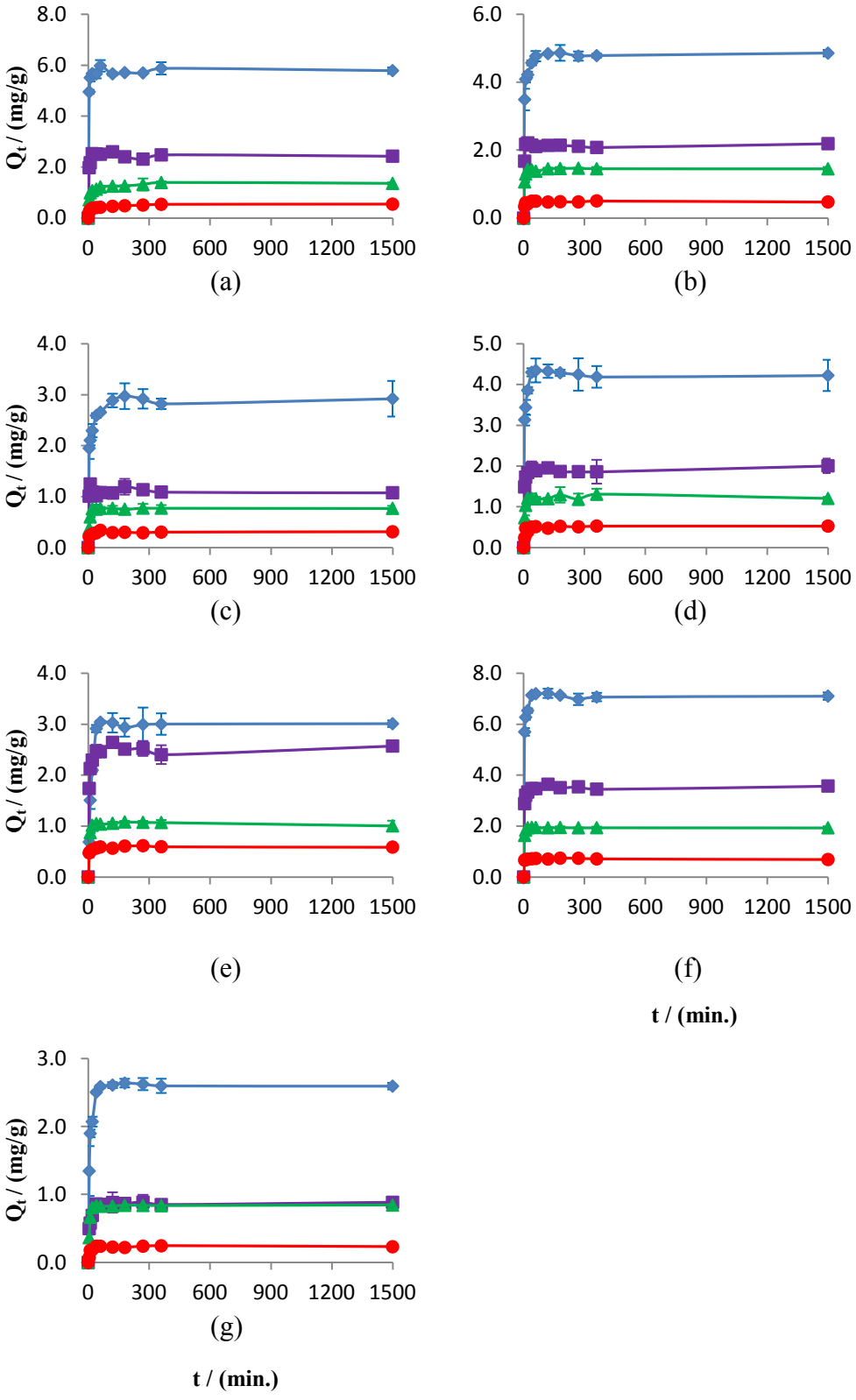

Figure 6.2 Sorption capacity vs. time graphs for zeolite: (a) Cu; (b) Ni; (c) Cd; (d) Pb; (e) Cr; (f) Al; (g) Zn (Legend: 200 mg/L; 100 mg/L; 50 mg/L; 20 mg/L)

According to Figure 6.2, the sorption of metals by zeolite was a rapid process and the system reached the equilibrium or near equilibrium within the first 60 minutes in most cases when considered with the experimental error. Hence, thermodynamics experiments described in Sections 4.3.4 (B) were conducted for one hour. The equilibrium time found in this study is comparable to the values reported in research literature. Kocaoba et al. (2007) found that equilibrium was achieved within 80 minutes in the sorption of Cd, Cu and Ni by natural clinoptilolite. Biškup and Subotic (1998) reported that the equilibrium time for Cd sorption by zeolite was less than 30 minutes.

6.3.2 SORPTION KINETICS

The sorption kinetics experiments were conducted as described in Section 4.3.4 (A). The sorption capacity data (Q_t) (Tables B.1-B.7 in Appendix B) were plotted against the square root of time ($\sqrt{t}$) as shown in Figure 6.3.

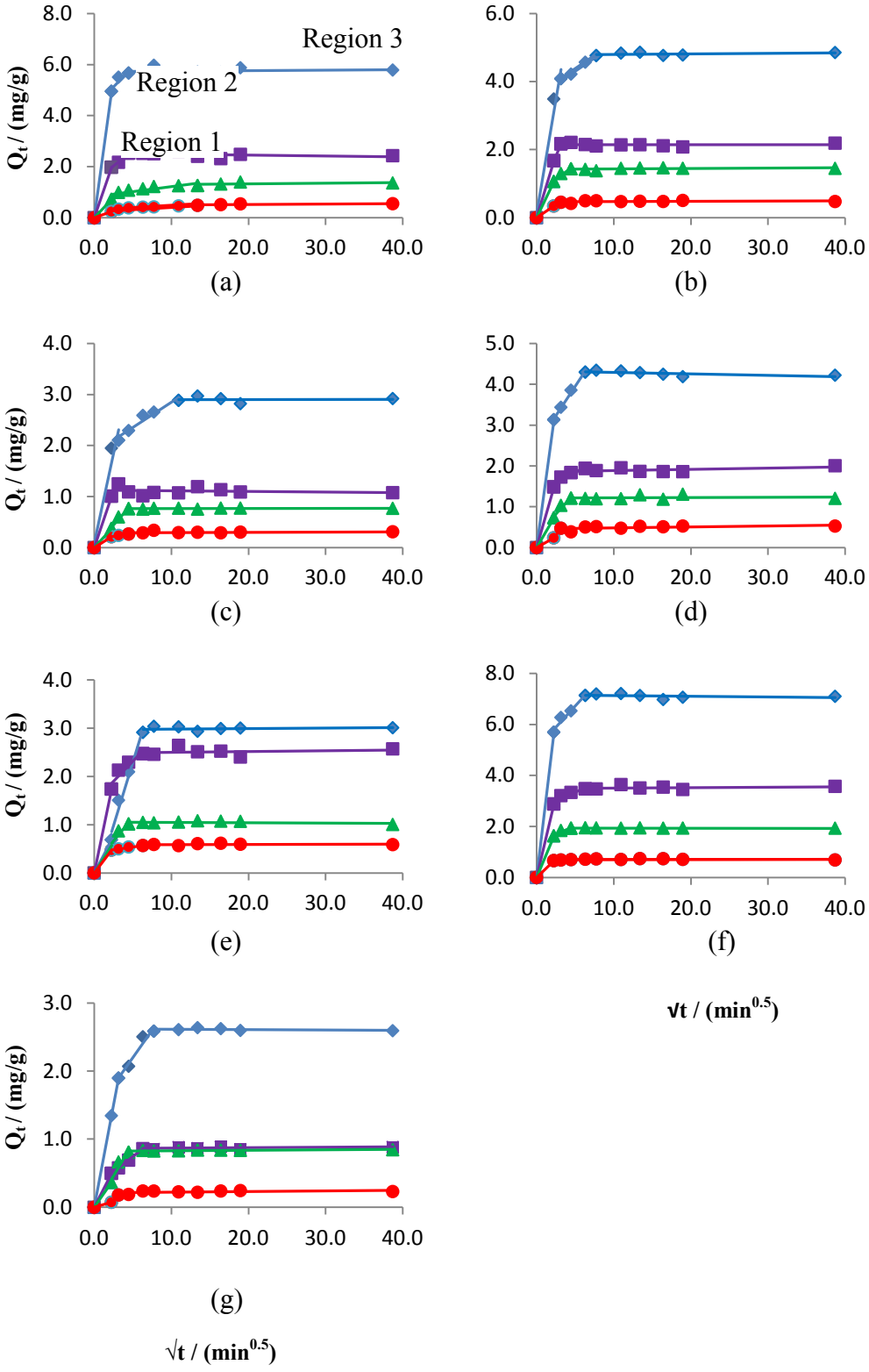

Figure 6.3 Q_t vs. √t graphs for zeolite: (a) Cu; (b) Ni; (c) Cd; (d) Pb; (e) Cr; (f) Al; (g) Zn (Legend: 200 mg/L; 100 mg/L; 50 mg/L; 20 mg/L)

In general, the graphs exhibit three linear regions (Figure 6.3a):

1. The initial linear portion corresponding to the boundary layer diffusion;
2. The second linear region corresponding to the intraparticle diffusion and
3. The plateau attributed to the equilibrium state.

Similar observations have previously been reported for the sorption of metals by zeolite (Zou et al. 2006; Apiratikul et al. 2008). The existence of three linear regions indicates that the overall metal removal rate of zeolite is governed by both boundary layer and intraparticle diffusion processes (Al-Johani and Salam 2011). However, according to Weber and Morris (1965), the relationship between sorption capacity and square root of time can only provide information on the diffusion processes, but does not provide any information regarding the influence of the metal binding process. Consequently, the diffusion and metal binding rates were calculated using the relevant mathematical models explained in Section 3.4 to further investigate the metal sorption kinetics of zeolite.

(A) BOUNDARY LAYER DIFFUSION

The boundary layer diffusion rates were determined from the kinetics experimental data (Tables B.1 – B.7 in Appendix B) using equation (3.8) and tabulated in Table 6.1:

Table 6.1 Boundary layer diffusion rates for zeolite

Metal ion	Initial metal concentrations (mg/L)			
	200	**100**	**50**	**20**
Cu	0.050	0.040	0.029	0.024
Ni	0.020	0.033	0.026	0.034
Cd	0.011	0.020	0.012	0.021
Pb	0.031	0.030	0.029	0.024
Cr	0.007	0.035	0.023	0.047
Al	0.057	0.058	0.065	0.066
Zn	0.009	0.010	0.015	0.007

According to Table 6.1, the boundary layer diffusion rates decrease in the order shown in Table 6.2:

Table 6.2 Boundary layer diffusion rate series for zeolite

Initial metal concentration/ (mg/L)	Series
200	Al ≥ Cu > Pb > Ni > Cd ≥ Zn ≥ Cr
100	Al > Cu ≥ Cr ≥ Ni ≈ Pb > Cd > Zn
50	Al > Pb ≈ Cu ≥ Ni ≥ Cr > Zn ≥ Cd
20	Al > Cr > Ni > Pb ≈ Cu ≥ Cd > Zn

Though the series is not consistent across the initial metal concentrations, a general trend can be observed. A driving force, which can be either physical factors such as concentration gradient (Fick 1855) or chemical factors, for example, chemical potential (Fisher 1973), is responsible for the diffusion of metal ions. In general, the boundary layer diffusion is driven by the molar concentration gradient, i.e. the difference between the metal concentration in solution and that in sorbent. Accordingly, the rate is directly proportional to the molar concentration gradient (Katsou et al. 2010). In this study, the experiments were conducted for equimass concentration. Hence, their molar concentration decreased with increasing molecular weight in the order of Al > Cr > Ni > Cu > Zn > Cd > Pb. Thus, the highest boundary layer diffusion rate of Al observed in the study can be attributed to its highest molar concentration in solution. Similarly, Cu and Ni were also present in relatively higher molar concentration. Hence, their boundary layer diffusion rates were generally higher. Furthermore, the lower molar concentration of Cd can be the reason for its lower boundary layer diffusion rate. The relationship predicted by Wilke and Chang (1955) suggested that the diffusion rate is low for ions with high molar volume. The diffusion rate of Cr was lower than that of Cu in most cases, even though molar concentration of Cr was higher than that of Cu. This is attributed to the relatively higher molar volume of Cr than that of Cu (Singman 1984).

The molar concentration of Zn was approximately similar to that of Ni and Cu. However, the boundary layer diffusion rate of Zn was lower than for the latter metal

ions. This is attributed to the inert electron structure of Zn^{2+}cation, the valence orbital of which is full ($3d^{10}$). Consequently, the tendency of forming strong bonds with the active sites of zeolite is weak (Liu et al. 2009). Therefore, the diffusion of Zn is retarded due to the low chemical driving force, though Zn has a significant physical driving force such as high molar concentration. Pb and Cd have low hydration energy, which can facilitate their exchange for extra framework cations of zeolite (Ouki and Kavannagh 1997). Therefore, despite their very low molar concentration, the chemical driving force resulting from the low hydration energy is attributed to the high diffusion rates of Pb and Cd in comparison to Zn. Therefore, it can be concluded that both physical and chemical driving forces can have an influence on the diffusion of metal ions through the boundary layer.

(B) INTRAPARTICLE DIFFUSION

Vermeulen (equation 3.9) and Weber-Morris (equation 3.10) models were used to determine the intraparticle diffusion rates. As discussed in Section 4.6.2, non-linear regression analysis was used to determine Vermeulen diffusion rates, while the Weber-Morris diffusion rate was calculated based on the second linear region of Q_t vs. $\sqrt{t}$ plots (Figure 6.3). The intraparticle diffusion rates calculated for 200 mg/L initial metal concentration using both models are presented in Table 6.3 for comparison.

Table 6.3 Intraparticle diffusion rates for 200 mg/L initial metal concentration

Metal ion	Vermeulen model		Weber-Morris model		
	^1D_v ($\times 10^{-7}$ m^2min^{-1})	R^2	$^1K_{WM}$ ($mg.g^{-1}min^{-0.5}$)	R^2	$^1D_{WM}$ ($\times 10^{-9}$ m^2min^{-1})
Cu	1.8	0.997	0.31	0.844	1.6
Ni	0.9	0.990	0.21	0.906	1.0
Cd	0.5	0.966	0.11	1.000	1.6
Pb	0.8	0.991	0.28	0.993	2.4
Cr	0.1	0.936	0.52	0.974	16
Al	1.2	0.992	0.33	0.964	1.2
Zn	0.4	0.995	0.21	0.909	3.6

Notes:

[1]Vermeulen intraparticle diffusion rate (D_v); Weber-Morris constant related to intraparticle diffusion rate (K_{WM}); Weber-Morris intraparticle diffusion rate (D_{WM})

From Table 6.3, it can be observed that the Vermeulen diffusion rates are higher than the Weber-Morris diffusion rate. Additionally, the Vermeulen rates decrease in the order of Cu > Al > Ni > Pb > Cd > Zn > Cr, while the Weber-Morris rates decrease in the order of Cr > Zn > Pb > Cu > Cd >Al > Ni. Difference in the intraparticle diffusion rates predicted by Vermeulen and Weber-Morris models has been reported in past research literature (Apiratikul and Pavasant 2008). The reliability of Weber-Morris model prediction depends on the data points present in the second linear region. As can be seen from Figure 6.3 above, there are only a few data points present in the second linear region of Q_t vs. $\sqrt{t}$ graph. Thus, the prediction of intraparticle diffusion rates using the Weber-Morris model cannot be considered as reliable. Consequently, the Vermeulen model was used for the subsequent calculation of intraparticle diffusion rates and tabulated in Table 6.4.

Table 6.4 Intraparticle diffusion rates for zeolite

Metal ion	Initial metal concentration / (mg/L)					
	100		50		20	
	D_v ($\times 10^{-7}$ m^2min^{-1})	R^2	D_v ($\times 10^{-7}$ m^2min^{-1})	R^2	D_v ($\times 10^{-7}$ m^2min^{-1})	R^2
Cu	1.2	0.987	0.4	0.975	0.2	0.955
Ni	1.5	0.990	1.0	0.997	0.7	0.974
Cd	2.8	0.963	0.4	0.978	0.7	0.971
Pb	1.3	0.996	0.7	0.984	0.3	0.916
Cr	0.8	0.992	0.5	0.989	1.0	0.982
Al	1.3	0.995	1.6	1.000	2.4	0.996
Zn	0.4	0.990	0.4	0.966	0.2	0.915

Based on the Vermeulen intraparticle diffusion reported in Tables 6.3 and 6.4, the following intraparticle diffusion rate series can be deduced as listed in Table 6.5.

Table 6.5 Intraparticle diffusion rate series for zeolite

Initial metal concentration / (mg/L)	Series
200	Cu > Al > Ni ≥ Pb > Cd ≥ Zn > Cr
100	Cd > Ni ≥ Pb ≈ Al ≥ Cu > Cr > Zn
50	Al > Ni > Pb ≥ Cr ≥ Cu ≈ Cd ≈ Zn
20	Al > Cr > Ni ≈ Cd >Pb ≥ Cu ≈ Zn

The intraparticle diffusion rate is dependent on the size of the metal ions such that the rate is higher for relatively smaller metal ions (Saucedo et al. 1992). This is because a metal ion with a smaller ionic diameter can easily diffuse through the pores of zeolite in comparison to larger metal ions. The metal ions in the solution are present as their hydrated complexes (Ouki and Kavannagh 1997). Hence, hydrated diameter of metal ions must be considered when investigating the intraparticle diffusion of porous materials. Additionally, metal ions with low hydration energy can lose some of the water molecules from their hydrated structure (Álvarez-Ayuso et al. 2003). As a result, the intraparticle diffusion of those metal ions can be enhanced (Erdem et al. 2004). However, additional energy needs to be provided to break the

bond between the water molecules and metals. In this study, the experiment was conducted under room temperature. Thus, no additional energy was provided. Therefore, metal ions are likely to remain in their hydrated form.

The hydrated diameter of metal ions decreases in the order of Al > Cr > Zn > Cd > Cu > Ni > Pb (Pfleger and Wolf 1975). Thus, ideally, the intraparticle diffusion rates have to increase in the reverse order, i.e. Pb > Ni > Cu > Cd > Zn > Cr > Al. According to Table 6.5, the intraparticle diffusion rates of Ni and Pb were generally higher, while that of Zn was generally lower. Additionally, the intraparticle diffusion rate of Cd was generally moderate. These observations are in agreement with the series derived for intraparticle series based on hydrated ionic diameter. However, Al was found to have a high intraparticle diffusion rate despite its larger hydrated ionic diameter. This indicates that other factors also influenced the intraparticle diffusion rates in addition to the hydrated ionic diameter. The existence of a larger physical driving force for the diffusion of Al ions resulting from its higher molar concentration is attributed to the higher intraparticle diffusion of Al. Additionally, Al is a hard acid, the sorption of which is preferred by the hard bases (Pearson 1968). As discussed in Section 6.2.2, zeolite consists of hydroxyl functional group, which is a hard base (Pearson 1968). Therefore, sorption of Al is preferred by zeolite, which provides the chemical driving force required for the intraparticle diffusion of Al.

Similarly, the intraparticle diffusion rate of Cr, which is another hard acid, was also generally high despite its larger hydrated ionic diameter. On the other hand, the intraparticle diffusion rate of Cu was relatively low, though the hydrated ionic diameter of Cu is small. This is because Cu is a soft acid, which is not generally preferred by the hard bases present in zeolite (Pearson 1968). Hence, the chemical driving force for its diffusion is relatively smaller. However, it should be noted that the larger intraparticle diffusion rates for metal ions with larger hydrated ionic diameter imply that diffusion occurred into the cracks on the surface of zeolite rather than inside the pores as explained in Section 3.4.2. It is worthy to note that the relatively low intraparticle diffusion rate of Zn can also be attributed to its inert valence structure in addition to its larger ionic diameter.

Though a general trend can be observed as discussed above, the intraparticle diffusion rate series is inconsistent across the initial metal concentration. As discussed above, this is attributed to the involvement of above-mentioned physical and chemical properties of the sorbent, metals and the solution in conjunction during the sorption of metals, which result in different sorption scenarios. Additionally, the properties of natural zeolites depend on factors such as the presence of impurities and the pore geometry. Thus, these factors can vary from one batch to the other as evident from the standard deviation of ECEC and the amount of negative sites as discussed in Section 6.2. Consequently, each batch of zeolites can have different metal removal characteristics. This may be another reason for the inconsistency observed for the intraparticle diffusion rate series.

(C) METAL BINDING PROCESS

Metal binding rate corresponds to the rate, at which the metal ions are sorbed to the active sites after the intraparticle diffusion step. As discussed in Section 3.4.2 (B), pseudo first order and pseudo second order models are widely used to determine the metal binding rates. The metal binding rates were determined by fitting the sorption kinetics experimental data (Tables B.1-B.7 in Appendix B) to the pseudo first order (equation 3.17) and second order (equation 3.15) models using the non-linear regression analysis and presented in Table 6.6.

Table 6.6 Pseudo first and pseudo second order metal binding rates for zeolite

Metal ion	Initial metal concentration															
	200 mg/L				100 mg/L				50 mg/L				20 mg/L			
	First order		Second order		First order		Second order		First order		Second order		First order		Second order	
	$^{1}K_1$	R^2	$^{1}K_2$	R^2	K_1	R^2	K_2	R^2	K_1	R^2	K_2	R^2	K_1	R^2	K_2	R^2
Cu	0.40	0.996	0.29	0.995	0.29	0.984	0.34	0.982	0.12	0.958	0.19	0.988	0.09	0.931	0.26	0.975
Ni	0.24	0.983	0.12	0.997	0.35	0.993	0.65	0.977	0.26	0.996	0.41	0.993	0.22	0.974	0.87	0.978
Cd	0.16	0.941	0.11	0.983	0.56	0.964	6.85	0.958	0.14	0.996	0.31	0.971	0.20	0.958	1.47	0.971
Pb	0.23	0.979	0.12	0.993	0.31	0.995	0.52	0.992	0.20	0.988	0.35	0.977	0.12	0.922	0.37	0.926
Cr	0.06	0.993	0.03	0.963	0.22	0.987	0.19	0.992	0.16	0.998	0.26	0.984	0.28	0.974	1.14	0.992
Al	0.30	0.988	0.12	0.996	0.32	0.993	0.25	0.998	0.36	0.999	0.67	0.997	0.52	0.995	4.20	0.997
Zn	0.13	0.981	0.09	0.993	0.14	0.968	0.31	0.984	0.13	0.991	0.24	0.962	0.08	0.959	0.46	0.933

Notes:

[1]Pseudo first order metal binding rate (K_1); Pseudo second order metal binding rate (K_2)

The R^2 values for both models were above 0.9 in all cases indicating a good fit with the experimental data. The following order as shown in Table 6.7 can be deduced for metal binding rates at different initial metal concentrations based on K_1 and K_2 values.

Table 6.7 Metal binding rate series for zeolite

Initial metal concentration / (mg/L)	Pseudo first order	Pseudo second order
200	Cu > Al > Ni ≥ Pb > Cd ≥ Zn > Cr	Cu > Al ≈ Ni ≈ Pb ≥ Cd ≥ Zn > Cr
100	Cd > Ni ≥ Al ≥ Pb ≥ Cu ≥ Cr > Zn	Cd > Ni ≥ Pb ≥ Cu ≥ Zn ≥ Al ≥ Cr
50	Al > Ni > Pb ≥ Cr ≥ Cd ≥ Zn ≥ Cu	Al > Ni ≥ Pb ≥ Cd > Cr ≥ Zn ≥ Cu
20	Al > Cr ≥ Ni ≥ Cd > Pb ≥ Cu ≥ Zn	Al > Cd ≥ Cr ≥ Ni ≥ Zn ≥ Pb ≥ Cu

The metal binding rate series predicted by both pseudo first and pseudo second order models is similar. Additionally, the rate series is approximately similar to the series predicted for the intraparticle diffusion rates presented in Table 6.5. This indicates that the metals that diffused relatively rapidly inside the intraparticle structures of zeolite were rapidly sorbed to the active sites. Therefore, a majority of the active sites must be present in the intraparticle structure of zeolite. For subsequent analysis of sorption kinetics, the model that had relatively high R^2 values in most cases was selected. Accordingly, for initial metal concentration of 200, 100, 50 and 20 mg/L, pseudo second, first, first and second order models were selected, respectively, based on their R^2 values.

(D) IDENTIFICATION OF RATE-LIMITING STEP

In Section 3.4.2 (C), it was concluded that it is necessary to develop a mathematically rigorous analytical approach to determine the degree of contribution of the sorption kinetics steps in limiting the overall metal removal rate. For this purpose, a parameter, namely, 'average specific metal removal rate (Z)', was introduced in this study to account for the overall metal removal rate. This term was defined as the rate, at which the metal ions are removed by a unit mass of a sorbent material, and was theoretically established as follows:

According to the above definition,

$$Z = \frac{1}{m_s}\frac{dm_m}{dt} \tag{6.1}$$

where dm_m is the amount of metal ions removed by the sorbent of mass m_s in time dt.

However, $m_m = (C_0 - C_t)\, v$ (6.2)

Therefore, $Z = \frac{1}{m_s}\frac{d}{dt}[(C_0 - C_t)\, v]$ (6.3)

The volume of the solution can be assumed constant if the reduction in the volume of the solution due to sample withdrawal is less than 10% of the initial volume.

Hence, $Z = \frac{v}{m_s}\frac{d}{dt}[(C_0 - C_t)]$ (6.4)

The initial metal concentration C_0 is constant.

Thus, $Z = -\frac{v}{m_s}\frac{dC_t}{dt}$ (6.5)

$$dC_t = -\frac{Zm_s dt}{v} \tag{6.6}$$

Integrating equation (6.6) with the following boundary conditions:

($t = 0$, $C_t = C_0$) and ($t = t_e$, $C_t = C_e$), where t_e is the time taken for the system to achieve equilibrium.

$$\int_{C_0}^{C_e} dC_t = -\frac{Zm_s \int_0^{t_e} dt}{v} \tag{6.7}$$

$$C_e - C_0 = -\frac{Zm_s t_e}{v} \tag{6.8}$$

$$Z = \frac{v\,(C_0 - C_e)}{m_s t_e} \tag{6.9}$$

However, $$Q_e = \frac{C_0 - C_e}{m_s/v} \tag{6.10}$$

Therefore, $$Z = \frac{Q_e}{t_e} \tag{6.11}$$

The parameter 'Z' was determined from the Q_t vs. t plots presented in Figure 6.2. The values are tabulated in Table 6.8.

Table 6.8 Z values for zeolite

Metal ion	Initial metal concentration / (mg/L)			
	[1]200	[1]100	[1]50	[1]20
Cu	0.071	0.042	0.009	0.003
Ni	0.053	0.042	0.013	0.005
Cd	0.024	0.110	0.007	0.005
Pb	0.047	0.024	0.013	0.003
Cr	0.014	0.019	0.009	0.005
Al	0.059	0.018	0.016	0.018
Zn	0.026	0.015	0.005	0.002

The rate of the overall metal removal is dependent on the rate-limiting step. Therefore, in principle, the rate of overall metal removal should be positively correlated to that of the rate-limiting step. Consequently, the rate-limiting step was identified by analysing the correlation of the average specific metal removal rate (Z) with the boundary layer diffusion rate (BLDR), Vermeulen intraparticle diffusion rate (D_v) and the metal binding rate (K_1 or K_2). Initially, Spearman correlation analysis was used to determine whether there is any correlation between the rate variables. The results of the Spearman correlation analysis are presented in Table 6.9.

Table 6.9 Correlation of Z with diffusion and metal binding rates

Rate parameter	Initial metal concentration/ (mg/L)	[1]r_s	[1]P
[2]BLDR	200	0.929	0.007
	100	-0.071	0.906
	50	0.857	0.024
	20	0.858	0.012
[2]D_v	200	1.000	0.000
	100	0.821	0.034
	50	0.929	0.007
	20	0.955	0.003
[2]K_1 or K_2	200	0.893	0.012
	100	0.750	0.066
	50	0.857	0.024
	20	0.839	0.024

Notes:

[1]Spearman ranking coefficient (r_s); Significance of correlation (P)

[2]Boundary layer diffusion (BLDR); Vermeulen intraparticle diffusion (D_v); Pseudo first order metal binding rate (K_1) or Pseudo second order metal binding rate (K_2)

The significance (P) of the correlations presented in Table 6.9 is less than 0.05 in all cases except for the boundary layer diffusion and the metal binding rates of 100 mg/L initial metal concentration. This indicates that the results of the analysis are generally reliable. According to r_s values, the intraparticle diffusion, boundary layer diffusion and metal binding rates are correlated to the average specific metal removal rate (Z) in all cases. However, the correlation of Z with the boundary layer diffusion and metal binding rates is inconclusive for 100 mg/L initial metal concentration since the significance was larger than 0.05. Except that, it can be concluded that all three rates have contributed to the overall metal removal rate.

However, r_s values cannot be used to interpret the strength of the relationship between variables (Bolboaca and Jantschi 2006). Therefore, multivariate analysis, PROMETHEE and GAIA, was employed to investigate the strength of the

correlations predicted by the Spearman correlation analysis. The PROMETHEE and GAIA techniques require the assignment of three modelling parameters: a ranking sense (maximum or minimum); a preference function; and a weight. Since rapid rates are favourable for good sorption performance, the rate variables were maximised. V-shaped preference function (Table 4.3) was assigned based on the data characteristics and a weight of 1 was allocated to all criteria to avoid any bias in the analysis.

According to the GAIA biplot for 200 mg/L initial metal concentration (Figure 6.4; 99% variance accounted), the average specific metal removal rate (Z) is correlated with both diffusion rates (D_v and BLDR) and the metal binding rate (K_2) indicating that the overall metal removal rate depends on both diffusion and metal binding processes. This is consistent with the results of Spearman correlation analysis for this particular scenario. Among them, the primary rate-limiting step is intraparticle diffusion since the correlation of Z with the intraparticle diffusion rate is relatively stronger.

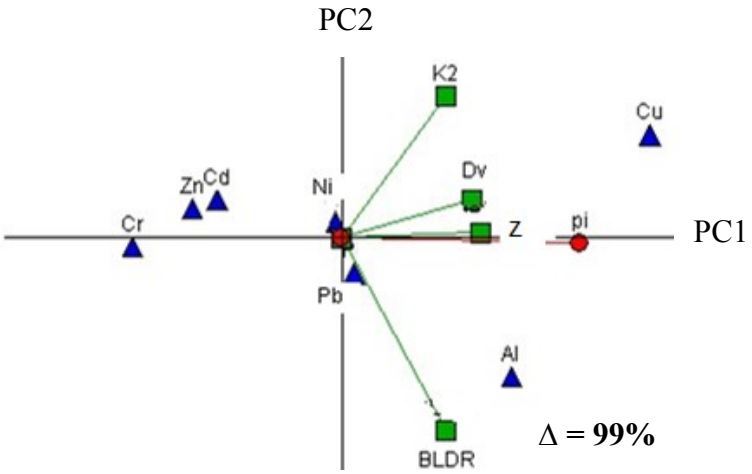

Figure 6.4 GAIA biplot for 200 mg/L initial metal concentration - Zeolite

The Spearman correlation analysis for 100 mg/L was inconclusive. However, the GAIA biplot (Figure 6.5; 99% variance accounted) confirms that Z is independent of the boundary layer diffusion rate as both vectors are approximately orthogonal. Both, metal binding and intraparticle diffusion rates are strongly correlated to Z, among which the intraparticle diffusion rate is stronger than the metal binding rate. Therefore, the primary rate-limiting step in this case is intraparticle diffusion.

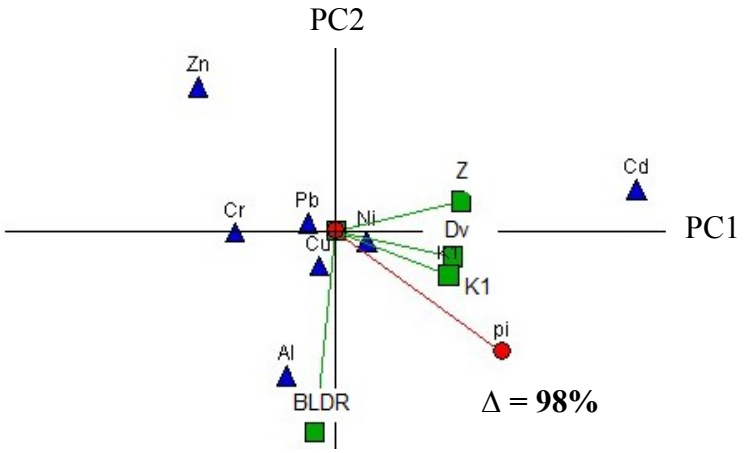

Figure 6.5

Figure 6.5 GAIA biplot for 100 mg/L initial metal concentration - Zeolite

In the case of 50 mg/L initial metal concentration, Spearman correlation predicted that diffusion and metal binding rates contributed in limiting the overall metal removal rate. However, according to the corresponding GAIA biplot (Figure 6.6; 96% variance described), the correlation of Z is stronger with the metal binding rate and the intraparticle diffusion rate, while it is approximately at right angle to the boundary layer diffusion rate. Thus, the primary rate-limiting steps are the metal binding and the intraparticle diffusion processes. Additionally, the boundary layer diffusion did not have any influence in limiting the overall metal removal rate, which is in disagreement with the Spearman correlation prediction. Hence, the influence of boundary layer diffusion on limiting the overall metal removal rate is inconclusive.

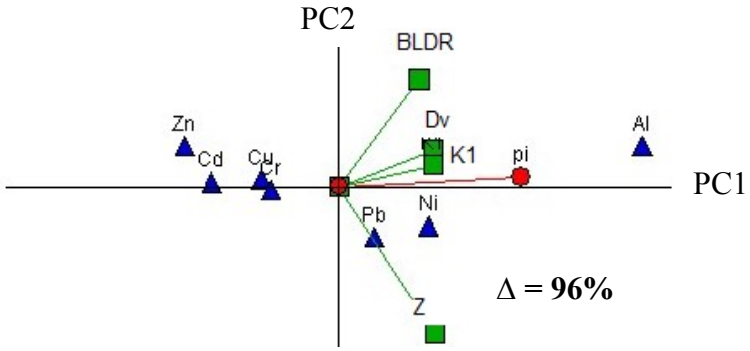

Figure 6.6 GAIA biplot for 50 mg/L initial metal concentration - Zeolite

The primary rate-limiting step is the metal binding process according to the GAIA biplot (Figure 6.7; 100% variance accounted) for 20 mg/L initial metal concentration,

as it is strongly correlated to Z. The intraparticle diffusion rate has also shown a strong correlation to Z suggesting that it is also significantly limiting the overall metal removal rate. However, the boundary layer diffusion rate vector is at right angle to Z indicating that it has not contributed in limiting the overall rate. On the other hand, the Spearman correlation analysis showed that the overall metal removal rate is limited by the boundary layer diffusion, intraparticle diffusion and metal binding steps. Therefore, similar to 50 mg/L initial metal concentration, the role of the boundary layer diffusion on limiting the overall metal removal rate is inconclusive.

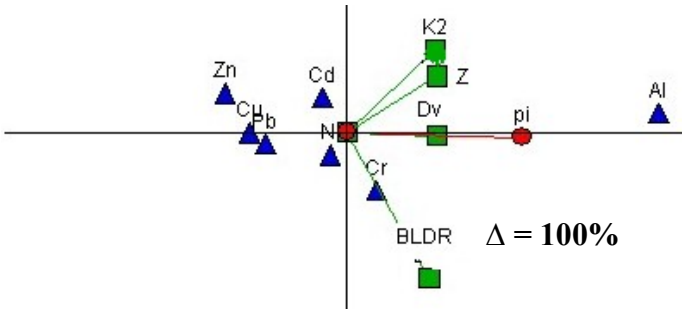

Figure 6.7 GAIA biplot for 20 mg/L initial metal concentration - Zeolite

In conclusion, the overall metal removal rate of zeolite was found to be influenced primarily by the intraparticle diffusion and the metal binding rates. In general, intraparticle diffusion has a significant influence in limiting the overall removal rate. This can be due to the porous networks of zeolite, through which the metal ions have to diffuse during their sorption process. The role of the boundary layer diffusion in limiting the overall metal removal rate of zeolite is generally inconclusive due to the contradiction in the Spearman and GAIA predictions. Therefore, further investigation is necessary in such cases. This can be achieved by determining the boundary layer diffusion rates at different agitation speeds. The diffusion rate will increase with the increase in the agitation speed if the boundary layer diffusion is the rate-limiting step (McKay and Poots 1980). This is because agitation reduces the thickness of the boundary layer resulting in the reduction of boundary layer diffusion resistance.

As discussed in Section 3.4.2 (C), it is commonly assumed that metal binding is not a rate-limiting step. However, Ho and McKay (1998) stated that this step could limit the overall metal removal rate. The findings from this study confirmed the hypothesis

by Ho and McKay (1998) since the metal binding process was found to be limiting the overall metal removal rate of zeolite. This can specially be the case in a multi metal system, in which a metal has to overcome the competition from other metal ions to sorb to active sites. Consequently, this can slow the binding rate of the metal ions. Furthermore, the competition between metals for the active sites can lead to a cycle of sorption and desorption of metal ions. Consequently, the rate, at which the metals are sorbed to the active sites, can be slow.

6.3.3 SORPTION THERMODYNAMICS

Thermodynamics parameters, namely enthalpy change (ΔH^0) and entropy change (ΔS^0), were determined from the slope and y-intercept of the log (K_d) vs. (1/T) graphs (Figure 6.8). The K_d values were calculated from the thermodynamics experimental data (Table B.8 in Appendix B) using equation (3.21). Finally, the Gibbs free energy change (ΔG^0) was calculated using equation (3.22) and equation (3.23), respectively. The parameters are presented in Table 6.10.

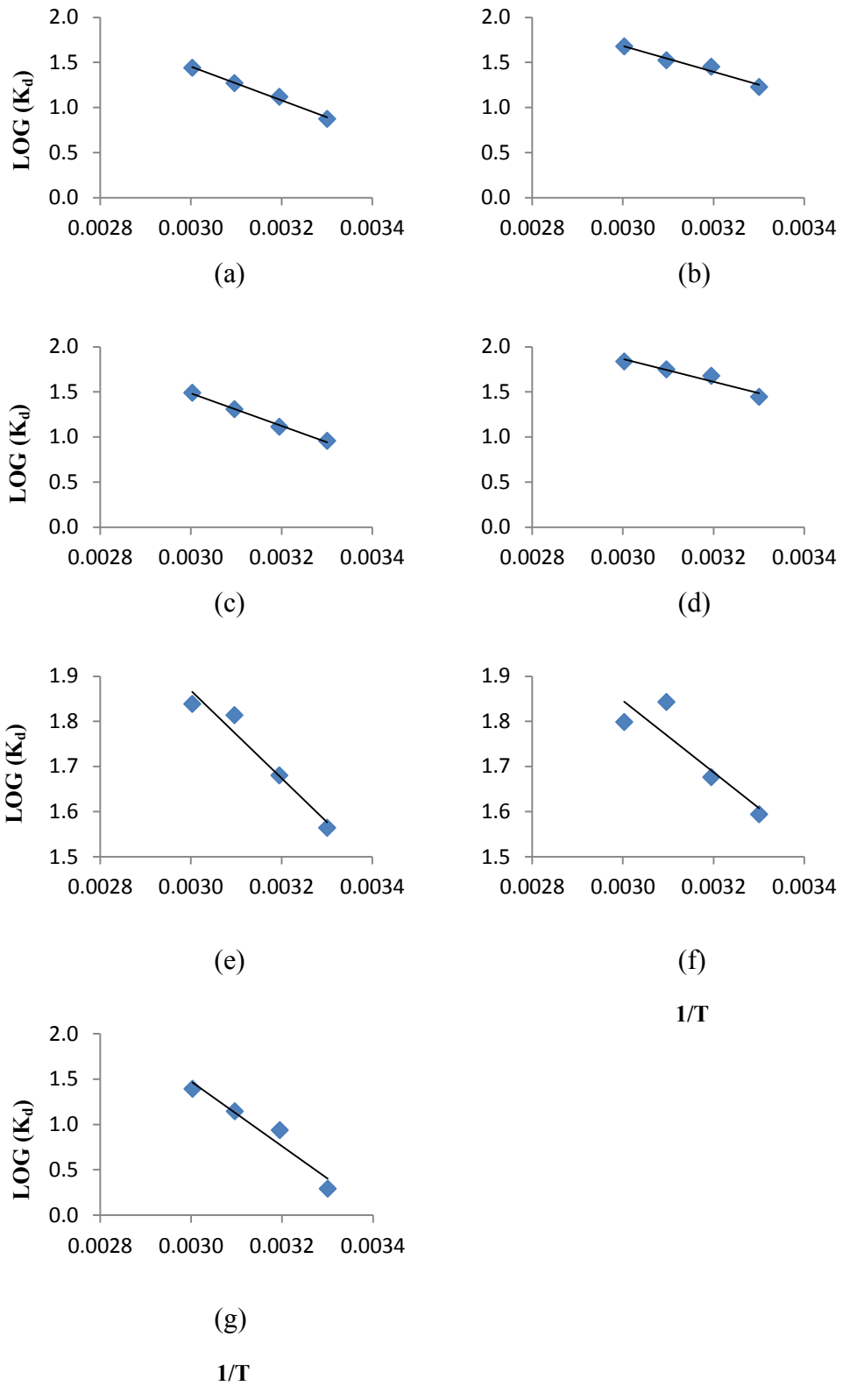

Figure 6.8 LOG(K_D) vs. 1/T plots for zeolite: (a) Cu; (b) Ni; (c) Cd; (d) Pb; (e) Cr; (f) Al; (g) Zn

Table 6.10 Thermodynamics parameters for zeolite

Metal ion	ΔH^0 /(kJ/mol)	ΔS^0 /(J/mol.K)	ΔG^0/(kJ/mol)			
			303[1]	313[1]	323[1]	333[1]
Cu	35.8	135.4	-5.2	-6.6	-7.9	-9.3
Ni	27.5	114.9	-7.2	-8.4	-9.6	-10.7
Cd	34.6	132.1	-5.5	-6.8	-8.1	-9.4
Pb	24.3	108.6	-8.6	-9.7	-10.8	-11.9
Cr	18.6	91.5	-9.1	-10.1	-11.0	-11.9
Al	15.2	81.0	-9.3	-10.1	-11.0	-11.8
Zn	68.2	232.6	-2.3	-4.6	-7.0	-9.3

Notes:

[1] Absolute temperature / (K)

ΔG^0 for all the metals was negative at the investigated temperatures. As such, the sorption of metals by zeolite can begin spontaneously (Lyubchik et al. 2004). ΔG^0 values decrease with the increase in temperature suggesting that metal sorption is more favourable at a higher temperature (Zaki et al. 2000).

Positive ΔH^0 indicates that the sorption of the investigated metal ions is endothermic (El-Kamash et al. 2005). Among the metal ions, sorption of Zn is more endothermic than the rest. Cu and Cd sorption is also highly endothermic, while Ni and Pb have a moderately endothermic nature. Cr and Al have the least ΔH^0 indicating that they have the lowest endothermic character. This suggests that the sorption of Zn is more favourable at high temperatures, while sorption of Cr and Al can occur at relatively low temperatures. Hence, more energy, i.e. high temperature, is required to make the bonding between Zn and the active sites in zeolite energetically favourable. Based on thermodynamics parameters, the energetically favourable nature of sorption increases as follows: Zn < Cu < Cd < Ni < Pb < Cr < Al. Accordingly, sorption of Al, Cr and Pb is thermodynamically more favourable, while that of Zn, Cu and Cd is less favourable. Furthermore, positive values for entropy change (ΔS^0) suggest that changes have occurred in the structure of zeolite due to the sorption of metals. These changes are attributed to the cation exchange or formation of bonds with active sites (Mohan and Singh 2002).

6.3.4 SORPTION ISOTHERM

Langmuir and Freundlich isotherm models were used in this study to understand the interaction between the sorbent surface and metal ions. Firstly, the equilibrium

sorption data (Tables B.9 in Appendix B) were fitted to the Langmuir isotherm model as shown in Figure 6.9. Notably, the isotherm plot corresponding to Cr shows a reasonably good fit (R^2 = 0.82) suggesting that Cr sorption could occur in monolayer. Hard acidic nature of Cr can facilitate the formation of a stable complex with hard bases of zeolite (Pearson 1968). Hence, the bonding of Cr with the active sites of zeolite can be of a chemisorption nature, which exhibits monolayer characteristics. However, though it is a hard acid, Al did not exhibit the monolayer characteristics as can be seen from its R^2 value in Figure 6.9 (f). Al is found in larger molar concentration. Hence, it requires relatively higher amount of active sites for sorption. Consequently, the sorption of Al could occur via forming hydrogen bonds with the metal ions sorbed to active sites instead of all Al ions being directly sorbed to the active sites. This can result in multilayer sorption characteristics.

The model also showed poor fit with other metals as evident from the R^2 values of Figure 6.9 indicating that the metal sorption was not of monolayer nature. This is because the metal ions can form hydrogen bond with the metal ions sorbed to active sites resulting in a multilayer on the surface of sorbent. In such a case, Freundlich model is more suitable in describing the sorption system (Section 3.4.1B).

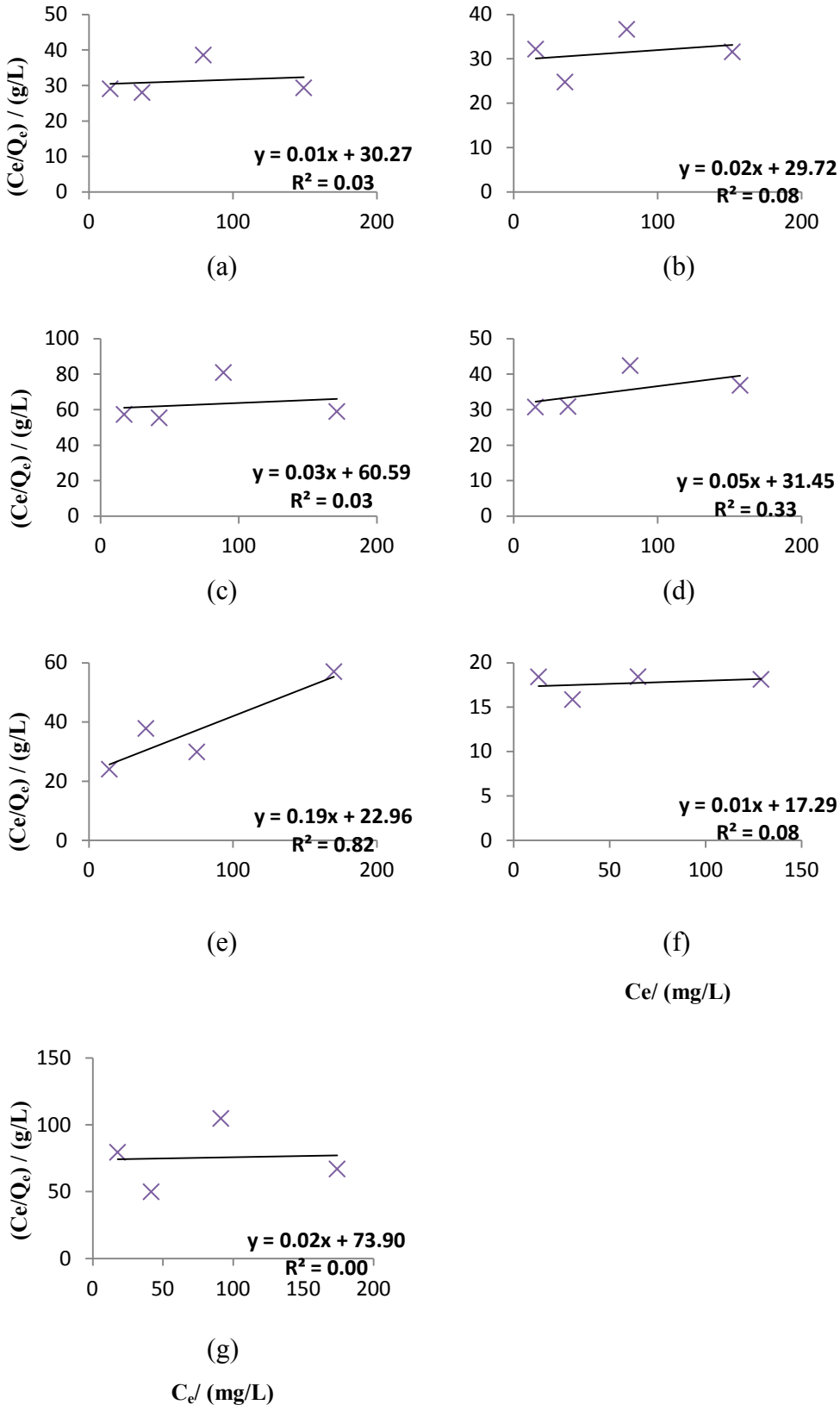

Figure 6.9 Langmuir isotherm plots for zeolite: (a) Cu; (b) Ni; (c) Cd; (d) Pb; (e) Cr; (f) Al; (g) Zn

Consequently, the isotherm experimental data were fitted to the linearised Freundlich isotherm model (equation 3.7) as shown in Figure 6.10.

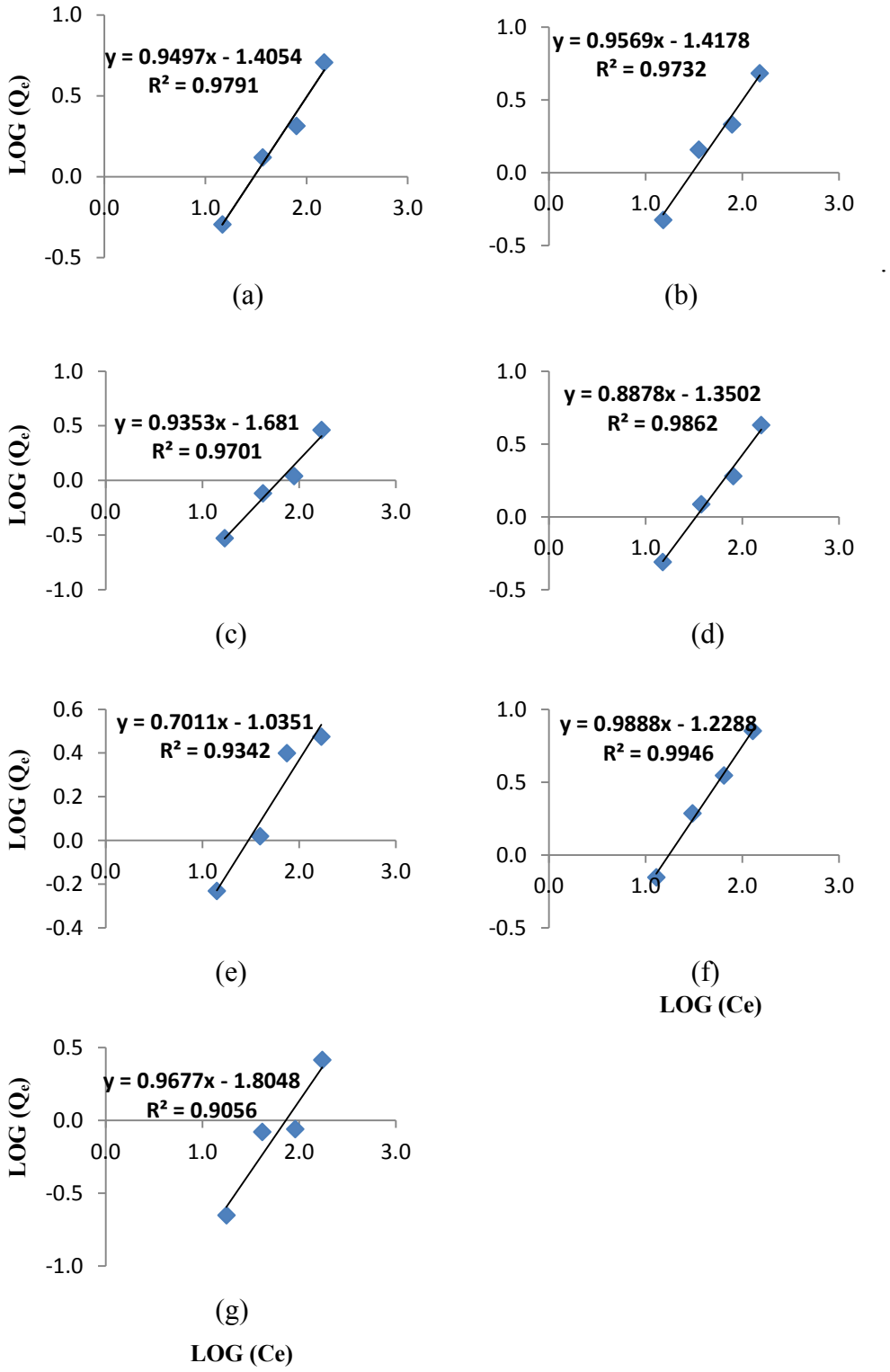

Figure 6.10 Freundlich isotherm models for: (a) Cu; (b) Ni; (c) Cd; (d) Pb; (e) Cr; (f) Al; (g) Zn

The Freundlich isotherm constants were calculated from the slope and y-intercept of the Freundlich isotherm plots and are presented in Table 6.11. The R^2 values of the model fit are above 0.9 indicating a good fit with the experimental data. This confirms that the sorption occurred in multilayer, which is the general case in a multi metal system (Genç-Fuhrman et al. 2007; Ünlü and Ersoz 2006).

Table 6.11 Freundlich isotherm constants

Metal ion	K_F/ $((mg/g)/(mg/L)^{1/n})$	n	R^2
Cu	0.039	1.05	0.979
Ni	0.038	1.05	0.973
Cd	0.021	1.07	0.970
Pb	0.045	1.13	0.986
Cr	0.092	1.43	0.934
Al	0.059	1.01	0.994
Zn	0.016	1.03	0.905

According to K_F values (Table 6.11), the affinity of zeolite for metal ions decreases in the order of Cr > Al > Pb > Cu ≈ Ni > Cd > Zn. As discussed in Section 6.2.2, zeolite predominantly consists of the hydroxyl functional group, which is a hard base. Hence, according to the HSAB principle, zeolite prefers to sorb with hard metals (Pearson 1968). According to Table 3.4, the hard acidic nature of the investigated metals decreases in the order of Al > Cr > Pb > Zn > Ni > Cd > Cu, which is generally in agreement with the predicted affinity series. Therefore, the predicted affinity series can be considered to reflect the HSAB principle. Additionally, the affinity series approximately reflects the thermodynamics series derived in Section 6.3.5 suggesting that the sorption affinity of zeolites is closely associated to the sorption thermodynamics.

However, Zn and Cu did not follow the HSAB principle. Zn exhibits a relatively high hard acidic property (Table 3.4). However, zeolite has the lowest affinity for Zn sorption. The possible reason is the inert valence electron structure of Zn cation, due to which the tendency of Zn to form bonds is low as explained in Section 6.3.2 (A). Additionally, the diffusion and metal binding rates of Zn were also lower compared to other metal ions (Section 6.3.2). Therefore, other metal ions reached the active sites faster and occupied the sites. This can be another reason for zeolite to have low affinity for Zn. In contrast, Cu is the softest acid among the metals investigated

(Table 3.4), to which zeolite has relatively less affinity. Thus, the high sorption of Cu is attributed to its high boundary layer diffusion rate, which can facilitate Cu to reach the active sites more rapidly than certain other metals.

Similarly, the sorption affinity for other metals can also be explained based on the physical and chemical factors. The reason for high affinity for Al can be attributed to its high diffusion and metal binding rates (Section 6.3.2). Consequently, Al can reach the active sites rapidly resulting in high probability of bonding with the active sites. Despite relatively lower kinetics rates of Cr in most cases, zeolite was found to have high affinity for Cr. This is attributed to the high charge density of Cr (Table 3.2), which facilitates a strong physisorption bond between metals and active sites. Consequently, sorbents prefer to sorb metals with high charge densities for stable bonds. Similarly, the high affinity for Al is attributed to the high charge density in addition to its high kinetics rates as described above. Additionally, a relatively higher affinity for Pb is attributed to its higher rates and low hydration energy. Ni has hydration energy higher than Pb and the differences in hydration energies of Cu and Ni are not significant (Table 3.1). Hence, K_F values for Cu and Ni are almost similar, while lower than for Pb (Table 6.11). This indicates that Ni sorption was mainly influenced by the hydration energy. The hydration energy of Cd is lower than that of Cu and Ni. Hence, ideally zeolite should have a high preference for Cd. However, the low affinity of zeolite for Cd is attributed to its low charge density (Table 3.2) and low kinetics rates.

The n values calculated from Freundlich model can be used to predict the nature of the interaction between metal and the sorbent as described in Section 3.4.1. According to Table 6.11, the n values for the metals are greater than 1 indicating that sorption is of a chemical nature. However, except for Pb and Cr, the values are very close to 1. Therefore, physisorption and ion exchange could contribute to the sorption process along with chemisorption. In contrast, the mechanism employed by zeolite for the sorption of Pb and Cr is chemisorption. This is attributed to their harder acidic nature that results in stronger complexation with the hydroxyl functional group.

6.4 METAL SORPTION MECHANISM - SEAWEED

A similar approach explained in Section 6.3 for zeolite was adopted to characterise the metal sorption mechanism employed by seaweed.

6.4.1 DETERMINATION OF EQUILIBRIUM TIME

The equilibrium time for metal sorption by seaweed was determined using batch kinetics experiment conducted as described in Section 4.3.4 (A). The metal sorption capacity of seaweed (Tables B.10-B.16 in Appendix B) was plotted against time as shown in Figure 6.11.

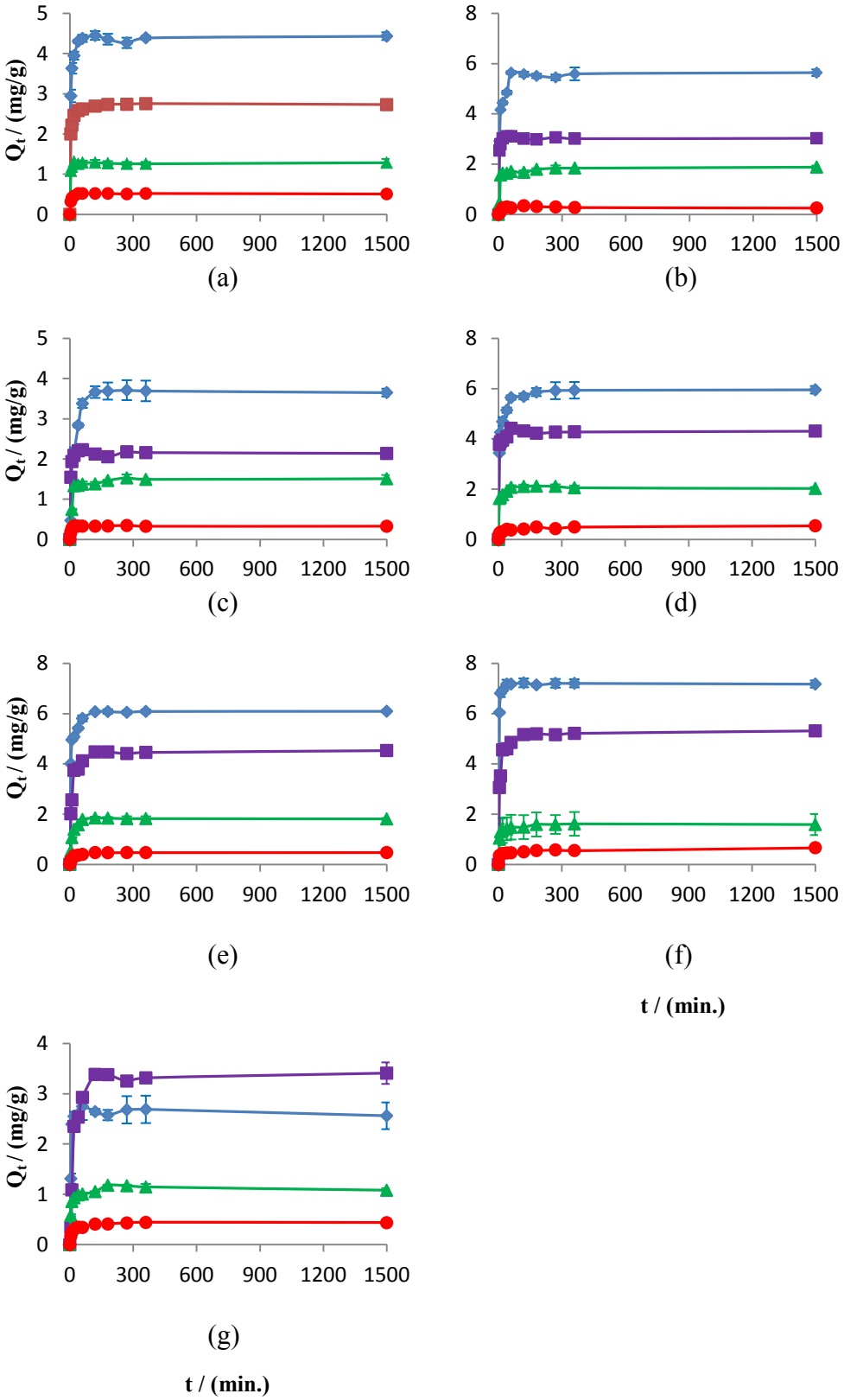

Figure 6.11 Sorption capacity vs. time graphs for seaweed: (a) Cu; (b) Ni; (c) Cd; (d) Pb; (e) Cr; (f) Al; (g) Zn (Legend: 200 mg/L; 100 mg/L; 50 mg/L; 20 mg/L)

Similar to zeolite, the sorption of metals by seaweed was a rapid process. In general, the equilibrium or near equilibrium condition was achieved within the first 60 minutes when considered with the experimental errors. Previous studies reported similar rapid sorption of metals by seaweed. For example, Sheng et al. (2004) found that 90% of total metal sorption occurred within the first hour, whilst Romero-González (2001) reported that 91% of Cd in the solution was removed by seaweed in the first 5 minutes. Therefore, the isotherm and thermodynamics experiments described in Sections 4.3.4 (B) for seaweed were conducted for one hour.

6.4.2 SORPTION KINETICS

The sorption capacity data (Q_t) (Tables B.10-B.16 in Appendix B) when plotted against the square root of time ($\sqrt{t}$) as shown in Figure 6.12, three linear regions are generally present. Thus, it can be concluded that the overall metal removal rate of seaweed is governed by both boundary layer and intraparticle diffusion processes. Gupta and Rastogi (2009) found that both diffusion processes influenced the sorption of Cr by seaweed. Similar conclusions were drawn by Jha et al. (2009) for the sorption Pb and Cd by seaweed as well.

The diffusion and metal binding rates were determined using the kinetics models (Section 3.4.2) to further investigate the metal sorption kinetics of seaweed.

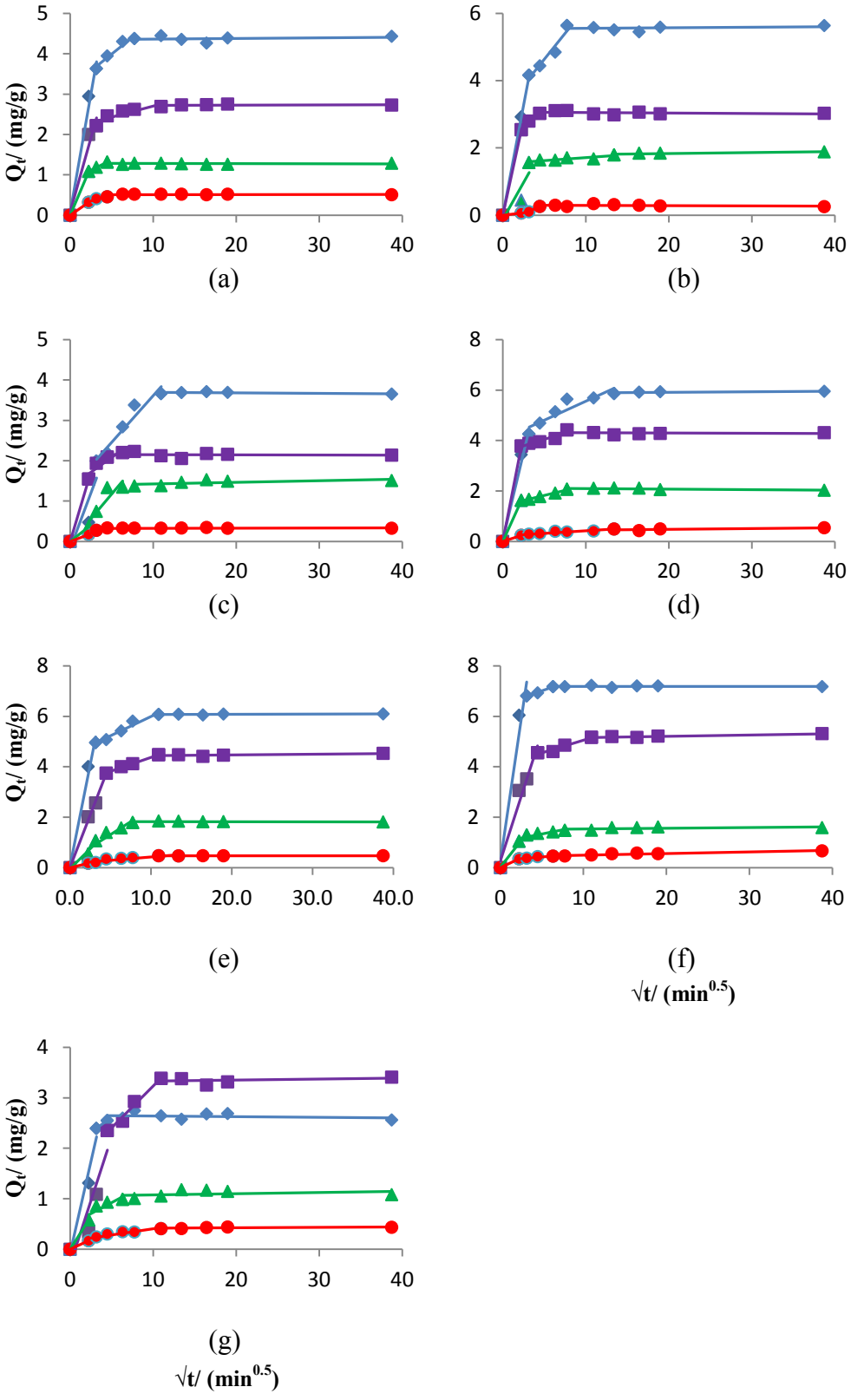

Figure 6.12 Q_t Vs. √t graphs for seaweed: (a) Cu; (b) Ni; (c) Cd; (d) Pb; (e) Cr; (f) Al; (g) Zn (Legend: 200 mg/L; 100 mg/L; 50 mg/L; 20 mg/L)

(A) BOUNDARY LAYER DIFFUSION

Equation (3.8) was used to calculate the boundary layer diffusion rates. The batch kinetics experimental data (Tables B.10-B.16 in Appendix B) were used for this purpose. The boundary layer diffusion rates are tabulated in Table 6.12:

Table 6.12 Boundary layer diffusion for seaweed

Metal ion	Initial metal concentration / (mg/L)			
	200	100	50	20
Cu	0.029	0.040	0.043	0.032
Ni	0.029	0.051	0.018	0.006
Cd	0.005	0.031	0.015	0.017
Pb	0.034	0.076	0.065	0.024
Cr	0.040	0.040	0.022	0.017
Al	0.060	0.061	0.042	0.035
Zn	0.013	0.007	0.017	0.017

Based on Table 6.12, the series presented in Table 6.13 can be derived for the boundary layer diffusion rates:

Table 6.13 Boundary layer diffusion rate series for seaweed

Initial metal concentration/ (mg/L)	Series
200	$Al > Cr \geq Pb \geq Cu \geq Ni > Zn > Cr$
100	$Pb > Al > Ni > Cu \approx Cr > Cd > Zn$
50	$Pb > Cu \geq Al > Cr \geq Ni \geq Zn \geq Cd$
20	$Al \geq Cu > Pb > Cr \approx Cd \approx Zn > Ni$

In comparison to the series derived for zeolite (Table 6.2), the series for seaweed shows more variation. This is attributed to more heterogeneity in the properties of seaweed than that of zeolite (Section 6.2). However, a general trend in the rate series can be observed. Accordingly, Al and Cu generally have a high boundary layer diffusion rate and Ni and Cr have a moderate boundary layer diffusion rate. This is attributed to the large driving force resulting from the high molar concentration of these metals. On the other hand, Cd and Zn exhibit a low boundary layer diffusion rate. Low molar concentration of Cd and the inert valence electron structure of Zn

cation are the reasons for their low boundary layer diffusion rates. Pb was an exception since it had relatively higher boundary layer diffusion despite its low concentration. This is attributed to its large chemical driving force as a result of low hydration energy (Table 3.1).

(B) INTRAPARTICLE DIFFUSION

In Section 6.3.2 (B), it was concluded that determination of the intraparticle diffusion rate using Weber-Morris model is not reliable if the number of data points in the second linear region of Q_t vs. $\sqrt{t}$ plot is small. As can be seen from Figure 6.12, the data points are few in the second linear region. Hence, only the Vermeulen model was used to calculate the intraparticle diffusion rates. Accordingly, the Vermeulen intraparticle diffusion rates (D_v) were determined using the batch sorption kinetics data (Tables B.10-B.16 in Appendix B) and are presented in Table 6.14:

Table 6.14 Intraparticle diffusion rates for seaweed

Metal ion	Initial metal concentration / (mg/L)							
	200		100		50		20	
	D_v ($\times 10^{-7}$ m^2min^{-1})	R^2	D_v ($\times 10^{-7}$ m^2min^{-1})	R^2	D_v ($\times 10^{-7}$ m^2min^{-1})	R^2	D_v ($\times 10^{-7}$ m^2min^{-1})	R^2
Cu	0.72	0.997	1.8	0.962	1.8	0.996	0.59	0.997
Ni	0.44	0.984	1.5	0.997	0.15	0.810	0.12	0.873
Cd	0.05	0.895	0.94	0.995	0.14	0.911	0.54	0.979
Pb	0.43	0.984	1.7	0.987	1.8	0.951	0.36	0.931
Cr	0.63	0.980	0.28	0.989	0.18	0.979	0.16	0.986
Al	1.2	0.995	0.44	0.988	0.61	0.978	0.41	0.940
Zn	0.47	0.960	0.04	0.853	0.38	0.968	0.19	0.979

The R^2 values are generally high indicating a good fit of the Vermeulen model with the experimental data. The intraparticle diffusion rates in Table 6.14 show the trends given in Table 6.15.

Table 6.15 Intraparticle diffusion rate series for seaweed

Initial metal concentration/ (mg/L)	Series
200	Al > Cu > Cr > Zn ≥ Ni ≥ Pb > Cd
100	Cu ≥ Pb > Ni > Cd > Al > Cr > Zn
50	Cu ≈ Pb > Al > Zn > Cr ≥ Ni ≥ Cd
20	Cu ≥ Cd > Al ≥ Pb > Zn ≥ Cr ≥ Ni

Seaweed does not have a well established porous structure compared to zeolite (Park et al. 2004). Hence, the pore diffusion is not the primary intraparticle diffusion mechanism in seaweed. As can be seen from Table 6.15, the intraparticle diffusion rate series does not reflect the hydrated ionic diameter series (Table 2.1). Thus, the observed intraparticle diffusion is attributed to their surface roughness. Similar to zeolite, the intraparticle rate series is not consistent and the heterogeneity of the properties of seaweed is the reason for the variation in the intraparticle diffusion rate series (Section 6.2). In the study by Brayan and Hummerstone (1973), the sorption of metals to seaweed was found to be dependent on the portion of the plant. Seaweed consists of hard stipes and blades, which have different chemical composition. Hence, different parts of seaweed exhibit different metal sorption properties (Leusch et al. 1997). The heterogeneity of seaweed properties would make the design of a treatment system for practical water treatment application, difficult. Thus, an in-depth investigation of the heterogeneity of seaweed properties can be the starting point for utilising seaweed for practical applications.

Nevertheless, a general trend can be observed for the intraparticle diffusion rates. In general, Cu and Al have a higher intraparticle diffusion rate, which is attributed to large physical driving force developed due to high molar concentration. Notably, the intraparticle diffusion rate of Zn is moderate for seaweed in contrast to zeolite, which is attributed to its moderate hydration energy (Table 3.1). This suggests that Zn is sorbed via ion exchange mechanism as discussed in Section 3.2. However, Sheng et al. (2004) attributed similar observation to the sorption through ionic bonding resulting from a strong attraction between Zn^{2+} and anionic active sites (Sheng et al. 2004). Therefore, an isotherm or thermodynamics study is necessary to confirm which of these mechanisms are employed by seaweed for the sorption of Zn. The intraparticle diffusion rates of Cr, Ni, Cd and Pb show variation, i.e. these metals

have both high and low diffusion rates (Table 6.15). The higher diffusion of Cr and Ni is attributed to the large physical driving force resulting from high molar concentration. In contrast, Pb and Cd have relatively higher intraparticle diffusion rates despite the low molar concentration. In such cases, the intraparticle diffusion of Pb and Cd is governed by the chemical driving force created by low hydration energy. Similarly, high hydration energy is the reason for low diffusion rates of Cr. Furthermore, low diffusion rates of Cd and Pb is attributed to their high molar volume, which can retard their intraparticle diffusion (Wilke and Chang 1955).

(C) METAL BINDING PROCESS

Pseudo first order and pseudo second order models were fitted to the kinetics experimental data to determine the metal binding rates and presented in Table 6.16.

Table 6.16 Pseudo first and pseudo second order sorption rates for seaweed

Metal ion	Initial metal concentration / (mg/L)															
	200				100				50				20			
	First order		Second order		First order		Second order		First order		Second order		First order		Second order	
	$^1K_1$	R^2	$^1K_2$	R^2	K_1	R^2	K_2	R^2	K_1	R^2	K_2	R^2	K_1	R^2	K_2	R^2
Cu	0.21	0.990	0.10	0.996	0.23	0.981	0.18	0.998	0.38	0.996	1.2	0.993	0.17	0.989	0.66	0.994
Ni	0.13	0.970	0.04	0.988	0.36	0.995	0.35	0.995	0.07	0.869	0.05	0.855	0.06	0.934	0.27	0.899
Cd	0.04	0.958	0.01	0.952	0.25	0.994	0.26	0.988	0.06	0.965	0.06	0.946	0.16	0.994	0.90	0.969
Pb	0.14	0.963	0.04	0.994	0.40	0.986	0.12	0.971	0.26	0.957	0.12	0.951	0.08	0.894	0.27	0.947
Cr	0.19	0.970	0.06	0.993	0.10	0.978	0.04	0.991	0.07	0.990	0.06	0.987	0.07	0.965	0.21	0.985
Al	0.36	0.998	0.16	0.999	0.14	0.973	0.05	0.994	0.19	0.971	0.22	0.992	0.14	0.912	0.45	0.964
Zn	0.15	0.981	0.09	0.955	0.03	0.953	0.01	0.940	0.13	0.960	0.19	0.984	0.08	0.949	0.27	0.988

Notes:

[1]Pseudo first order metal binding rate (K_1); Pseudo second order metal binding rate (K_2)

Both models fit the experimental data well since the R^2 values are above 0.9 in almost all the cases. Pseudo second order model showed better fit in most cases for 200, 100 and 20 mg/L initial metal concentration. In contrast, pseudo first order model fitted well for 50 mg/L initial metal concentration for most metal ions. Based on K_1 and K_2 values, the rate series shown in Table 6.17 was derived for the metal binding rates.

Table 6.17 Metal binding rate series for seaweed

Initial metal concentration / (mg/L)	First order	Second order
200	Al > Cu ≥ Cr > Zn ≥ Pb ≥ Ni > Cd	Al > Cu ≥ Zn ≥ Cr > Pb ≥ Ni ≥ Cd
100	Pb ≥ Ni > Cd ≥ Cu > Al ≥ Cr > Zn	Ni ≥ Cd > Cu ≥ Pb > Al ≥ Cr ≥ Zn
50	Cu > Pb ≥ Al > Zn ≥ Cr ≈ Ni > Cd	Cu > Al ≥ Zn > Pb ≥ Cr ≥ Cd > Ni
20	Cu ≥ Cd > Al > Pb ≈ Zn ≥ Cr ≥ Ni	Cd > Cu > Al > Pb ≥ Ni ≥ Zn > Cr

Except for Pb and Al, there is no significant difference between the series derived by both models. Additionally, the series is similar to the intraparticle diffusion rate order. This implies that more active sites are exposed to the metal ions in the cracks relative to its external surfaces. Furthermore, the ions can be physically trapped inside the cracks, which can reduce the possibility of the metal ions being desorbed back to the solution. This can facilitate the rapid sorption on the active sites inside the cracks. On the other hand, the metal ions sorbed to the external surfaces can be easily desorbed back to solution in an agitated system. In such cases, the sorption of metal ions can be slow.

(D) IDENTIFICATION OF RATE-LIMITING STEP

The approach adopted for zeolite (Section 6.3.2 D) was also employed for determining the rate-limiting step in the sorption of metals by seaweed. The average specific metal removal rate (Z) (equation 6.11) was calculated by dividing Q_e by t_e obtained from Figure 6.11 and presented in Table 6.18:

Table 6.18 Z values for seaweed

Metal ion	Initial metal concentration / (mg/L)			
	200	**100**	**50**	**20**
Cu	0.049	0.045	0.026	0.004
Ni	0.035	0.052	0.008	0.002
Cd	0.019	0.037	0.008	0.002
Pb	0.033	0.036	0.008	0.003
Cr	0.047	0.021	0.011	0.002
Al	0.090	0.029	0.013	0.004
Zn	0.045	0.028	0.010	0.002

Spearman analysis was conducted to investigate the correlations of Z with diffusion and metal binding rates and the results are tabulated in Table 6.19.

Table 6.19 Correlation of Z with diffusion and reaction rates

Rate parameter	Initial metal concentration/ (mg/L)	[1]r_s	[1]P
[2]BLDR	200	0.628	0.139
	100	0.193	0.662
	50	0.500	0.267
	20	0.933	0.003
[2]D_v	200	1.000	0.000
	100	0.786	0.048
	50	0.646	0.110
	20	0.447	0.302
[2]K_1 or K_2	200	0.929	0.007
	100	0.929	0.007
	50	0.714	0.088
	20	0.139	0.783

Notes:

[1]Spearman ranking coefficient (r_s); Significance of correlation (P)

[2]Boundary layer diffusion (BLDR); Vermeulen intraparticle diffusion (D_v); Pseudo first order metal binding rate (K_1) or Pseudo second order metal binding rate (K_2)

According to Table 6.19, it can be concluded that Z is correlated with the boundary layer diffusion rate for 20 mg/L initial metal concentration. In the case of 200mg/L, the intraparticle diffusion and metal binding rates are correlated with Z. Similarly, the metal binding rate is correlated with Z for 100 mg/L initial metal concentration. However, for the rest of the scenarios, the P values of the Spearman correlations are more than 0.05 indicating that the spearman correlation analysis is inconclusive in these cases.

The GAIA biplot for 200 mg/L initial metal concentration is given in Figure 6.13 (100% variance accounted).

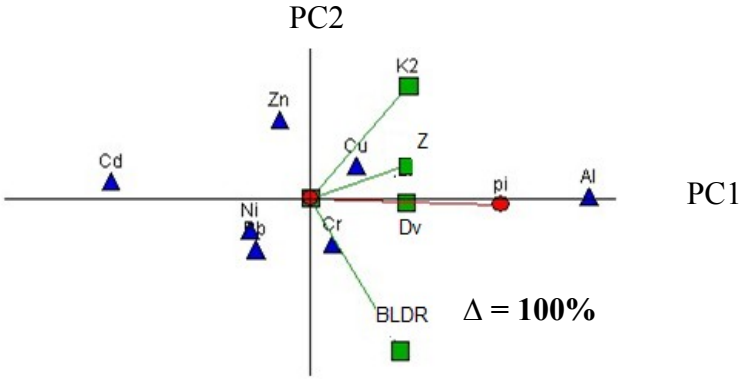

Figure 6.13 GAIA biplot for 200 mg/L initial metal concentration - Seaweed

According to the GAIA biplot, the overall metal removal rate of seaweed is controlled by the intraparticle diffusion and metal binding steps, which is similar to Spearman correlation analysis prediction (Table 6.19). In contrast, the influence of the boundary layer diffusion in limiting the overall metal removal rate is inconclusive in Spearman correlation due to high P value. However, GAIA biplot predicts that the boundary layer diffusion is not a rate-limiting step.

Spearman correlation for 100 mg/L initial metal concentration predicted that both intraparticle and metal binding kinetics steps were rate limiting. However, the significance of correlation between Z and the boundary layer diffusion rate is more than 0.05. Hence, the influence of boundary layer diffusion is not conclusive. Nevertheless, the GAIA biplot (Figure 6.14; 93% variance accounted) suggests that the boundary layer diffusion is not a rate-limiting step. In contrast, the intraparticle

and metal binding steps have an influence on the overall metal removal rate, among which the metal binding process is the primary rate-limiting step.

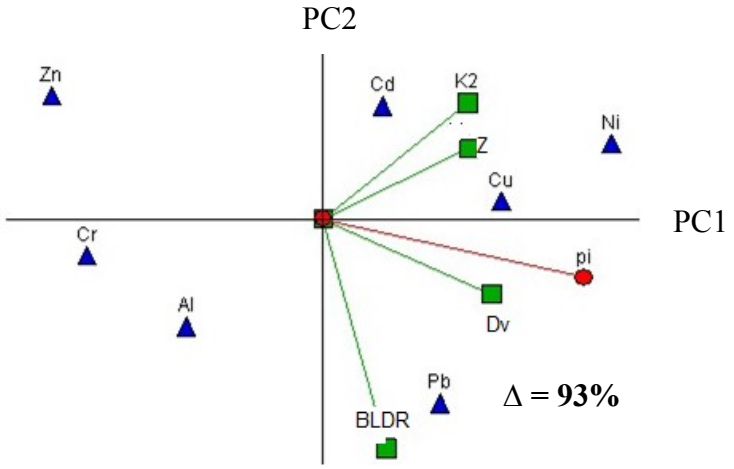

Figure 6.14 GAIA biplot for 100 mg/L initial metal concentration - Seaweed

The GAIA biplot for 50 mg/L (Figure 6.15; 98% variance accounted) indicates that the overall metal removal rate is controlled only by the metal binding step. Hence, the sorption mechanism is slow chemisorption process. The Spearman analysis for 50 mg/L initial metal concentration was inconclusive since the significance of the analysis was more than 0.05 in all cases.

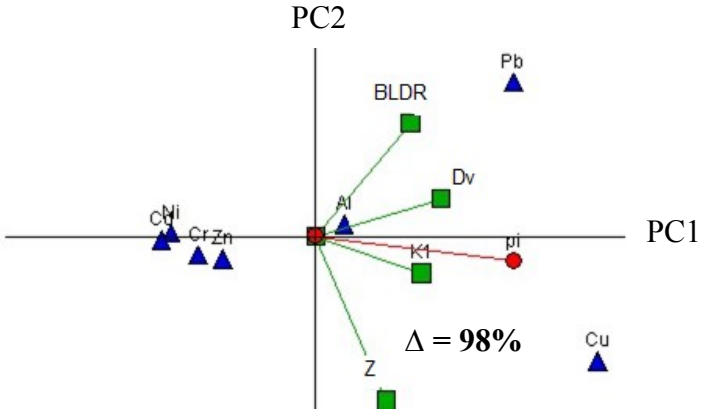

Figure 6.15 GAIA biplot for 100 mg/L initial metal concentration - Seaweed

According to the GAIA biplot for 20 mg/L initial metal concentration (Figure 6.16; 98% variance described), the correlation of Z is relatively stronger with the boundary layer diffusion rate. This is in agreement with the Spearman correlation analysis. This can be possible since at low concentration, the active sites present in seaweed are adequate for the sorption of all metal ions. Thus, diffusion inside the cracks and

metal binding can be rapid. However, due to relatively low molar concentration gradient, the boundary layer diffusion can be slow.

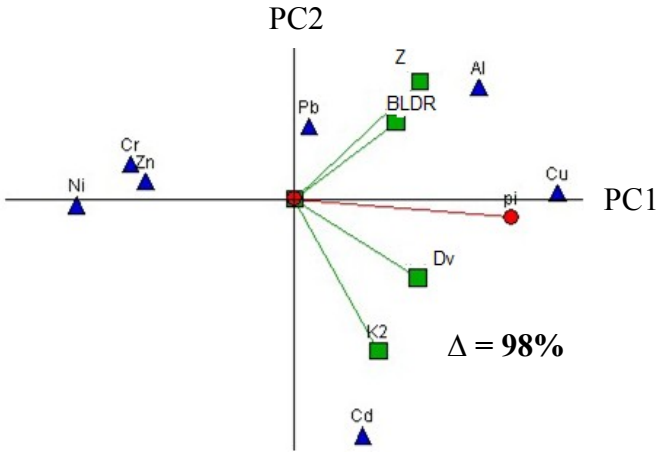

Figure 6.16 GAIA biplot for 20 mg/L initial metal concentration - Seaweed

6.4.3 SORPTION THERMODYNAMICS

By following the similar approach adopted in Section 6.3.4, the thermodynamics parameters were determined based on the plots shown in Figure 6.17 and are tabulated in Table 6.20. The experimental data used for the analysis can be found in Table B.17 in Appendix B.

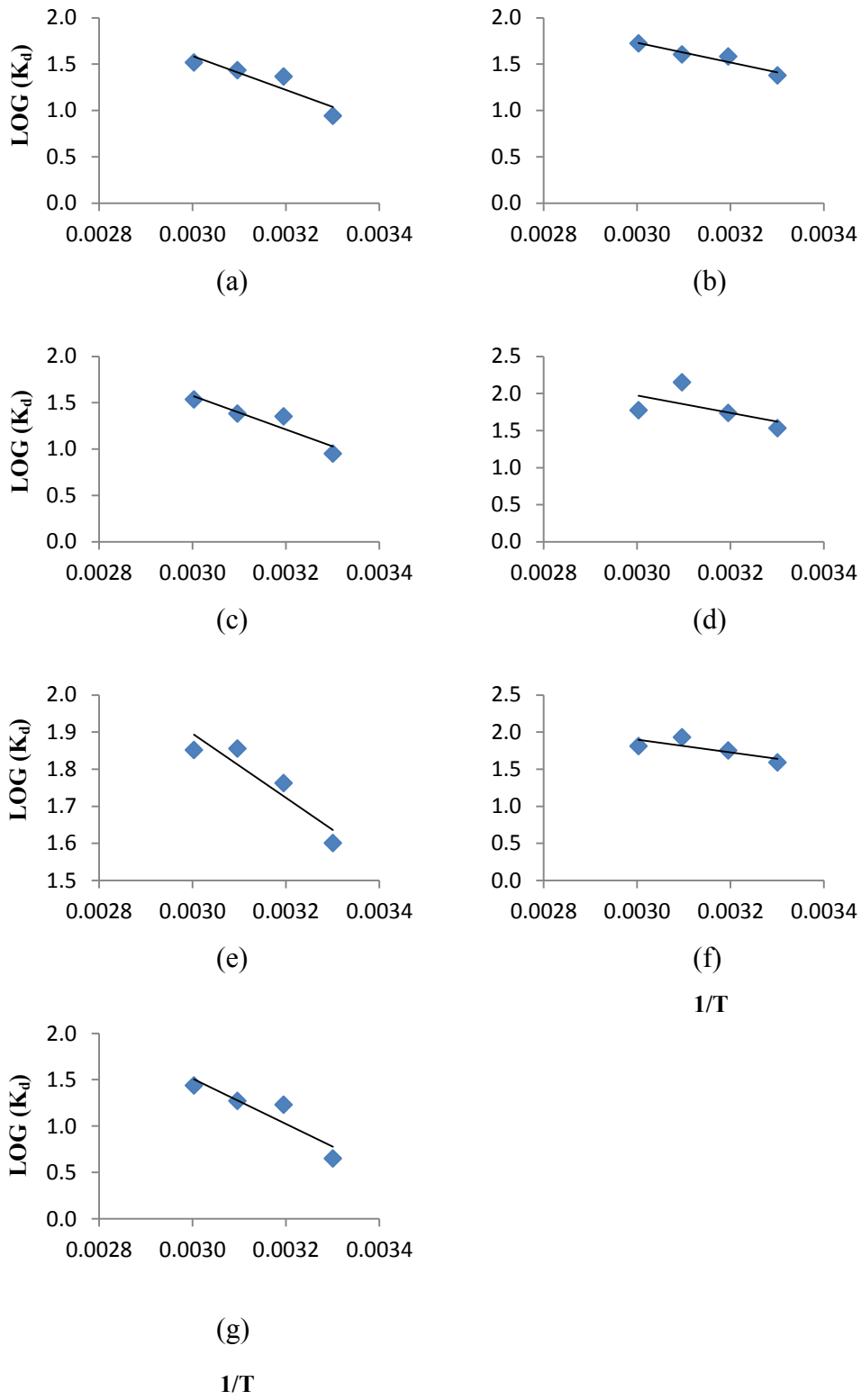

Figure 6.17 LOG(K_D) vs. 1/T plots for seaweed: (a) Cu; (b) Ni; (c) Cd; (d) Pb; (e) Cr; (f) Al; (g) Zn

Table 6.20 Thermodynamics parameters for seaweed

Metal ion	ΔH^o /(kJ/mol)	ΔS^o /(J/mol.K)	ΔG^o/(kJ/mol)			
			[1]303	[1]313	[1]323	[1]333
Cu	35.1	135.6	-6.0	-7.4	-8.7	-10.1
Ni	20.5	94.8	-8.2	-9.1	-10.1	-11.0
Cd	34.7	134.4	-6.0	-7.3	-8.7	-10.0
Pb	22.7	105.7	-9.4	-10.4	-11.5	-12.5
Cr	16.5	86.0	-9.5	-10.4	-11.2	-12.1
Al	16.5	86.0	-9.5	-10.4	-11.2	-12.1
Zn	46.9	169.6	-4.5	-6.2	-7.9	-9.6

Notes:

[1] Absolute temperature / (K)

The negative Gibbs free energy change (ΔG^0) for the metal ions at the investigated temperatures indicates that sorption of metals by seaweed can begin spontaneously. The metal sorption is more favourable at higher temperature since the ΔG^0 values decrease with increasing temperature. The enthalpy change (ΔH^0) is positive for all metal ions. Hence, the metal sorption by seaweed is of endothermic nature. According to the ΔH^0 values, the energetically favourable nature of metal sorption increases in the following order: Zn < Cu < Cd < Cr ≈ Al < Pb < Ni. Accordingly, high temperature is necessary for the sorption of Zn. However, ΔH^0 for Ni, Pb, Cr, Cu and Zn in seaweed is lower compared to zeolite. This suggests that the sorption of these metals by seaweed is thermodynamically favourable than the sorption by zeolite. In contrast, zeolite can be thermodynamically the better option for the sorption of Cd and Al. Positive ΔS^0 indicates that changes occurred in the seaweed structure due to the sorption of metals, which are attributed to cation exchange or formation of bonds with the active sites (Mohan and Singh 2002).

6.4.4 SORPTION ISOTHERM

The equilibrium sorption data (Tables B.18 in Appendix B) were initially fitted with the Langmuir isotherm model and presented in Figure 6.18. Similar to zeolite, the R^2 values are low suggesting that sorption occurred in multilayer as described for zeolite in Section 6.3.3. Therefore, the equilibrium sorption data were fitted to the Freundlich model as shown in Figure 6.19.

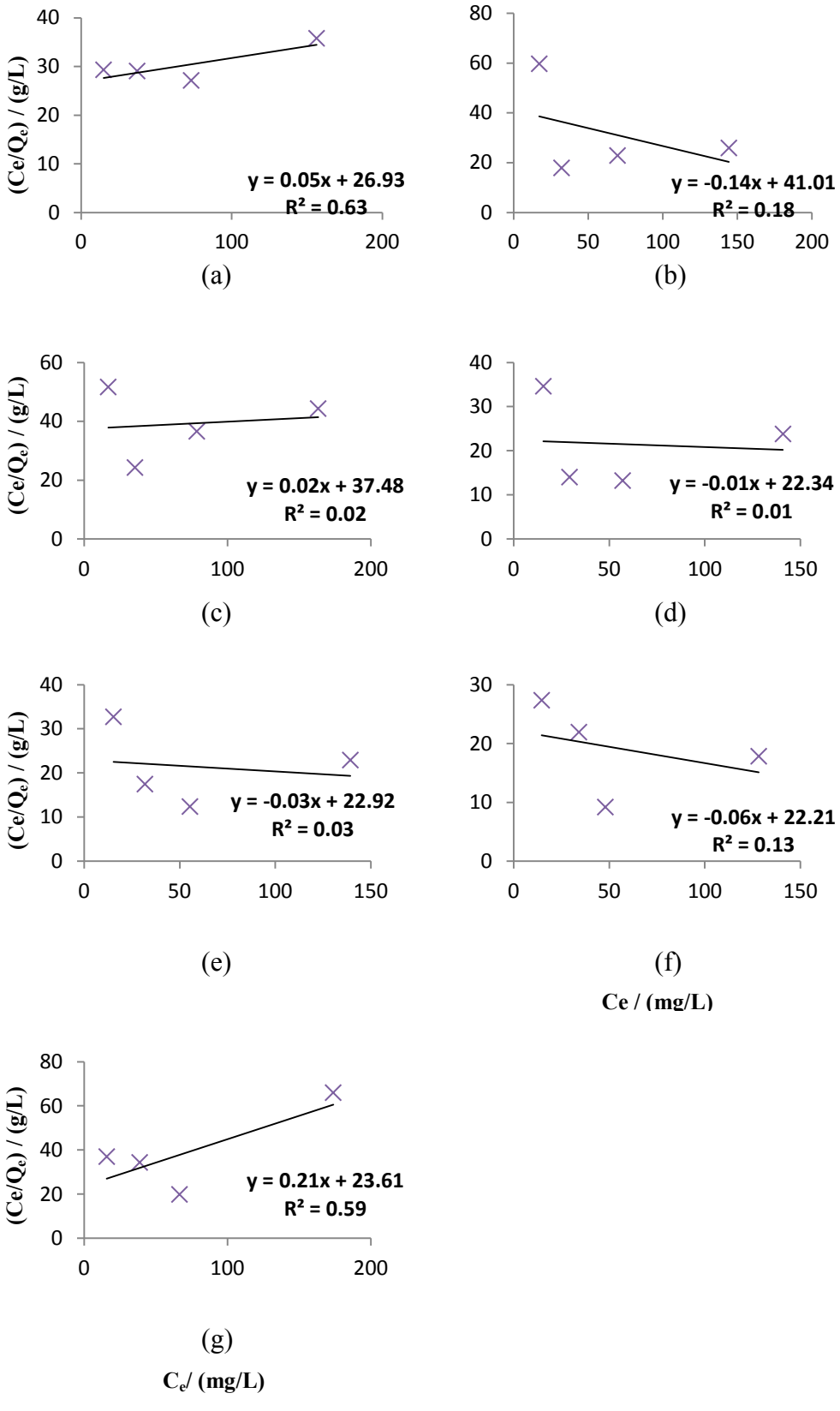

Figure 6.18 Langmuir isotherm models for seaweed: (a) Cu; (b) Ni; (c) Cd; (d) Pb; (e) Cr; (f) Al; (g) Zn

The isotherm constants derived from the slope and y-intercept of Freundlich plots are tabulated in Table 6.21. The R^2 values are high indicating a good fit of Freundlich isotherm with the experimental data. Aravindhan et al. (2004) and Antunes et al. (1996) also reported similar results with the Freundlich isotherm model.

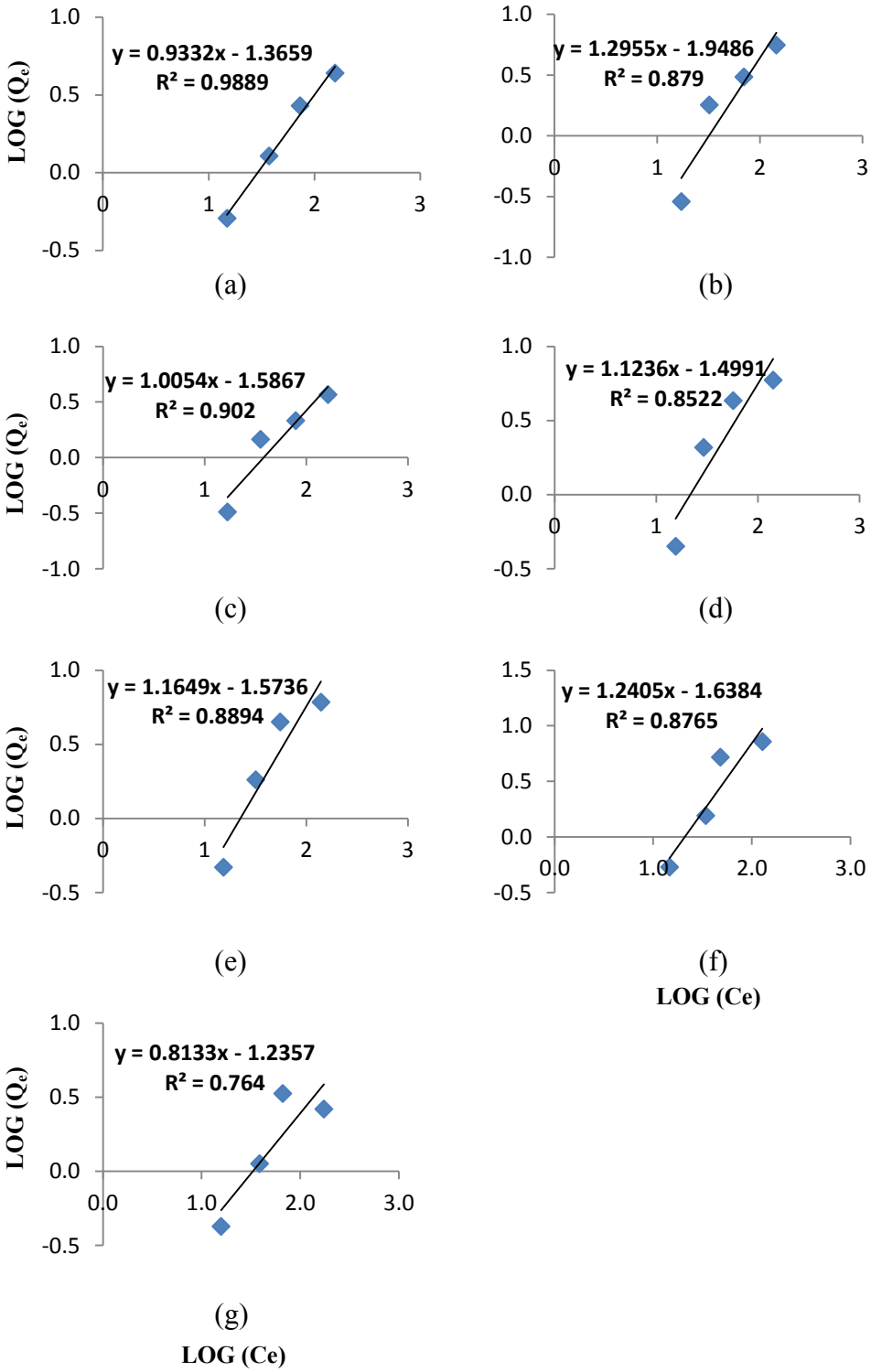

Figure 6.19 Freundlich isotherm models for seaweed: (a) Cu; (b) Ni; (c) Cd; (d) Pb; (e) Cr; (f) Al; (g) Zn

Table 6.21 Freundlich isotherm constants for seaweed

Metal ion	K_F/ ((mg/g)/(mg/L)$^{1/n}$)	n	R^2
Cu	0.04	1.07	0.989
Ni	0.01	0.76	0.879
Cd	0.03	1.00	0.902
Pb	0.03	0.89	0.852
Cr	0.03	0.86	0.889
Al	0.02	0.81	0.876
Zn	0.06	1.23	0.764

In Section 6.4.2 (B), it was concluded that either ion exchange mechanism or ionic bonding was responsible for the sorption of Zn by seaweed. According to the n values, it is confirmed that the sorption of Zn occurred via ionic bonding since the n value for Zn suggests that the sorption bond is strong, which is a characteristic of the ionic bond. On the other hand, sorption of Ni, Pb, Cr and Al occurred via physisorption or ion exchange. The n values of Cd and Cu are 1 or close to 1 suggesting that physisorption can have an influence on the sorption of these metals along with chemisorption. The affinity of seaweed for metal was deduced based on the K_F values (Table 6.21) and it is as follows: Zn > Cu > Pb ≈ Cd ≈ Cr > Al > Ni. This affinity series is not in agreement with the series predicted by the thermodynamics study (Section 6.4.3) suggesting that the sorption thermodynamics has little impact on the metal sorption affinity of seaweed.

High affinity for Cu can be attributed to high intraparticle diffusion rate, which helped Cu to reach the active sites faster and, consequently, increased the possibility of Cu sorption. Pb and Cd exhibited similar affinity, which can be due to their low hydration energy. Therefore, Pb and Cd are sorbed via ion exchange mechanism as predicted based on the n values. Seaweed contains hard bases such as the carboxylic and hydroxyl functional groups. However, the affinity of seaweed for hard acids such as Cr and Al was low. As suggested by the n values (Table 6.21), the primary mechanism employed by seaweed for the sorption of Cr and Al is ion exchange. This is possible since seaweed contains a large number of ion exchange sites (Section 6.2.1). However, Cr and Al have larger hydration energies. Hence, it is difficult for Al and Cr to participate in the ion exchange mechanism. Consequently, sorption affinity for Al and Cr is low. Furthermore, sorption of Ni by seaweed that has a large

number of hard bases occurred via physisorption, according to the n values (Table 6.21). However, Ni has low charge density that can retard its physisorption, which is the reason for seaweed having low affinity for Ni.

6.5 CONCLUSIONS

Kinetics, isotherm and thermodynamics characteristics of metal sorption mechanism were investigated for zeolite and seaweed. The sorption system attained equilibrium within an hour for zeolite and seaweed. The boundary layer diffusion of metals in zeolite was primarily influenced by the molar metal concentration, molar volume, valence electron configuration and hydration energy. The intraparticle diffusion rates were determined using both Weber-Morris and Vermeulen models. Vermeulen intraparticle model is recommended over Weber-Morris model for determining the intraparticle diffusion rates when only a few data points are present in the second linear region of Q_t vs. $\sqrt{t}$ plot. Furthermore, the intraparticle diffusion rate series was inconsistent for different initial metal concentration, which was attributed to the variation of zeolite properties.

However, in general, the Vermeulen intraparticle diffusion rates are governed by hydrated ionic size, chemical hardness and molar concentration of metal ions. Furthermore, the metal binding rates can be described by both pseudo first order and second order kinetics models and the metal binding rate series is approximately similar to the intraparticle rate series. Hence, it was concluded that the active sites in zeolite should be present in the pores. A parameter called average specific metal removal rate was proposed to account for overall metal removal rate and mathematically established. This parameter was used to develop an analytical approach based on the Spearman correlation and GAIA techniques to identify the rate-limiting steps. The primary rate-limiting step of the sorption kinetics of zeolite was found to be intraparticle diffusion followed by the metal binding process. The effect of the boundary layer diffusion on the overall metal removal rate of zeolite was inconclusive.

Thermodynamics studies were conducted to further investigate the zeolite sorption system. Negative Gibbs free energy change suggested that sorption of metal ions by

zeolite is favourable at high temperatures. Sorption of metals by zeolite is endothermic and changed the structure of zeolite. Furthermore, sorption is energetically favourable in the order of Al > Cr > Pb > Ni > Cd > Cu > Zn. The affinity of zeolite for metal sorption was found to be influenced by the sorption thermodynamics. In general, the characteristics of zeolite are best described by the Freundlich model indicating that metal sorption by zeolite is of multilayer nature. In addition, charge density, hydration energy, valence electron configuration of the ion and the kinetics rates influence the affinity of zeolite for the sorption of metal ions. The sorption mechanism employed by zeolite is chemisorption for Pb and Cr, while ion exchange or physisorption also contribute in the sorption of Al, Cd, Zn, Ni and Cu.

The analytical approach similar to zeolite was adopted to define the mechanisms employed by seaweed for metal sorption. The boundary layer diffusion is primarily influenced by the molar metal concentration and hydration energy, while the intraparticle diffusion rate is governed by the molar concentration, hydration energy and molar volume of metal ions. Similar to zeolite, inconsistency in the intraparticle diffusion rate series for different initial metal concentration was observed, which was attributed to the heterogeneity of seaweed properties. Both pseudo first order and second order kinetics models can be used to describe the metal binding process of seaweed. It was hypothesised that the sorption sites in seaweed are predominantly found inside the cracks on the external surface since the metal binding rate series was approximately similar to the intraparticle rate series. The primary rate-limiting step is the metal binding process and the intraparticle diffusion also has an influence on metal sorption. The boundary layer diffusion also limits the overall metal removal rate in certain cases.

Thermodynamics study suggested that the metal sorption is energetically favourable in the following order: Zn < Cu < Cd < Cr ≈ Al < Pb < Ni. However, this order does not reflect the affinity order derived from the Freundlich constants indicating that sorption thermodynamics has limited influence on the metal sorption. In contrast, kinetics rates, hydration energies and charge densities of metal ions influence the sorption affinity of seaweed. Additionally, the sorption of Ni, Pb, Cu, Cr and Zn by

seaweed is thermodynamically favourable than by zeolite, while zeolite is thermodynamically the best option for Cu, Cd and Al. Zn sorption by seaweed occur via ionic interaction with the anionic sites of seaweed. Cr, Al, Pb and Cd are sorbed by seaweed via ion exchange mechanism, whilst sorption of Ni occurs via physisorption.

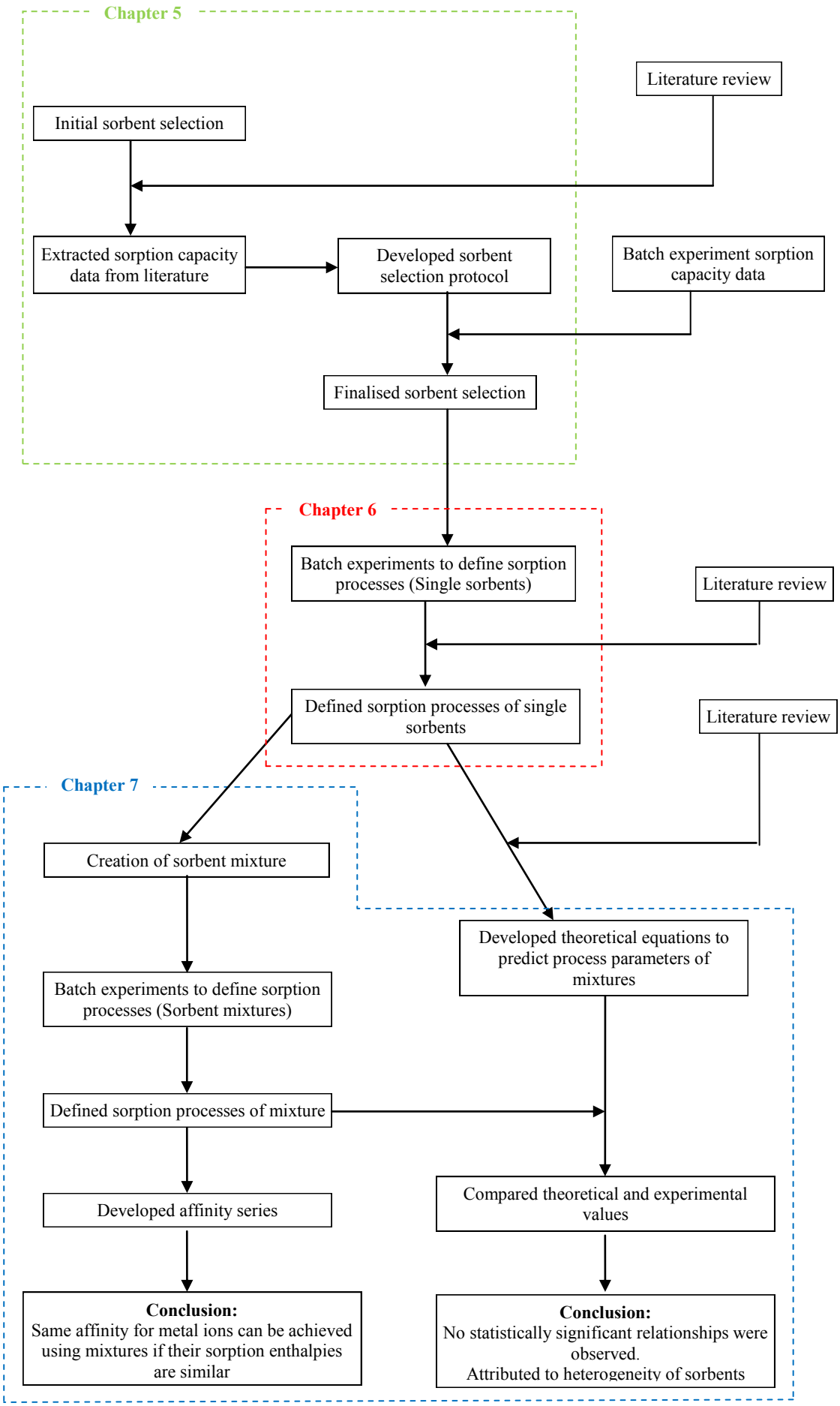

Schematic diagram showing the research methodology and the development of analytical chapters

Chapter 7: Isotherm, kinetics and thermodynamics of metal sorption by innovative mixtures

7.1 INTRODUCTION

The outcomes from Chapter 6 confirmed that the sorption of metal ions is influenced by the isotherm, thermodynamics and kinetics characteristics of the mechanisms employed by the sorbents. Depending on these characteristics, zeolite and seaweed prefer to sorb specific metal ions, which in turn can result in poor removal of the less preferred metal ions. Therefore, it was hypothesised that affinity for the sorption of metals can be enhanced by using mixtures of seaweed and zeolite, whereby the different isotherm, kinetics and thermodynamics characteristics of both sorbents can be utilised. Additionally, it was also hypothesised that the thermodynamics and kinetics aspects of metal sorption by zeolite-seaweed mixtures can be mathematically related to those of individual sorbents based on the mass conservation principle.

In order to test these hypotheses, batch sorption experiments for mixtures were conducted as described in Section 4.3.4 and the kinetics, isotherm and thermodynamics parameters were determined using a similar approach as described in Section 6.3. In this chapter, firstly, the metal sorption kinetics, isotherm and thermodynamics characteristics of mechanisms employed by the mixtures are discussed. Thereafter, the determination of theoretical kinetics and thermodynamics parameters for mixtures from the mathematical relationships derived based on mass conservation principle are discussed. The applicability of these theoretical relationships is investigated using the experimental values. Finally, the effect of mixing the sorbent materials on sorption affinity is evaluated.

7.2 DETERMINATION OF EQUILIBRIUM TIME

Four mixtures were prepared by mixing zeolite and seaweed in the proportions given in Table 7.1:

Table 7.1 Composition of mixtures

Mixture	% zeolite	% seaweed
1	80	20
2	60	40
3	40	60
4	20	80

The kinetics batch experiments were conducted for mixtures as described in Section 4.3.4 (A). The time required for each mixture to attain equilibrium or near equilibrium state was determined from the plots of the kinetics experimental data (Tables C.1-C.4 in Appendix C) shown in Figure 7.1:

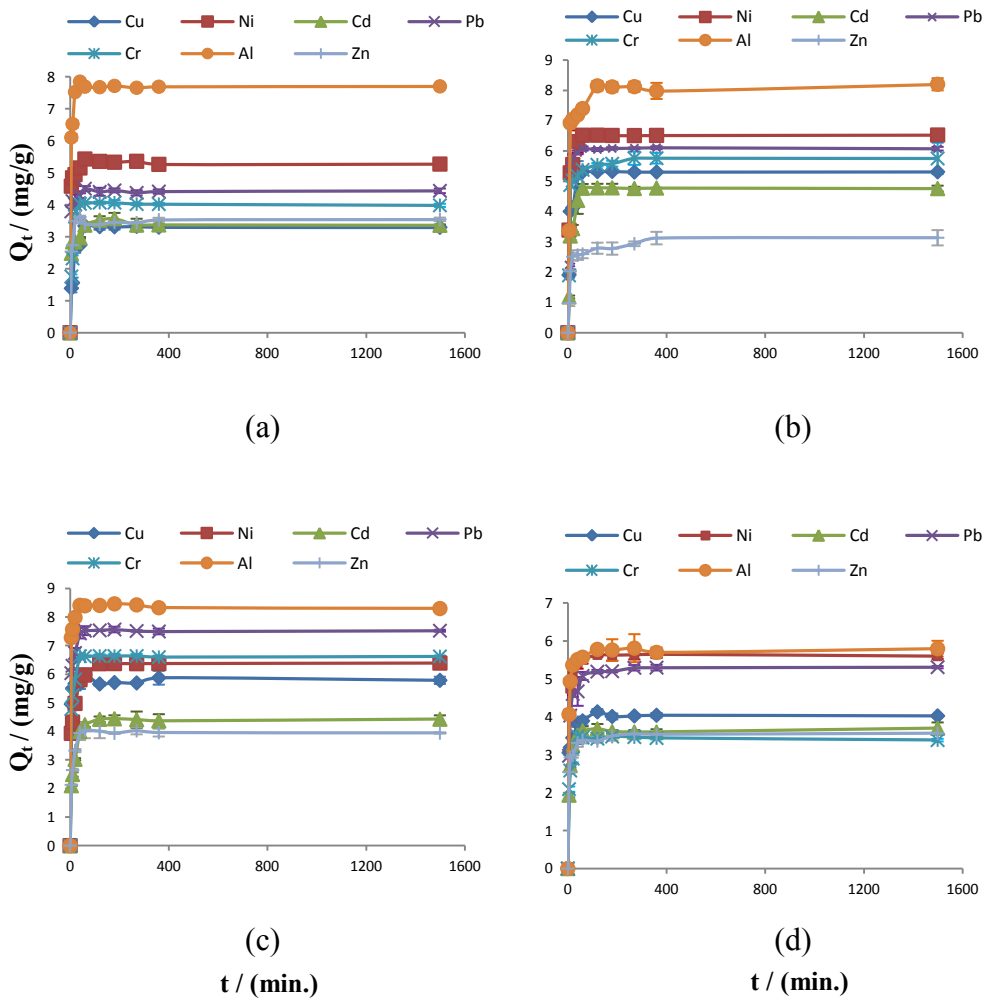

Figure 7.1 Sorption capacity vs. time graphs for mixtures: (a) mixture 1; (b) mixture 2; (c) mixture 3; (d) mixture 4

According to Figure 7.1, the sorption of metals by mixtures was rapid. In Chapter 6, it was found that the sorption of metals by seaweed and zeolite was also rapid. Similar to zeolite and seaweed, the sorption equilibrium or near equilibrium was achieved in less than 60 minutes for the investigated metal ions. Therefore, the thermodynamics experiments for mixtures were conducted for one hour.

7.3 METAL SORPTION MECHANISMS OF MIXTURES

7.3.1 SORPTION KINETICS

The sorption capacity data (Q_t) (Tables C.1-C.4 in Appendix C) vs. square root of time ($\sqrt{t}$) plots for mixtures are presented in Figure 7.2. The plots show three linear regions indicating that both boundary layer and intraparticle diffusion processes are involved in the sorption of metals by mixtures.

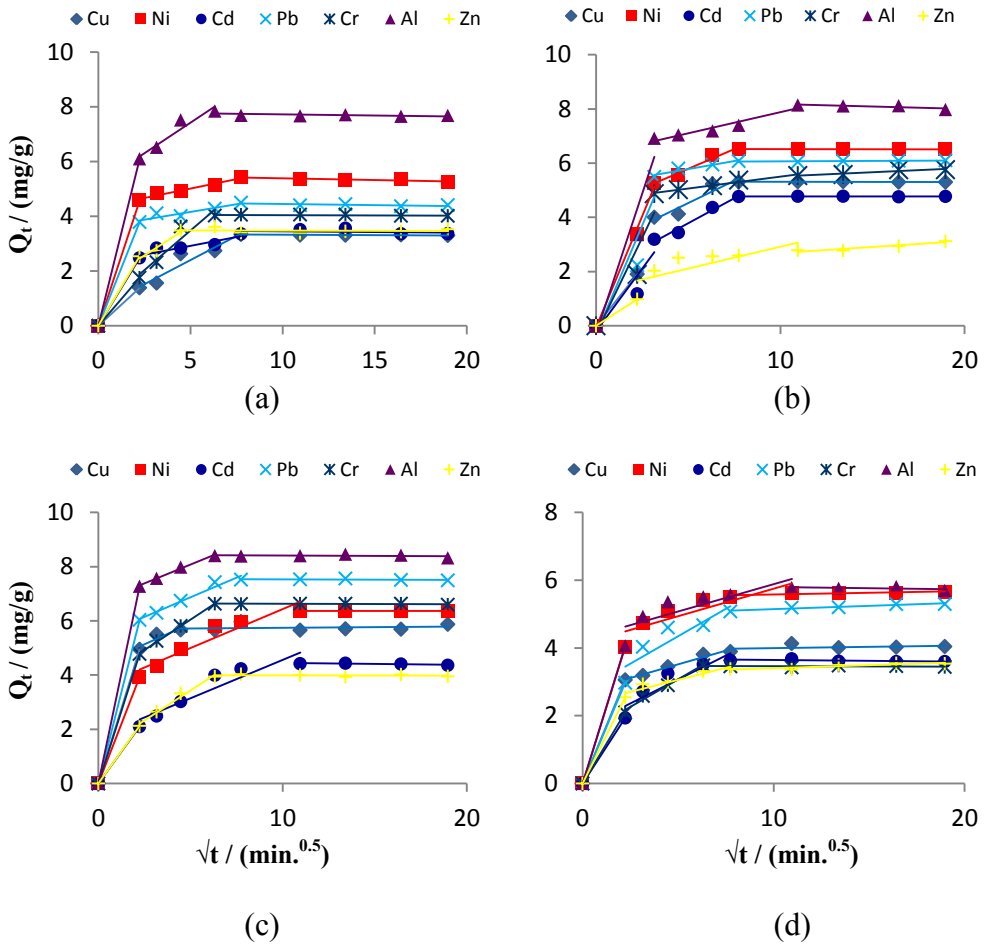

Figure 7.2 Q_t vs. $\sqrt{t}$ plot for mixtures: (a) mixture 1; (b) mixture 2; (c) mixture 3; (d) mixture 4

The boundary layer diffusion rates for mixtures were determined using equation (3.8) and the values are tabulated in Table 7.2 along with the boundary layer diffusion rates for zeolite and seaweed.

Table 7.2 Boundary layer diffusion rates for mixtures / (min^{-1})

Metal ion	Cu	Ni	Cd	Pb	Cr	Al	Zn
Zeolite	0.050	0.020	0.011	0.031	0.007	0.057	0.009
Mixture 1	0.014	0.046	0.025	0.038	0.018	0.061	0.025
Mixture 2	0.019	0.034	0.012	0.022	0.019	0.034	0.010
Mixture 3	0.050	0.039	0.021	0.060	0.048	0.073	0.021
Mixture 4	0.031	0.040	0.019	0.030	0.021	0.041	0.025
Seaweed	0.029	0.029	0.005	0.034	0.040	0.060	0.013

According to Table 7.2, the boundary layer rates decrease in the order shown in Table 7.3.

Table 7.3 Boundary layer diffusion rate series

Metal ion	Boundary layer rate series
Zeolite	$Al \geq Cu > Pb > Ni > Cd \geq Zn \geq Cr$
Mixture 1	$Al > Ni > Pb > Cd \approx Zn > Cr \geq Cu$
Mixture 2	$Ni \approx Al > Pb \geq Cu \approx Cr > Cd \geq Zn$
Mixture 3	$Al > Pb > Cu \geq Cr > Ni > Cd \approx Zn$
Mixture 4	$Al \geq Ni > Cu \geq Pb \geq Zn \geq Cr \geq Cd$
Seaweed	$Al > Cr \geq Pb \geq Cu \geq Ni > Zn > Cd$

In Chapter 6, it was found that the boundary layer diffusion rates of Al, Ni, Cu and Cd in both seaweed and zeolite are influenced by the molar concentration. Similarly, in both sorbents, the boundary layer diffusion rates of Pb and Zn are governed by the hydration energy and valence electron configuration, respectively. Hence, the boundary layer diffusion rate series of these metals can be expected to be unaffected in mixtures since the boundary layer diffusion rates depend on the properties of metal ions and not on the properties of the sorbents.

As evident in Table 7.3, for mixtures, the boundary layer diffusion rates of Al, Cu and Ni were generally higher than other investigated metals due to their relatively higher molar concentration. On the other hand, the molar concentration of Cd was low in the solution, due to which the boundary layer diffusion rates of Cd were generally lower for mixtures as was the case for zeolite and seaweed. Pb exhibited higher boundary layer diffusion rates due to its low hydration energy, while Zn had low boundary layer diffusion rates due to its inert valence electron structure. However, the boundary layer rate of Cr was influenced by the molar volume in zeolite and by the molar concentration in seaweed (Sections 6.3 and 6.4). Accordingly, high molar concentration of Cr can enhance its boundary layer diffusion by providing a large physical driving force, while its high molar volume can retard its diffusion as suggested by Wilke and Chang (1955). Hence, in mixtures, the boundary layer diffusion rate order of Cr varied depending on whether molar concentration or molar volume governed the boundary layer diffusion.

The intraparticle diffusion rates for mixtures were determined by fitting the batch kinetics experimental data presented in Tables C.1-C.4 in Appendix C with the Vermeulen model (equation 3.9). The Vermeulen rates are tabulated in Table 7.4 along with the rates for zeolite and seaweed.

Table 7.4 Intraparticle diffusion rates for mixtures ($D_v \times 10^{-8}$ $m^2 min^{-1}$)

Metal ion	Cu	Ni	Cd	Pb	Cr	Al	Zn
Zeolite	18.0	9.0	5.0	8.0	1.0	12	4.0
Mixture 1	2.1	16.2	8.2	15.7	3.0	10.8	8.6
Mixture 2	2.6	4.6	1.5	3.0	2.3	3.3	2.2
Mixture 3	17.8	4.3	2.7	10.4	7.6	15.0	4.1
Mixture 4	7.9	8.2	4.8	4.8	5.2	8.1	7.7
Seaweed	7.2	4.4	0.5	4.3	6.3	15	4.7

The intraparticle diffusion rate series was derived based on the rates in Table 7.4 and is given in Table 7.5.

Table 7.5 Intraparticle diffusion rate series

Metal ion	Intraparticle diffusion rate series
Zeolite	Cu > Al > Ni ≥ Pb > Cd ≥ Zn > Cr
Mixture 1	Ni > Pb > Al > Zn ≥ Cd > Cr ≥ Cu
Mixture 2	Ni > Al ≥ Pb ≥ Cu ≥ Cr ≥ Zn > Cd
Mixture 3	Cu > Al > Pb > Cr > Ni ≥ Zn ≥ Cd
Mixture 4	Ni ≥ Al ≥ Cu ≥ Zn > Cr ≥ Cd ≈ Pb
Seaweed	Al > Cu ≥ Cr > Zn ≥ Ni ≥ Pb > Cd

The molar concentration and hydrated ionic size governed the intraparticle diffusion of Ni in seaweed and zeolite, respectively (Sections 6.3.2B and 6.4.2B). Consequently, in mixtures, Ni had relatively higher intraparticle diffusion rates (Table 7.5), which is attributed to high molar concentration and small hydrated ionic diameter. Similarly, the intraparticle diffusion rate of Al was high. This is attributed to the high molar concentration of Al in solution, which was the reason for higher intraparticle diffusion observed in both zeolite and seaweed.

The intraparticle diffusion rate of Zn varied between moderate and low. In zeolite, the intraparticle diffusion of Zn was low due to relatively larger hydrated ionic diameter, whereas the rate was moderate in seaweed because of ionic bonding with anionic sites of seaweed. Consequently, the lower intraparticle diffusion rate observed in mixtures indicates that Zn is sorbed to zeolite, whilst sorption occurred in seaweed when the intraparticle diffusion rate was high. Similarly, the intraparticle diffusion rate of Cr varied between moderate and low. The moderate diffusion rate is attributed to the high chemical hardness, which was responsible for the high intraparticle diffusion rate of Cr in zeolite. In contrast, high hydration energy of Cr retarded the intraparticle diffusion of Cr in seaweed, which is attributed to be the reason for low intraparticle diffusion rate observed in certain mixtures.

In general, Cu has a moderate intraparticle diffusion rate. Though Cu had relatively large driving force resulting from its high molar concentration, its soft acidic nature reduced its driving force for intraparticle diffusion. This is because zeolite and seaweed have hard bases, which prefer to bond with metals with hard acidic nature according to the HSAB principle (Pearson 1968). Hence, Cu does not have a large

chemical driving force. Similarly, the intraparticle diffusion of Pb is also moderate. This is attributed to high molar volume of Pb despite its small ionic diameter. In seaweed, high molar volume of Pb reduced its intraparticle diffusion rate. However, in zeolite, Pb had a relatively higher rate due to its smaller ionic diameter. In mixtures, the intraparticle diffusion rate is governed by both of these factors resulting in a moderate diffusion rate for Pb. Cd showed low intraparticle diffusion rate, which is attributed to its high molar volume. In seaweed, the intraparticle diffusion rate of Cd was low in certain cases, which was attributed to high molar volume of Cd. Therefore, it can be concluded that in mixtures, the sorption of Cd primarily occurs in seaweed. This is possible since seaweed has carboxylic functional groups (Section 6.2.2), which are relatively softer than the hydroxyl groups present in zeolite (Hancock and Martell 1989). Hence, Cd, which is a relatively softer acid among the investigated metals, would have preferentially sorbed to the carboxylic sites in seaweed.

The pseudo second order model provides a good description of the metal binding process in zeolite and seaweed. Hence, pseudo second order metal binding rates for mixtures were determined using the batch kinetics experimental data presented in Tables C.1-C.4 in Appendix C. The values are tabulated in Table 7.6.

Table 7.6 Pseudo second order metal binding rates for mixtures

	Cu	Ni	Cd	Pb	Cr	Al	Zn
Zeolite	0.29	0.12	0.11	0.12	0.03	0.12	0.09
Mixture 1	0.04	0.24	0.15	0.26	0.04	0.10	0.14
Mixture 2	0.03	0.04	0.02	0.03	0.02	0.02	0.04
Mixture 3	0.29	0.04	0.04	0.10	0.07	0.14	0.06
Mixture 4	0.12	0.09	0.07	0.05	0.09	0.08	0.13
Seaweed	0.10	0.04	0.01	0.04	0.06	0.16	0.09

Based on Table 7.6, the following rate series given in Table 7.7 was developed.

Table 7.7 Pseudo second order rate series for mixtures

Metal ion	Intraparticle diffusion rate series
Zeolite	Cu > Ni ≈ Pb ≈ Al ≥ Cd ≥ Zn > Cr
Mixture 1	Pb ≥ Ni > Cd ≥ Zn > Al > Cu ≈ Cr
Mixture 2	Ni ≈ Zn ≥ Cu ≈ Pb ≥ Cd ≈ Cr ≈ Al
Mixture 3	Cu > Al > Pb ≥ Cr ≈ Zn ≈ Ni ≈ Cd
Mixture 4	Zn ≥ Cu > Ni ≈ Cr ≥ Al ≥ Cd ≥ Pb
Seaweed	Al > Cu ≥ Zn > Cr ≥ Ni ≈ Pb > Cd

Except for mixture 2, in general, the order for the metal binding rates in Table 7.7 reflects the intraparticle diffusion rate order given in Table 7.5. Similar phenomenon was observed for seaweed and zeolite in Sections 6.3.2 (C) and 6.4.2 (C) and was attributed to the fact that the metal sorption predominantly occurred in the intraparticle sites of the sorbents. Therefore, the similarity in intraparticle diffusion and metal binding rate series for mixtures is attributed to the occurrence of sorption primarily in the intraparticle sites.

The average specific metal removal rates (Z) for mixtures were determined using equation (6.11) and presented in Table 7.8.

Table 7.8 Z values for mixtures

Metal ion	Zeolite	Mixture 1	Mixture 2	Mixture 3	Mixture 4	Seaweed
Cu	0.071	0.025	0.038	0.095	0.057	0.049
Ni	0.053	0.088	0.050	0.058	0.043	0.035
Cd	0.024	0.057	0.034	0.034	0.036	0.019
Pb	0.047	0.055	0.047	0.075	0.041	0.033
Cr	0.014	0.029	0.045	0.060	0.035	0.047
Al	0.059	0.064	0.036	0.119	0.034	0.090
Zn	0.026	0.058	0.023	0.040	0.035	0.045

The correlation of Z with the boundary layer diffusion (BLDR), Vermeulen intraparticle diffusion (D_v) and metal binding (K_2) rates was used as the basis to

determine the rate-limiting step. Spearman correlation analysis was used to observe whether there is a correlation between variables (Table 7.9).

Table 7.9 Correlation of Z with diffusion and reaction rates

Rate parameter	Mixtures	r_s	P
BLDR	Mixture 1	0.857	0.024
	Mixture 2	0.750	0.066
	Mixture 3	0.964	0.003
	Mixture 4	0.084	0.840
D_v	Mixture 1	0.786	0.048
	Mixture 2	0.714	0.088
	Mixture 3	0.964	0.003
	Mixture 4	0.084	0.840
K_2	Mixture 1	0.500	0.267
	Mixture 2	0.143	0.783
	Mixture 3	0.929	0.007
	Mixture 4	0.120	0.783

For significance (P) greater than 0.05, the Spearman correlation analysis is inconclusive. As such, Spearman correlation is not suitable for the analysis of mixtures except for mixture 3 as the P values are greater than 0.05. For mixture 3, it can be concluded that Z is correlated to the boundary layer diffusion, intraparticle diffusion and the metal binding rates. Thus, all three processes limit the overall metal removal rate in mixture 3.

The strength of the correlations between the rates was investigated using the GAIA approach described in Section 6.3. The corresponding GAIA biplot for each mixture is given in Figure 7.3. The PROMETHEE modelling parameters used in this analysis was similar to the parameters described in Section 6.3.2 (D).

For mixture 1 (Figure 7.3 (a); 96% variance accounted), the parameter Z is correlated with both diffusion rates (D_v and BLDR) and the metal binding rate (K_2). This suggests that the overall metal removal rate depends on both diffusion and metal

binding processes, among which the primary rate-limiting step is the intraparticle diffusion due to a relatively stronger correlation with Z.

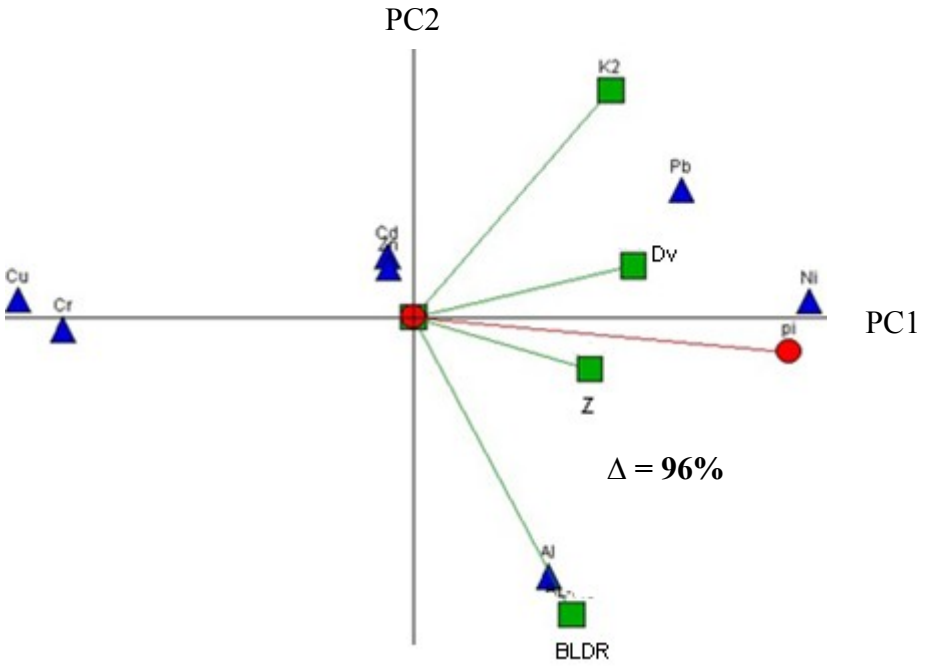

(a)

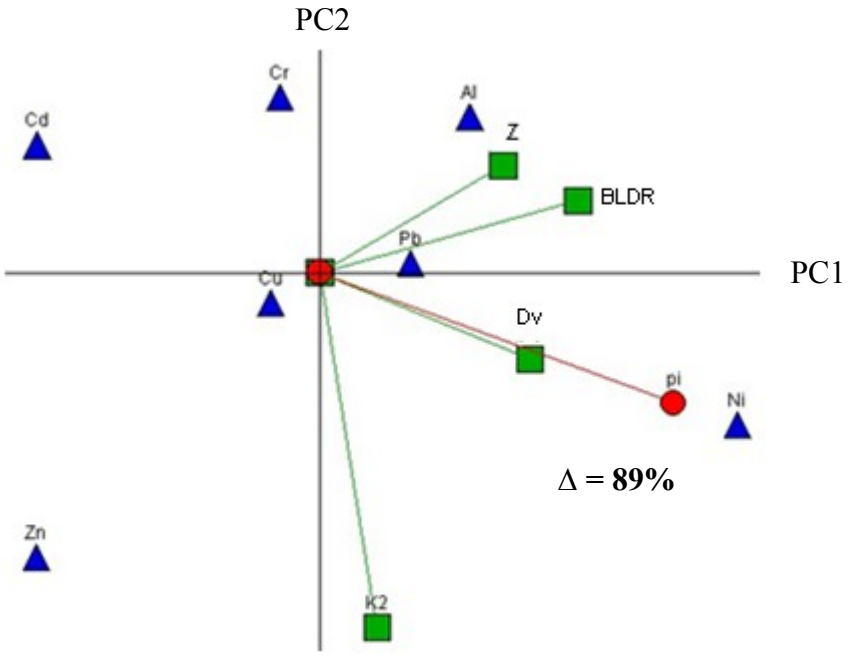

(b)

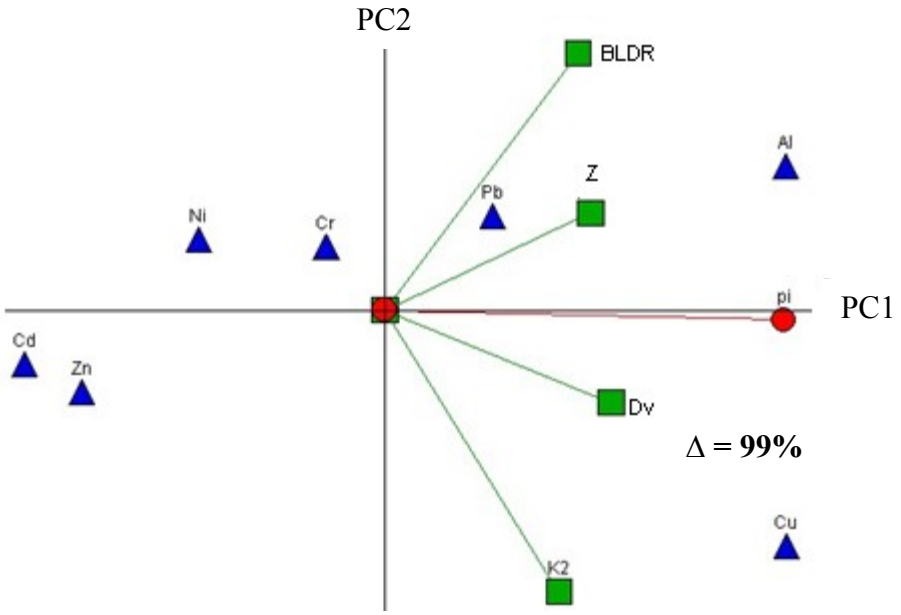

(c)

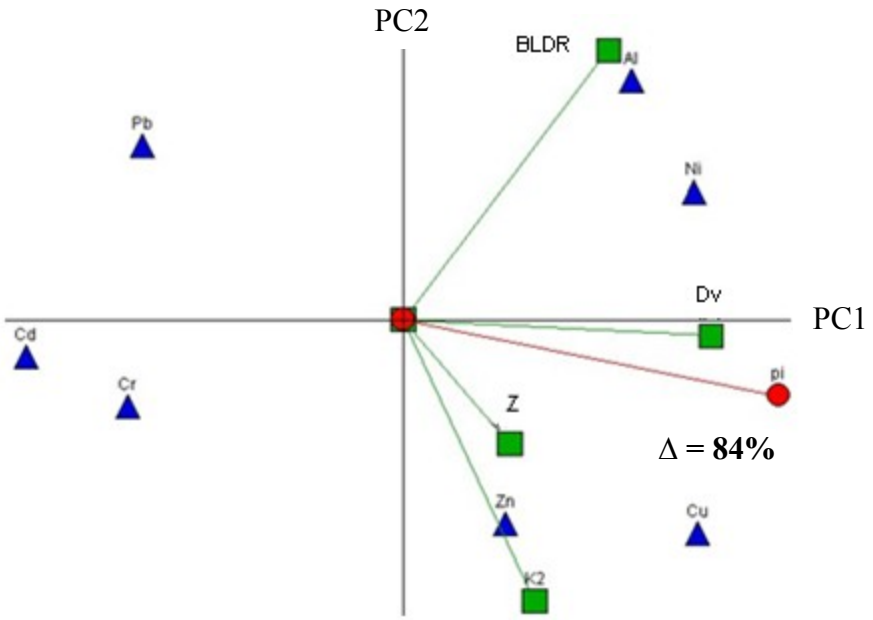

(d)

Figure 7.3 GAIA biplots for (a) mixture 1; (b) mixture 2; (c) mixture 3; (d) mixture 4

The GAIA biplot for mixture 2 (Figure 7.3(b); 89% variance accounted) and mixture 3 (Figure 7.3 (c); 99% variance accounted) predict that the primary rate-limiting step is the boundary layer diffusion followed by the intraparticle diffusion. The metal binding rate does not control the overall metal removal rate in both cases since the

vector is approximately at right angle to Z. In mixture 4 (Figure 7.3 (d); 84% variance accounted), the metal binding rate is the primary rate-limiting step followed by the intraparticle diffusion. The boundary layer diffusion rate vector is at right angle to Z. Hence, it is not limiting the overall metal removal rate.

The major component in mixture 1 is zeolite, the rate of which was limited by the pore diffusion as noted in Section 6.3.2 (D). Hence, the pore diffusion was the main rate-limiting step in the kinetics of metal sorption in mixture 1. Mixture 2 and 3 consisted of a significant amount of seaweed. Thus, the overall metal removal rate was limited by both intraparticle and boundary layer diffusion processes since the boundary layer diffusion was also a rate-limiting step in metal sorption by seaweed (Section 6.4.2D). However, the overall metal removal rate by seaweed was primarily limited by the metal binding rate (Section 6.4.2D). Thus, the metal binding rate was found to be the primary rate-limiting step in mixture 4, which consisted of 80% seaweed.

7.3.2 SORPTION ISOTHERM

The equilibrium experimental data (Tables C.5-C.8 in Appendix C) were first fitted with the Langmuir isotherm model. As evident from Figures C.1-C.4 in Appendix C, the model did not fit the experimental data well in most cases. Therefore, the Freundlich isotherm model was fitted with the experimental data as shown in Figures 7.4-7.7. The isotherm constants were calculated as described in Section 3.4.1.

Figure 7.4 shows the isotherm plots for mixture 1 for the investigated metals.

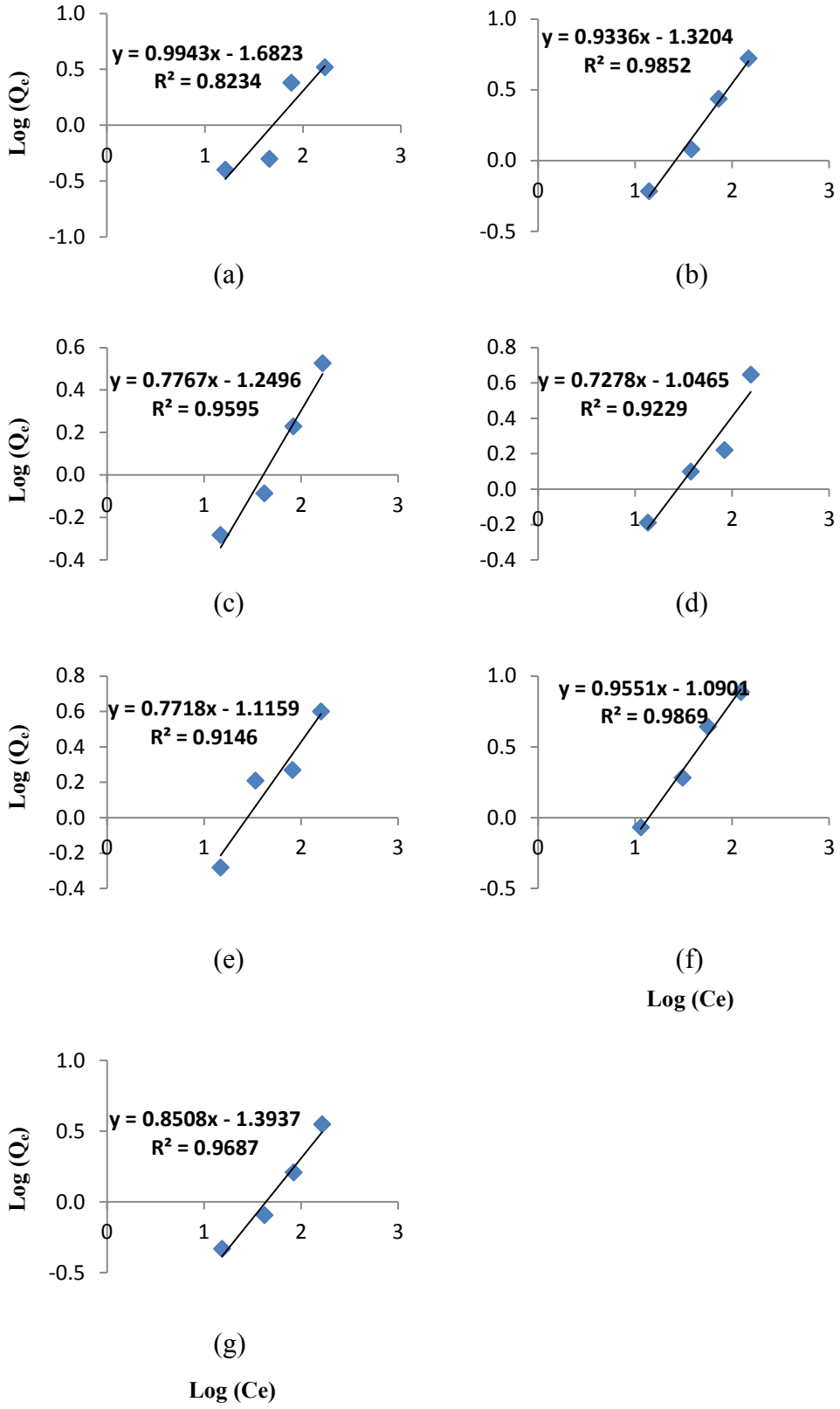

Figure 7.4 Freundlich isotherm models for mixture 1: (a) Cu; (b) Ni; (c) Cd; (d) Pb; (e) Cr; (f) Al; (g) Zn

The Freundlich isotherm constants were calculated from the slope and y-intercept of the plots shown in Figure 7.4 and are tabulated in Table 7.10:

Table 7.10 Freundlich isotherm constants for mixture 1

Metal ion	K_F/ ((mg/g)/(mg/L)$^{1/n}$)	n	R^2
Cu	0.021	1.01	0.8234
Ni	0.008	1.07	0.9852
Cd	0.056	1.29	0.9595
Pb	0.090	1.37	0.9229
Cr	0.077	1.30	0.9146
Al	0.081	1.05	0.9869
Zn	0.040	1.18	0.9687

High R^2 values indicate a good fit of the Freundlich model with the experimental data. Thus, it can be concluded that sorption occurred in multilayer similar to the metal sorption by zeolite and seaweed. The metal sorption affinity of mixture 1 can be derived based on K_F values (Table 7.10) and it decreases in the following order: Pb > Al > Cr > Cd > Zn > Cu > Ni. Based on the affinity series of zeolite (Cr > Al > Pb > Cu ≈ Ni > Cd > Zn) and that of seaweed (Zn > Cu > Pb ≈ Cd ≈ Cr > Al > Ni), it can be concluded that the sorption of Cr, Pb and Zn by mixture 1 is generally influenced by the presence of both sorbents. Zn was the most preferred metal ion by seaweed and the least preferred by zeolite. Similarly, Cr was the most preferred by zeolite and moderately preferred by seaweed. As a result, mixture 1 had a moderate affinity for the sorption of Zn and Cr. On the other hand, Pb was moderately preferred by both sorbents. Therefore, the highest preference for Pb by mixture 1 is attributed to the cumulative effect of both sorbents. In contrast, sorption affinity of Ni and Cd reflects the affinity order of seaweed. Hence, seaweed in mixture 1 is primarily responsible for the sorption of Ni and Cd. Sorption of Al occurred in zeolite since the affinity order of mixture 1 for Al reflects that of zeolite for Al. In the case of Cu, zeolite and seaweed had low and high affinity, respectively. The low affinity of mixture 1 indicates that the presence of seaweed did not have any effect on the sorption affinity of Cu. Therefore, Cu sorption would have occurred predominantly in zeolite.

The sorption of Pb, Cr, Cd, Ni and Zn by mixture 1 was of chemical nature since the n values are well above 1 according to Table 7.10. The n values for Cu, Ni and Al are

close to 1 in comparison to the other metals. Therefore, physisorption and ion exchange have also contributed to the sorption process along with chemical sorption. However, the nature of mechanisms employed for the sorption of a certain metal by mixture 1 did not always reflect that of individual sorbents. For example, sorption of Ni by mixture 1 was associated with seaweed. However, the n value for the sorption of Ni by mixture 1 is close to 1, whilst it was 0.76 for seaweed (Table 6.21). This suggests that other factors such as sorption kinetics and thermodynamics also had an influence on the sorption of metals along with the nature of mechanisms employed for the metal sorption.

The Freundlich isotherm plots and constants for mixture 2 are presented in Figure 7.5 and Table 7.11.

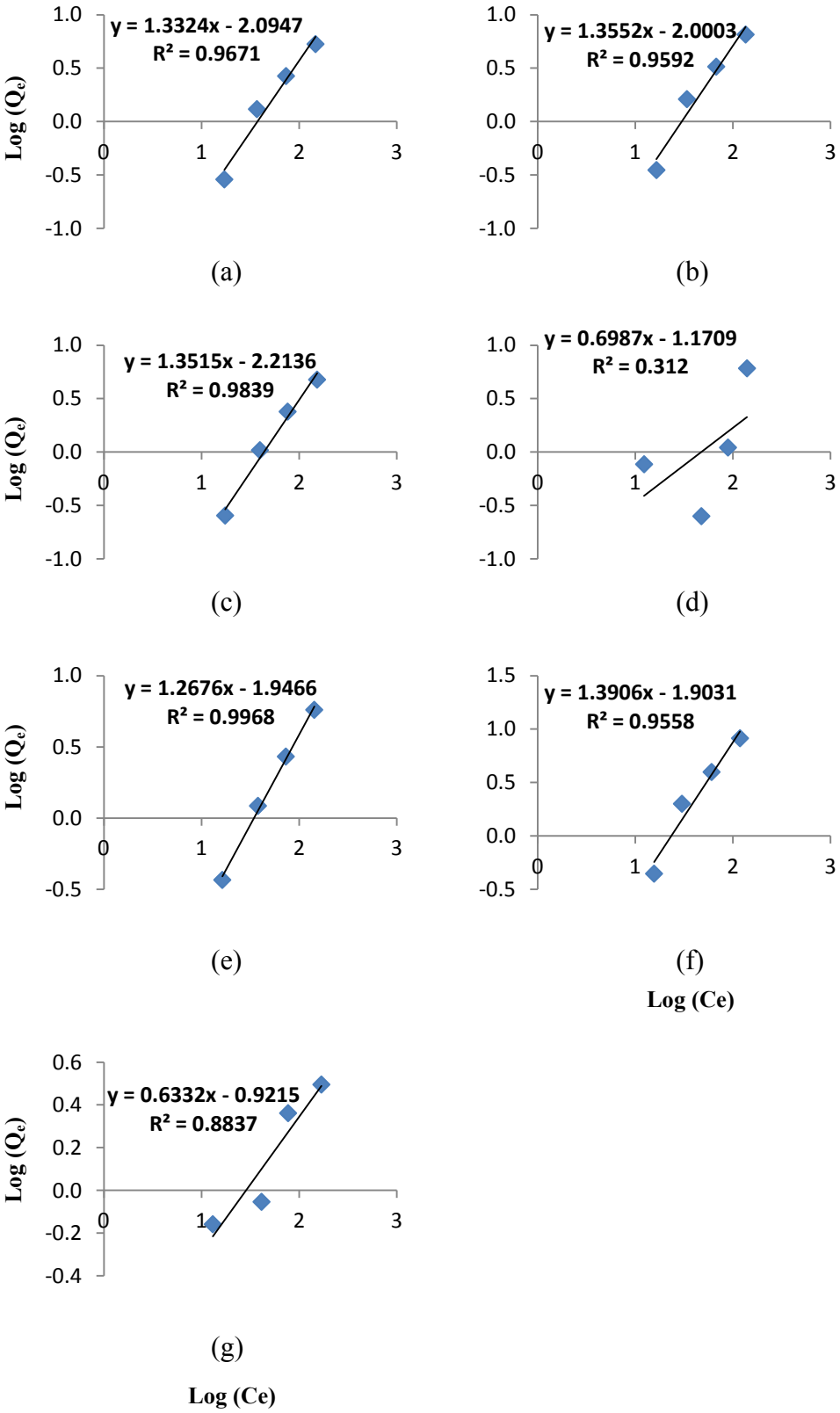

Figure 7.5 Freundlich isotherm models for mixture 2: (a) Cu; (b) Ni; (c) Cd; (d) Pb; (e) Cr; (f) Al; (g) Zn

Table 7.11 Freundlich isotherm constants for mixture 2

Metal ion	K_F/ ((mg/g)/(mg/L)$^{1/n}$)	n	R^2
Cu	0.008	0.75	0.9671
Ni	0.010	0.74	0.9592
Cd	0.006	0.74	0.9839
Pb	0.067	1.43	0.3120
Cr	0.011	0.79	0.9968
Al	0.012	0.72	0.9558
Zn	0.120	1.58	0.8837

The R^2 values are generally high indicating a good fit of the model with the experimental data. The metal sorption affinity for mixture 2 decreased in the order of Zn > Pb > Al ≈ Cr ≈ Ni ≈ Cu ≈ Cd. However, it should be noted that the isotherm constants calculated for Pb is not reliable since it has a low R^2 value. The affinity series indicates that mixture 2 has a high preference for the sorption of Zn. Notably, the affinity for the sorption of Al, Cr, Ni, Cu and Cd is approximately similar. However, the K_F values for these metals are much lower than those for Zn. The n values for Zn and Pb indicate that these metals were sorbed via chemisorption. The n values for the other metals are much less than 1, indicating that the sorption was primarily of a physical nature and the contribution by the chemisorption mechanism is limited.

The Freundlich isotherm plots and constants for mixture 3 are provided in Figure 7.6 and Table 7.12.

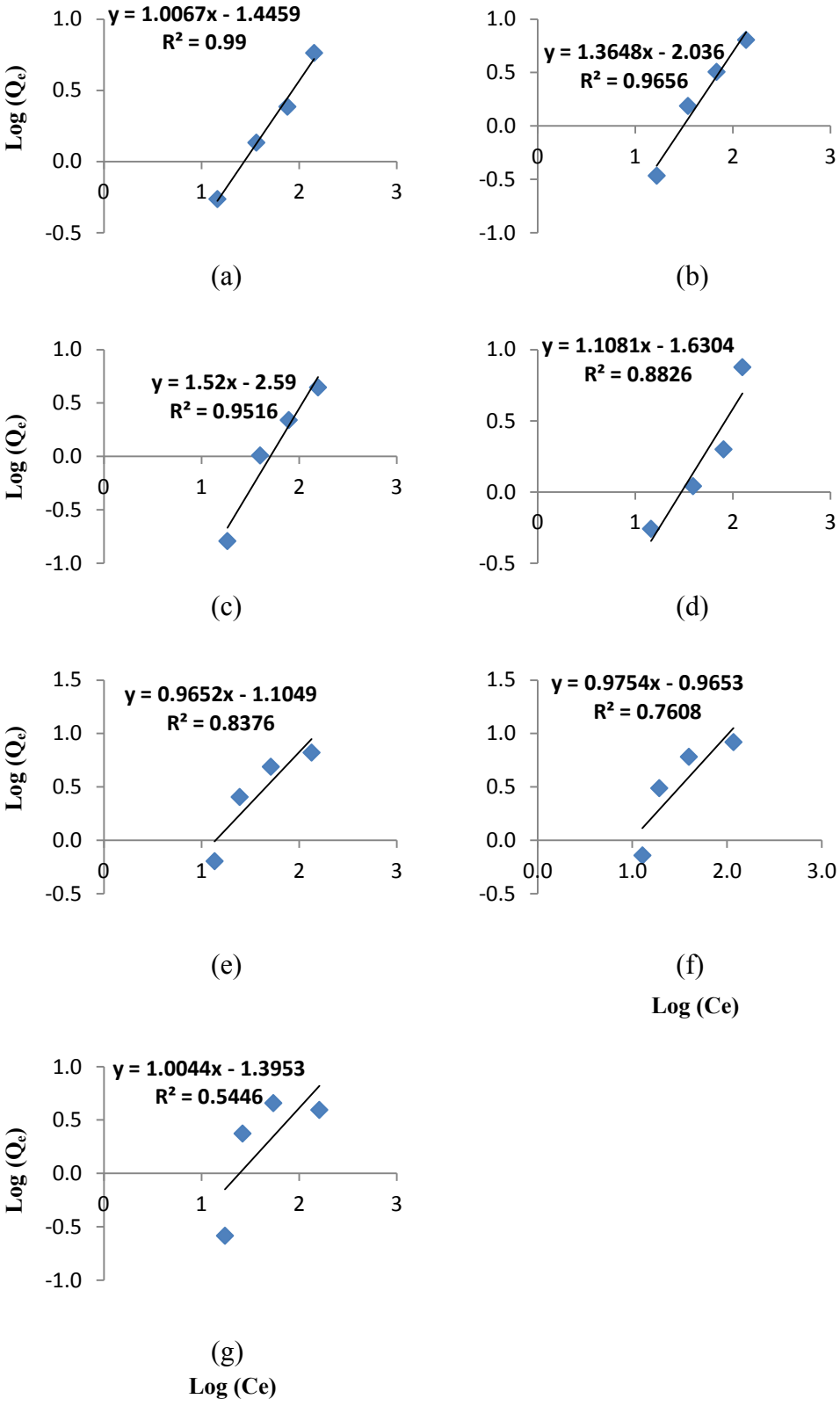

Figure 7.6 Freundlich isotherm models for mixture 3: (a) Cu; (b) Ni; (c) Cd; (d) Pb; (e) Cr; (f) Al; (g) Zn

Table 7.12 Freundlich isotherm constants for mixture 3

Metal ion	K_F/ ((mg/g)/(mg/L)$^{1/n}$)	n	R^2
Cu	0.036	0.99	0.9900
Ni	0.009	0.73	0.9656
Cd	0.003	0.66	0.9516
Pb	0.045	1.13	0.8826
Cr	0.079	1.04	0.8376
Al	0.108	1.03	0.7608
Zn	0.040	1.00	0.5446

High R^2 values indicate that the Freundlich isotherm model describes the experimental data well. According to K_F values, the affinity order is Al > Cr > Pb ≥ Zn ≥ Cu > Ni ≥ Cd. When compared to the affinity series of zeolite and seaweed, sorption of Al, Cr, Cd and Cu reflects the affinity order for zeolite, whilst sorption of Zn and Ni reflects the order for seaweed. The sorption affinity order for Pb in seaweed and zeolite was similar. Hence, it is difficult to conclude whether the sorption of Pb in mixture 3 occurred in seaweed or zeolite. According to the n values, Ni and Cd have n values less than 1 suggesting physical sorption was responsible for their sorption, while Pb was sorbed via chemisorption since the n value is greater than 1. As other metals have n values closer to 1, both physisorption and chemisorption contributed to their sorption by mixture 3.

The Freundlich isotherm plots and the isotherm constants for mixture 4 are given in Figure 7.7 and Table 7.13:

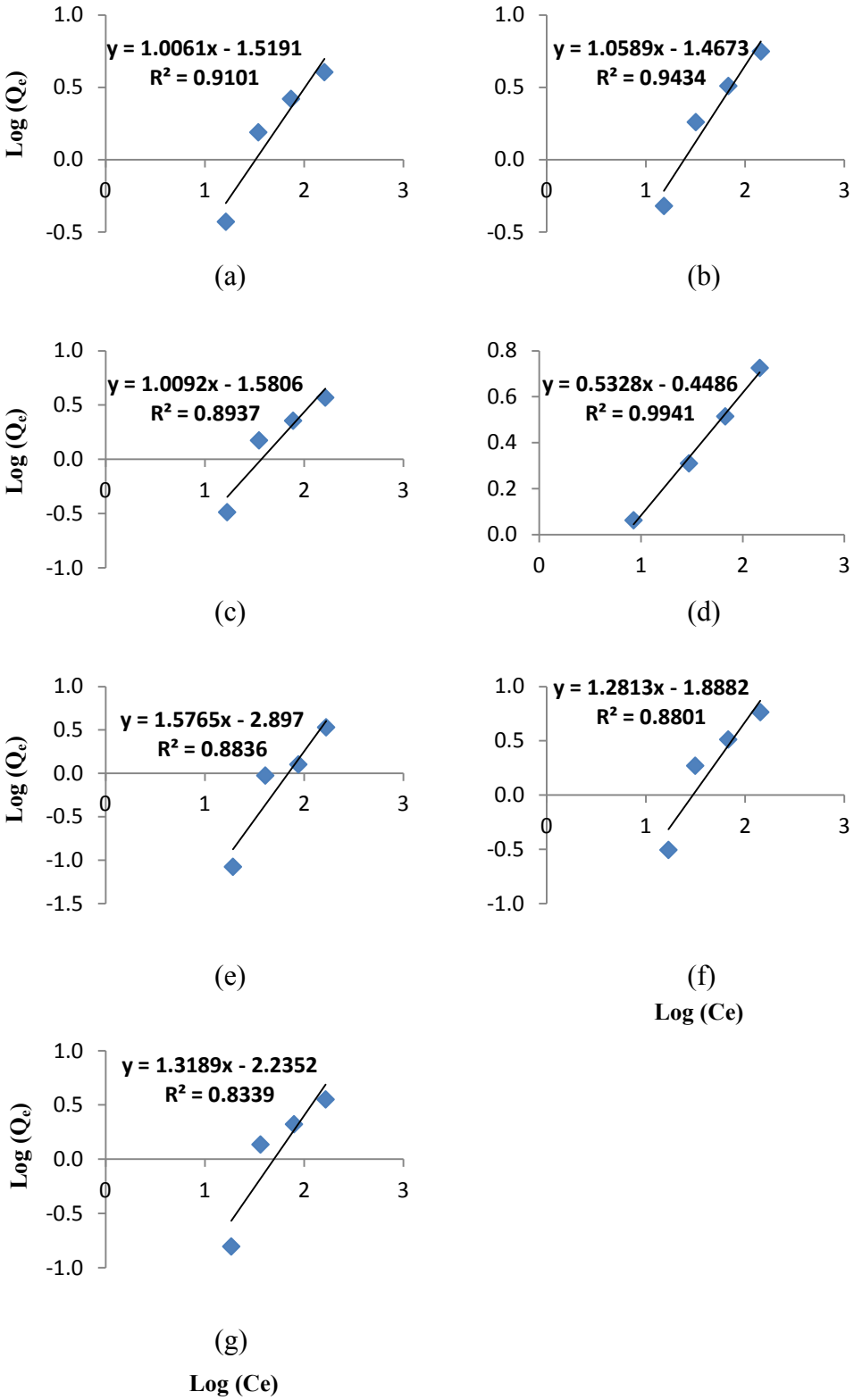

Figure 7.7 Freundlich isotherm models for mixture 4: (a) Cu; (b) Ni; (c) Cd; (d) Pb; (e) Cr; (f) Al; (g) Zn

Table 7.13 Freundlich isotherm constants for mixture 4

Metal ion	K_F/ ((mg/g)/(mg/L)$^{1/n}$)	n	R^2
Cu	0.030	0.99	0.9101
Ni	0.034	0.94	0.9434
Cd	0.026	0.99	0.8937
Pb	0.356	1.88	0.9941
Cr	0.001	0.63	0.8836
Al	0.013	0.78	0.8801
Zn	0.006	0.76	0.8339

The affinity series for mixture 4 is in the order of Pb > Ni ≈ Cu ≈ Cd > Al > Zn > Cr. Seaweed in mixture 4 was responsible for the sorption of Cd, Cr, Al and Zn since the affinity order for these metals reflects that of seaweed. Zn was sorbed by zeolite present in mixture 4 according to its affinity order, whilst the sorption of Pb was by both zeolite and seaweed. According to the n values, sorption of Cr, Al and Zn occurred via physical sorption and chemisorption was responsible for the sorption of Pb. Both physical and chemical sorption contributed in the sorption of Cu, Cd and Ni.

7.3.3 SORPTION THERMODYNAMICS

The thermodynamics parameters presented in Tables 7.14-7.16 were calculated from the slopes and y-intercepts of graphs in Figures 7.8-7.11 plotted using the thermodynamics experimental data for mixtures given in Tables C.9-C.12 in Appendix C. As evident from Tables 7.14-7.16, the Gibbs free energy change (ΔG^o) for the sorption of metal ions by mixtures is negative indicating that the sorption process was spontaneous. Furthermore, ΔG^o values decreased when the temperature was increased indicating that metal sorption by mixtures is more favourable at higher temperatures. The enthalpy change (ΔH^o) for metal ions was positive. Hence, metal sorption by mixtures was an endothermic process.

Thermodynamics parameters for mixture 1 were calculated from the plots given in Figure 7.8:

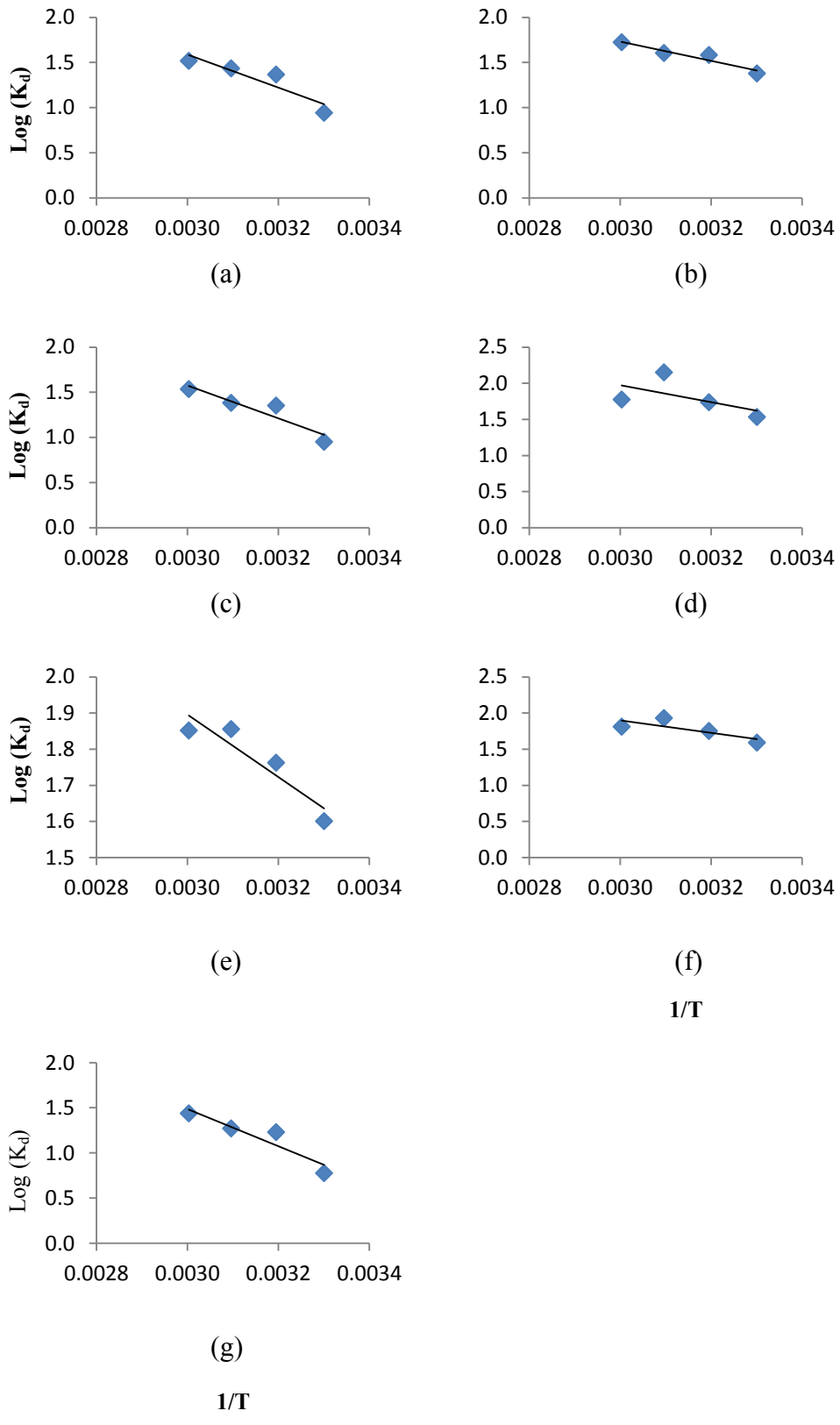

Figure 7.8 Log(K_D) vs. 1/T plots for mixture 1: (a) Cu; (b) Ni; (c) Cd; (d) Pb; (e) Cr; (f) Al; (g) Zn

The corresponding thermodynamics parameters are presented in Table 7.14.

Table 7.14 Thermodynamics parameters for mixture 1

Metal ion	ΔH^o /(kJ/mol)	ΔG^o/(kJ/mol)			
		[1]303	[1]313	[1]323	[1]333
Cu	35.1	-6.0	-7.4	-8.7	-10.1
Ni	20.5	-8.2	-9.1	-10.1	-11.0
Cd	34.7	-6.0	-7.3	-8.7	-10.0
Pb	22.7	-9.4	-10.4	-11.5	-12.5
Cr	16.5	-9.5	-10.4	-11.2	-12.1
Al	16.5	-9.5	-10.4	-11.2	-12.1
Zn	39.5	-5.0	-6.5	-8.0	-9.5

Notes:

[1] Absolute temperature / (K)

Al, Cr, Ni and Pb have relatively lower enthalpy change than Zn, Cd and Cu. Hence, the sorption of the former can occur at relatively lower temperature than the latter. As such, the sorption of Zn, Cd and Cu by mixture 1 is energetically favourable compared to that of Al, Cr, Ni and Pb. This is a primary reason for the low affinity of mixture 1 in the sorption of Zn, Cd and Cu observed in Section 7.3.2.

Similarly, the thermodynamics characteristics of the sorption by mixture 2 were investigated using the parameters in Table 7.15 derived from plots given in Figure 7.9.

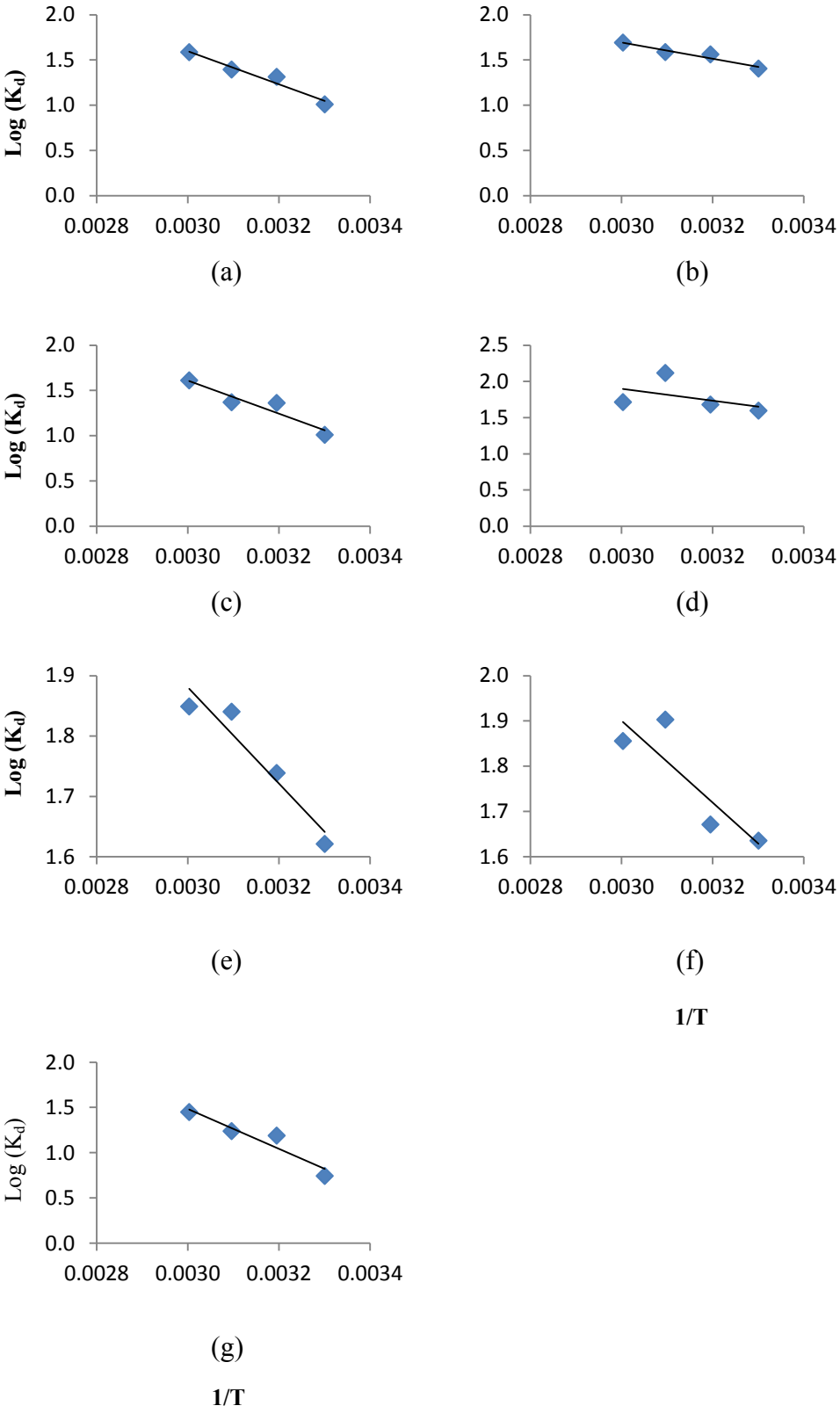

Figure 7.9 Log(K_D) vs. 1/T plots for mixture 2: (a) Cu; (b) Ni; (c) Cd; (d) Pb; (e) Cr; (f) Al; (g) Zn

Table 7.15 Thermodynamics parameters for mixture 2

Metal ion	ΔH^o /(kJ/mol)	ΔG^o/(kJ/mol)			
		[1]303	[1]313	[1]323	[1]333
Cu	35.1	-6.1	-7.5	-8.8	-10.2
Ni	17.2	-8.3	-9.1	-10	-10.8
Cd	35.2	-6.2	-7.5	-8.9	-10.2
Pb	15.8	-9.6	-10.4	-11.3	-12.1
Cr	15.3	-9.5	-10.4	-11.2	-12.0
Al	17.3	-9.4	-10.3	-11.2	-12.1
Zn	42.1	-4.7	-6.3	-7.8	-9.4

Notes:

[1] Absolute temperature / (K)

According to ΔH^o values, the sorption of Al, Cr, Ni and Pb by mixture 2 is energetically favourable, whilst Zn, Cd and Cu require a relatively higher temperature for the sorption. In general, this agrees with the affinity series for mixture 2. The exception was Zn, for which mixture 2 had a higher affinity even though the sorption of Zn is not energetically favourable. This is attributed to the higher metal binding rate of Zn, which resulted in its rapid sorption to the active sites of mixture 2.

Figure 7.10 shows Log (K_D) vs. 1/T plots for mixture 3 and the thermodynamics parameters for mixture 3 were determined from these plots:

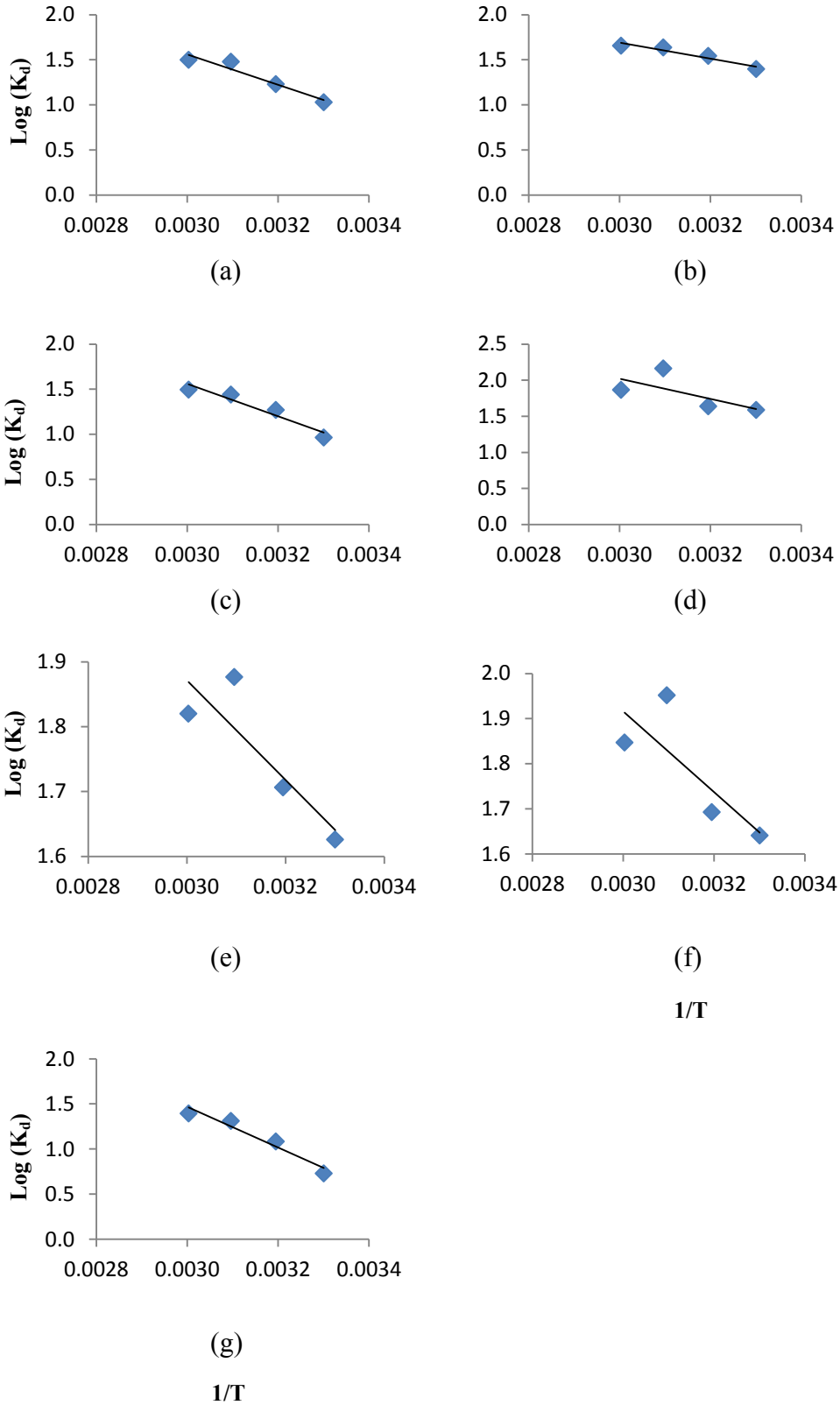

Figure 7.10 Log(K_D) vs. 1/T plots for mixture 3: (a) Cu; (b) Ni; (c) Cd; (d) Pb; (e) Cr; (f) Al; (g) Zn

The thermodynamics parameters for mixture 3 are presented in Table 7.16.

Table 7.16 Thermodynamics parameters for mixture 3

Metal ion	ΔH^o /(kJ/mol)	ΔG^o/(kJ/mol)			
		[1]303	[1]313	[1]323	[1]333
Cu	32.2	-6.1	-7.4	-8.6	-9.9
Ni	16.9	-8.2	-9.1	-9.9	-10.7
Cd	34.3	-5.9	-7.3	-8.6	-9.9
Pb	26.7	-9.3	-10.5	-11.7	-12.9
Cr	14.7	-9.5	-10.3	-11.1	-11.9
Al	17.1	-9.6	-10.4	-11.3	-12.2
Zn	43.3	-4.6	-6.2	-7.7	-9.3

Notes:

[1] Absolute temperature / (K)

Al, Cr, Pb and Ni have a relatively low ΔH^o indicating that the sorption of these metals by mixture 3 can occur at relatively low temperature. However, sorption of Zn, Cd and Cu by mixture 3 is more favourable at a high temperature. Accordingly, sorption of Al, Cr, Pb and Ni by mixture 3 is more energetically favourable than the sorption of Zn, Cd and Cu. Though the metal affinity series for mixture 3 is generally in agreement with this conclusion, mixture 3 had low affinity for Ni despite the energetically favourable nature of Ni sorption. This is because, Ni had relatively low diffusion and metal binding rates, which retarded the probability of Ni reaching the active sites of mixture 3.

The thermodynamics characteristics of the sorption by mixture 4 were investigated using the parameters in Table 7.17 derived from plots given in Figure 7.11.

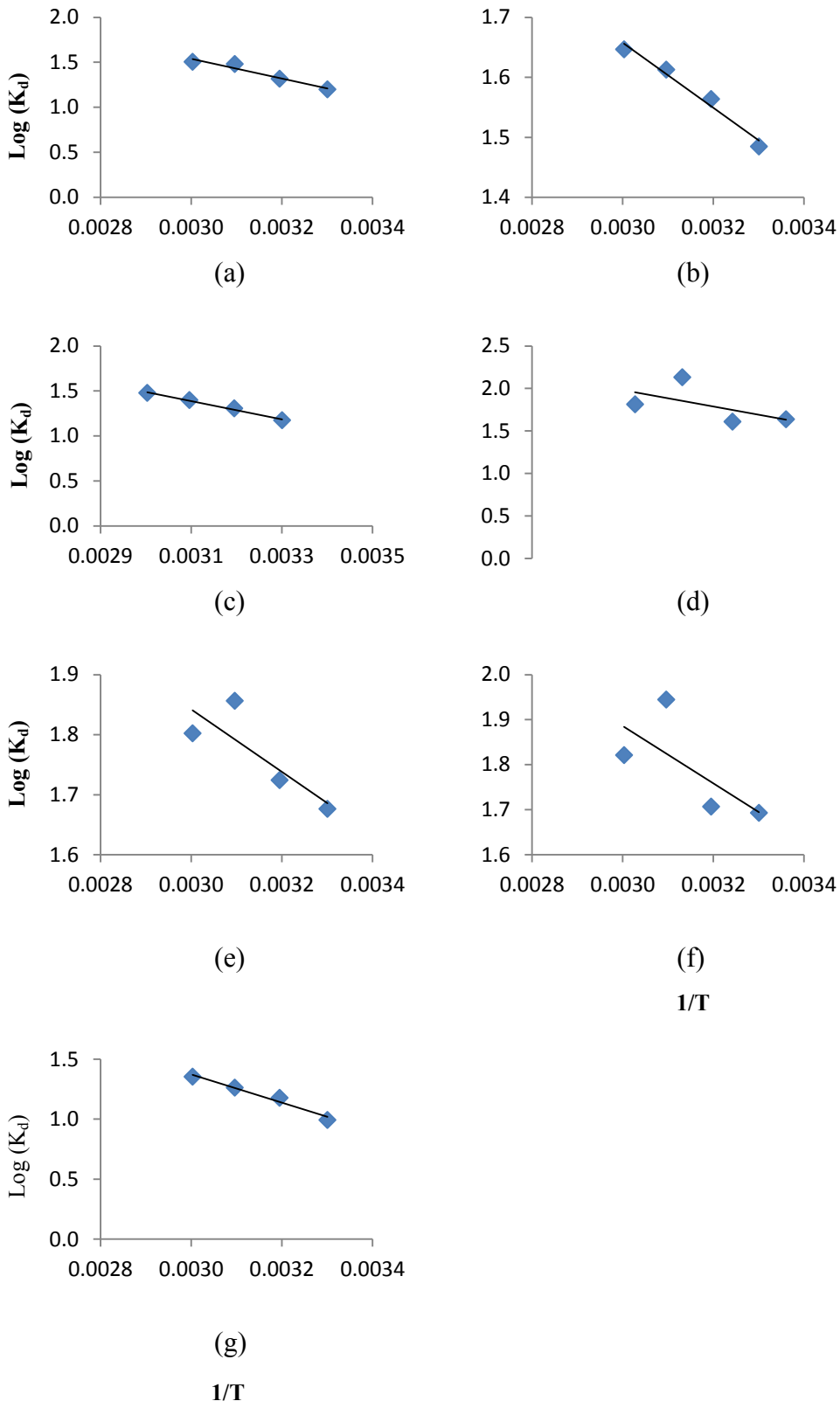

Figure 7.11 Log(K_D) vs. 1/T plots for mixture 4: (a) Cu; (b) Ni; (c) Cd; (d) Pb; (e) Cr; (f) Al; (g) Zn

Table 7.17 Thermodynamics parameters for mixture 4

Metal ion	ΔH^o /(kJ/mol)	ΔG^o/(kJ/mol)			
		[1]303	[1]313	[1]323	[1]333
Cu	21	-7.0	-8.0	-8.9	-9.8
Ni	10.4	-8.7	-9.3	-9.9	-10.5
Cd	19.4	-6.9	-7.7	-8.6	-9.5
Pb	20.6	-9.5	-10.5	-11.5	-12.5
Cr	10.0	-9.8	-10.4	-11.1	-11.7
Al	12.2	-9.8	-10.5	-11.3	-12.0
Zn	22.6	-5.9	-6.8	-7.8	-8.7

Notes:

[1] Absolute temperature / (K)

Sorption of Zn, Pb and Cu by mixture 4 is less energetically favourable compared to that of Ni, Cd, Cr and Al. However, according to the affinity series predicted for mixture 4, sorption of Pb, Ni, Cu and Cd was more favourable than that of Al, Zn, and Cr. Both affinity and the enthalpy change series are in agreement in the case of Zn, Ni and Cd. The discrepancy in relation to the other metals confirm that other factors such as kinetics rates also have an influence on the affinity of sorbents for the sorption of metal ions.

7.4 RELATIONSHIP BETWEEN MIXTURES AND INDIVIDUAL SORBENTS

In the research study, it was hypothesised that the kinetics and thermodynamics parameters of mixtures are mathematically related to those of individual sorbents via mass conservation principle. Such a relationship will be helpful in the creation of mixtures to control the kinetics and thermodynamics of metal sorption, which, in turn, can be used to enhance the affinity for the less preferred metal ions. In this section, theoretical mathematical relationships are initially provided and then investigated using the experimental values.

7.4.1 DERIVATION OF THEORETICAL MATHEMATICAL RELATIONSHIPS

If one gram of mixture contains 'f' grams of zeolite and (1-f) grams of seaweed, then the amount of metals in the mixture (m_{mix}) can be given as (Helmy et al. 1999):

$$m_{mix} = f.m_z + (1 - f).m_{sw} \quad (7.1)$$

where, m_z and m_{sw} are the amount of metals in a gram of zeolite and seaweed, respectively.

During boundary layer diffusion, a certain amount of metal ions (m) present in solution diffuses into the boundary layer of the sorbent material and it can be given as (Section 3.4.2 A):

$$m = (C_0 - C_5).v \quad (7.2)$$

Combining equation (7.2) with equation (7.1) results in:

$$(C_0 - C_{5-mix})v = f.(C_0 - C_{5-z})v + (1 - f).(C_0 - C_{5-SW})v \quad (7.3)$$

Dividing both sides by $5C_0$ (5 corresponds to 5 minutes, during which the boundary layer diffusion was assumed to occur as discussed in Section 3.4.2A) gives:

$$\frac{(C_0 - C_{5-mix})}{5C_0} = \frac{f.(C_0 - C_{5-z})}{5C_0} + \frac{(1 - f).(C_0 - C_{5-sw})}{5C_0} \quad (7.4)$$

According to the definition (Section 3.4.2A):

$$\text{Boundary layer diffusion rate (BLDR)} = \frac{(C_0 - C_5)}{5C_0} \quad (7.5)$$

Hence, the boundary layer diffusion rate of a mixture can be mathematically related to that of the individual sorbents using the following equation:

$$BLDR_{mix} = f.BLDR_z + (1 - f).BLDR_{SW} \quad (7.6)$$

Similarly, the amount of metal ions (m) in a mixture at time 't' can be given as:

$$m = (C_0 - C_t).v \tag{7.7}$$

The following equation can be obtained from equations (7.1) and (7.7):

$$(C_0 - C_{t-mix})v = f.(C_0 - C_{t-z})v + (1 - f).(C_0 - C_{t-sw})v \tag{7.8}$$

Dividing both sides by the mass of sorbents used for the sorption (m_s) gives:

$$\frac{(C_0 - C_{t-mix})v}{m_s} = \frac{f.(C_0 - C_{t-z})v}{m_s} + \frac{(1 - f).(C_0 - C_{t-sw})v}{m_s} \tag{7.9}$$

However,

$$Q_t = \frac{(C_0 - C_t).v}{m_s} \tag{7.10}$$

Substituting equation (7.10) in equation (7.9) gives:

$$Q_{t-mix} = f.Q_{t-z} + (1 - f).Q_{t-SW} \tag{7.11}$$

Theoretical sorption capacities of mixtures for different time intervals was calculated using equation (7.11) using the sorption capacities of zeolite (Tables B.1-B.7 in Appendix B) and those of seaweed (Tables B.10-B.16 in Appendix B). These values were fitted with the Vermeulen and pseudo second order models to determine the theoretical intraparticle diffusion rate and metal binding rates, respectively.

The distribution coefficient (K_d) is given by the following equation:

$$K_d = \frac{(C_0 - C_e).v}{m_s C_e} \tag{7.12}$$

From equation (7.10), the equation for the equilibrium sorption capacity (Q_e) is as follows:

$$Q_e = \frac{(C_0 - C_e).v}{m_s} \tag{7.13}$$

The following equation can be derived based on equations (7.12) and (7.13):

$$Q_e = K_d C_e \quad (7.14)$$

Substituting equation (7.14) in equation (7.11) for equilibrium condition gives:

$$K_{d-mix}\, C_{e-mix} = f.\, K_{d-z}\, C_{e-z} + (1 - f).\, K_{d-SW}\, C_{e-SW} \quad (7.15)$$

Theoretical K_d values were calculated based on the experimental K_d values for seaweed and zeolite and the enthalpy change can be determined as described in Section 3.4.3.

7.4.2 RESULTS AND DISCUSSION

The theoretical boundary layer diffusion rates for mixtures calculated using equation (7.6) are shown in Table 7.18:

Table 7.18 Theoretical boundary layer diffusion rates

Metal ion	Cu	Ni	Cd	Pb	Cr	Al	Zn
Zeolite	0.050	0.020	0.011	0.031	0.007	0.057	0.009
Mixture 1	0.046	0.022	0.010	0.032	0.014	0.058	0.010
Mixture 2	0.042	0.024	0.009	0.032	0.020	0.058	0.011
Mixture 3	0.037	0.025	0.007	0.033	0.027	0.059	0.011
Mixture 4	0.033	0.027	0.006	0.033	0.033	0.059	0.012
Seaweed	0.029	0.029	0.005	0.034	0.040	0.060	0.013

The theoretical values were plotted against the experimental values (Table 7.2) as shown in Figure 7.12:

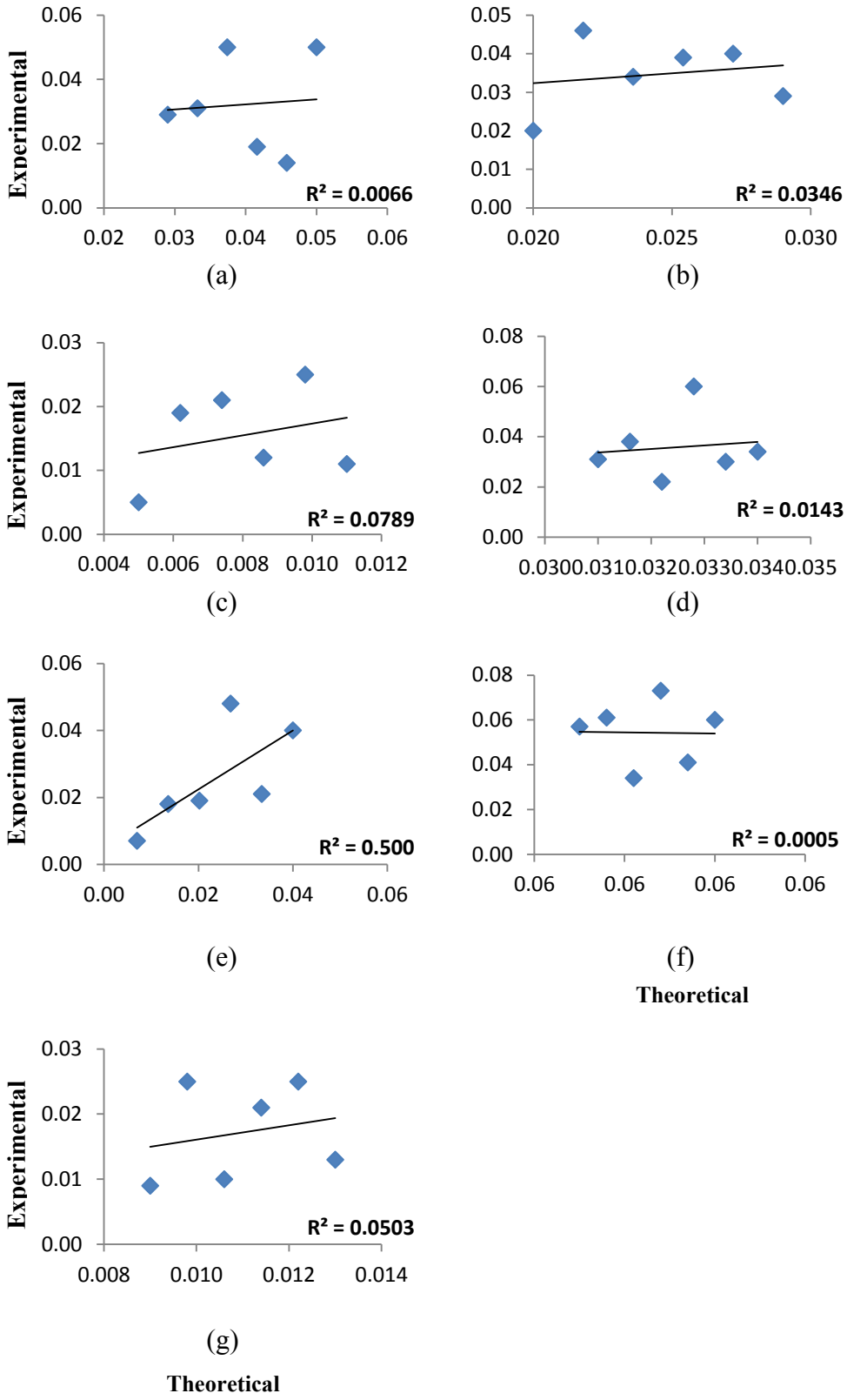

Figure 7.12 Theoretical vs. experimental boundary layer diffusion rates for: (a) Cu; (b) Ni; (c) Cd; (d) Pb; (e) Cr; (f) Al; (g) Zn

According to Figure 7.12, it can be seen that the R^2 values is very low indicating that the boundary layer diffusion rates did not follow equation (7.6). Therefore, the

boundary layer diffusion characteristics of mixtures are independent from those of the individual sorbents. The primary reason for this observation is that the boundary layer diffusion of metals in zeolite and seaweed is governed by the properties of metals such as molar concentration and molar volume and not by the properties of sorbents. Therefore, mixing of sorbents did not have an effect on the boundary layer diffusion rates.

Theoretical intraparticle diffusion rates were determined by fitting the Vermeulen model (equation 3.9) to the sorption capacity values calculated using equation (7.11). The values are tabulated in Table 7.19:

Table 7.19 Theoretical intraparticle diffusion rates ($D_v \times 10^{-8}$ $m^2 min^{-1}$)

Metal ion	Cu	Ni	Cd	Pb	Cr	Al	Zn
Zeolite	18.0	9.0	5.0	8.0	1.0	12.0	4.0
Mixture 1	15.0	7.8	4.0	7.4	2.3	12.8	4.2
Mixture 2	13.0	6.6	2.6	6.6	3.4	13.5	4.4
Mixture 3	11.0	5.7	1.7	6.0	4.6	14.2	4.5
Mixture 4	8.8	5.0	1.0	5.5	6.0	14.9	4.6
Seaweed	7.2	4.4	0.5	4.3	6.3	15.0	4.7

The theoretical (Table 7.19) and the experimental (Table 7.4) intraparticle diffusion rates were plotted against each other as shown in Figure 7.13:

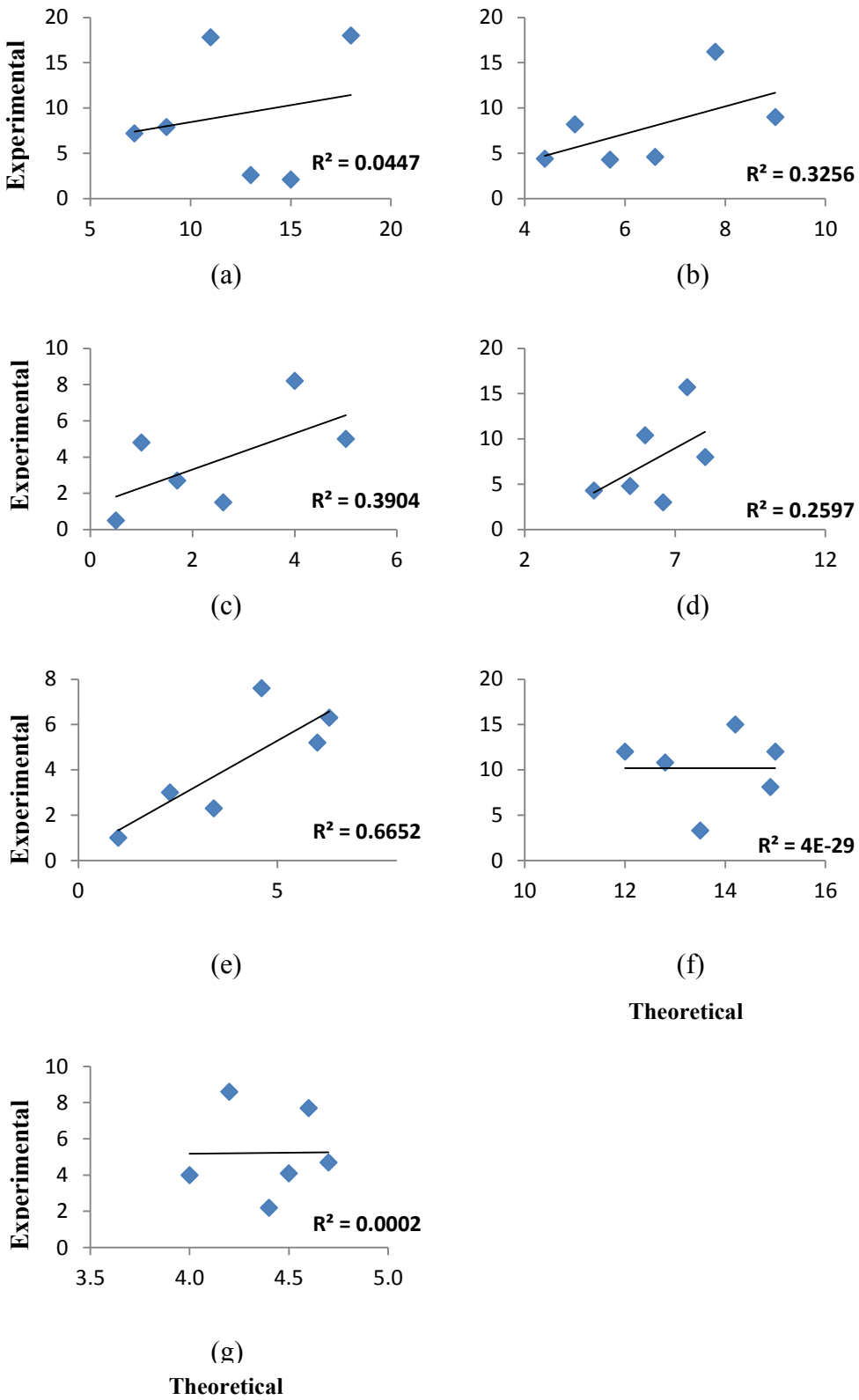

Figure 7.13 Theoretical vs. experimental intraparticle diffusion rates for: (a) Cu; (b) Ni; (c) Cd; (d) Pb; (e) Cr; (f) Al; (g) Zn

Similar to the boundary layer diffusion, the R^2 values for intraparticle diffusion is low. However, relative to boundary layer diffusion rates, intraparticle diffusion rates generally had higher R^2 values suggesting that intraparticle diffusion rates of mixtures have some relationship with that of individual sorbents. However, this relationship is statistically not significant. Notably, the R^2 value for Cr had relatively higher values ($R^2 = 0.6652$). Intraparticle diffusion of Cr in zeolite was found to be governed by the hardness of the functional groups present in the sorbents, while it was influenced by the molar concentration in the case of seaweed. Therefore, the intraparticle diffusion of Cr in mixtures is influenced by both factors. Since the properties of zeolite has an influence on the intraparticle diffusion of Cr, the intraparticle diffusion characteristics of mixtures exhibited a reasonably good relationship for equation (7.13).

Theoretical pseudo second order metal binding rates were determined based on equation (7.11) and tabulated in Table 7.20 below.

Table 7.20 Theoretical pseudo second order metal binding rates

	Cu	Ni	Cd	Pb	Cr	Al	Zn
Zeolite	0.29	0.12	0.11	0.12	0.03	0.12	0.09
Mixture 1	0.178	0.083	0.071	0.088	0.030	0.111	0.077
Mixture 2	0.149	0.067	0.043	0.072	0.040	0.119	0.078
Mixture 3	0.126	0.055	0.026	0.060	0.049	0.127	0.078
Mixture 4	0.107	0.046	0.015	0.052	0.056	0.137	0.078
Seaweed	0.10	0.04	0.01	0.04	0.06	0.16	0.09

Theoretical and experimental (Table 7.6) metal binding rates were plotted against each other as shown in Figure 7.14.

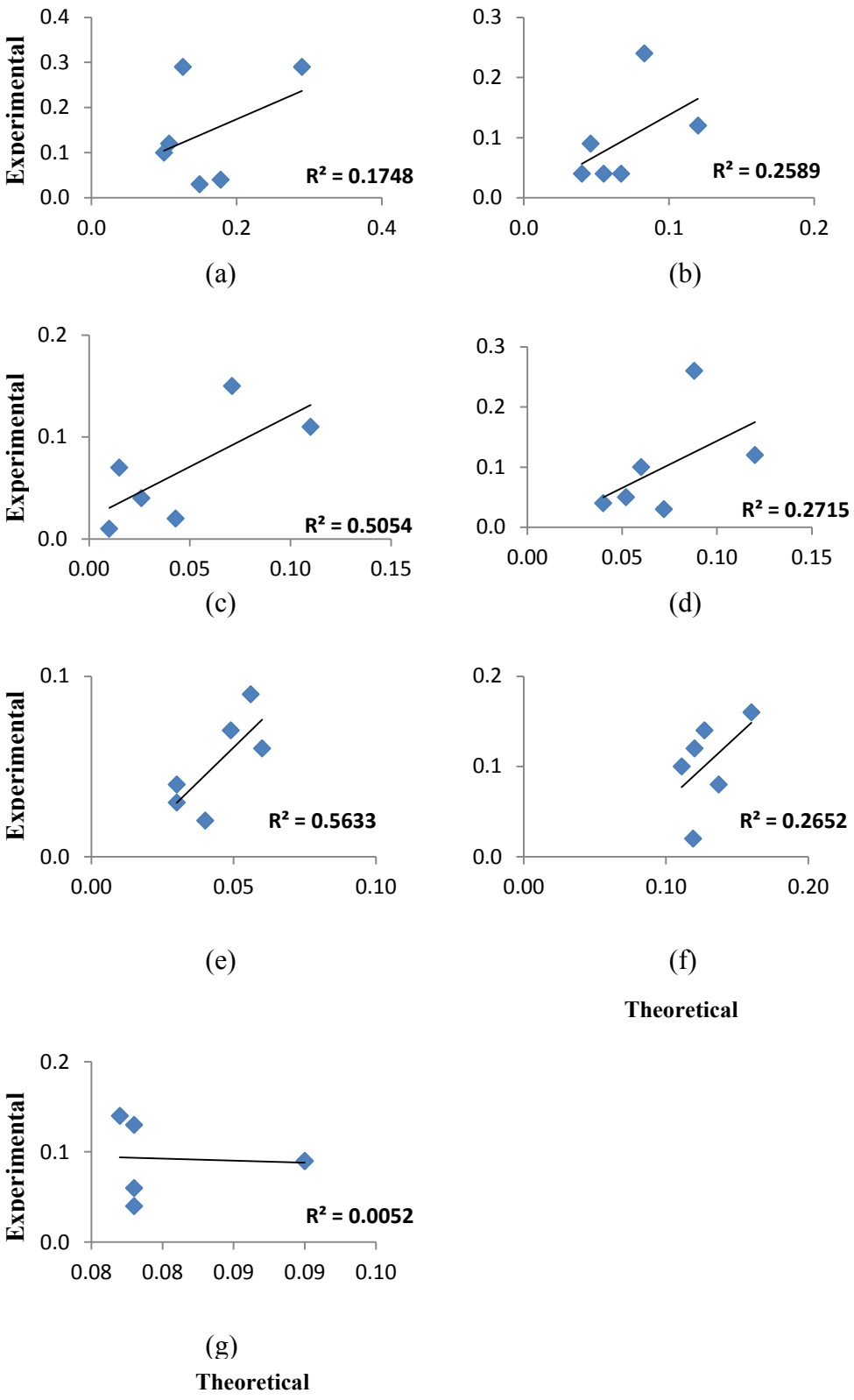

Figure 7.14 Theoretical vs. experimental metal binding rates for: (a) Cu; (b) Ni; (c) Cd; (d) Pb; (e) Cr; (f) Al; (g) Zn

The R^2 values are low. However, they are generally higher than the intraparticle diffusion rates. It is worthy to note that the R^2 values of Cr and Cd are relatively higher, suggesting that their metal binding rates in mixtures have some relationship with that for individual sorbents.

Theoretical K_d values for mixtures were determined using equation (7.15) and the enthalpy change (ΔH^0) was calculated as described in Section 4.3.4 (B). The values are tabulated in Table 7.21 and plotted against the experimental values in Tables 7.14-7.17 as shown in Figure 7.15.

Table 7.21 Theoretical enthalpy change

	Cu	**Ni**	**Cd**	**Pb**	**Cr**	**Al**	**Zn**
Zeolite	35.8	27.5	34.6	24.3	18.6	15.2	68.2
Mixture 1	33.4	24.2	32.3	22.6	17.0	15.1	54.8
Mixture 2	34.0	23.3	33.1	20.3	16.6	15.6	55.1
Mixture 3	33.3	23.1	32.2	24.6	16.4	15.6	55.0
Mixture 4	31.9	21.6	30.4	22.3	14.8	13.9	53.1
Seaweed	25.4	15.2	24.3	13.5	11.5	10.8	33.6

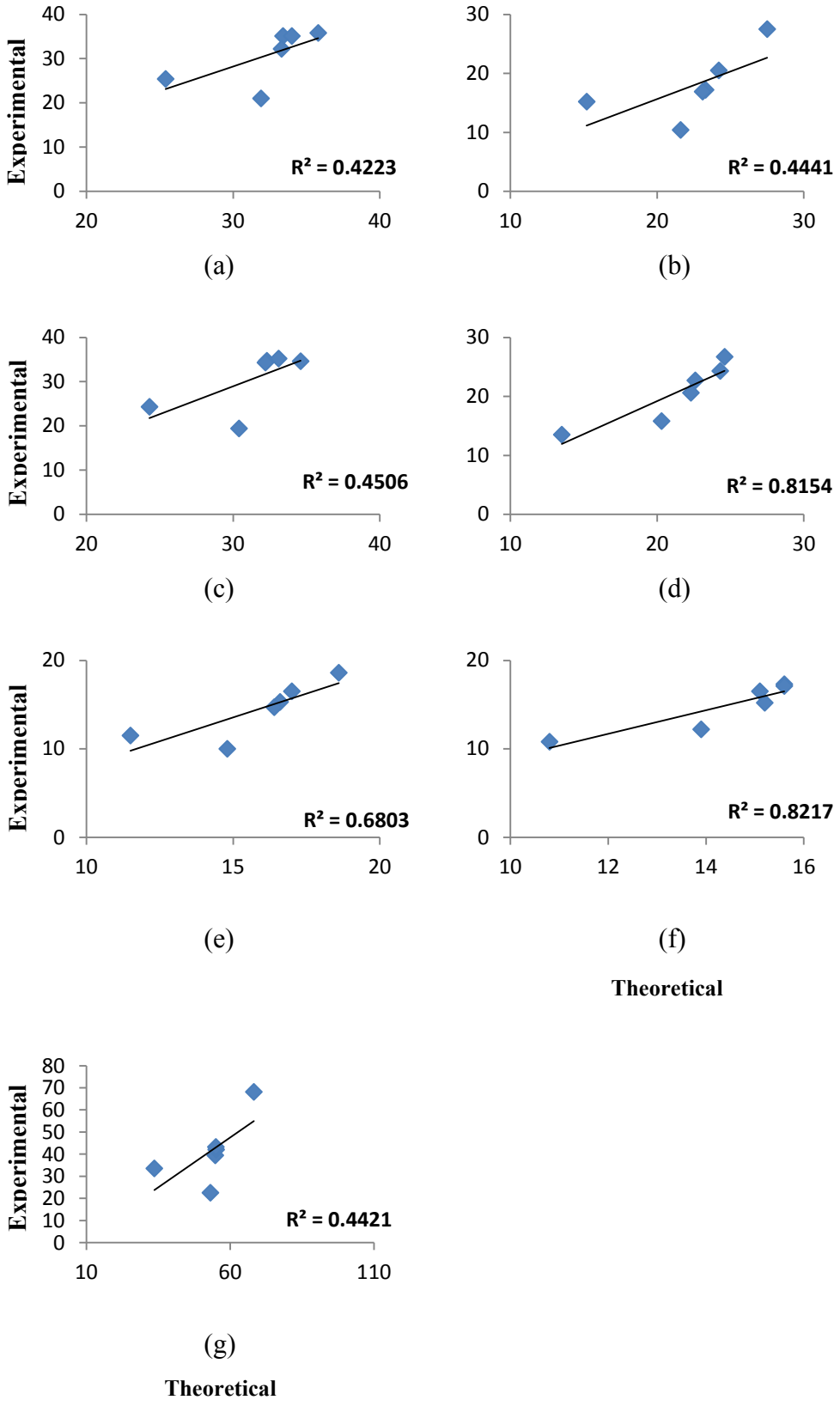

Figure 7.15 Theoretical vs. experimental enthalpy change for: (a) Cu; (b) Ni; (c) Cd; (d) Pb; (e) Cr; (f) Al; (g) Zn

The R^2 values are relatively higher than the kinetics rates indicating that thermodynamics parameters obey equation (7.15) to a greater extent than the kinetics parameters obeying their corresponding mathematical relationships. Specifically, Pb, Cr and Al had satisfactory R^2 values suggesting that the derived relationship in equation (7.15) can be used to predict the enthalpy of mixtures based on that of individual sorbents.

It is important to note that zeolite and seaweed used in this research study are natural materials, the properties of which can vary considerably. Additionally, the batch experiments were conducted at laboratory scale, in which a maximum of 5 g of sorbent per batch were used. Thus, the variation in properties can be significant and this can be a reason for the poor relationship observed between theoretical and experimental values for thermodynamics and kinetics parameters.

7.5 EFFECT OF SORBENT MIXTURES ON METAL AFFINITY

The effect of mixing sorbents based on the affinity for the sorption of metals was investigated using the Freundlich constant responsible for the affinity (K_F). Figure 7.16 shows the K_F values of metal ions for each mixture:

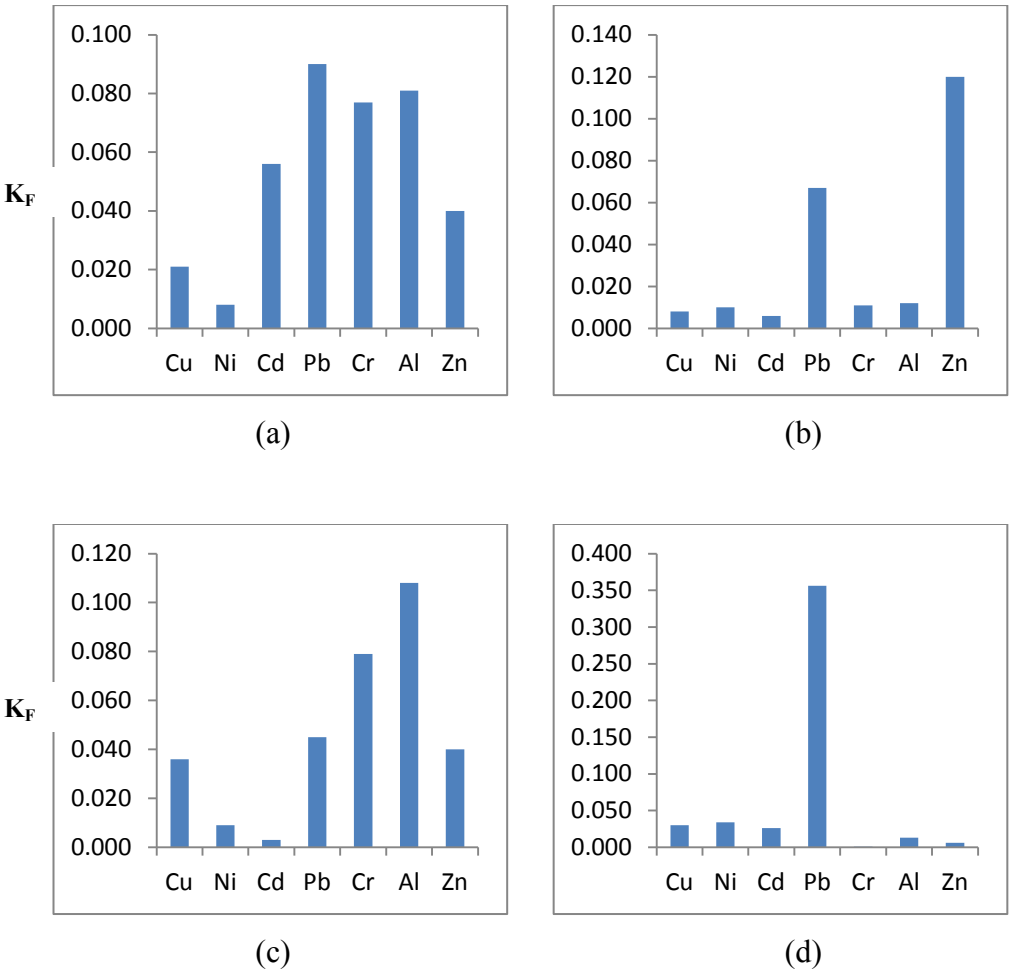

Figure 7.16 K_F values of metal ions: (a) Mixture 1; (b) Mixture 2; (c) Mixture 3; (d) Mixture 4

It is evident from Figure 7.16, that sorbent mixtures also preferentially sorb certain metal ions similar to the individual sorbents, which led to the rejection of the hypothesis of this research study. However, important information was derived regarding the affinity for the sorption of metal ions. As discussed in Section 7.3.2 and evident from Figure 7.16 (b), mixture 2 showed interesting characteristics regarding metal affinity. Mixture 2 had high affinity for Pb and Zn. Though the affinity was low for the other metals, their K_F values were approximately similar, i.e. mixture 2 had similar affinity for the sorption of these metal ions. Therefore, the isotherm, kinetics and thermodynamics parameters were subjected to PROMETHEE and GAIA analysis to identify the process parameter/s responsible for the observed phenomenon.

The data matrix used for the analysis consisted of five metal ions and their isotherm, kinetics and thermodynamics parameters as shown in Table 7.22:

Table 7.22 Data matrix for PROMETHEE and GAIA analysis

	[1]BLDR	[1]D_v	[1]K_2	[1]H	[1]K_F
Cu	0.019	2.6	0.03	35.1	0.008
Ni	0.034	4.6	0.04	17.2	0.010
Cd	0.012	1.5	0.02	35.2	0.006
Cr	0.019	2.3	0.02	15.3	0.011
Al	0.034	3.3	0.02	17.3	0.012

Notes:

[1]Boundary layer diffusion rate (BLDR); Intraparticle diffusion rate (D_v); Metal binding rate (K_2); Enthalpy change (H); Freundlich constant related to the affinity (K_F)

PROMETHEE analysis requires the assignment of three modelling parameters: a ranking sense, a weight and a preference function. The weight was set to 1 to avoid any bias in the analysis and V-shape preference function (Table 4.3) was selected based on the characteristics of the data. The boundary layer diffusion, intraparticle diffusion and metal binding rates were maximised since high kinetics rates are preferred for good sorption performance. Similarly, K_F value was also maximised since high K_F value indicates good affinity for the sorption of metals. The enthalpy change was minimised since the sorption is energetically favourable if the sorption enthalpy is small. The corresponding GAIA biplot for this analysis is given in Figure 7.17.

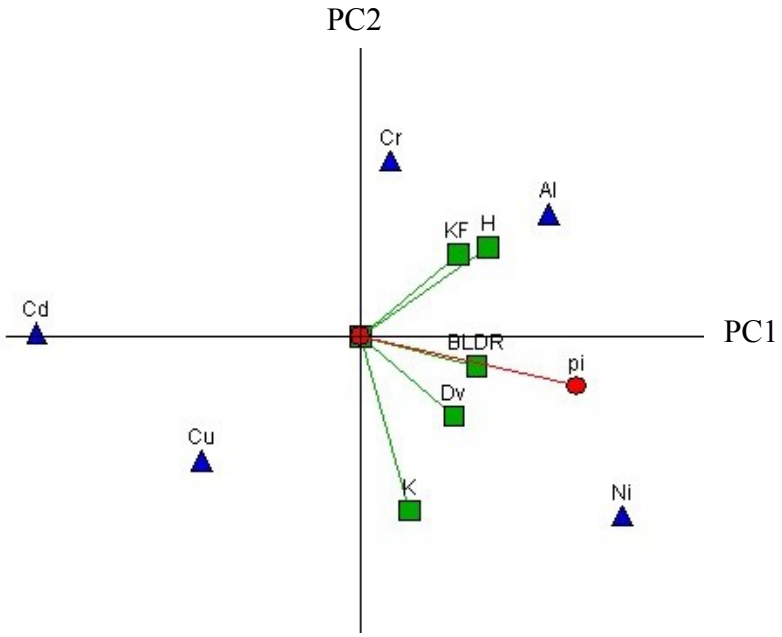

Figure 7.17 GAIA biplot for mixture 2

According to the GAIA biplot (Figure 7.17), it is evident that the boundary layer diffusion and sorption enthalpy have relatively more influence on the affinity (K_F) for the sorption of the investigated metals. The enthalpy vector is strongly correlated to the K_F vector suggesting that sorption thermodynamics is the primary reason for similar affinity for the sorption of Cd, Cu, Ni, Al and Cr by mixture 2. Consulting the data matrix in Table 7.11 indicates that Ni, Cr and Al have approximately similar K_F values. On the other hand, K_F values for Cu and Cd are closer than those of Ni, Cr and Al. The enthalpy value reflects the K_F values such that Ni, Cr and Al have very similar enthalpy values, whilst enthalpy values of Cu and Cd are almost similar.

7.6 CONCLUSIONS

This chapter investigated the removal of metal ions by mixtures of zeolite and seaweed. Firstly, kinetics, isotherm and thermodynamics characteristics of metal sorption mechanisms employed by the mixtures were characterised. Equilibrium was attained within one hour similar to zeolite and seaweed. The boundary layer diffusion rates in mixtures were found to be influenced by the properties of metal ions such as initial metal concentration, molar volume, valence electron configuration and hydration energy. On the other hand, mixing sorbent materials had an effect on the intraparticle diffusion rates. Intraparticle diffusion rates of Ni and Al were high, which was the case for the individual sorbents. However, intraparticle diffusion rates

of Cr, Zn, Cu and Pb exhibited a compromise scenario, i.e. one sorbent in the mixture provided a large driving force for the intraparticle diffusion, while the other sorbent diminished the driving force. As a result, the intraparticle diffusion rates of these metals were either moderate or low. Furthermore, the intraparticle diffusion of Cd primarily occurred in seaweed. The metal binding rate series indicated that the active sites were predominantly present in the intraparticle sites of the mixture. Additionally, the primary kinetics rate-limiting step reflected the composition of the mixtures such that the intraparticle diffusion was rate limiting when zeolite was the major component. Both intraparticle and boundary layer diffusion processes were limiting the overall metal removal rate when both seaweed and zeolite were present. Metal binding step was rate limiting if seaweed was present as a high fraction.

In general, the Langmuir isotherm model did not accurately describe the isotherm characteristics of metal sorption by mixtures. Hence, it was concluded that sorption occurred primarily in multilayer. This was further confirmed by the good fit of the Freundlich isotherm with the experimental data. The affinity of mixtures for metals was influenced by the individual sorbents present in mixtures. However, the nature of mechanism employed by the mixtures did not always reflect that of the individual sorbents. According to the thermodynamics parameters, the sorption of metals by mixtures was a spontaneous and endothermic process, which was favourable at high temperatures. Based on the enthalpy change, it was found that sorption of certain metals such as Al, Cr and Ni were energetically favourable, while others such as Cu and Zn were not. Thus, high temperature is necessary for the sorption of the latter group of metal ions by mixtures. In addition, the affinity of mixtures was found to be influenced by the enthalpy of sorption.

Mathematical relationships were developed based on the conservation of mass principle to determine the theoretical boundary layer diffusion rate, intraparticle diffusion rate, metal binding rate and enthalpy of sorption. The theoretical values were plotted against the experimental values and no statistically significant relationship was generally found between the theoretical and experimental values. However, the intraparticle diffusion rate, metal binding rate and enthalpy of sorption showed relatively high R^2 values suggesting that there is some relationship between the kinetics and thermodynamics parameters of mixtures and that of sorbents. The

effect of mixing sorbents in relation to the affinity for the sorption of metals was investigated and it was found that mixtures also exhibited preferential sorption of metals as the case in individual sorbents. However, mixture 2 showed approximately the same affinity for the sorption of Cu, Ni, Cd, Cr and Al and further analysis was performed using GAIA approach to identify the process parameters responsible. It was found that enthalpy of sorption was the primary reason for similar metal sorption affinity observed in mixture 2. This suggests that the mixtures of seaweed and zeolite have the potential to make the affinity for different metals in a multi component system similar if the enthalpy of metal sorption can be controlled.

Chapter 8: Conclusions and recommendation for future research

8.1 CONCLUSIONS

This research study investigated the removal of metals from a multi metal system using sorbents with the aim of employing sorption in tertiary stormwater treatment. The metals investigated were, Pb, Cu, Cd, Zn, Cr, Al and Ni as these are commonly present in urban stormwater. As individual sorbents exhibit a preferential sorption for metal ions, it was hypothesised in the study that a mixture of sorbents with different affinity patterns can result in similar preference for the sorption of all metal ions leading to enhanced metal removal. To test this hypothesis, firstly, suitable sorbents were selected and their metal removal processes were characterised. Then, the characteristics of sorbent mixtures in relation to metal sorption affinity and metal removal processes were investigated.

8.1.1 SORBENT SELECTION

A multi-criteria protocol was developed based on the multi criteria decision making methods, PROMETHEE and GAIA, for the selection of sorbents. The protocol was used to evaluate six sorbents, namely, seaweed, zeolite, sugarcane bagasse, clay, activated carbon and corncob against a suite of technical and non-technical selection criteria. The criteria considered were metal sorption capacity, cost, environmental, operational and biodegradability factors. The following conclusions were derived based on the analysis undertaken:

- Seaweed has affinity for the sorption of Al, Ni, Cr and Zn, while zeolite and clay preferred the sorption of Pb and Cd. Seaweed, zeolite and clay had equal affinity for Cu.
- Based on all the criteria considered, zeolite, seaweed and clay were the best performers, while sugarcane bagasse, corncob and activated carbon were the poor performers.

- Based on the overall performance including the affinity for the sorption of metals, it was found that zeolite and seaweed or clay and seaweed were preferable for creating the mixtures to meet the study objectives. Accordingly, zeolite and seaweed were selected for further study.

The multi-criteria protocol developed in the study is a contribution to knowledge as conventional methods for sorbent evaluation are based on their metal sorption capacity alone and, do not consider the important real-world factors such as cost and environmental impacts. Additionally, the protocol is useful to readily understand how each criterion affects the selection of sorbents, which provides the decision maker with the ability to evaluate different selection scenarios. Furthermore, this protocol can be used as the basis to create novel sorbent mixtures for the removal of diverse pollutants from water. However, the major limitation of the multi-criteria protocol is the sensitivity of the decision, which is dependent on PROMETHEE modelling parameters such as the choice of preference function. Therefore, the decision maker must be aware of the data characteristics and choose the preference function accordingly.

8.1.2 ISOTHERM, KINETICS AND THERMODYNAMICS OF SORPTION MECHANISM EMPLOYED BY ZEOLITE AND SEAWEED

The isotherm, kinetics and thermodynamics characteristics were investigated to understand the metal sorption processes employed by zeolite and seaweed.

The following conclusions were derived from the metal sorption study using zeolite:

- Initial molar metal concentration, molar volume, valence electron configuration and hydration energy influenced the boundary layer diffusion of metal ions. On the other hand, hydrated ionic size, chemical hardness and molar concentration of metal ions influenced the intraparticle diffusion of metal ions. The metal binding process was well described by both pseudo first order and second order kinetics models. Furthermore, the metal binding and the intraparticle rate series were approximately similar.

Hence, it was concluded that the sorption of metals occurred predominantly inside the intraparticle sites.

The primary rate-limiting step in the sorption of metals by zeolite was intraparticle diffusion followed by the metal binding process. The boundary layer diffusion did not have a significant effect on limiting the overall metal removal rate. The sorption system attained equilibrium or near equilibrium status within an hour.

- According to the thermodynamics study, sorption of metals by zeolite is energetically favourable at high temperatures. According to the Gibbs free energy and the enthalpy change, metal sorption by zeolite is a random process. Furthermore, sorption of metals by zeolite is endothermic and changes the structure of zeolite. The sorption is energetically favourable in the order of Al > Cr > Pb > Ni > Cd > Cu > Zn. The affinity of zeolite for metal sorption was found to be influenced by the sorption thermodynamics.
- The Freundlich model fitted the isotherm experimental data better than the Langmuir isotherm model. Hence, it was concluded that metal sorption by zeolite occurred in multilayer. The affinity of zeolite for metal ions is dependent on the charge density, hydration energy, valence electron configuration of the ion and the kinetics rates. The ion exchange or physisorption mechanisms also contributed to the sorption of Al, Cd, Zn, Ni and Cu along with chemisorption. In contrast, Pb and Cr were predominantly removed via chemisorption.

The following conclusions were derived from the metal sorption study using seaweed:

- The molar metal concentration and hydration energy are influential in boundary layer diffusion, while molar concentration, hydration energy and molar volume of metals govern intraparticle diffusion. Both pseudo first order and second order models can be used to describe the metal binding process. Metal sorption in seaweed occurred inside the cracks on the

external surface since the metal binding rate series is similar to the intraparticle rate series.

The primary rate-limiting step is the metal binding process. Intraparticle diffusion also influences sorption, whereas boundary layer diffusion controls the overall metal removal rate at a low concentration. The equilibrium or near equilibrium for metal sorption by seaweed is achieved within one hour.

- According to the Gibbs free energy and the entropy change values, metal sorption by seaweed is a random process. Based on the enthalpy change, sorption of Ni, Pb, Cu, Cr and Zn by seaweed is thermodynamically favourable compared to zeolite, while sorption of Cu, Cd and Al by zeolite is thermodynamically favourable. The metal sorption by seaweed is energetically favourable in the following order: Zn < Cu < Cd < Cr ≈ Al < Pb < Ni and this order does not reflect the sorption affinity order derived from the Freundlich constants. Thus, the affinity of seaweed for the sorption of metals is not influenced by the sorption thermodynamics.
- The Freundlich isotherm model describes the isotherm characteristics of the metal sorption by seaweed. Kinetics rates, hydration energies and charge densities of metal ions influence the sorption affinity of seaweed. Sorption of Cr, Al, Pb and Cd occur via ion exchange, while physisorption is responsible for the sorption of Ni by seaweed. Zn is sorbed via ionic interaction with the anionic sites of seaweed.

In summary, the boundary layer diffusion process in seaweed and zeolite is influenced by the metal properties. The intraparticle diffusion in zeolite is governed by properties of metals and zeolite, while that in seaweed is predominantly influenced by the metal properties. Furthermore, it was found that sorption in both sorbents occur mainly in the intraparticle sites. The primary rate-limiting steps are intraparticle diffusion followed by the metal binding process for zeolite and for seaweed it is the metal binding process followed by the intraparticle and boundary layer diffusion.

Sorption begins spontaneously, is favourable at higher temperatures and is of endothermic nature for both sorbents. Furthermore, thermodynamics have an influence on the metal sorption affinity in case of zeolite, while it has little effect in seaweed. Based on the analysis of both sorbents, it was concluded that the heterogeneity of sorbent properties made the sorption kinetics characteristics system specific.

The major advancement of knowledge contributed by this part of the research study was in the area of sorption kinetics investigations. This research proposed a novel approach for the kinetics rate-limiting investigations including the introduction of a new parameter, namely, average specific metal removal rate, which is defined as the average metal sorption rate per a unit mass of sorbent, to account for the overall metal removal rate. The advantage of this approach over conventional techniques is that the former predicts to what extent a particular kinetic step limits the overall metal removal rate, which is imperative to decide whether any process modification can result in a significant increase in the overall metal removal rate. Additionally, the new approach considers the metal binding process in the analysis of the rate-limiting step in addition to the diffusion processes, while the conventional methods assume only the diffusion processes are responsible for limiting the overall metal removal rate.

8.1.3 ISOTHERM, KINETICS AND THERMODYNAMICS OF SORPTION MECHANISM EMPLOYED BY THE MIXTURES

The effect of mixing sorbents was investigated by characterising the mechanism employed by the mixtures. The following conclusions were derived in relation to the metal sorption mechanisms of mixtures:

- Similar to zeolite and seaweed individually, the sorption equilibrium was achieved within one hour, for the mixtures. The boundary layer diffusion rate series was not affected by mixing sorbent materials. However, in mixtures, the boundary layer diffusion was affected by the properties of metals such as molar concentration, molar volume, valence electron configuration and hydration energy.

- Mixing sorbent materials had either cumulative or compromise effects on the intraparticle diffusion rates. The cumulative effect on the intraparticle diffusion rate in mixtures was observed when the driving force for the intraparticle diffusion in the individual sorbents for a particular metal had a similar trend. For example, the intraparticle diffusion rate of Al was high in zeolite and seaweed. Consequently, in mixtures, the intraparticle diffusion rate of Al was also high.

  In contrast, for the compromise scenario, one sorbent in the mixture can provide a large driving force, while the other sorbent can reduce the driving force for intraparticle diffusion. Furthermore, the metal binding rate series was similar to the intraparticle diffusion rate series indicating that the active sites were primarily present in the intraparticle sites.

- The intraparticle diffusion was the rate-limiting step in mixtures when zeolite was present in high fraction, and the metal binding process was rate limiting when seaweed was the primary component in mixtures. The overall metal removal rate was limited by both intraparticle and boundary layer diffusion processes when both seaweed and zeolite were present in an approximately equal amount.

- The Freundlich isotherm model described the isotherm characteristics of metal sorption by mixtures. Though the affinity for metals was affected by the individual sorbents present in mixtures, the nature of the mechanism did not always reflect that of the individual sorbents. The process of metal sorption by mixtures was spontaneous, endothermic and favourable at high temperatures. The affinity of mixtures for the sorption of metals was found to be dependent on the sorption enthalpy.

In summary, the boundary layer diffusion process in mixtures was found to be influenced by the properties of metals. However, the intraparticle diffusion and the metal binding processes in mixtures exhibited a compromise or cumulative effects depending on the characteristics of these processes in individual sorbents. The primary rate-limiting step in mixtures depended on the composition of mixtures such that the rate-limiting step was intraparticle diffusion if zeolite was the major

component, the metal binding process if seaweed was the main component and both intraparticle and boundary diffusion processes if both sorbents were present in an approximately equal amount. Furthermore, sorption by mixtures began spontaneously, was favourable at higher temperature and was of endothermic nature.

Based on the study outcomes, the advancement of knowledge by this research study relate to the development of the mathematical relationships to predict the sorption kinetics and thermodynamics of mixtures based on those of individual sorbents. Such relationships can be useful in creating customised sorbent mixtures for the sorption of specific metal ions. The theoretical values calculated from the mathematical relationships discussed above were plotted against the experimental data to investigate the applicability of the equations.

From the analyses, it was found that the boundary layer diffusion rate, intraparticle diffusion rate, metal binding rate and enthalpy of sorption did not completely obey the mathematical relationships derived in this research study to predict the kinetics and thermodynamics of sorption in mixtures based on individual sorbents. Nevertheless, intraparticle diffusion rate, metal binding rate and sorption enthalpy of mixtures displayed higher coefficient of determination (R^2 values) in comparison to the boundary layer diffusion rate, thus indicating a certain degree of relationship with that of sorbents. However, this relationship was not strong enough to be statistically significant, which was attributed to the heterogeneity of sorbent properties.

Furthermore, it was hypothesised in the research study that mixtures of sorbents will result in a similar affinity for the sorption of metal ions in a multi metal system. Approximately the same affinity for the sorption of Cu, Ni, Cd, Cr and Al was observed for mixture 2 (80% zeolite and 20% seaweed) and similar sorption enthalpy was found to be responsible for similar metal sorption affinity. Hence, it was concluded that the sorbent mixtures can be used to obtain similar affinity for metal ions if the metal sorption enthalpy is similar.

8.2 RECOMMENDATIONS FOR FUTURE RESEARCH

This research study created new knowledge regarding the mechanisms employed by zeolite, seaweed and their mixtures in the sorption of dissolved metals and the effect of mixing sorbent materials on the sorption kinetics and thermodynamics. Additionally, the research study established that there is a potential for mixtures to be used to control the affinity for the sorption of metals. The following future studies are recommended to bridge the knowledge gaps identified to further advance the use of sorbent mixtures to enhance the sorption affinity of metals in a multi metal system:

- The system investigated in this study is complex with seven metal ions in competition for the active sites present in sorbent materials. Important physico-chemical properties such as hydration energy and molar volume responsible for metal diffusion are different for each metal. Consequently, many important parameters cannot be adequately controlled in a multi metal system. Therefore, further investigations are necessary to identify the critical physical and chemical factors responsible for enhancing the affinity for the sorption of metal ions in a mixture using well-controlled single metal systems.
- The mixtures were found to have the potential to change the sorption enthalpy, on which the sorption affinity was found to be dependent. Knowledge of the fundamental physical and chemical factors responsible for the change in sorption enthalpy in mixtures is important to influence the affinity for the sorption of metal ions. Hence, further studies are required to identify these factors. The experimental conditions that have an influence on the metal sorption mechanism were controlled in this study. However, the properties of sorbent materials also affect metal sorption processes. Thus, the sensitivity of influential properties of sorbents on metal removal performance needs to be investigated. This knowledge is essential in robust design of a treatment system for real-world application.
- The mathematical equations derived in this study did not show statistically significant relationships with the experimental data. This was attributed to the heterogeneity of the properties of sorbents used in this study. The

applicability of these equations to mixtures that are made up of sorbents with relatively homogenous properties needs to be investigated to identify the properties of sorbents responsible for the deviation from theoretical relationships observed in this research. This knowledge is essential to enhance the mathematical relationships derived in this research and consequently, to create custom designed sorbent mixtures to enhance the affinity for the sorption of specific metal ions in a multi metal system.

- The metal removal performance of sorbent mixtures needs to be optimised for various factors such as agitation speed, pH, initial metal concentration and adsorbent dose. Furthermore, column experiments provide vital information for the design of a treatment system based on continuous flow, which is considered a more practical form. Hence, column experimental studies should be undertaken for sorbent mixtures and the parameters such as flow rate, temperature and bed volume should be optimised to achieve the best metal removal performance. Finally, sorbent regeneration needs to be investigated in order to understand the potential for reusing sorbents and recovering the sorbed metals for safe disposal.

Chapter 9: References

ABS (Australian Bureau of Statistics). 2005. Water Account Australia 2004-05. Australian Bureau of Statistics,Canberra, Australia.

Adebowale, K. O., Unuabonah, E. I. and Olu-Owolabi, B. I. 2008. Kinetic and thermodynamic aspects of the adsorption of Pb^{2+} and Cd^{2+} ions on tripolyphosphate-modified kaolinite clay. *Chemical Engineering Journal*, 136(2-3): 99-107.

Adhoum, N., Monser, L., Bellakhal, N. and Belgaied, J.-E. 2004. Treatment of electroplating wastewater containing Cu^{2+}, Zn^{2+} and Cr(VI) by electrocoagulation. *Journal of Hazardous Materials*, 112(3): 207-213.

Aharon, A. 2001. Removal of heavy metals from wastewater using natural zeolites, PhD Thesis, University of New South Wales, Australia.

Ahmadi, F., Sarrafi, A. and Ghashghaee, M. 2009. Spectrophotometric evaluation of stability constants of copper, cobalt, nickel and zinc with 2-Thiobarbituric acid in aqueous solution. *E-Journal of Chemistry*, 6(S1): S47-S52.

Ahmed, S., Chughtai, S. and Keane, M. A. 1998. The removal of cadmium and lead from aqueous solution by ion exchange with Na-Y zeolite. *Separation and Purification Technology*, 13(1): 57-64.

Ajmal, M., Hussain Khan, A., Ahmad, S. and Ahmad, A. 1998. Role of sawdust in the removal of copper(II) from industrial wastes. *Water Research*, 32(10): 3085-3091.

Al-Johani, H. and Salam, M. A. 2011. Kinetics and thermodynamic study of aniline adsorption by multi-walled carbon nanotubes from aqueous solution. *Journal of Colloid and Interface Science*, 360(2): 760-767.

Allen, S. J., McKay, G. and Porter, J. F. 2004. Adsorption isotherm models for basic dye adsorption by peat in single and binary component systems. *Journal of Colloid and Interface Science*, 280(2): 322-333.

Allison, R. A., Walker, T. A., Chiew, F. H. S., O'Neill, I. C. and McMahon, T. A. 1998. From roads to rivers: gross pollutant removal from urban waterways. Cooperative Research Centre for Catchment Hydrology, Clayton**.**

Altin, O., Özbelge, H. O. and Dogu, T. 1998. Use of general purpose adsorption isotherms for heavy metal-clay mineral interactions. *Journal of Colloid and Interface science*, 198(1): 130-140.

Álvarez-Ayuso, E., García-Sánchez, A. and Querol, X. 2003. Purification of metal electroplating waste waters using zeolites. *Water Research*, 37(20): 4855-4862.

Angove, M. J., Johnson, B. B. and Wells, J. D. 1997. Adsorption of cadmium(II) on kaolinite. *Colloids and Surfaces A: Physicochemical and Engineering Aspects*, 126(2-3): 137-147.

Antunes, W. M., Luna, A. S., Henriques, C. A. and da Costa, A. C. A. 2003. An evaluation of copper biosorption by a brown seaweed under optimized conditions. *Electronic Journal of Biotechnology*, 6(3): 174-184.

Apiratikul, R. and Pavasant, P. 2008. Sorption of Cu^{2+}, Cd^{2+}, and Pb^{2+} using modified zeolite from coal fly ash. *Chemical Engineering Journal*, 144(2): 245-258.

Arámbula-Villazana, V., Solache-Ríos, M. and Olguín, M. 2006. Sorption of cadmium from aqueous solutions at different temperatures by Mexican HEU-type zeolite rich tuff. *Journal of Inclusion Phenomena and Macrocyclic Chemistry*, 55(3): 229-236.

Aravindhan, R., Madhan, B., Rao, J. R. and Nair, B. U. 2004. Recovery and reuse of chromium from tannery wastewaters using Turbinaria ornata seaweed. *Journal of Chemical Technology and Biotechnology*, 79(11): 1251-1258.

Argun, M. E., Dursun, S., Ozdemir, C. and Karatas, M. 2007. Heavy metal adsorption by modified oak sawdust: Thermodynamics and kinetics. *Journal of Hazardous Materials*, 141(1): 77-85.

Ayoub, G. M., Semerjian, L., Acra, A., El Fadel, M. and Koopman, B. 2001. Heavy metal removal by coagulation with seawater liquid bittern. *Journal of Environmental Engineering*, 127(3): 196-207.

Babel, S. and Kurniawan, T. A. 2003. Low-cost adsorbents for heavy metals uptake from contaminated water: a review. *Journal of Hazardous Materials*, 97(1-3): 219-243.

Bailey, S. E., Olin, T. J., Bricka, R. M. and Adrian, D. D. 1999. A review of potentially low-cost sorbents for heavy metals. *Water Research*, 33(11): 2469-2479.

Baker, H., Massadeh, A. and Younes, H. 2009. Natural Jordanian zeolite: removal of heavy metal ions from water samples using column and batch methods. *Environmental Monitoring and Assessment*, 157(1): 319-330.

Bansemir, A., Blume, M., Schröder, S. and Lindequist, U. 2006. Screening of cultivated seaweeds for antibacterial activity against fish pathogenic bacteria. *Aquaculture*, 252(1): 79-84.

Baran, A., Bıçak, E., Baysal, Ş. H. and Önal, S. 2007. Comparative studies on the adsorption of Cr(VI) ions on to various sorbents. *Bioresource Technology*, 98(3): 661-665.

Barnes, L.-M., Phillips, G. J., Davies, J. G., Lloyd, A. W., Cheek, E., Tennison, S. R., Rawlinson, A. P., Kozynchenko, O. P. and Mikhalovsky, S. V. 2009. The cytotoxicity of highly porous medical carbon adsorbents. *Carbon*, 47(8): 1887-1895.

Barros, M., Arroyo, P. A., Sousa-Aguiar, E. F. and Tavares, C. R. G. 2004. Thermodynamics of the exchange processes between K^+, Ca^{2+} and Cr^{3+} in zeolite NaA. *Adsorption*, 10(3): 227-235.

Basha, S. and Murthy, Z. V. P. 2007. Kinetic and equilibrium models for biosorption of Cr(VI) on chemically modified seaweed, Cystoseira Indica. *Process Biochemistry*, 42(11): 1521-1529.

Basso, M. C., Cerrella, E. G. and Cukierman, A. L. 2002. Lignocellulosic materials as potential biosorbents of trace toxic metals from wastewater. *Industrial & Engineering Chemistry Research*, 41(15): 3580-3585.

Bates, D. M. and Watts, D. G. 1988. Nonlinear regression analysis and its applications. John Wiley and Sons, New York.

Beasley, G. and Kneale, P. 2002. Reviewing the impact of metals and PAHs on macroinvertebrates in urban watercourses. *Progress in Physical Geography*, 26(2): 236.

Beck, M., Dellwig, O., Fischer, S., Schnetger, B. and Brumsack, H.-J. 2012. Trace metal geochemistry of organic carbon-rich watercourses draining the NW German coast. *Estuarine, Coastal and Shelf Science,* In Press, Corrected Proof.

Begum, S., Rasul, M. and Brown, R. J. 2008. Stormwater treatment and reuse techniques: A review. WSEAS Press, New York, USA.

Behzadian, M., Kazemzadeh, R. B., Albadvi, A. and Aghdasi, M. 2010. PROMETHEE: A comprehensive literature review on methodologies and applications. *European Journal of Operational Research*, 200(1): 198-215.

Bektas, N. and Kara, S. 2004. Removal of lead from aqueous solutions by natural clinoptilolite: equilibrium and kinetic studies. *Separation and Purification Technology*, 39(3): 189-200.

Bhattacharyya, K. G. and Gupta, S. S. 2006. Kaolinite, montmorillonite, and their modified derivatives as adsorbents for removal of Cu(II) from aqueous solution. *Separation and Purification Technology*, 50(3): 388-397.

Birch, G. F., Matthai, C., Fazeli, M. S. and Suh, J. Y. 2004. Efficiency of a constructed wetland in removing contaminants from stormwater. *Wetlands*, 24(2): 459-466.

Biškup, B. and Subotic, B. 1998. Removal of heavy metal ions from solutions by means of zeolites. I. Thermodynamics of the exchange processes between cadmium ions from solution and sodium ions from zeolite A. *Separation Science and Technology*, 33(4): 449 - 466.

Biswas, N. and Lazarescu, G. 1991. Removal of oil from emulsions using electrocoagulation. *International Journal of Environmental Studies*, 38(1): 65-75.

Blanchard, G., Maunaye, M. and Martin, G. 1984. Removal of heavy metals from waters by means of natural zeolites. *Water Research*, 18(12): 1501-1507.

Boehm, H. P. 1994. Some aspects of the surface chemistry of carbon blacks and other carbons. *Carbon*, 32(5): 759-769.

Boehm, H. P. 2002. Surface oxides on carbon and their analysis: a critical assessment. *Carbon*, 40(2): 145-149.

Bohdziewicz, J., Bodzek, M. and Wasik, E. 1999. The application of reverse osmosis and nanofiltration to the removal of nitrates from groundwater. *Desalination*, 121(2): 139-147.

Bolboaca, S. D. and Jantschi, L. 2006. Pearson versus Spearman, Kendall's tau correlation analysis on structure-activity relationships of biologic active compounds. *Leonardo Journal of Sciences*, 5(9): 179-200.

Bose, P., Aparna Bose, M. and Kumar, S. 2002. Critical evaluation of treatment strategies involving adsorption and chelation for wastewater containing copper, zinc and cyanide. *Advances in Environmental Research*, 7(1): 179-195.

Bosma, J. C. and Wesselingh, J. A. 1998. pH dependence of ion-exchange equilibrium of proteins. *AIChE Journal*, 44(11): 2399-2409.

Bougen, A., Rabiller-Baudry, M., Chaufer, B. and Michel, F. 2001. Retention of heavy metal ions with nanofiltration inorganic membranes by grafting chelating groups. *Separation and Purification Technology*, 25(1-3): 219-227.

Bradl, H. B. 2004. Adsorption of heavy metal ions on soils and soils constituents. *Journal of Colloid and Interface Science*, 277(1): 1-18.

Brans, J. P., Vincke, P. and Mareschal, B. 1986. How to select and how to rank projects: The PROMETHEE method. *European Journal of Operational Research*, 24(2): 228-238.

Brown, J. N. and Peake, B. M. 2006. Sources of heavy metals and polycyclic aromatic hydrocarbons in urban stormwater runoff. *Science of the Total Environment*, 359(1-3): 145-155.

Bryan, G. W. and Hummerstone, L. G. 1973. Brown seaweed as an indicator of heavy metals in estuaries in south-west England. *Journal of the Marine Biological Association of the United Kingdom*, 53(03): 705-720.

Bubb, J. M. and Lester, J. N. 1994. Anthropogenic heavy metal inputs to lowland river systems, a case study. The River Stour, U.K. *Water, Air, & Soil Pollution*, 78(3): 279-296.

Bunzl, K., Schmidt, W. and Sansoni, B. 1976. Kinetics of ion exchange in soil organic matter. IV. Adsorption and desorption of Pb^{2+}, Cu^{2+}, Cd^{2+}, Zn^{2+} and Ca^{2+} by peat. *Journal of Soil Science*, 27(1): 32-41.

Burns, M. and Mitchell, V. 2007. An evaluation of the design, implementation and operation of 3 stormwater reuse systems across Melbourne. Proceedings of the 13th International Rainwater Catchment Systems Conference, Sydney, Australia.

Carleton, J. N., Grizzard, T. J., Godrej, A. N. and Post, H. E. 2001. Factors affecting the performance of stormwater treatment wetlands. *Water Research*, 35(6): 1552-1562.

Carmody, O., Frost, R., Xi, Y. and Kokot, S. 2007. Adsorption of hydrocarbons on organo-clays-Implications for oil spill remediation. *Journal of Colloid and Interface Science*, 305(1): 17-24.

Carpenter, S. R., Caraco, N. F., Correll, D. L., Howarth, R. W., Sharpley, A. N. and Smith, V. H. 1998. Nonpoint pollution of surface waters with phosphorus and nitrogen. *Ecological Applications*, 8(3): 559-568.

Cenkin, V. and Belevtsev, A. 1985. Electrochemical treatment of industrial wastewater. *Effluent and Water Treatment Journal*, 25(7): 243-249.

Cerniglia, C. E. 1992. Biodegradation of polycyclic aromatic hydrocarbons. *Biodegradation*, 3(2): 351-368.

Chaabane, T., Taha, S., Taleb Ahmed, M., Maachi, R. and Dorange, G. 2006. Removal of copper from industrial effluent using a spiral wound module - film theory and hydrodynamic approach. *Desalination*, 200(1-3): 403-405.

Chang, Q. and Wang, G. 2007. Study on the macromolecular coagulant PEX which traps heavy metals. *Chemical Engineering Science*, 62(17): 4636-4643.

Charerntanyarak, L. 1999. Heavy metals removal by chemical coagulation and precipitation. *Water Science and Technology*, 39(10-11): 135-138.

Chaudhari, S. and Tare, V. 1999. Heavy metal–soluble starch xanthate interactions in aqueous environments. *Journal of Applied Polymer Science*, 71(8): 1325-1332.

Chen, G. 2004. Electrochemical technologies in wastewater treatment. *Separation and Purification Technology*, 38(1): 11-41.

Colella, C. 1996. Ion exchange equilibria in zeolite minerals. *Mineralium Deposita*, 31(6): 554-562.

Collins, K. D. 1997. Charge density-dependent strength of hydration and biological structure. *Biophysical Journal*, 72(1): 65-76.

Conrad, K. and Bruun Hansen, H. C. 2007. Sorption of zinc and lead on coir. *Bioresource Technology*, 98(1): 89-97.

Crank, J. 1975. The mathematics of diffusion. Clarendon Press, Oxford.

Crear, R. 2001. Engineering and design precipitation/coagulation/flocculation. US Army Crops of Engineers, Washington DC, USA.

Curkovic, L., Cerjan-Stefanovic, S. and Filipan, T. 1997. Metal ion exchange by natural and modified zeolites. *Water Research*, 31(6): 1379-1382.

Dabrowski, A., Hubicki, Z., Podkoscielny, P. and Robens, E. 2004. Selective removal of the heavy metal ions from waters and industrial wastewaters by ion-exchange method. *Chemosphere*, 56(2): 91-106.

Davis, A. P., Shokouhian, M. and Ni, S. 2001. Loading estimates of lead, copper, cadmium, and zinc in urban runoff from specific sources. *Chemosphere*, 44(5): 997-1009.

Davis, T. A., Volesky, B. and Vieira, R. H. S. F. 2000. Sargassum seaweed as biosorbent for heavy metals. *Water Research*, 34(17): 4270-4278.

Dayan, A. D. and Paine, A. J. 2001. Mechanisms of chromium toxicity, carcinogenicity and allergenicity: Review of the literature from 1985 to 2000. *Human and Experimental Toxicology*, 20(9): 439-451.

De Brucker, K., Verbeke, A. and Macharis, C. 2004. The applicability of multicriteria-analysis to the evaluation of intelligent transport systems (ITS). *Research in Transportation Economics*, 8(1): 151-179.

De Villiers, P. G. R., Van Deventer, J. S. J. and Lorenzen, L. 1997. The use of ion-exchange resins for the recovery of valuable species from slurries of sparingly soluble solids. *Minerals Engineering*, 10(9): 929-945.

Dean, J. G., Bosqui, F.L., and Lanouette, K.H. 1972. Removing heavy metals from waste water. *Environmental Science & Technology*, 6(6): 518-522.

Del Campillo, M. C., Van Der Zee, S. E. A. T. M. and Torrent, J. 1999. Modelling long-term phosphorus leaching and changes in phosphorus fertility in excessively fertilized acid sandy soils. *European Journal of Soil Science*, 50(3): 391-399.

Deliyanni, E. A. and Matis, K. A. 2005. Sorption of Cd ions onto akaganéite-type nanocrystals. *Separation and Purification Technology*, 45(2): 96-102.

Demirbas, A. 2008. Heavy metal adsorption onto agro-based waste materials: A review. *Journal of Hazardous Materials*, 157(2-3): 220-229.

Dils, R. M. and Heathwaite, A. L. 1998. Development of an iron oxide-impregnated paper strip technique for the determination of bioavailable phosphorus in runoff. *Water Research*, 32(5): 1429-1436.

Dorota, K. 2011. Green complexing agent — EDDS in removal of heavy metal ions on strongly basic anion exchangers. *Desalination*, 280(1-3): 44-57.

Drapper, D., Tomlinson, R. and Williams, P. 2000. Pollutant concentrations in road runoff: Southeast Queensland case study. *Journal of Environmental Engineering*, 126(4): 313-320.

Egodawatta, P., Goonetilleke, A., Ayoko, G. A. and Thomas, E. 2006. Understanding the interrelationships between stormwater quality and rainfall and runoff factors in residential catchments. Proceedings of the Seventh International Conference on Urban Drainage Modelling and the Fourth International Conference on Water Sensitive Urban Design, Melbourne, Australia.

Eisenman, G. 1962. Cation selective glass electrodes and their mode of operation. *Biophysical Journal*, 2(2): 259.

El-Bishtawi, R. F. and Ali, A. A. H. 2001. Sorption kinetics of lead ions by zeolite tuff. *Journal of Environmental Science and Health, Part A*, 36(6): 1055-1072.

Ellis, J. B. 1976. Sediments and water quality of urban storm water. *Water Service* 80(970): 730-734.

Erdem, E., Karapinar, N. and Donat, R. 2004. The removal of heavy metal cations by natural zeolites. *Journal of Colloid and Interface Science*, 280(2): 309-314.

Erdogan, S., Önal, Y., Akmil-Basar, C., Bilmez-Erdemoglu, S., SarIcI-Özdemir, Ç., Köseoglu, E. and Içduygu, G. 2005. Optimization of nickel adsorption from aqueous solution by using activated carbon prepared from waste apricot by chemical activation. *Applied Surface Science*, 252(5): 1324-1331.

Espinasse, B., Picolet, G. and Chouraqui, E. 1997. Negotiation support systems: A multi-criteria and multi-agent approach. *European Journal of Operational Research*, 103(2): 389-409.

Feng, D., Aldrich, C. and Tan, H. 2000. Treatment of acid mine water by use of heavy metal precipitation and ion exchange. *Minerals Engineering*, 13(6): 623-642.

Ferella, F., Prisciandaro, M., De Michelis, I. and Veglio, F. 2007. Removal of heavy metals by surfactant-enhanced ultrafiltration from wastewaters. *Desalination*, 207(1-3): 125-133.

Fick, A. 1855. On liquid diffusion. *Philosophical Magazine Series 4*, 10(63): 30-39.

Fisher, G. W. 1973. Nonequilibrium thermodynamics as a model for diffusion-controlled metamorphic processes. *American Journal of Science*, 273(10): 897-924.

Foo, K. Y. and Hameed, B. H. 2010. Insights into the modeling of adsorption isotherm systems. *Chemical Engineering Journal*, 156(1): 2-10.

Forman, R. T. T. and Alexander, L. E. 1998. Roads and their major ecological effects. *Annual Review of Ecology and Systematics*, 29: 207-231.

Forster, C. F., Mehrotra, I. and Alibhai, K. R. K. 1985. The multiple binding of heavy metals by digested sludge. *Journal of Chemical Technology and Biotechnology*, 35(2): 145-154.

Freundlich, H. 1906. Over the adsorption in solution. *Journal of Physical Chemistry*, 57: 385–470.

Fu, F. and Wang, Q. 2011. Removal of heavy metal ions from wastewaters: A review. *Journal of Environmental Management*, 92(3): 407-418.

García-Sánchez, A., Alastuey, A. and Querol, X. 1999. Heavy metal adsorption by different minerals: application to the remediation of polluted soils. *Science of the Total Environment*, 242(1-3): 179-188.

Garg, U., Kaur, M. P., Jawa, G. K., Sud, D. and Garg, V. K. 2008. Removal of cadmium (II) from aqueous solutions by adsorption on agricultural waste biomass. *Journal of Hazardous Materials*, 154(1-3): 1149-1157.

Genç-Fuhrman, H., Mikkelsen, P. S. and Ledin, A. 2007. Simultaneous removal of As, Cd, Cr, Cu, Ni and Zn from stormwater: Experimental comparison of 11 different sorbents. *Water Research*, 41(3): 591-602.

Ghobarkar, H., Schäf, O. and Guth, U. 1999. Zeolites-from kitchen to space. *Progress in Solid State Chemistry*, 27(2-4): 29-73.

Gleick, P. 2002. The world's water: The biennial report on freshwater resources 2002-2003. Island Press, Washington, DC, USA.

Gnecco, I., Berretta, C., Lanza, L. G. and La Barbera, P. 2005. Storm water pollution in the urban environment of Genoa, Italy. *Atmospheric Research*, 77(1-4): 60-73.

Gosset, T., Trancart, J.-L. and Thévenot, D. R. 1986. Batch metal removal by peat: Kinetics and thermodynamics. *Water Research*, 20(1): 21-26.

Gregor, J. E., Nokes, C. J. and Fenton, E. 1997. Optimising natural organic matter removal from low turbidity waters by controlled pH adjustment of aluminium coagulation. *Water Research*, 31(12): 2949-2958.

Guibal, E., Milot, C. and Tobin, J. M. 1998. Metal-anion sorption by chitosan beads: Equilibrium and kinetic Studies. *Industrial & Engineering Chemistry Research*, 37(4): 1454-1463.

Guo, Q. 1997. Sediment and heavy metal accumulation in dry storm water detention basin. *Journal of Water Resources Planning and Management*, 123(5): 295-301.

Gupta, S. S. and Bhattacharyya, K. G. 2005. Interaction of metal ions with clays: I. A case study with Pb(II). *Applied Clay Science*, 30(3-4): 199-208.

Gupta, S. S. and Bhattacharyya, K. G. 2006. Adsorption of Ni(II) on clays. *Journal of Colloid and Interface Science*, 295(1): 21-32.

Gupta, S. S. and Bhattacharyya, K. G. 2006. Removal of Cd(II) from aqueous solution by kaolinite, montmorillonite and their poly(oxo zirconium) and tetrabutylammonium derivatives. *Journal of Hazardous Materials*, 128(2-3): 247-257.

Gupta, V., Carrott, P. and Ribeiro Carrott, M. 2009. Low-cost adsorbents: Growing approach to wastewater treatment - a review. *Critical Reviews in Environmental Science and Technology*, 39(9-12): 783-842.

Haggerty, G. M. and Bowman, R. S. 1994. Sorption of chromate and other inorganic anions by organo-zeolite. *Environmental Science & Technology*, 28(3): 452-458.

Hamilton, R. S., Revitt, D. M. and Warren, R. S. 1984. Levels and physico-chemical associations of Cd, Cu, Pb and Zn in road sediments. *Science of the Total Environment*, 33(1–4): 59-74.

Hancock, R. D. and Marsicano, F. 1978. Parametric correlation of formation constants in aqueous solution. 1. Ligands with small donor atoms. *Inorganic Chemistry*, 17(3): 560-564.

Hancock, R. D. and Martell, A. E. 1989. Ligand design for selective complexation of metal ions in aqueous solution. *Chemical Reviews*, 89(8): 1875-1914.

Haque, R., Lindstrom, F. T., Freed, V. H. and Sexton, R. 1968. Kinetic study of the sorption of 2,4-D on some clays. *Environmental Science & Technology*, 2(3): 207-211.

Hatt, B., Deletic, A. and Fletcher, T. 2007. Stormwater reuse: designing biofiltration systems for reliable treatment. *Water Science and Technology*, 55(4): 201.

Haydn, H. M. 1991. Overview — clay mineral applications. *Applied Clay Science*, 5(5-6): 379-395.

Helmy, A. K., de Bussetti, S. G. and Ferreiro, E. A. 1999. Monolayer coverage–sorbate area relationship for mixtures of sorbents. *Journal of Colloid and Interface Science*, 219(1): 149-154.

Henley, W. F., Patterson, M. A., Neves, R. J. and Lemly, A. D. 2000. Effects of sedimentation and turbidity on lotic food webs: a concise review for natural resource managers. *Reviews in Fisheries Science*, 8(2): 125-139.

Herngren, L., Goonetilleke, A. and Ayoko, G. A. 2005. Understanding heavy metal and suspended solids relationships in urban stormwater using simulated rainfall. *Journal of Environmental Management*, 76(2): 149-158.

Herngren, L., Goonetilleke, A. and Ayoko, G. A. 2006. Analysis of heavy metals in road-deposited sediments. *Analytica Chimica Acta*, 571(2): 270-278.

Herngren, L., Goonetilleke, A., Ayoko, G. A. and Mostert, M. M. M. 2010. Distribution of polycyclic aromatic hydrocarbons in urban stormwater in Queensland, Australia. *Environmental Pollution*, 158(9): 2848-2856.

Herngren, L. F. 2005. Build-up and wash-off process kinetics of PAHs and heavy metals on paved surfaces using simulated rainfall, PhD Thesis, Queensland University of Technology.

Herrero, R., Lodeiro, P., García-Casal, L. J., Vilariño, T., Rey-Castro, C., David, C. and Rodríguez, P. 2011. Full description of copper uptake by algal biomass combining an equilibrium NICA model with a kinetic intraparticle diffusion driving force approach. *Bioresource Technology*, 102(3): 2990-2997.

Hill, J.-R., Freeman, C. M. and Delley, B. 1999. Bridging hydroxyl groups in faujasite: periodic vs cluster density functional calculations. *The Journal of Physical Chemistry A*, 103(19): 3772-3777.

Ho, Y., Porter, J. and McKay, G. 2002. Equilibrium isotherm studies for the sorption of divalent metal ions onto peat: copper, nickel and lead single component systems. *Water, Air, and Soil Pollution*, 141(1): 1-33.

Ho, Y. S. and McKay, G. 1998. A comparison of chemisorption kinetic models applied to pollutant removal on various sorbents. *Process Safety and Environmental Protection*, 76(4): 332-340.

Ho, Y. S. and McKay, G. 1999. The sorption of lead (II) ions on peat. *Water Research*, 33(2): 578-584.

Ho, Y. S., Wase, D. A. J. and Forster, C. F. 1996. Kinetic studies of competitive heavy metal adsorption by sphagnum moss peat. *Environmental Technology*, 17(1): 71-77.

Hogan, D. M. and Walbridge, M. R. 2007. Best management practices for nutrient and sediment retention in urban stormwater runoff. *Journal of Environmental Quality*, 36(2): 386-395.

Holan, Z. and Volesky, B. 1995. Accumulation of cadmium, lead, and nickel by fungal and wood biosorbents. *Applied Biochemistry and Biotechnology*, 53(2): 133-146.

Homagai, P. L., Ghimire, K. N. and Inoue, K. 2010. Adsorption behavior of heavy metals onto chemically modified sugarcane bagasse. *Bioresource Technology*, 101(6): 2067-2069.

Horsfall Jnr, M. and Spiff, A. I. 2005. Effects of temperature on the sorption of Pb^{2+} and Cd^{2+} from aqueous solution by Caladium bicolor (Wild Cocoyam) biomass. *Electronic Journal of Biotechnology*, 8: 43-50.

Horvath, A. and Chester, M. 2009. Greenhouse gas assessment of expanded polystyrene food containers and alternative products used in Los Angeles County. The Center for a New American Dream, Los Angeles, California.

Hui, K. S., Chao, C. Y. H. and Kot, S. C. 2005. Removal of mixed heavy metal ions in wastewater by zeolite 4A and residual products from recycled coal fly ash. *Journal of Hazardous Materials*, 127(1-3): 89-101.

Ibrahim, H. S., Jamil, T. S. and Hegazy, E. Z. 2010. Application of zeolite prepared from Egyptian kaolin for the removal of heavy metals: II. Isotherm models. *Journal of Hazardous Materials*, 182(1-3): 842-847.

Inglezakis, V. and Poulopoulos, S. 2006. Adsorption, ion exchange and catalysis: design of operations and environmental applications. Elsevier Science Ltd.

Inglezakis, V. J. 2005. The concept of "capacity" in zeolite ion-exchange systems. *Journal of Colloid and Interface Science*, 281(1): 68-79.

Inglezakis, V. J. and Grigoropoulou, H. 2004. Effects of operating conditions on the removal of heavy metals by zeolite in fixed bed reactors. *Journal of Hazardous Materials*, 112(1-2): 37-43.

Inglezakis, V. J., Loizidou, M. D. and Grigoropoulou, H. P. 2003. Ion exchange of Pb^{2+}, Cu^{2+}, Fe^{3+}, and Cr^{3+} on natural clinoptilolite: selectivity determination and influence of acidity on metal uptake. *Journal of Colloid and Interface Science*, 261(1): 49-54.

Inglezakis, V. J., Papadeas, C. D., Loizidou, M. D. and Grigoropoulou, H. P. 2001. Effects of pretreatment on physical and ion exchange properties of natural clinoptilolite. *Environmental Technology*, 22(1): 75-82.

Ismail, A. A., Mohamed, R. M., Ibrahim, I. A., Kini, G. and Koopman, B. 2010. Synthesis, optimization and characterization of zeolite A and its ion-exchange properties. *Colloids and Surfaces A: Physicochemical and Engineering Aspects*, 366(1-3): 80-87.

ISRIC, FAO, 2002. Procedures for soil analysis, sixth ed., ISRIC, Wageningen, The Netharlands.

Jacobs, R. M., Fox, M. R. S. and Aldridge, M. H. 1969. Changes in plasma proteins associated with the anemia produced by dietary cadmium in Japanese quail. *Journal of Nutrition*, 99(2): 119-128.

Jamil, T. S., Ibrahim, H. S., Abd El-Maksoud, I. H. and El-Wakeel, S. T. 2010. Application of zeolite prepared from Egyptian kaolin for removal of heavy metals: I. Optimum conditions. *Desalination*, 258(1-3): 34-40.

Jha, B., Basha, S., Jaiswar, S., Mishra, B. and Thakur, M. 2009. Biosorption of Cd(II) and Pb(II) onto brown seaweed, Lobophora variegata (Lamouroux): kinetic and equilibrium studies. *Biodegradation*, 20(1): 1-13.

Jiang, J.-Q., Cooper, C. and Ouki, S. 2002. Comparison of modified montmorillonite adsorbents: Part I: preparation, characterization and phenol adsorption. *Chemosphere*, 47(7): 711-716.

Juang, R.-S. and Shiau, R.-C. 2000. Metal removal from aqueous solutions using chitosan-enhanced membrane filtration. *Journal of Membrane Science*, 165(2): 159-167.

Jüttner, K., Galla, U. and Schmieder, H. 2000. Electrochemical approaches to environmental problems in the process industry. *Electrochimica Acta*, 45(15-16): 2575-2594.

Kadirvelu, K. and Namasivayam, C. 2003. Activated carbon from coconut coirpith as metal adsorbent: adsorption of Cd(II) from aqueous solution. *Advances in Environmental Research*, 7(2): 471-478.

Kalavathy, M. H., Karthikeyan, T., Rajgopal, S. and Miranda, L. R. 2005. Kinetic and isotherm studies of Cu(II) adsorption onto H_3PO_4-activated rubber wood sawdust. *Journal of Colloid and Interface Science*, 292(2): 354-362.

Kang, S.-Y., Lee, J.-U., Moon, S.-H. and Kim, K.-W. 2004. Competitive adsorption characteristics of Co^{2+}, Ni^{2+}, and Cr^{3+} by IRN-77 cation exchange resin in synthesized wastewater. *Chemosphere*, 56(2): 141-147.

Karnitz, J. O., Gurgel, L. V. A., de Melo, J. C. P., Botaro, V. R., Melo, T. M. S., de Freitas Gil, R. P. and Gil, L. F. 2007. Adsorption of heavy metal ion from aqueous single metal solution by chemically modified sugarcane bagasse. *Bioresource Technology*, 98(6): 1291-1297.

Katsou, E., Malamis, S. and Haralambous, K. 2010. Examination of zinc uptake in a combined system using sludge, minerals and ultrafiltration membranes. *Journal of Hazardous Materials*, 182(1-3): 27-38.

Katsou, E., Malamis, S., Tzanoudaki, M., Haralambous, K. J. and Loizidou, M. 2011. Regeneration of natural zeolite polluted by lead and zinc in wastewater treatment systems. *Journal of Hazardous Materials*, 189(3): 773-786.

Keller, H. R., Massart, D. L. and Brans, J. P. 1991. Multicriteria decision making: A case study. *Chemometrics and Intelligent Laboratory Systems*, 11(2): 175-189.

Keskinkan, O., Goksu, M. Z. L., Basibuyuk, M. and Forster, C. F. 2004. Heavy metal adsorption properties of a submerged aquatic plant (Ceratophyllum demersum). *Bioresource Technology*, 92(2): 197-200.

Kesraoui-Ouki, S., Cheeseman, C. and Perry, R. 1993. Effects of conditioning and treatment of chabazite and clinoptilolite prior to lead and cadmium removal. *Environmental Science and Technology*, 27(6): 1108-1116.

Kesraoui-Ouki, S., Cheeseman, C. R. and Perry, R. 1994. Natural zeolite utilisation in pollution control: a review of applications to metals' effluents. *Journal of Chemical Technology & Biotechnology*, 59(2): 121-126.

Khalil, W. A.-S., Goonetilleke, A., Kokot, S. and Carroll, S. 2004. Use of chemometrics methods and multicriteria decision-making for site selection for sustainable on-site sewage effluent disposal. *Analytica Chimica Acta*, 506(1): 41-56.

Klopman, G. 1968. Chemical reactivity and the concept of charge- and frontier-controlled reactions. *Journal of the American Chemical Society*, 90(2): 223-234.

Kocaoba, S., Orhan, Y. and Akyuz, T. 2007. Kinetics and equilibrium studies of heavy metal ions removal by use of natural zeolite. *Desalination*, 214(1-3): 1-10.

Kokot, S. and Phuong, T. D. 1999. Elemental content of Vietnamese rice. Part 2. Multivariate data analysis. *Analyst*, 124(4): 561-569.

Kongsricharoern, N. and Polprasert, C. 1995. Electrochemical precipitation of chromium (Cr^{6+}) from an electroplating wastewater. *Water Science and Technology*, 31(9): 109-117.

Kumar, R., Bishnoi, N. R., Garima and Bishnoi, K. 2008. Biosorption of chromium(VI) from aqueous solution and electroplating wastewater using fungal biomass. *Chemical Engineering Journal*, 135(3): 202-208.

Kundu, S. and Gupta, A. K. 2006. Arsenic adsorption onto iron oxide-coated cement (IOCC): Regression analysis of equilibrium data with several isotherm models and their optimization. *Chemical Engineering Journal*, 122(1-2): 93-106.

Kurniawan, T. A., Chan, G. Y. S., Lo, W. and Babel, S. 2006. Comparisons of low-cost adsorbents for treating wastewaters laden with heavy metals. *Science of the Total Environment*, 366(2-3): 409-426.

Kurniawan, T. A., Chan, G. Y. S., Lo, W. H. and Babel, S. 2006. Physico-chemical treatment techniques for wastewater laden with heavy metals. *Chemical Engineering Journal*, 118(1-2): 83-98.

Kwon, J.-S., Yun, S.-T., Lee, J.-H., Kim, S.-O. and Jo, H. Y. 2010. Removal of divalent heavy metals (Cd, Cu, Pb, and Zn) and arsenic(III) from aqueous solutions using scoria: Kinetics and equilibria of sorption. *Journal of Hazardous Materials*, 174(1–3): 307-313.

Lagergren, S. 1898. About the theory of so-called adsorption of soluble substances (Zur theorie der sogenannten adsorption geloster stoffe) *Kungliga Svenska Vetenskapsakademiens. Handlingar*, 24 (4): 1-39.

Langmuir, I. 1916. The constitution and fundamental properties of solids and liquids. Part I. Solids. *Journal of the American Chemical Society*, 38(11): 2221-2295.

Laszlo, K., Josepovits, K. and Tombacz, E. 2001. Analysis of active sites on synthetic carbon surfaces by various methods. *Analytical Sciences*, 17: i1741-i1744.

Lau, S.-L. and Stenstrom, M. K. 2005. Metals and PAHs adsorbed to street particles. *Water Research*, 39(17): 4083-4092.

Le Chatelier, H. L. 1884. Sur un énoncé général des lois des équilibres chimiques (About a general statement of the chemical equilibrium laws). *Comptes Rendus Académie de Sciences*, 99: 786-789.

Legret, M., and Pagotto, C. 1999. Evaluation of pollutant loadings in the runoff waters from a major rural highway. *Science of the Total Environment*, 235(1-3): 143-150.

Leusch, A., Holan, Z. and Volesky, B. 1997. Solution and particle effects on the biosorption of heavy metals by seaweed biomass. *Applied Biochemistry and Biotechnology*, 61(3): 231-249.

Lewis, A. E. 2010. Review of metal sulphide precipitation. *Hydrometallurgy*, 104(2): 222-234.

Leyva-Ramos, R., Bernal-Jacome, L. A. and Acosta-Rodriguez, I. 2005. Adsorption of cadmium(II) from aqueous solution on natural and oxidized corncob. *Separation and Purification Technology*, 45(1): 41-49.

Li, Y., Zeng, X., Liu, Y., Yan, S., Hu, Z. and Ni, Y. 2003. Study on the treatment of copper-electroplating wastewater by chemical trapping and flocculation. *Separation and Purification Technology*, 31(1): 91-95.

Liu, C.-C., Wang, M.-K., Chiou, C.-S., Li, Y.-S., Yang, C.-Y. and Lin, Y.-A. 2009. Biosorption of chromium, copper and zinc by wine-processing waste sludge: Single and multi-component system study. *Journal of Hazardous Materials*, 171(1-3): 386-392.

Liu, F., Zhang, G., Meng, Q. and Zhang, H. 2008. Performance of nanofiltration and reverse osmosis membranes in metal effluent treatment. *Chinese Journal of Chemical Engineering*, 16(3): 441-445.

Luo, J. and Lindsey, S. 2006. The use of pine bark and natural zeolite as biofilter media to remove animal rendering process odours. *Bioresource Technology*, 97(13): 1461-1469.

Lyubchik, S. I., Lyubchik, A. I., Galushko, O. L., Tikhonova, L. P., Vital, J., Fonseca, I. M. and Lyubchik, S. B. 2004. Kinetics and thermodynamics of the Cr(III) adsorption on the activated carbon from co-mingled wastes. *Colloids and Surfaces A: Physicochemical and Engineering Aspects*, 242(1-3): 151-158.

Mabeau, S. and Fleurence, J. 1993. Seaweed in food products: biochemical and nutritional aspects. *Trends in Food Science and Technology*, 4(4): 103-107.

Madhava Rao, M., Ramesh, A., Purna Chandra Rao, G. and Seshaiah, K. 2006. Removal of copper and cadmium from the aqueous solutions by activated carbon derived from Ceiba pentandra hulls. *Journal of Hazardous Materials*, 129(1-3): 123-129.

Maldonado-Magaña, A., E. Favela-Torres, F. Rivera-Cabrera and T. Volke-Sepulveda. 2011. Lead bioaccumulation in <i>Acacia farnesiana</i> and its effect on lipid peroxidation and glutathione production. *Plant and Soil,* 339(1): 377-389.

Malliou, E., Loizidou, M. and Spyrellis, N. 1994. Uptake of lead and cadmium by clinoptilolite. *Science of the Total Environment*, 149(3): 139-144.

Mangani, G., Berloni, A., Bellucci, F., Tatano, F. and Maione, M. 2005. Evaluation of the pollutant content in road runoff first flush waters. *Water, Air, and Soil Pollution*, 160(1): 213-228.

Marcus, Y. 1988. Ionic radii in aqueous solutions. *Chemical Reviews*, 88(8): 1475-1498.

Marcus, Y. 1991. Thermodynamics of solvation of ions. Part 5 - Gibbs free energy of hydration at 298.15 K. *Journal of the Chemical Society, Faraday Transactions*, 87(18): 2995-2999.

Martell, A. and Hancock, R. 1996. Metal complexes in aqueous solutions. Springer, New York.

Martin, E. H. 1988. Effectiveness of an urban runoff detention pond-wetlands system. *Journal of Environmental Engineering*, 114(4): 810-827.

Matin, A., Khan, Z., Zaidi, S. M. J. and Boyce, M. C. 2011. Biofouling in reverse osmosis membranes for seawater desalination: Phenomena and prevention. *Desalination*, 281(0): 1-16.

McKay, G., Otterburn, M. S. and Aga, J. A. 1987. Intraparticle diffusion process occurring during adsorption of dyestuffs. *Water, Air, and Soil Pollution*, 36(3): 381-390.

McKay, G. and Poots, V. J. P. 1980. Kinetics and diffusion processes in colour removal from effluent using wood as an adsorbent. *Journal of Chemical Technology and Biotechnology*, 30(1): 279-292.

Miguntanna, N. P. 2009. Nutrients build-up and wash-off processes in urban land uses, PhD Thesis, Queensland University of Technology.

Miguntanna, N. P., Goonetilleke, A., Egodowatta, P. and Kokot, S. 2010. Understanding nutrient build-up on urban road surfaces. *Journal of Environmental Sciences*, 22(6): 806-812.

Minceva, M., Fajgar, R., Markovska, L. and Meshko, V. 2008. Comparative study of Zn^{2+}, Cd^{2+}, and Pb^{2+} removal from water solution using natural clinoptilolitic zeolite and commercial granulated activated carbon. Equilibrium of adsorption. *Separation Science and Technology*, 43(8): 2117-2143.

Mishra, T. and Tiwari, S. K. 2006. Studies on sorption properties of zeolite derived from Indian fly ash. *Journal of Hazardous Materials*, 137(1): 299-303.

Mohan, D. and Singh, K. P. 2002. Single- and multi-component adsorption of cadmium and zinc using activated carbon derived from bagasse—an agricultural waste. *Water Research*, 36(9): 2304-2318.

Mohsen-Nia, M., Montazeri, P. and Modarress, H. 2007. Removal of Cu^{2+} and Ni^{2+} from wastewater with a chelating agent and reverse osmosis processes. *Desalination*, 217(1-3): 276-281.

Mostert, M. M. R., Ayoko, G. A. and Kokot, S. 2010. Application of chemometrics to analysis of soil pollutants. *Trends in Analytical Chemistry*, 29(5): 430-445.

Motoyuki, S. 1994. Activated carbon fiber: Fundamentals and applications. *Carbon*, 32(4): 577-586.

Motsi, T., Rowson, N. A. and Simmons, M. J. H. 2009. Adsorption of heavy metals from acid mine drainage by natural zeolite. *International Journal of Mineral Processing*, 92(1-2): 42-48.

Mozgawa, W. and Bajda, T. 2005. Spectroscopic study of heavy metals sorption on clinoptilolite. *Physics and Chemistry of Minerals*, 31(10): 706-713.

Murphy, V., Hughes, H. and McLoughlin, P. 2008. Comparative study of chromium biosorption by red, green and brown seaweed biomass. *Chemosphere*, 70(6): 1128-1134.

Murzin, D. and Salmi, T. 2005. Catalytic kinetics. Elsevier Science Ltd, Amsterdam .

Muthukrishnan, M. and Guha, B. K. 2006. Heavy metal separation by using surface modified nanofiltration membrane. *Desalination*, 200(1-3): 351-353.

Nagao, M. 1971. Physisorption of water on zinc oxide surface. *The Journal of Physical Chemistry*, 75(25): 3822-3828.

Ndabigengesere, A., Narasiah, K. S. and Talbot, B. G. 1995. Active agents and mechanism of coagulation of turbid waters using Moringa oleifera. *Water Research*, 29(2): 703-710.

Nestorov, I., Rowland, M., Hadjitodorov, S. and Petrov, I. 1999. Empirical versus mechanistic modelling: comparison of an artificial neural network to a mechanistically based model for quantitative structure pharmacokinetic relationships of a homologous series of barbiturates. *The AAPS Journal*, 1(4): 5-13.

NHMRC (National Health and Medical Research Council), 2004. Australian Drinking Water Guidelines.

Ni, Y., Lai, Y., Brandes, S. and Kokot, S. 2009. Multi-wavelength HPLC fingerprints from complex substances: An exploratory chemometrics study of the Cassia seed example. *Analytica Chimica Acta*, 647(2): 149-158.

Nightingale, E. R. 1959. Phenomenological theory of ion solvation. effective radii of hydrated ions. *The Journal of Physical Chemistry*, 63(9): 1381-1387.

Norkus, E., Stalnionien , I. and Crans, D. C. 2003. Interaction of pyridine and 4 hydroxypyridine 2, 6 dicarboxylic acids with heavy metal ions in aqueous solutions. *Heteroatom Chemistry*, 14(7): 625-632.

NWQMS (The National Water Quality Management Strategy). 2009. Australian guidelines for water recycling: Managing health and environmental risks - Stormwater harvesting and reuse. Retrieved 20 May, 2012 URL: http://www.ephc.gov.au/sites/default/files/WQ_AGWR_GL__Stormwater_Harvesting_and_Reuse_Final_200907.pdf

Ogunlaja, O. and Aemere, O. 2009. Evaluating the efficiency of a textile wastewater treatment plant located in Oshodi, Lagos. *African Journal of Pure and Applied Chemistry*, 3(9): 189-196.

Ok, Y. S., Yang, J. E., Zhang, Y. S., Kim, S. J. and Chung, D. Y. 2007. Heavy metal adsorption by a formulated zeolite-Portland cement mixture. *Journal of Hazardous Materials*, 147(1-2): 91-96.

Oren, A. H. and Kaya, A. 2006. Factors affecting adsorption characteristics of Zn^{2+} on two natural zeolites. *Journal of Hazardous Materials*, 131(1-3): 59-65.

Ouki, S. and Kavannagh, M. 1997. Performance of natural zeolites for the treatment of mixed metal-contaminated effluents. *Waste Management & Research*, 15(4): 383-394.

Oumi, Y., Mizuno, R., Azuma, K., Nawata, S., Fukushima, T., Uozumi, T. and Sano, T. 2001. Reversibility of dealumination–realumination process of BEA zeolite. *Microporous and Mesoporous Materials*, 49(1–3): 103-109.

Pagnanelli, F., Esposito, A. and Vegliò, F. 2002. Multi-metallic modelling for biosorption of binary systems. *Water Research*, 36(16): 4095-4105.

Panayotova, M. I. 2001. Kinetics and thermodynamics of copper ions removal from wastewater by use of zeolite. *Waste Management*, 21(7): 671-676.

Park, D., Yun, Y.-S., Cho, H. Y. and Park, J. M. 2004. Chromium biosorption by thermally treated biomass of the brown seaweed, Ecklonia sp. *Industrial & Engineering Chemistry Research*, 43(26): 8226-8232.

Park, H. G., Kim, T. W., Chae, M. Y. and Yoo, I.-K. 2007. Activated carbon-containing alginate adsorbent for the simultaneous removal of heavy metals and toxic organics. *Process Biochemistry*, 42(10): 1371-1377.

Parr, R. G. and Pearson, R. G. 1983. Absolute hardness: companion parameter to absolute electronegativity. *Journal of the American Chemical Society*, 105(26): 7512-7516.

Patterson, J. W., Allen, H. E. and Scala, J. J. 1977. Carbonate precipitation for heavy metals pollutants. *Journal of Water Pollution Control Federation*, 49(12): 2397-2410.

Pearson, R. 1963. Hard and soft acids and bases. *Journal of the American Chemical Society*, 85(22): 3533-3539.

Pearson, R. G. 1968. Hard and soft acids and bases, HSAB, part 1: Fundamental principles. *Journal of Chemical Education*, 45(9): 581-587.

Peric, J., Trgo, M. and Vukojevic Medvidovic, N. 2004. Removal of zinc, copper and lead by natural zeolite-a comparison of adsorption isotherms. *Water Research*, 38(7): 1893-1899.

Pfleger, H. and Wolf, H. 1975. Activation of membrane-bound high-affinity calcium ion-sensitive adenosine triphosphatase of human erythrocytes by bivalent metal ions. *Biochemical Journal*, 147(2): 359.

Pigram, J. J. 2006. Australia's water resources. CSIRO Publishing, Melbourne, Australia.

Pitcher, S. K., Slade, R. C. T. and Ward, N. I. 2004. Heavy metal removal from motorway stormwater using zeolites. *Science of the Total Environment*, 334-335: 161-166.

Pontier, H., May, E. and Williams, J. B. 2001. Constructed wetlands for the treatment of runoff from the Newbury bypass. *Water and Environment Journal*, 15(2): 125-129.

Potts, D. E., Ahlert, R. C. and Wang, S. S. 1981. A critical review of fouling of reverse osmosis membranes. *Desalination*, 36(3): 235-264.

Qu, W. and Kelderman, P. 2001. Heavy metal contents in the Delft canal sediments and suspended solids of the River Rhine: multivariate analysis for source tracing. *Chemosphere*, 45(6-7): 919-925.

Rai, L. C., Gaur, J. P. and Kumar, H. D. 1981. Phycology and heavy metal pollution. *Biological Reviews*, 56(2): 99-151.

Rao, G. P. C., Satyaveni, S., Ramesh, A., Seshaiah, K., Murthy, K. S. N. and Choudary, N. V. 2006. Sorption of cadmium and zinc from aqueous solutions by zeolite 4A, zeolite 13X and bentonite. *Journal of Environmental Management*, 81(3): 265-272.

Ray, W. J. 1983. Rate-limiting step: a quantitative definition. Application to steady-state enzymic systems. *Biochemistry*, 22(20): 4625-4637.

Reddy, K. R. and Parupudi, U. S. 1997. Removal of chromium, nickel and cadmium from clays by in-situ electrokinetic remediation. *Journal of Soil Contamination*, 6(4): 391-407.

Rengaraj, S., Joo, C. K., Kim, Y. and Yi, J. 2003. Kinetics of removal of chromium from water and electronic process wastewater by ion exchange resins: 1200H, 1500H and IRN97H. *Journal of Hazardous Materials*, 102(2-3): 257-275.

Rengaraj, S., Yeon, K. H. and Moon, S. H. 2001. Removal of chromium from water and wastewater by ion exchange resins. *Journal of Hazardous Materials*, 87(1-3): 273-287.

Rivera, A., Rodríguez-Fuentes, G. and Altshuler, E. 2000. Time evolution of a natural clinoptilolite in aqueous medium: conductivity and pH experiments. *Microporous and Mesoporous Materials*, 40(1-3): 173-179.

Robertson, G. P., Sollins, P., Ellis, B. G. and Lajtha, K. 1999. Exchangeable ions, pH, and cation exchange capacity. In: Robertson, G. P., Coleman, D. C., Bledsoe, C. S. and Sollins, P. (eds.). *Standard soil methods in long-term ecological research*. Oxford University Press, Oxford, UK.

Rogge, W. F., Hildemann, L. M., Mazurek, M. A., Cass, G. R. and Simoneit, B. R. T. 1993. Sources of fine organic aerosol. 2. Noncatalyst and catalyst-equipped automobiles and heavy-duty diesel trucks. *Environmental Science & Technology*, 27(4): 636-651.

Romero-González, M. E., Williams, C. J. and Gardiner, P. H. E. 2001. Study of the mechanisms of cadmium biosorption by dealginated seaweed waste. *Environmental Science and Technology*, 35(14): 3025-3030.

Rupérez, P. and Saura-Calixto, F. 2001. Dietary fibre and physicochemical properties of edible Spanish seaweeds. *European Food Research and Technology*, 212(3): 349-354.

Sağ, Y. and Aktay, Y. 2000. Mass transfer and equilibrium studies for the sorption of chromium ions onto chitin. *Process Biochemistry*, 36(1-2): 157-173.

Sansalone, J. J. and Buchberger, S. G. 1997. Partitioning and first flush of metals in urban roadway storm water. *Journal of Environmental Engineering*, 123(2): 134-143.

Sansalone, J. J., Buchberger, S. G. and Al-Abed, S. R. 1996. Fractionation of heavy metals in pavement runoff. *Science of the Total Environment*, 189: 371-378.

Sansalone, J. J. and Kim, J.-Y. 2008. Suspended particle destabilization in retained urban stormwater as a function of coagulant dosage and redox conditions. *Water Research*, 42(4–5): 909-922.

Sapari, N., Idris, A. and Hamid, N. H. A. 1996. Total removal of heavy metal from mixed plating rinse wastewater. *Desalination*, 106(1-3): 419-422.

Sartor, J. D., Boyd, G. B. and Agardy, F. J. 1974. Water pollution aspects of street surface contaminants. *Journal of Water Pollution Control Federation*, 46(3): 458-467.

Satarug, S. and Michael, R. M. 2004. Adverse health effects of chronic exposure to low-level cadmium in foodstuffs and cigarette smoke. *Environmental Health Perspectives*, 112(10): 1099-1103.

Saucedo, I., Guibal, E., Roulph, C. and Le Cloirec, P. 1992. Sorption of uranyl ions by a modified chitosan: Kinetic and equilibrium studies. *Environmental Technology*, 13(12): 1101-1115.

Schoonover, J. E. and Lockaby, B. G. 2006. Land cover impacts on stream nutrients and fecal coliform in the lower Piedmont of West Georgia. *Journal of Hydrology*, 331(3-4): 371-382.

Selcuk, H. 2005. Decolorization and detoxification of textile wastewater by ozonation and coagulation processes. *Dyes and Pigments*, 64(3): 217-222.

Semerjian, L. and Ayoub, G. M. 2003. High-pH–magnesium coagulation–flocculation in wastewater treatment. *Advances in Environmental Research*, 7(2): 389-403.

Seward, T. M., Henderson, C. M. B., Charnock, J. M. and Driesner, T. 1999. An EXAFS study of solvation and ion pairing in aqueous strontium solutions to 300°C. *Geochimica et Cosmochimica Acta*, 63(16): 2409-2418.

Shen, J. and Duvnjak, Z. 2005. Adsorption kinetics of cupric and cadmium ions on corncob particles. *Process Biochemistry*, 40(11): 3446-3454.

Sheng, P. X., Ting, Y.-P., Chen, J. P. and Hong, L. 2004. Sorption of lead, copper, cadmium, zinc, and nickel by marine algal biomass: characterization of biosorptive capacity and investigation of mechanisms. *Journal of Colloid and Interface Science*, 275(1): 131-141.

Sheppard, D. M., Demir, H. and Melville, B. 2011. Scour at Wide Piers and Long Skewed Piers. Transportation Research Board of National Academies, Washington, DC, USA.

Singman, C. N. 1984. Atomic volume and allotropy of the elements. *Journal of Chemical Education*, 61(2): 137.

Smith, J., Sievers, M., Huang, S. and Yu, S. 2000. Occurrence and phase distribution of polycyclic aromatic hydrocarbons in urban storm-water runoff. *Water Science and Technology* 42(3-4): 383-388.

Smolka, A. and Schmidt, K.-G. 1997. Gas/particle partitioning before and after flue gas purification by an activated-carbon-filter. *Chemosphere*, 34(5–7): 1075-1082.

Sukola, K., Wang, F. and Tessier, A. 2005. Metal-sulfide species in oxic waters. *Analytica Chimica Acta*, 528(2): 183-195.

Sultana, B., Anwar, F. and Przybylski, R. 2007. Antioxidant potential of corncob extracts for stabilization of corn oil subjected to microwave heating. *Food Chemistry*, 104(3): 997-1005.

Takada, H., Onda, T., Harada, M. and Ogura, N. 1991. Distribution and sources of polycyclic aromatic hydrocarbons (PAHs) in street dust from the Tokyo Metropolitan area. *Science of the Total Environment*, 107: 45-69.

Tan, G., Yuan, H., Liu, Y. and Xiao, D. 2010. Removal of lead from aqueous solution with native and chemically modified corncobs. *Journal of Hazardous Materials*, 174(1-3): 740-745.

Terry, P. A. and Stone, W. 2002. Biosorption of cadmium and copper contaminated water by Scenedesmus abundans. *Chemosphere*, 47(3): 249-255.

Terzano, R., Spagnuolo, M., Medici, L., Tateo, F. and Ruggiero, P. 2005. Zeolite synthesis from pre-treated coal fly ash in presence of soil as a tool for soil remediation. *Applied Clay Science*, 29(2): 99-110.

Tillinghast, E. D., Hunt, W. F. and Jennings, G. D. 2011. Stormwater control measure (SCM) design standards to limit stream erosion for Piedmont North Carolina. *Journal of Hydrology*, 411(3–4): 185-196.

Tsihrintzis, V. A. and Hamid, R. 1997. Modeling and management of urban stormwater runoff quality: A review. *Water Resources Management*, 11(2): 136-164.

Tunell, I. and Lim, C. 2006. Factors governing the metal coordination number in isolated group IA and IIA metal hydrates. *Inorganic Chemistry*, 45(12): 4811-4819.

Türkman, A., Aslan, Ş. and Ege, I. 2004. Treatment of metal containing wastewaters by natural zeolites. *Fresenius Environmental Bulletin*, 13(6): 574-580.

Uluozlu, O. D., Sari, A., Tuzen, M. and Soylak, M. 2008. Biosorption of Pb(II) and Cr(III) from aqueous solution by lichen (Parmelina tiliaceae) biomass. *Bioresource Technology*, 99(8): 2972-2980.

Ünlü, N. and Ersoz, M. 2006. Adsorption characteristics of heavy metal ions onto a low cost biopolymeric sorbent from aqueous solutions. *Journal of Hazardous Materials*, 136(2): 272-280.

Uusitalo, R., Yli-Halla, M. and Turtola, E. 2000. Suspended soil as a source of potentially bioavailable phosphorus in surface runoff waters from clay soils. *Water Research*, 34(9): 2477-2482.

Vaca Mier, M., López Callejas, R., Gehr, R., Jiménez Cisneros, B. E. and Alvarez, P. J. J. 2001. Heavy metal removal with Mexican clinoptilolite: multi-component ionic exchange. *Water Research*, 35(2): 373-378.

Vadivelan, V. and Kumar, K. V. 2005. Equilibrium, kinetics, mechanism, and process design for the sorption of methylene blue onto rice husk. *Journal of Colloid and Interface Science*, 286(1): 90-100.

van den Broek, R., van den Burg, T., van Wijk, A. and Turkenburg, W. 2000. Electricity generation from eucalyptus and bagasse by sugar mills in Nicaragua: A comparison with fuel oil electricity generation on the basis of costs, macro-economic impacts and environmental emissions. *Biomass and Bioenergy*, 19(5): 311-335.

Vaughan, T., Seo, C. W. and Marshall, W. E. 2001. Removal of selected metal ions from aqueous solution using modified corncobs. *Bioresource Technology*, 78(2): 133-139.

Vaze, J. and Chiew, F. H. S. 2004. Nutrient Loads Associated with Different Sediment Sizes in Urban Stormwater and Surface Pollutants. *Journal of Environmental Engineering*, 130(4): 391-396.

Vázquez, G., Antorrena, G., González, J. and Doval, M. D. 1994. Adsorption of heavy metal ions by chemically modified Pinus pinaster bark. *Bioresource Technology*, 48(3): 251-255.

Vengris, T., Binkiene, R. and Sveikauskaite, A. 2001. Nickel, copper and zinc removal from waste water by a modified clay sorbent. *Applied Clay Science*, 18(3-4): 183-190.

Vermeulen, T. 1953. Theory for Irreversible and Constant-Pattern Solid Diffusion. *Industrial and Engineering Chemistry*, 45(8): 1664-1670.

Vigneswaran, S., Ngo, H. H., Chaudhary, D. S. and Hung, Y.-T. 2005. Physicochemical Treatment Processes for Water Reuse. In: Wang, L. K., Hung, Y.-T. and Shammas, N. K. (eds.). *Physicochemical Treatment Processes*. Humana Press, 3: 635-676.

Vijayaraghavan, K., Padmesh, T. V. N., Palanivelu, K. and Velan, M. 2006. Biosorption of nickel(II) ions onto Sargassum wightii: Application of two-parameter and three-parameter isotherm models. *Journal of Hazardous Materials*, 133(1-3): 304-308.

Vijayavel, K. and Balasubramanian, M. P. 2006. Changes in oxygen consumption and respiratory enzymes as stress indicators in an estuarine edible crab Scylla serrata exposed to naphthalene. *Chemosphere*, 63(9): 1523-1531.

Visual Decision Inc. 1999. Decision Lab 2000 Executive Edition. Montreal, Quebec, Canada.

Volesky, B. 2003. Biosorption process simulation tools. *Hydrometallurgy*, 71(1-2): 179-190.

Vuckovic, D., Cudjoe, E., Musteata, F. M. and Pawliszyn, J. 2010. Automated solid-phase microextraction and thin-film microextraction for high-throughput analysis of biological fluids and ligand-receptor binding studies. *Nature Protocols*, 5(1): 140-161.

Wan Ngah, W. S. and Hanafiah, M. A. K. M. 2008. Removal of heavy metal ions from wastewater by chemically modified plant wastes as adsorbents: A review. *Bioresource Technology*, 99(10): 3935-3948.

Wang, J. and Chen, C. 2009. Biosorbents for heavy metals removal and their future. *Biotechnology Advances*, 27(2): 195-226.

Wang, S. and Peng, Y. 2010. Natural zeolites as effective adsorbents in water and wastewater treatment. *Chemical Engineering Journal*, 156(1): 11-24.

Wang, S., Soudi, M., Li, L. and Zhu, Z. H. 2006. Coal ash conversion into effective adsorbents for removal of heavy metals and dyes from wastewater. *Journal of Hazardous Materials*, 133(1-3): 243-251.

Wang, X.-C., Zhang, Y.-X. and Chen, R. F. 2001. Distribution and Partitioning of Polycyclic Aromatic Hydrocarbons (PAHs) in Different Size Fractions in Sediments from Boston Harbor, United States. *Marine Pollution Bulletin*, 42(11): 1139-1149.

Wark, M., Lutz, W., Schulz-Ekloff, G. and Dyer, A. 1993. Quantitative monitoring of side products during high loading of zeolites by heavy metals via pH measurements. *Zeolites*, 13(8): 658-662.

Weber, W. J. and Morris, J. C. 1962. Removal of biological resistant pollutions from wastewater by adsorption. Proceedings of the first International Conference on Water Pollution Research, New York, USA.

White, P. J., M. R. Broadley and J. P. Gregory. 2012. Managing the Nutrition of Plants and People. *Applied and Environmental Soil Science* 2012: 13.

WHO (World Health Organization). 2000. Global water supply and sanitation assessment 2000 report. World Health Organization.

WHO (World Health Organization). 2008. Progress on Drinking Water and Sanitation: Special Focus on Sanitation. WHO and UNICEF Joint Monitoring Programme for Water Supply and Sanitation, Geneva and New York. Retrieved 6

Sept, 2010, URL: http://www.who.int/water_sanitation_health/monitoring/jmp_report_7_10_lores.pdf

Wilke, C. R. and Chang, P. 1955. Correlation of diffusion coefficients in dilute solutions. *AIChE Journal*, 1(2): 264-270.

Wingenfelder, U., Nowack, B., Furrer, G. and Schulin, R. 2005. Adsorption of Pb and Cd by amine-modified zeolite. *Water Research*, 39(14): 3287-3297.

Wu, D., Sui, Y., Chen, X., He, S., Wang, X. and Kong, H. 2008. Changes of mineralogical-chemical composition, cation exchange capacity, and phosphate immobilization capacity during the hydrothermal conversion process of coal fly ash into zeolite. *Fuel*, 87(10-11): 2194-2200.

Wu, P. and Zhou, Y.-s. 2009. Simultaneous removal of coexistent heavy metals from simulated urban stormwater using four sorbents: A porous iron sorbent and its mixtures with zeolite and crystal gravel. *Journal of Hazardous Materials*, 168(2-3): 674-680.

Yang, X. J., Livingston, A. G. and Freitas dos Santos, L. 2001. Experimental observations of nanofiltration with organic solvents. *Journal of Membrane Science*, 190(1): 45-55.

Yousef, Y. A., Hvitved-Jacobsen, T., Harper, H. H. and Lin, L. Y. 1990. Heavy metal accumulation and transport through detention ponds receiving highway runoff. *Science of the Total Environment*, 93: 433-440.

Yu, B., Zhang, Y., Shukla, A., Shukla, S. S. and Dorris, K. L. 2001. The removal of heavy metals from aqueous solutions by sawdust adsorption — removal of lead and comparison of its adsorption with copper. *Journal of Hazardous Materials*, 84(1): 83-94.

Yun, Y. 2004. Characterization of functional groups of protonated sargassum polycystum biomass capable of binding protons and metal Ions. *Journal of Microbiology and Biotechnology*, 14.

Yurlova, L., Kryvoruchko, A. and Kornilovich, B. 2002. Removal of Ni(II) ions from wastewater by micellar-enhanced ultrafiltration. *Desalination*, 144(1-3): 255-260.

Zafra, C. A., Temprano, J. and Tejero, I. 2008. Particle size distribution of accumulated sediments on an urban road in rainy weather. *Environmental Technology*, 29(5): 571 - 582.

Zaki, A. B., El-Sheikh, M. Y., Evans, J. and El-Safty, S. A. 2000. Kinetics and mechanism of the sorption of some aromatic amines onto Amberlite IRA-904 anion-exchange Resin. *Journal of Colloid and Interface Science*, 221(1): 58-63.

Zamzow, M. J., Eichbaum, B. R., Sandgren, K. R. and Shanks, D. E. 1990. Removal of heavy metals and other cations from wastewater using zeolites. *Separation Science and Technology*, 25(13): 1555-1569.

Zenk, M. H. 1996. Heavy metal detoxification in higher plants - a review. *Gene*, 179(1): 21-30.

Ziyath, A. M., Mahbub, P., Goonetilleke, A., Adebajo, M. O., Kokot, S. and Oloyede, A. 2011. Influence of physical and chemical parameters on the treatment of heavy metals in polluted stormwater using zeolite – A review. *Journal of Water Resource and Protection*, 3(10): 758-767.

Zou, W., Han, R., Chen, Z., Jinghua, Z. and Shi, J. 2006. Kinetic study of adsorption of Cu (II) and Pb (II) from aqueous solutions using manganese oxide coated zeolite in batch mode. *Colloids and Surfaces A: Physicochemical and Engineering Aspects*, 279(1-3): 238-246.

Appendix A
Experimental metal sorption capacities from research literature

Table A.1 Metal sorption capacities of sorbents

Sorbent	Metal ion	Sorption capacity (mmol/g)	Reference/s
[1]SW	Ni	0.61	Sheng et al. (2004)
	Cu	0.99	
	Zn	0.50	
	Cd	0.76	
	Pb	1.16	
[1]CC	Ni	0.37	Vaughan et al. (2001)
	Cu	0.49	Leyva-Ramos et al. (2005)
	Zn	0.40	Vaughan et al. (2001)
	Cd	0.49	Leyva-Ramos et al. (2005)
	Pb	0.40	Vaughan et al. (2001)
[1]SB	Ni	2.80	Homagai et al. (2010)
	Cu	2.09	Karnitz et al. (2007)
	Zn	2.54	Homagai et al. (2010)
	Cd	2.78	Karnitz et al. (2007)
	Pb	1.51	
[1]AC	Ni	1.72	Erdogan et al. (2005)
	Cu	1.16	Park et al. (2007)
	Zn	0.18	
	Cd	0.17	Madhava Rao et al. (2006)
	Pb	0.72	Park et al. (2007)
[1]Z	Ni	0.03	Alvarez-Ayuso et al. (2003)
	Cu	0.09	
	Zn	0.05	
	Cd	0.04	
	Pb	0.07	Turkman et al. (2004)
[1]C	Ni	0.48	Sengupta et al. (2006)
	Cu	0.40	Bhattacharyya et al. (2006)
	Zn	0.23	Vengris et al. (2001)
	Cd	0.29	Gupta et al. (2006)
	Pb	0.16	Gupta et al. (2005)

Notes:[1] Seaweed (SW); Corncob (CC); Sugarcane bagasse (SB); Activated carbon (AC); Zeolite (Z); Clay (C)

Table A.2 Experimental equilibrium sorption capacities (in μmol/g)

Sorbent materials	Equilibrium sorption capacity (in μmol/g)						
	Al	**Cr**	**Ni**	**Cu**	**Zn**	**Cd**	**Pb**
Seaweed	0.08	0.40	0.75	0.47	0.34	0.08	0.13
Corncob	0.07	0.06	0.09	0.06	0.03	0.04	0.03
Sugarcane bagasse	0.00	0.50	0.27	0.25	0.08	0.16	0.05
Activated carbon	0.00	0.10	0.25	0.01	0.04	0.10	0.02
Zeolite	0.00	0.31	0.28	0.39	0.08	0.20	0.50
Clay	0.00	0.42	0.42	0.53	0.00	0.31	0.27

Appendix B
Sorption experimental data for zeolite and seaweed

Kinetics experimental data for zeolite

Table B.1 Cu sorption capacity of zeolite (mg/g)

Time (min.)	Initial metal concentration / (mg/L)							
	200		100		50		20	
	Mean	SD[1]	Mean	SD	Mean	SD	Mean	SD
5	0.0	0.0	0.0	0.0	0.0	0.0	0.0	0.0
10	5.0	0.1	2.0	0.0	0.7	0.0	0.2	0.0
20	5.5	0.1	2.2	0.0	1.0	0.0	0.3	0.0
40	5.7	0.1	2.5	0.0	1.1	0.0	0.4	0.0
60	5.7	0.2	2.5	0.0	1.1	0.0	0.4	0.0
120	6.0	0.2	2.5	0.0	1.2	0.0	0.4	0.0
180	5.7	0.1	2.6	0.0	1.3	0.0	0.5	0.0
270	5.7	0.0	2.4	0.0	1.3	0.0	0.5	0.0
360	5.7	0.0	2.3	0.1	1.3	0.2	0.5	0.0
1500	5.9	0.2	2.5	0.1	1.4	0.0	0.5	0.0

Notes:
[1]Standard deviation (SD)

Table B.2 Ni sorption capacity of zeolite (mg/g)

Time (min.)	Initial metal concentration / (mg/L)							
	200		100		50		20	
	Mean	SD	Mean	SD	Mean	SD	Mean	SD
5	0.0	0.0	83.3	0.0	0.0	0.0	0.0	0.0
10	3.5	0.3	78.3	0.0	1.1	0.0	0.3	0.1
20	4.1	0.1	77.9	0.0	1.3	0.0	0.5	0.0
40	4.2	0.1	78.5	0.1	1.4	0.0	0.4	0.0
60	4.6	0.1	78.9	0.0	1.4	0.1	0.5	0.0
120	4.8	0.2	78.6	0.1	1.4	0.0	0.5	0.0
180	4.8	0.0	78.6	0.1	1.4	0.0	0.5	0.0
270	4.9	0.2	78.9	0.1	1.5	0.0	0.5	0.0
360	4.8	0.1	79.2	0.1	1.5	0.0	0.5	0.0
1500	4.8	0.1	78.1	0.1	1.5	0.1	0.5	0.0

Table B.3 Cd sorption capacity of zeolite (mg/g)

Time (min.)	Initial metal concentration / (mg/L)							
	200		100		50		20	
	Mean	SD	Mean	SD	Mean	SD	Mean	SD
5	0.0	0.0	0.0	0.0	0.0	0.0	0.0	0.0
10	1.9	0.2	1.0	0.0	0.4	0.0	0.2	0.0
20	2.1	0.1	1.2	0.1	0.6	0.0	0.2	0.0
40	2.3	0.1	1.1	0.1	0.8	0.0	0.3	0.0
60	2.6	0.0	1.0	0.2	0.8	0.0	0.3	0.0
120	2.7	0.0	1.1	0.0	0.8	0.0	0.3	0.0
180	2.9	0.1	1.1	0.1	0.8	0.0	0.3	0.0
270	3.0	0.3	1.2	0.2	0.8	0.0	0.3	0.0
360	2.9	0.2	1.1	0.1	0.8	0.1	0.3	0.0
1500	2.8	0.1	1.1	0.1	0.8	0.1	0.3	0.0

Table B.4 Pb sorption capacity of zeolite (mg/g)

Time (min.)	Initial metal concentration / (mg/L)							
	200		100		50		20	
	Mean	SD	Mean	SD	Mean	SD	Mean	SD
5	0.0	0.0	0.0	0.0	0.0	0.0	0.0	0.0
10	3.1	0.1	1.5	0.2	0.7	0.1	0.2	0.1
20	3.4	0.2	1.7	0.2	1.0	0.0	0.5	0.1
40	3.9	0.1	1.8	0.1	1.2	0.1	0.4	0.0
60	4.3	0.1	1.9	0.2	1.2	0.1	0.5	0.0
120	4.3	0.3	1.9	0.1	1.2	0.0	0.5	0.0
180	4.3	0.2	2.0	0.0	1.2	0.0	0.5	0.1
270	4.3	0.1	1.9	0.1	1.3	0.2	0.5	0.0
360	4.2	0.4	1.9	0.1	1.2	0.1	0.5	0.0
1500	4.2	0.3	1.9	0.3	1.3	0.1	0.5	0.0

Table B.5 Cr sorption capacity of zeolite (mg/g)

Time (min.)	Initial metal concentration / (mg/L)							
	200		100		50		20	
	Mean	SD	Mean	SD	Mean	SD	Mean	SD
5	0.0	0.0	0.0	0.0	0.0	0.0	0.0	0.0
10	0.7	0.1	1.7	0.1	0.6	0.0	0.5	0.1
20	1.5	0.2	2.1	0.0	0.9	0.0	0.5	0.0
40	2.1	0.0	2.3	0.0	1.0	0.0	0.5	0.0
60	2.9	0.1	2.5	0.1	1.0	0.0	0.6	0.0
120	3.0	0.0	2.5	0.1	1.0	0.0	0.6	0.0
180	3.0	0.2	2.6	0.1	1.1	0.0	0.6	0.0
270	2.9	0.2	2.5	0.1	1.1	0.0	0.6	0.0
360	3.0	0.3	2.5	0.1	1.1	0.0	0.6	0.0
1500	3.0	0.2	2.4	0.2	1.1	0.0	0.6	0.0

Table B.6 Al sorption capacity of zeolite (mg/g)

Time (min.)	Initial metal concentration / (mg/L)							
	200		100		50		20	
	Mean	SD	Mean	SD	Mean	SD	Mean	SD
5	0.0	0.0	0.0	0.0	0.0	0.0	0.0	0.0
10	5.7	0.1	2.9	0.0	1.6	0.0	0.7	0.1
20	6.3	0.1	3.2	0.0	1.8	0.0	0.7	0.0
40	6.5	0.1	3.3	0.0	1.9	0.0	0.7	0.0
60	7.1	0.0	3.5	0.1	1.9	0.1	0.7	0.0
120	7.2	0.0	3.5	0.1	1.9	0.0	0.7	0.0
180	7.2	0.2	3.6	0.1	1.9	0.0	0.7	0.0
270	7.1	0.1	3.5	0.1	1.9	0.0	0.7	0.0
360	7.0	0.2	3.5	0.1	1.9	0.0	0.7	0.0
1500	7.1	0.2	3.4	0.2	1.9	0.0	0.7	0.0

Table B.7 Zn sorption capacity of zeolite (mg/g)

Time (min.)	Initial metal concentration / (mg/L)							
	200		100		50		20	
	Mean	SD	Mean	SD	Mean	SD	Mean	SD
5	0.0	0.0	0.0	0.0	0.0	0.0	0.0	0.0
10	1.3	0.4	0.5	0.0	0.4	0.0	0.1	0.0
20	1.9	0.1	0.6	0.1	0.7	0.0	0.2	0.0
40	2.1	0.1	0.7	0.1	0.8	0.0	0.2	0.0
60	2.5	0.0	0.9	0.1	0.8	0.0	0.2	0.0
120	2.6	0.0	0.9	0.0	0.8	0.0	0.2	0.0
180	2.6	0.0	0.9	0.1	0.8	0.0	0.2	0.0
270	2.6	0.1	0.9	0.1	0.8	0.0	0.2	0.0
360	2.6	0.1	0.9	0.1	0.8	0.0	0.2	0.0
1500	2.6	0.1	0.9	0.1	0.8	0.1	0.2	0.0

Thermodynamics experimental data for zeolite

Table B.8 Distribution coefficients for metal ions (L/g)

[1]T	Cu	Ni	Cd	Pb	Cr	Al	Zn
303	0.007	0.017	0.009	0.028	0.037	0.039	0.002
313	0.013	0.028	0.013	0.048	0.048	0.047	0.009
323	0.019	0.033	0.020	0.056	0.065	0.070	0.014
333	0.028	0.048	0.031	0.069	0.069	0.063	0.025

Notes:

[1]Absolute temperature (T) in K

Isotherm experimental data for zeolite

Table B.9 Equilibrium sorption capacity and metal concentration for zeolite

Cu		Ni		Cd		Pb		Cr		Al		Zn	
[1]Q_e	[1]C_e	Q_e	C_e	Q_e	C_e	Q_e	C_e	Q_e	C_e	Q_e	C_e	Q_e	C_e
5.1	149	4.8	152	2.9	171	4.3	157	3.0	170	7.1	129	2.6	174
2.1	79.4	2.1	78.6	1.1	88.9	1.9	80.9	2.5	74.9	3.5	64.8	0.9	91.3
1.3	36.8	1.4	35.6	0.8	42.4	1.2	37.8	1.0	39.5	1.9	30.7	0.8	41.7
0.5	14.7	0.5	15.3	0.3	17.0	0.5	15.1	0.6	14.1	0.7	13.0	0.2	17.8

Notes:

[1]Equilibrium sorption capacity (Q_e) in mg/g; Equilibrium metal concentration (C_e) in mg/L

Kinetics experimental data for seaweed

Table B.10 Cu sorption capacity of seaweed (mg/g)

Time /(min.)	Initial metal concentration / (mg/L)							
	200		100		50		20	
	Mean	SD[1]	Mean	SD	Mean	SD	Mean	SD
5	0.0	0.0	0.0	0.0	0.0	0.0	0.0	0.0
10	2.9	0.2	2.0	0.0	1.1	0.0	0.3	0.0
20	3.6	0.1	2.2	0.0	1.2	0.0	0.4	0.0
40	3.9	0.1	2.5	0.2	1.3	0.0	0.5	0.0
60	4.3	0.0	2.6	0.0	1.3	0.0	0.5	0.0
120	4.4	0.1	2.6	0.0	1.3	0.0	0.5	0.0
180	4.4	0.1	2.7	0.0	1.3	0.0	0.5	0.0
270	4.4	0.1	2.7	0.0	1.3	0.0	0.5	0.0
360	4.3	0.1	2.7	0.0	1.3	0.0	0.5	0.0
1500	4.4	0.0	2.8	0.0	1.3	0.0	0.5	0.0

Notes:
[1]Standard deviation (SD)

Table B.11 Ni sorption capacity of seaweed (mg/g)

Time /(min.)	Initial metal concentration / (mg/L)							
	200		100		50		20	
	Mean	SD	Mean	SD	Mean	SD	Mean	SD
5	0.0	0.0	0.0	0.0	0.0	0.0	0.0	0.0
10	2.9	0.0	2.5	0.1	0.4	0.0	0.1	0.0
20	4.2	0.0	2.8	0.0	1.6	0.0	0.1	0.0
40	4.4	0.1	3.0	0.0	1.6	0.0	0.3	0.0
60	4.8	0.1	3.1	0.0	1.6	0.0	0.3	0.0
120	5.6	0.1	3.1	0.1	1.7	0.0	0.3	0.0
180	5.6	0.1	3.0	0.0	1.7	0.1	0.3	0.0
270	5.5	0.1	3.0	0.0	1.8	0.0	0.3	0.0
360	5.5	0.1	3.1	0.1	1.8	0.2	0.3	0.1
1500	5.6	0.3	3.0	0.0	1.8	0.0	0.3	0.0

Table B.12 Cd sorption capacity of seaweed (mg/g)

Time /(min.)	Initial metal concentration / (mg/L)							
	200		100		50		20	
	Mean	SD	Mean	SD	Mean	SD	Mean	SD
5	0.0	0.0	0.0	0.0	0.0	0.0	0.0	0.0
10	0.5	0.1	1.5	0.0	0.4	0.0	0.2	0.0
20	2.0	0.1	1.9	0.1	0.7	0.0	0.3	0.0
40	2.2	0.1	2.1	0.1	1.3	0.0	0.3	0.0
60	2.8	0.1	2.2	0.1	1.3	0.0	0.3	0.0
120	3.4	0.2	2.2	0.0	1.4	0.0	0.3	0.0
180	3.7	0.2	2.1	0.0	1.4	0.1	0.3	0.0
270	3.7	0.0	2.1	0.0	1.5	0.0	0.3	0.0
360	3.7	0.1	2.2	0.1	1.5	0.0	0.3	0.0
1500	3.7	0.1	2.2	0.0	1.5	0.0	0.3	0.0

Table B.13 Pb sorption capacity of seaweed (mg/g)

Time /(min.)	Initial metal concentration / (mg/L)							
	200		100		50		20	
	Mean	SD	Mean	SD	Mean	SD	Mean	SD
5	0.0	0.0	0.0	0.0	0.0	0.0	0.0	0.0
10	3.4	0.1	3.8	0.0	1.6	0.0	0.2	0.0
20	4.3	0.1	3.9	0.1	1.7	0.0	0.3	0.0
40	4.7	0.1	4.0	0.1	1.8	0.0	0.3	0.0
60	5.1	0.1	4.1	0.1	1.9	0.0	0.4	0.0
120	5.6	0.2	4.4	0.0	2.1	0.0	0.4	0.0
180	5.7	0.2	4.3	0.0	2.1	0.1	0.4	0.0
270	5.9	0.0	4.2	0.0	2.1	0.0	0.5	0.0
360	5.9	0.1	4.3	0.1	2.1	0.0	0.4	0.0
1500	5.9	0.1	4.3	0.0	2.1	0.0	0.5	0.0

Table B.14 Cr sorption capacity of seaweed (mg/g)

Time /(min.)	Initial metal concentration / (mg/L)							
	200		100		50		20	
	Mean	SD	Mean	SD	Mean	SD	Mean	SD
5	0.0	0.0	0.0	0.0	0.0	0.0	0.0	0.0
10	4.0	0.1	2.0	0.0	0.5	0.0	0.2	0.1
20	5.0	0.1	2.6	0.0	1.1	0.0	0.2	0.0
40	5.1	0.0	3.7	0.1	1.4	0.0	0.3	0.0
60	5.4	0.1	3.8	0.0	1.6	0.0	0.4	0.0
120	5.8	0.1	4.1	0.0	1.8	0.0	0.4	0.0
180	6.1	0.0	4.5	0.0	1.8	0.1	0.5	0.0
270	6.1	0.1	4.5	0.0	1.8	0.0	0.5	0.0
360	6.0	0.1	4.4	0.0	1.8	0.1	0.5	0.0
1500	6.1	0.1	4.5	0.0	1.8	0.1	0.5	0.0

Table B.15 Al sorption capacity of seaweed (mg/g)

Time /(min.)	Initial metal concentration / (mg/L)							
	200		100		50		20	
	Mean	SD	Mean	SD	Mean	SD	Mean	SD
5	0.0	0.0	0.0	0.0	0.0	0.0	0.0	0.0
10	6.0	0.1	3.1	0.0	1.0	0.6	0.3	0.1
20	6.8	0.2	3.5	0.1	1.3	0.5	0.4	0.0
40	6.9	0.0	4.6	0.0	1.4	0.5	0.4	0.0
60	7.2	0.2	4.6	0.0	1.4	0.5	0.5	0.0
120	7.2	0.1	4.9	0.0	1.5	0.5	0.5	0.0
180	7.2	0.2	5.2	0.0	1.5	0.5	0.5	0.0
270	7.1	0.1	5.2	0.0	1.6	0.5	0.5	0.0
360	7.2	0.2	5.2	0.1	1.6	0.4	0.6	0.0
1500	7.2	0.2	5.2	0.0	1.6	0.5	0.6	0.0

Table B.16 Zn sorption capacity of seaweed (mg/g)

Time /(min.)	Initial metal concentration / (mg/L)							
	200		100		50		20	
	Mean	SD	Mean	SD	Mean	SD	Mean	SD
5	0.0	0.0	0.0	0.0	0.0	0.0	0.0	0.0
10	1.3	0.1	0.3	0.1	0.6	0.0	0.2	0.0
20	2.4	0.1	1.1	0.0	0.9	0.0	0.2	0.0
40	2.6	0.1	2.4	0.1	0.9	0.0	0.3	0.0
60	2.6	0.1	2.5	0.1	1.0	0.0	0.3	0.0
120	2.7	0.3	2.9	0.0	1.0	0.0	0.3	0.0
180	2.6	0.1	3.4	0.0	1.1	0.0	0.4	0.0
270	2.6	0.1	3.4	0.0	1.2	0.0	0.4	0.0
360	2.7	0.3	3.3	0.1	1.2	0.0	0.4	0.0
1500	2.7	0.3	3.3	0.0	1.1	0.1	0.4	0.0

Thermodynamics experimental data for seaweed

Table B.17 Distribution coefficients for metal ions (L/g)

[1]T	Cu	Ni	Cd	Pb	Cr	Al	Zn
303	0.016	0.029	0.015	0.063	0.050	0.055	0.009
313	0.025	0.039	0.024	0.055	0.057	0.057	0.017
323	0.031	0.045	0.030	0.065	0.063	0.060	0.026
333	0.040	0.051	0.037	0.103	0.076	0.083	0.031

Notes:

[1]Absolute temperature (T) in K

Isotherm experimental data for seaweed

Table B.18 Equilibrium sorption capacity and metal concentration for zeolite

Cu		Ni		Cd		Pb		Cr		Al		Zn	
$^{1}Q_e$	$^{1}C_e$	Q_e	C_e	Q_e	C_e	Q_e	C_e	Q_e	C_e	Q_e	C_e	Q_e	C_e
4.4	156	5.6	144	3.7	163	5.9	141	6.1	139	7.2	128	2.6	174
2.7	72.7	3.0	69.6	2.1	78.5	4.3	57.0	4.5	55.3	5.2	47.9	3.4	66.5
1.3	37.2	1.7	32.7	1.5	35.0	2.1	29.2	1.8	31.8	1.6	34.1	1.1	38.7
0.5	14.9	0.3	17.1	0.3	16.8	0.4	15.5	0.5	15.3	0.5	14.6	0.4	15.7

Notes:

[1]Equilibrium sorption capacity (Q_e) in mg/g; Equilibrium metal concentration (C_e) in mg/L

Appendix C
Sorption experimental data for mixtures of zeolite and seaweed

Kinetics experimental data for mixtures

Table C.1 Metal sorption capacities of mixture 1 (mg/g)

Time	Cu		Ni		Cd		Pb		Cr		Al		Zn	
/(min.)	[1]M	[1]SD	M	SD	M	SD	M	SD	M	SD	M	SD	M	SD
5	0.0	0.0	0.0	0.0	0.0	0.0	0.0	0.0	0.0	0.0	0.0	0.0	0.0	0.0
10	1.4	0.1	4.6	0.1	2.5	0.0	3.8	0.1	1.8	0.1	6.1	0.1	2.5	0.0
20	1.6	0.2	4.8	0.1	2.8	0.0	4.1	0.1	2.3	0.1	6.5	0.1	2.7	0.1
40	2.6	0.1	4.9	0.1	2.8	0.0	4.0	0.3	3.6	0.0	7.5	0.1	3.5	0.1
60	2.7	0.0	5.1	0.1	3.0	0.0	4.3	0.1	4.0	0.0	7.8	0.0	3.6	0.0
120	3.3	0.1	5.4	0.1	3.4	0.0	4.5	0.1	4.1	0.0	7.7	0.0	3.4	0.0
180	3.3	0.1	5.4	0.1	3.5	0.1	4.4	0.1	4.1	0.0	7.7	0.0	3.4	0.1
270	3.3	0.1	5.3	0.1	3.6	0.2	4.4	0.1	4.1	0.1	7.7	0.0	3.5	0.0
360	3.3	0.1	5.4	0.1	3.4	0.2	4.4	0.1	4.0	0.0	7.7	0.0	3.4	0.0
1500	3.3	0.1	5.3	0.1	3.4	0.0	4.4	0.1	4.0	0.0	7.7	0.1	3.5	0.1

Notes:

[1]Mean (M); Standard deviation (SD)

Table C.2 Metal sorption capacities of mixture 2 (mg/g)

Time	Cu		Ni		Cd		Pb		Cr		Al		Zn	
/(min.)	M	SD	M	SD	M	SD	M	SD	M	SD	M	SD	M	SD
5	0.0	0.0	0.0	0.0	0.0	0.0	0.0	0.0	0.0	0.0	0.0	0.0	0.0	0.0
10	1.9	0.1	3.4	0.0	1.2	0.0	2.2	0.0	1.9	0.0	3.4	0.1	1.0	0.1
20	4.0	0.1	5.3	0.1	3.2	0.1	5.5	0.2	4.9	0.1	6.9	0.0	2.0	0.1
40	4.1	0.0	5.5	0.1	3.4	0.1	5.8	0.1	5.0	0.0	7.0	0.1	2.5	0.1
60	5.2	0.4	6.3	0.4	4.4	0.4	5.9	0.1	5.2	0.1	7.2	0.1	2.6	0.2
120	5.3	0.1	6.5	0.0	4.8	0.1	6.1	0.1	5.4	0.1	7.4	0.0	2.6	0.1
180	5.3	0.1	6.5	0.1	4.8	0.1	6.0	0.0	5.5	0.1	8.1	0.2	2.8	0.2
270	5.3	0.0	6.5	0.0	4.8	0.1	6.1	0.0	5.6	0.1	8.1	0.2	2.8	0.2
360	5.3	0.1	6.5	0.0	4.8	0.1	6.1	0.0	5.8	0.2	8.1	0.2	2.9	0.1
1500	5.3	0.0	6.5	0.0	4.8	0.0	6.1	0.0	5.8	0.2	8.0	0.3	3.1	0.2

Table C.3 Metal sorption capacities of mixture 3 (mg/g)

Time	Cu		Ni		Cd		Pb		Cr		Al		Zn	
/(min.)	M	SD	M	SD	M	SD	M	SD	M	SD	M	SD	M	SD
5	0.0	0.0	0.0	0.0	0.0	0.0	0.0	0.0	0.0	0.0	0.0	0.0	0.0	0.0
10	5.0	0.1	3.9	0.0	2.1	0.0	6.0	0.1	4.8	0.0	7.3	0.0	2.1	0.0
20	5.5	0.1	4.3	0.1	2.5	0.1	6.3	0.2	5.3	0.0	7.6	0.1	2.6	0.0
40	5.7	0.1	5.0	0.1	3.0	0.0	6.7	0.2	5.8	0.1	8.0	0.1	3.3	0.1
60	5.7	0.2	5.8	0.1	4.0	0.1	7.4	0.2	6.6	0.0	8.4	0.1	3.9	0.2
120	6.0	0.2	6.0	0.1	4.2	0.1	7.5	0.2	6.6	0.0	8.4	0.2	4.0	0.3
180	5.7	0.1	6.4	0.2	4.4	0.1	7.5	0.0	6.6	0.1	8.4	0.1	4.0	0.2
270	5.7	0.0	6.4	0.1	4.4	0.1	7.6	0.1	6.6	0.1	8.5	0.0	3.9	0.0
360	5.7	0.0	6.4	0.1	4.4	0.3	7.5	0.0	6.6	0.1	8.4	0.0	4.0	0.1
1500	5.9	0.2	6.4	0.1	4.4	0.2	7.5	0.1	6.6	0.1	8.3	0.0	4.0	0.1

Table C.4 Metal sorption capacities of mixture 4 (mg/g)

Time	Cu		Ni		Cd		Pb		Cr		Al		Zn	
/(min.)	M	SD	M	SD	M	SD	M	SD	M	SD	M	SD	M	SD
5	0.0	0.0	0.0	0.0	0.0	0.0	0.0	0.0	0.0	0.0	0.0	0.0	0.0	0.0
10	3.1	0.1	4.0	0.0	1.9	0.1	3.0	0.1	2.1	0.1	4.1	0.1	2.5	0.0
20	3.2	0.0	4.7	0.2	2.7	0.0	4.0	0.1	2.6	0.0	4.9	0.0	2.9	0.0
40	3.4	0.1	5.1	0.2	3.2	0.2	4.6	0.1	2.9	0.1	5.4	0.1	3.0	0.1
60	3.8	0.1	5.4	0.1	3.5	0.2	4.7	0.4	3.5	0.1	5.5	0.0	3.3	0.1
120	3.9	0.1	5.5	0.1	3.6	0.1	5.1	0.1	3.5	0.0	5.6	0.1	3.4	0.1
180	4.1	0.1	5.6	0.1	3.7	0.1	5.2	0.0	3.4	0.0	5.8	0.0	3.4	0.0
270	4.0	0.1	5.6	0.1	3.6	0.0	5.2	0.0	3.5	0.0	5.8	0.3	3.5	0.1
360	4.0	0.0	5.6	0.1	3.6	0.1	5.3	0.1	3.5	0.1	5.8	0.4	3.5	0.0
1500	4.0	0.1	5.6	0.1	3.6	0.1	5.3	0.1	3.4	0.0	5.7	0.1	3.5	0.0

Isotherm experimental data for mixtures

Table C.5 Metal sorption capacities of mixture 1 (mg/g)

Cu		Ni		Cd		Pb		Cr		Al		Zn	
$^{1}Q_e$	$^{1}C_e$	Q_e	C_e	Q_e	C_e	Q_e	C_e	Q_e	C_e	Q_e	C_e	Q_e	C_e
3.3	167	5.3	147	3.4	166	4.4	155	4.0	160	7.7	123	3.5	165
2.4	76.0	2.7	72.7	1.7	83.1	1.7	83.4	1.9	81.4	4.4	56.1	1.6	83.8
0.5	45.4	1.2	38.0	0.8	41.8	1.3	37.4	1.6	33.8	1.9	30.9	0.8	41.9
0.4	16.1	0.6	13.9	0.5	14.8	0.6	13.5	0.5	14.8	0.9	11.5	0.5	15.3

Notes:

[1]Equilibrium sorption capacity (Q_e) in mg/g; Equilibrium metal concentration (C_e) in mg/L

Table C.6 Metal sorption capacities of mixture 2 (mg/g)

Cu		Ni		Cd		Pb		Cr		Al		Zn	
Q_e	C_e	Q_e	C_e	Q_e	C_e	Q_e	C_e	Q_e	C_e	Q_e	C_e	Q_e	C_e
5.3	147	6.5	135	4.8	152	6.1	139	5.7	143	8.2	118	3.1	169
2.7	73.3	3.3	67.4	2.4	76.1	1.1	89.0	2.7	73.0	4.0	60.4	2.3	77.0
1.3	36.9	1.6	33.8	1.0	39.6	0.3	47.5	1.2	37.8	2.0	30.0	0.9	41.1
0.3	17.1	0.4	16.5	0.3	17.5	0.8	12.3	0.4	16.3	0.4	15.6	0.7	13.0

Table C.7 Metal sorption capacities of mixture 3 (mg/g)

Cu		Ni		Cd		Pb		Cr		Al		Zn	
Q_e	C_e	Q_e	C_e	Q_e	C_e	Q_e	C_e	Q_e	C_e	Q_e	C_e	Q_e	C_e
5.8	142	6.4	136	4.4	156	7.5	125	6.6	134	8.3	117	3.9	161
2.4	75.7	3.2	67.9	2.2	78.1	2.0	80.1	4.9	51.2	6.0	39.5	4.6	54.3
1.4	36.4	1.5	34.6	1.0	39.8	1.1	39.0	2.5	24.6	3.1	19.2	2.4	26.3
0.5	14.5	0.3	16.6	0.2	18.4	0.6	14.5	0.6	13.6	0.7	12.8	0.3	17.4

Table C.8 Metal sorption capacities of mixture 4 (mg/g)

Cu		Ni		Cd		Pb		Cr		Al		Zn	
Q_e	C_e	Q_e	C_e	Q_e	C_e	Q_e	C_e	Q_e	C_e	Q_e	C_e	Q_e	C_e
4.0	160	5.6	144	3.7	163	5.3	147	3.4	166	5.8	142	3.6	164
2.6	73.7	3.2	67.7	2.3	77.3	3.3	67.3	1.3	87.3	3.2	67.5	2.1	78.9
1.5	34.5	1.8	31.8	1.5	35.1	2.0	29.6	0.9	40.6	1.9	31.4	1.4	36.3
0.4	16.3	0.5	15.2	0.3	16.7	1.2	8.5	0.1	19.2	0.3	16.9	0.2	18.4

Langmuir plots for mixtures

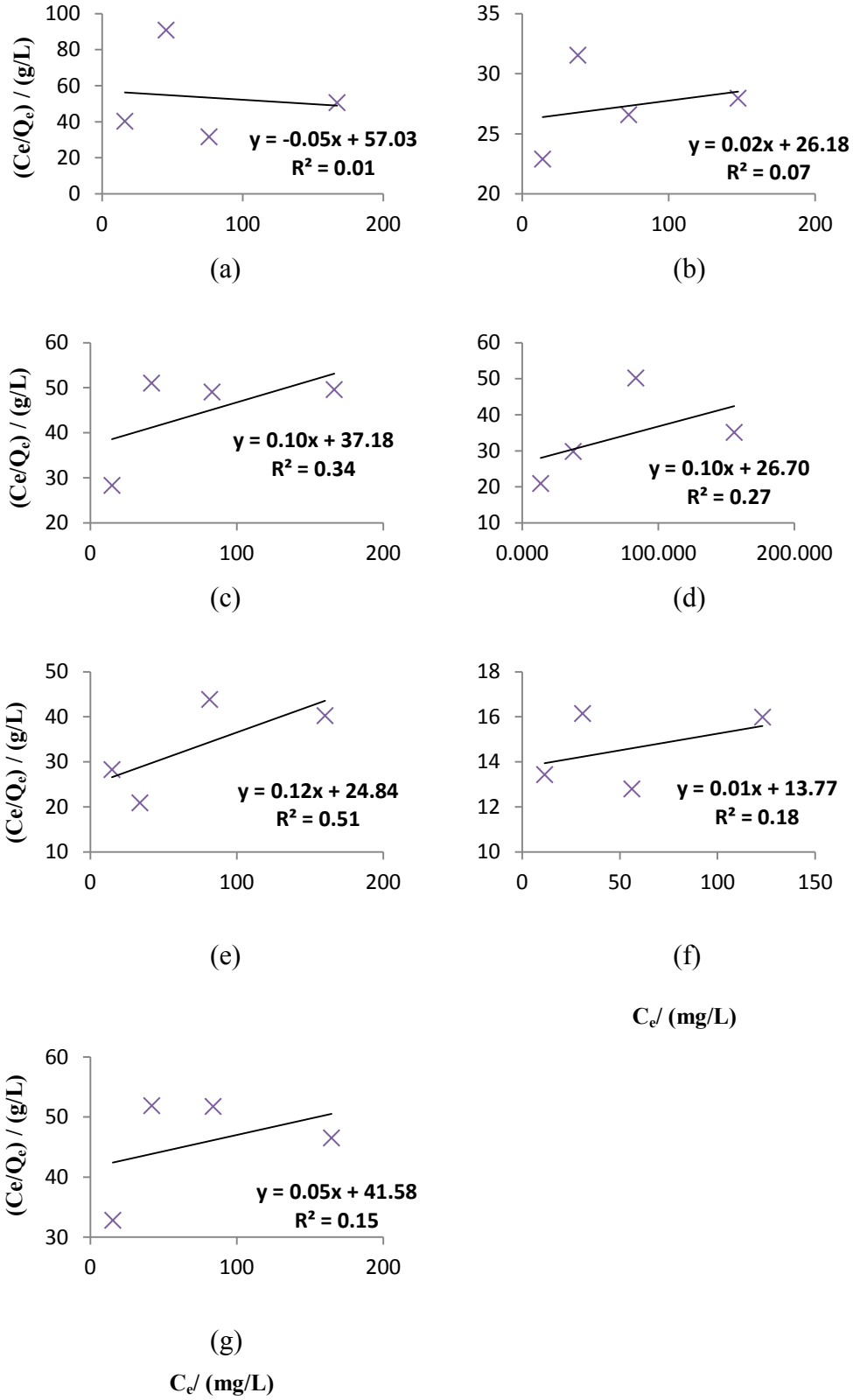

Figure C.1 Langmuir isotherm plots for mixture 1 for: (a) Cu; (b) Ni; (c) Cd; (d) Pb; (e) Cr; (f) Al; (g) Zn

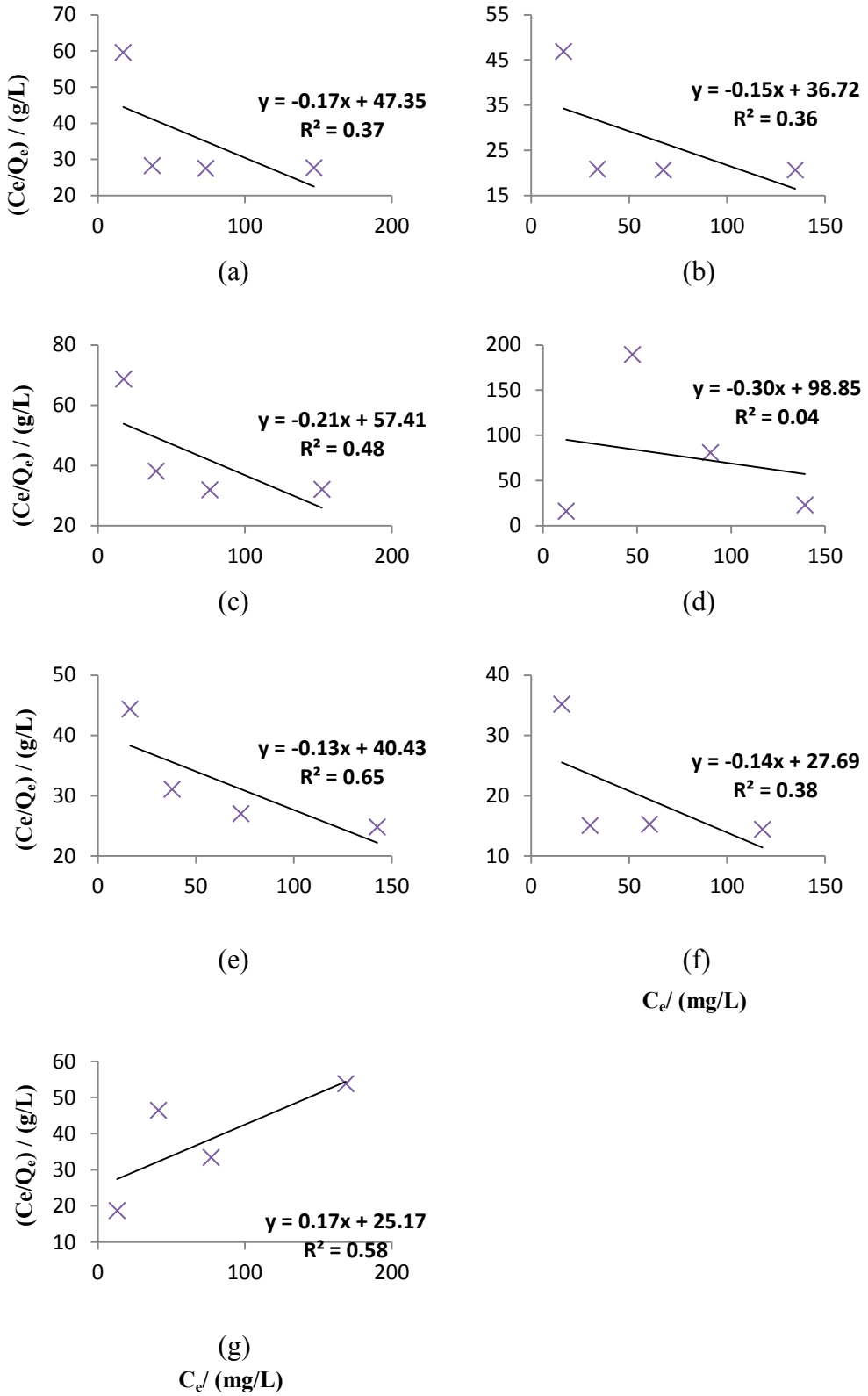

Figure C.2 Langmuir isotherm plots for mixture 2 for: (a) Cu; (b) Ni; (c) Cd; (d) Pb; (e) Cr; (f) Al; (g) Zn

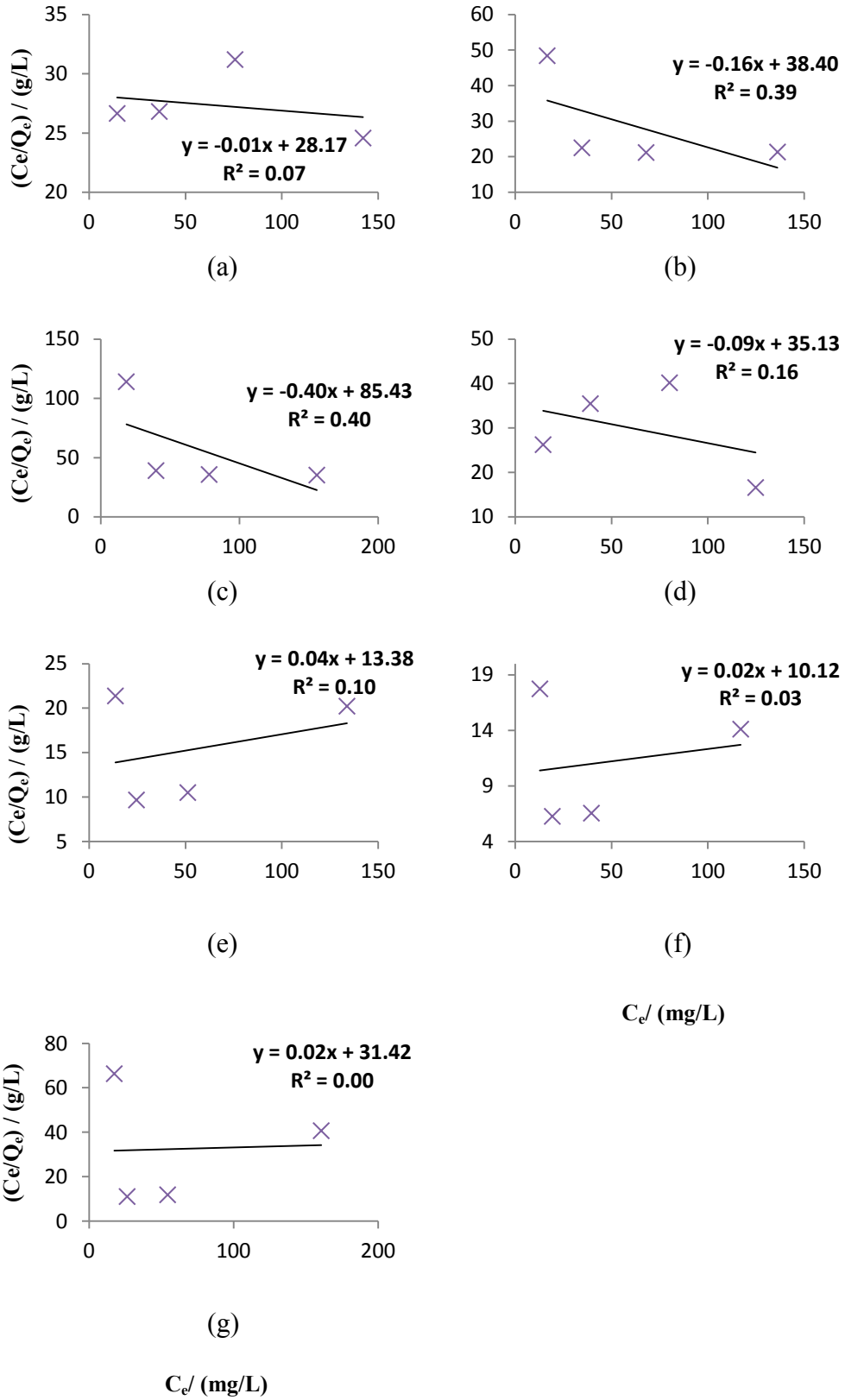

Figure C.3 Langmuir isotherm plots for mixture 3 for: (a) Cu; (b) Ni; (c) Cd; (d) Pb; (e) Cr; (f) Al; (g) Zn

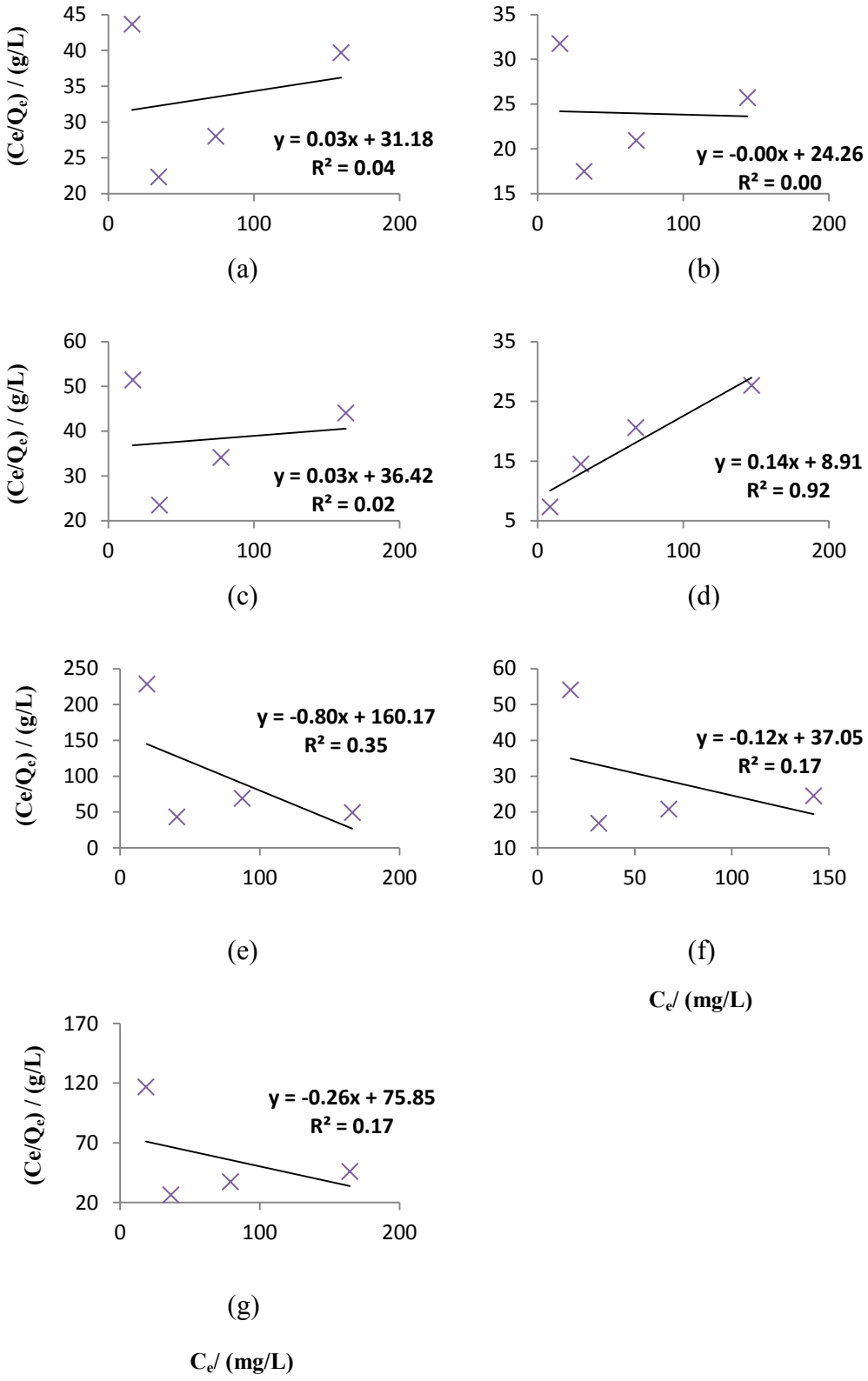

Figure C.4 Langmuir isotherm plots for mixture 4 for: (a) Cu; (b) Ni; (c) Cd; (d) Pb; (e) Cr; (f) Al; (g) Zn

Thermodynamics experimental data for mixtures

Table C.9 Distribution coefficient for mixture 1

[1]T	[2]Cu	[2]Ni	[2]Cd	[2]Pb	[2]Cr	[2]Al	[2]Zn
303	0.009	0.024	0.009	0.034	0.040	0.039	0.006
313	0.023	0.038	0.023	0.055	0.058	0.056	0.017
323	0.027	0.040	0.024	0.141	0.072	0.085	0.019
333	0.033	0.053	0.034	0.059	0.071	0.065	0.028

Notes:

[1]Absolute temperature (T) in K;

[2]Distribution coefficient (K_d) of corresponding metal ion in L/g

Table C.10 Distribution coefficient for mixture 2

T	Cu	Ni	Cd	Pb	Cr	Al	Zn
303	0.010	0.025	0.010	0.039	0.042	0.043	0.006
313	0.021	0.036	0.023	0.048	0.055	0.047	0.015
323	0.025	0.039	0.023	0.131	0.069	0.080	0.017
333	0.039	0.049	0.041	0.052	0.071	0.072	0.028

Table C.11 Distribution coefficient for mixture 3

T	Cu	Ni	Cd	Pb	Cr	Al	Zn
303	0.011	0.025	0.009	0.039	0.042	0.044	0.005
313	0.017	0.035	0.019	0.043	0.051	0.049	0.012
323	0.030	0.043	0.028	0.145	0.075	0.089	0.021
333	0.032	0.045	0.031	0.073	0.066	0.070	0.025

Table C.12 Distribution coefficient for mixture 4

T	Cu	Ni	Cd	Pb	Cr	Al	Zn
303	0.016	0.031	0.015	0.043	0.047	0.049	0.010
313	0.021	0.037	0.020	0.041	0.053	0.051	0.015
323	0.030	0.041	0.025	0.135	0.072	0.088	0.018
333	0.032	0.044	0.030	0.065	0.063	0.066	0.023